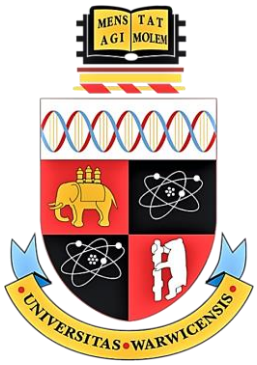

Biochemical characterization of multicopper oxidase enzymes from lignin degrading bacteria

Rommel Santiago Granja Trávez

A thesis submitted in partial fulfilment of the requirements for the degree of Doctor of Philosophy in Chemistry

University of Warwick

Department of Chemistry

October 2018

Supervisor: Professor Timothy D.H. Bugg

I. Table of Contents

II. List of Figures

III. List of Tables

IV. List of Abbreviations

ABTS	2,2'-azino-bis(3-ethylthiazoline-6- sulfonate)
BLAST	Basic local alignment search tool
B. xenovorans	*Burkholderia xenovorans*
° C	Degrees Celsius
Da	Dalton
DMP	2,6-dimethoxyphenol
DMSO	Dimethyl sulfoxide
DNA	Deoxyribonucleic acid
DyP	Dye-decolorizing peroxidases
DCP	2,4-dichlorophenol
dNTPs	Deoxynucleotide triphosphates
E. coli	*Escherichia coli*
EDTA	Ethylenediaminetetraacetic acid
EC	Enzyme commission
ε	Extinction coefficient
FADH	Flavin adenine dinucleotide (reduced)
FPLC	Fast protein liquid chromatograph
HEPES	4-(2-hydroxyethyl)-1-piperazineethanesulfonic acid
His	Histidine
His_6	Hexa-histidine
HPLC	High pressure liquid chromatography
HRMS	High resolution mass spectrometry
ICP-OES	Inductively coupled plasma optical emission spectrometry

IPTG	Isopropyl β-D-1-thiogalactopyranoside
kcat	Turnover number
KM	Michaelis constant
Kbp	Kilo base pair
kpsi	kilo pounds per square inch
LB	Luria broth
LiP	Lignin peroxidase
LC-MS	Liquid chromatography mass spectrometry
MnP	Manganese peroxidase
m/z	Mass to charge ratio
M. phyllosphaerae	*Microbacterium phyllosphaerae*
MS	Mass spectrometry
mV	Millivolt
NaOH	Sodium hydroxide
NADPH	Nicotinamide adenine dinucleotide phosphate (reduced)
Ni-NTA	Nickel-Nitrilotriacetic acid
OD	Optical density
PDB	Protein Data Bank
PCR	Polymerase chain reaction
pKa	Acid dissociation constant
P. fluorescens	*Pseudomonas fluorescens*
P. putida	*Pseudomonas putida*
RNA	Ribonucleic acid
R. jostii RHA1	*Rhodococcus jostii* Rha1
SDS	Sodium dodecyl sulphate

SDS-PAGE	Sodium dodecyl sulphate polyacrylamide gel electrophoresis
SGZ	Syringaldazine
TBE	Tris-borate-EDTA
T. fusca	*Thermomonaspora fusca*
TEV	Tobacco Etch Virus
UV	Ultraviolet
UV-Vis	Ultraviolet-visible
VP	Versatile peroxidise
λ	Wavelength

V. Acknowledgements

Firstly, I would like to express my sincere gratitude to my supervisor Prof. Timothy D.H. Bugg for giving me the opportunity to pursue my academic goal, for believe in me, for the continuous support during my PhD studies, for his patience, enthusiasm, vast knowledge and for his kind understanding of my personal circumstances. His guidance helped me all the way through the research and writing of this thesis.

Secondly, I would like to express my deepest thanks to the Scholarship program "Convocatoria Abierta 2014" granted by the Ecuadorian Government, through the Ministry of Higher Education, Science and Technology (SENESCYT), without which my studies abroad would not have been possible.

Besides my supervisor, I would like to thank my advisory Panel: Dr. Ann M. Dixon and Dr. Claudia A. Blindauer, for their insightful comments and encouragement that led me to widen my research from various perspectives.

My sincere thanks also go to Dr. Rachael Wilkinson and Prof. Vilmos Fulop, who provided me their help and suggestions on protein crystallography analysis and performed the crystallography work.

I thank my fellow lab mates for the stimulating discussions and for their academic and moral support throughout the journey. In particular, I am grateful to Dr. Rahman Rahmanpour for his friendship and his tireless effort to teach me most of the things that now I know about molecular biology, and to Dr. Goran Rashid for his help on chemistry matters. Thanks also to everyone in the CBRF for their help.

Last but not the least, I would like to thank my family: my parents Emilio and Mercedes, for their unconditional love and encouragement to chase my dreams; to my brothers Fernando and Julián, who always have the right words to cheer me up without even noticing; to my sister Johanna for listening me whenever I needed; to the love of my life, Laura, for being such an extraordinary wife, for giving me comfort, serenity and love; and to the three greatest joys of my life, Dario, Joaquin and Julia, who make me stronger and bring me all the happiness that I need to keep balanced my world. This accomplishment simply would not have been possible without their emotional support.

VI. Declaration

The work presented herein is my own work unless otherwise acknowledged and has not been submitted for a degree at another university.

Work in Chapter 2 on identity confirmation of CopC-Bx1 and CopC-Bx2 was performed by the Proteomics Research Technology Platform, School of Life Sciences, University of Warwick.

Work in Chapter 3 on LMCOs redox potential, was performed by Dr Rachael Wilkinson, Research Fellow at Life Science Department in the University of Warwick.

Work in Chapter 4 on activity of lignin 6 with Oc-CueO in combination with other enzymes was performed using the enzymes dihydrolipoamide dehydrogenase (DhLDh) from *Sphingobacterium sp*., and glutathione S-transferase (LigE) from *Agrobacterium sp.* cloned by Dr. Goran Rashid, in the TDHB research group; and the enzyme Dyp-type peroxidase (Dyp1B) from *Pseudomonas fluorescens Pf-5*, cloned by Dr. Rahman Rahmanpour, in the TDHB research group.

Work in Chapter 5 on protein crystallization, data analysis and protein modelling were carried out by Dr Rachael Wilkinson, Research Fellow at the School of Life Science, University of Warwick, under the supervision of Professor Vilmos Fulop, School of Life Sciences, University of Warwick.

Rommel Santiago Granja Trávez

VII. Scholarly outcomes

This investigation has made possible the generation of two scientific publications and three presentations in scientific events, as listed below:

Scientific publications

- Granja-Travez, R. S., Wilkinson, R. C., Persinoti, G. F., Squina, F. M., Fülöp, V., & Bugg, T. D. (2018). Structural and functional characterisation of multi-copper oxidase CueO from lignin-degrading bacterium Ochrobactrum sp. reveal its activity towards lignin model compounds and lignosulfonate. *The FEBS journal*, 285(9), 1684-1700.
- Granja-Travez, R. S., & Bugg, T. D. (in press). Characterisation of multicopper oxidase CopA from Pseudomonas putida KT2440 and Pseudomonas. *Archives of Biochemistry and Biophysics*.

Scientific presentations

As poster presentation:

- Granja-Travez, R. S. (2017). Oxidase activity of laccase-like multicopper oxidases from bacterial lignin degraders. Poster presented at: *The 13th International Conference on Renewable Resources and Biorefineries.* 7-9 June 2017. Wroclaw, Poland. Winner awarded as best poster.
- Granja-Travez, R. S. (2016). Biochemical characterization of copper enzymes from bacterial lignin degraders. Poster presented at: *Chemistry Postgraduate Symposium*. May 2016. University of Warwick, Coventry, United Kingdom.

As oral presentation:

- Granja-Travez, R. S. (2017). Oxidase activity of laccase-like multicopper oxidases and CopC proteins, from bacterial lignin degraders. Oral presentation at: *Chemistry Postgraduate Symposium*. April 2017. University of Warwick, Coventry, United Kingdom.

VIII. Abstract

Lignin is an abundant biopolymer found in nature. Because of its carbon content and aromatic nature, lignin is promising renewable feedstock for biotechnological applications. However, the resistance of lignin to chemical and microbial breakdown have limited its utilization. Some enzymes have been involved in lignin depolymerization, among them, the multicopper oxidase subgroup of laccase has shown oxidase activity towards lignin. In addition, since laccase activity only requires oxygen and the only by-product generated is water, these enzymes have been regarded as perfect green catalysts, offering a range of potential applications beyond lignin transformation. Multicopper oxidases (MCOs) have been found encoded in the genome of some bacterial lignin degraders, which might show laccase activity and maybe play a role in lignin degradation. In this study, three MCOs (Pp-CopA, Pf-CopA and Oc-CueO), have been expressed and reconstituted as recombinant laccase-like multicopper oxidases (LMCOs), and they have been kinetically characterized. Pp-CopA, Pf-CopA and Oc-CueO showed activity towards common laccases substrates, such as 2,2'-azino-bis(3-ethylbenzothiazoline-6-sulphonic acid) (ABTS); syringaldazine (SGZ); guiacol; 2,6-dimethoxyphenol (DMP); and 2,4-dichlorophenol (DCP). These enzymes showed further activity towards the lignin model compounds: guaiacylglycerol-beta-guaiacyl (GGE) and 2,2'-dihydroxy-3,3'-dimethoxy-5,5'-dicarboxybiphenyl (DDVA), generating oxidized dimeric products; and they were active with Ca-lignosulfonate (Borregaard), generating the low molecular weight product vanillic acid. The steady state kinetic parameters have been elucidated for these enzymes with ABTS and SGZ, and their pH profile showed an optimal pH value of ≈4.5 for ABTS and ≈7.5 for SGZ. The crystal structure of Oc-CueO has been determined at 1.1 Å resolution, showing a four-coordinate mononuclear type I copper centre with Met500 as an axial ligand, whereas the trinuclear type 2/3 copper cluster was modelled into the active site. Site-directed mutagenesis was carried out on amino acid residues found in the solvent tunnels, indicating the importance for residues Asp102, Gly103, Arg221, Arg223 and Asp462 for catalytic activity. The host organism of Pp-CopA, *Pseudomonas putida KT2440* has been subjected to a double deletion of *copA-I* and *copA-II* genes, which led to a diminished growth capability of this strain on different small aromatic compounds, related with lignin degradation, only if copper was present in the media. This study identifies new bacterial multicopper oxidase enzymes with laccase activity and activity for lignin oxidation.

1 Introduction

1.1 Lignin: function and structure

Lignin is a biopolymer derived from plants and some algae [1], whose main biological functions include, firstly, to provide mechanical and chemical resistance to plants, and secondly, to facilitate water transportation in vascular plants. Lignin plays an adhesive role between the polysaccharide components of the plant cell walls, as it is covalently linked with hemicellulose and forms cross-links with cellulose, especially in vascular and support tissues, such as xylem (tracheids and vessel elements), fibers and sclereid cells [2]. The importance of lignin for structural support of lignified cell walls is based on its function as a polymer glue, which gives cohesion to different layers of polysaccharides in the secondary cell wall, making fibers stiff and conferring mechanical strength to the cell and, by extension, the whole plant. In addition, lignin also glues different cells together, since it is the main component of middle lamella [2, 3]. Polysaccharide polymers are fastened by lignin in such a compact way, that degrading enzymes excreted by most microorganisms cannot penetrate the cell wall, which also makes lignified wood resistant to microbial attack, though there are some microorganisms able to degrade lignin [3, 4]. A chemical property that distinguishes lignin from other biopolymers found in the cell wall is that, while cellulose or hemicellulose are basically hydrophilic in nature, lignin is rather hydrophobic. Lignin hydrophobicity implies that tissues where lignin is located normally present a barrier to water diffusion, therefore water can be transported efficiently through lignified tissues as its absorption by cells is inhibited [3, 4].

Despite its importance and abundance in nature, a formal definition of lignin has been challenging. For its inherent molecular complexity and diverse structural composition, lignin should not be considered as a single compound but as a heterogeneous material. Lignin found in plants has been called “native lignin”, while there is another type of lignin that derives from the separation of different plant components in paper industry and biorefineries; being both substantially different from each other. Nevertheless, they share in common a phenolic nature, with a variety of compositions and linkages between subunits [3]. The basis of its complex architecture is the different combination of three phenylpropane derivatives, called monolignols, containing basically the same phenylpropane unit (M1) with different phenyl functionalization: coniferyl alcohol ($M1_G$), sinapyl alcohol ($M1_S$), and *p*-coumaryl alcohol ($M1_H$). When incorporated into lignin, these monolignols form the

phenylpropanoids units, guaiacyl (G), syringyl (S) and *p*-hydroxyphenyl (H), respectively (**Figure 1**) [3, 5, 6].

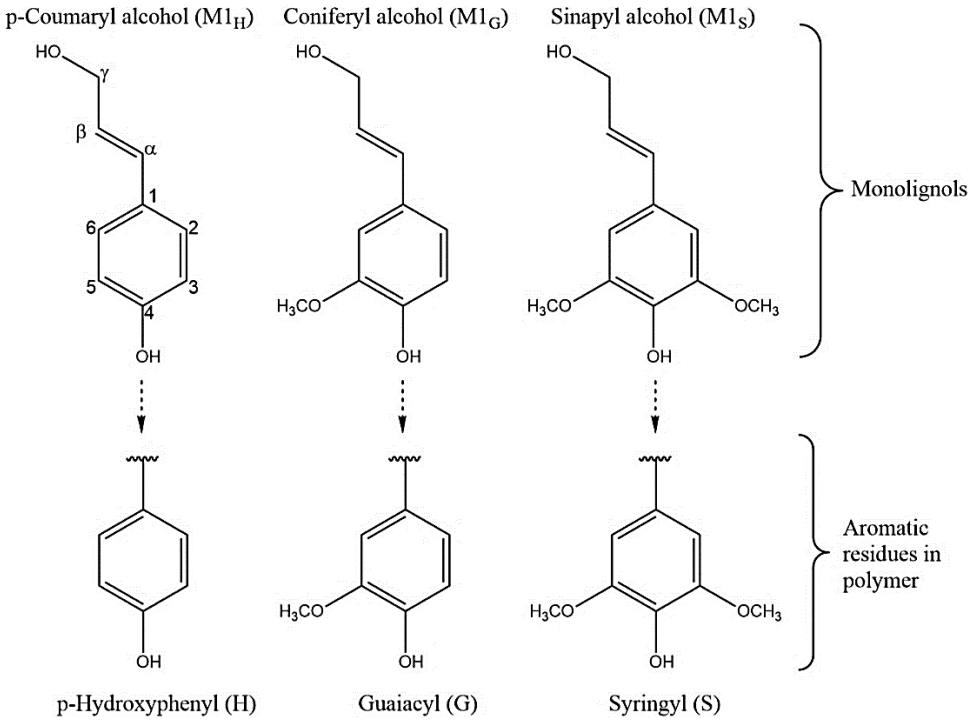

Figure 1. Chemical structure and atom numbering for the three more common monolignols and their corresponding phenylpropanoids in polymeric lignin. Adapted from [3].

Lignin distribution and its content in plants is influenced by the species of the plant, growth conditions and tissue type. The phenylpropanoid ratio in plants has been used as method of classification, giving three different lignin groups: softwood (gymnosperm), mainly composed of G-units and a lesser amount of H-units; hardwood (angiosperm-dicots), formed by G- and S-units in about equal ratios; and grass lignins (angiosperm-monocots), containing various ratios of all subunits, G-, S- and H-units [6-8]. This classification has many exceptions, however. Because of the different phenylpropanoid functionalization, their proportion and how they are combined can affect, to some extent, the type of bonds formed in the polymer. To represent an inter-unit linkage, the two carbons atoms involved in the chemical bond are denoted, distinguishing one subunit from the other by a prime (‘). For instance, the most common linkage in native lignin is the so called β-O-4’ (**Figure 2**), which means that a β-carbon from one subunit is forming a linkage to the carbon in position 4 of another subunit, through an ether bond (R-O-R’) [3, 6].

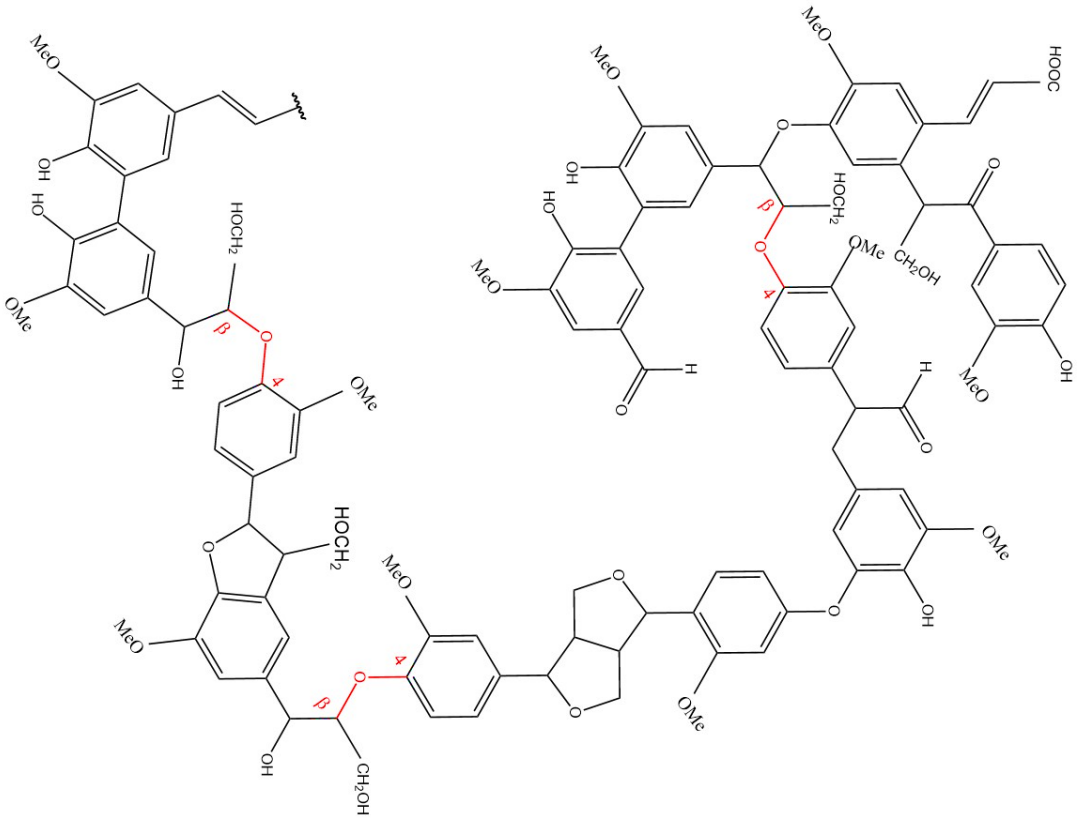

Figure 2. Hypothetical structure of a hardwood lignin fragment. β-O-4' inter-unit linkages are coloured in red. Adapted from [3].

The β-O-4' chemical bond comprises more than 50% of all linkages in all types of native lignin [8, 9]. Other linkages involving the β carbon include, β-5', β-β' and β-1'. Another kind of inter-unit linkages found in lignin that potentially could serve as branching points are 4-O-5' and 5-5' [6]. As noted, some subunits are linked through an ether bond, while others can form a direct linkage between two carbon atoms. The predominant type of inter-unit linkages in lignin can affect its susceptibility to degradation. Since the energy needed to break ether linkages tends to be lower (54 – 72 kcal/mol) than the energy needed to break carbon-carbon linkages (125 – 127 kcal/mol), lignins with high numbers of carbon-carbon are more rigid and less prone to degradation. These type of lignins are known as condensed lignins [10]. Native lignin can be structurally transformed by industrial processes by the oxidation of hydroxyl or ether groups, into a more condensed or less phenolic lignin, making it usually more resistant to degradation [10, 11]. These transformations are the main reason for the differences seen between the native and industrial lignin, and the differences among industrial lignins, whose properties depend on how they were isolated. As it can be inferred, the representation of a lignin structure is difficult, due to its complex and wide proportion of different monomers and inter-unit linkages. Several models have been proposed, as illustration, in **Figure 2**, a proposed model for hardwood lignin is shown [3].

1.2 Lignin biosynthesis

The complex structure of lignin requires a highly coordinated and accurate system of monolignol production, transportation, and polymerization, to assure the correct assembly of lignified secondary cell walls. Lignin biosynthesis commences with the amino acid L-phenylalanine as a precursor for the biosynthetic formation of all monolignols, then these monolignols are glycosylated in the cytosol to make monolignols more hydrophobic and less toxic, and then these molecules are transported to the apoplast, where the glucose is removed and polymerization occurs [5, 12].

Biosynthesis of monolignols begins with the deamination of phenylalanine, followed by consecutive hydroxylation and O-methylation reactions of the aromatic ring, and the transformation of the side chain carboxyl into an alcohol. A total of eleven enzymes have been identified to be involved in conversion of phenylalanine in any of the three main monolignols [5, 13]. **Figure 3** presents a summary of the most accepted biosynthetic pathways for generation of classical and recently discovered monolignols [13].

Once monolignols are formed, they are transported to cell wall for polymerization, in the form of monolignol-4-O-β-D-glucosides [14]. However, the exact translocation mechanism of monolignols to the cell wall remains unclear, though Golgi-derived vesicles and ABC transporters directly pumping monolignols through membrane, have been proposed as transportation models [12, 15]. Once monolignols reach the cell wall, they are oxidised to form radicals that can perform coupling reactions. Several groups of enzymes have been involved in this step, including peroxidases, laccases, polyphenol oxidases and coniferyl alcohol oxidases. Whether all enzymes or a combination of them are responsible for the dehydrogenation of monolignols, is unclear. Neither is it known if there are other redox molecules that can serve as mediators or another groups of accessory enzymes, such as those producing hydrogen peroxide (a molecule needed for peroxidases activity), involved in lignin polymerization [5, 15]. Many studies have been conducted to study the role of these enzymes in lignin polymerization, nevertheless, downregulation of genes encoding laccases or peroxidases has been shown to have little effect on lignin content, which might be attributed to the high redundancy of these enzymes in plant genomes [16, 17]. Finally, when the monolignol radical is formed, an oxidative radicalization of phenols leads to lignin polymerization. Two oxidised monolignols radicals couple to produce a dimer, forming a covalent bond between subunits, mainly favouring a linkage at the β-carbon position. Then,

the dimer is dehydrogenated once again, making it possible to combine with a new dehydrogenated monomer, allowing the polymerization by adding one unit at a time [15]. This coupling occurs in a chemical combinatorial manner, where the chemical nature of each monomer and also environmental conditions, including enzyme concentrations or supply of reactants, and other factors, affect the ratio of each possible coupling, therefore the result is the complex and random pattern seen in lignin [18].

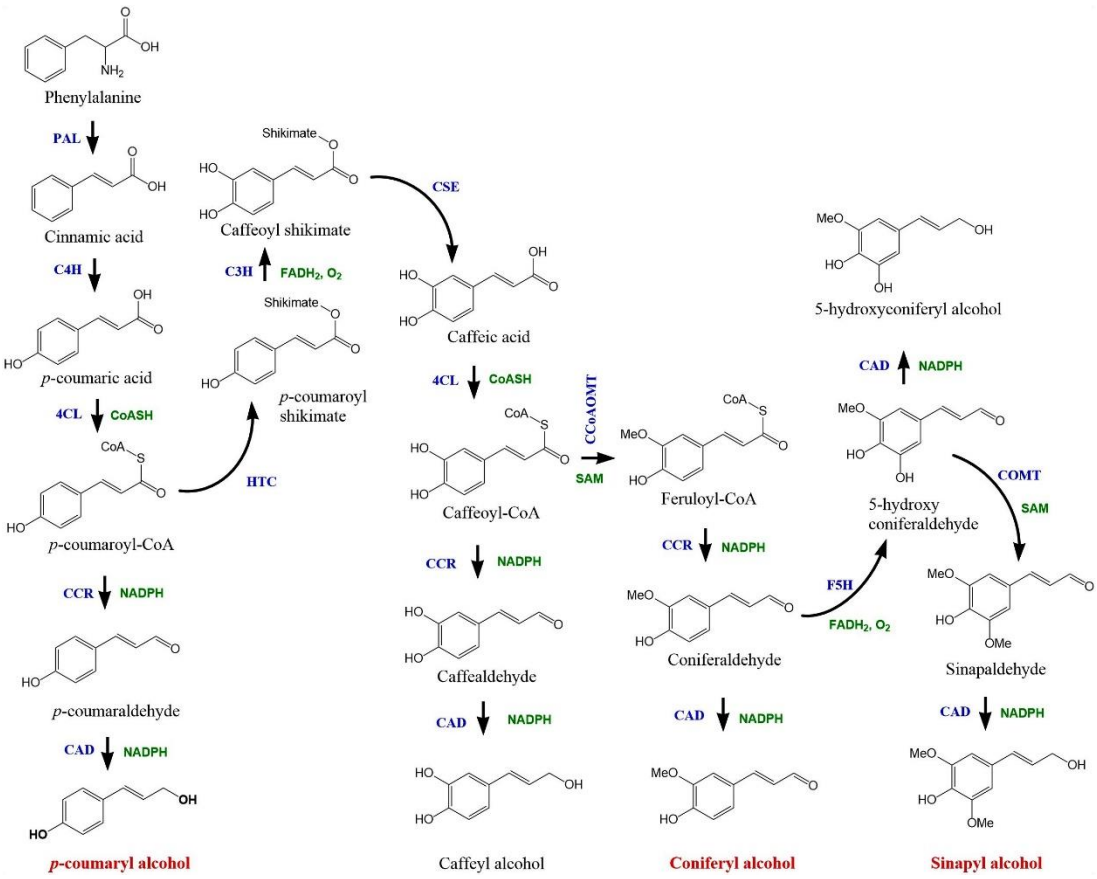

Figure 3. Monolignols biosynthetic pathways. Most common monolignols are labelled in red colour. Enzymes involved in bioconversions are labelled in blue, and are as follows: PAL, L-phenylalanine ammonia-lyase; C4H, cinnamate 4-hydroxylase; 4CL, 4-coumarate:CoA ligase; CCR, cinnamoyl-CoA reductase; CAD, cinnamyl alcohol dehydrogenase; HCT, hydroxycinnamoyl CoA:shikimate/quinate hydroxycinnamoyl transferase; C3H, 4-coumaroyl shikimate 3-hydroxylase; CSE, caffeoyl shikimate esterase; CCoAOMT, caffeoyl-CoA 3-O-methyltransferase; F5H, ferulate/coniferaldehyde 5-hydroxylase; and COMT, caffeic acid/5-hydroxyconiferaldehyde 3-O-methyltransferase. Cofactors are labelled in green: CoASH, reduced coenzyme A; NAPDH, reduced nicotinamide adenine dinucleotide phosphate; $FADH_2$, reduced flavin adenine dinucleotide; and SAM, S-adenosyl methionine. Adapted from [13].

1.3 Lignin sources and characterization

Since the term “lignin” refers to a heterogenous material and not a single compound, it is useful to group lignins based on some shared characteristics. The process by which lignins are obtained is an acceptable approach for this purpose. However, it should be noted that many differences will remain among lignins of the same group. For instance, the so called “native lignin” shares some properties, e.g. a relatively high number of β-O-4’ linkages, but lignins from wheat straw, spruce or eucalyptus, have been proven to be essentially different from each other, even though all of them were produced as native lignins [19].

Kraft lignin process: This is the main chemical pulping process and consists in the treatment of lignin at high pressure and temperatures of 150 to 180 °C, at a high pH conditions and in presence of NaOH, Na_2SO_4 and polysulfide. Lignin is solubilized and then recovered by precipitation, lowering the pH. The product is known as kraft lignin, it shows an average molecular weight between 1000 and 3000, and about 70% to 75% is chemically sulfonated, which makes it soluble in alkali and confers it with surfactant properties. In addition, it shows increased phenolic hydroxyl groups and biphenyl structures and it is bound to some residual carbohydrates. Kraft lignin represent the largest source of available lignin for the biorefinery [6, 11, 20].

Lignosulfonate process: Lignosulfonate is a by-product of wood pulp production when sulphite pulping has been used as the extract process. It consists in treatment of lignin at high temperatures and pressure, in presence of various salts of sulphurous acid, with a pH varying from 2 to 12, depending on the cationic compositions of the pulping liquor, though many processes are carried out in acidic conditions. The product, sulfonated lignin, contains many sulfonate groups in the aliphatic side chains and is negatively charged. A pH shift is not enough to isolate it, so desulfonation steps are needed before its precipitation, normally in presence of Ca. Its molecular weight ranges from 5000 to 20000 (higher than kraft lignin) and it is very soluble in water in the whole range of pH [6, 20, 21].

Organosolv process: Organosolv pulping is a process by which components of wood are separated by using organic solvents at high pressures and temperatures, giving separate streams of cellulose, hemicellulose and lignin. A list of some solvents used in this process include acetic acid, formic acid, peroxy-organic acids and ethanol. Some processes have been commercially registered and used at industrial scale, e.g. the Acell process, which uses a mixture of ethanol – water, or CIMV process, which uses a mixture of acetic acid – formic acid – water. Organosolv lignin is isolated easily by solvent removal or precipitation with water. This mean of extraction makes it possible to obtain a less modified lignins at a higher

purity. The average molecular weight is less than 1000, making it the lignin with the lower MW, and it is insoluble in water, though some organosolv lignins could be soluble in alkali conditions and may contain phosphorous groups [6, 20, 21].

Steam explosion process: In this process, lignin is treated for a short time, from 1 to 20 minutes, with steam at high temperature and pressure. Temperature ranges from 180 to 230 °C, while pressures can be between 200 to 500 psi. Then, the pressure is released rapidly, hence the name "steam explosion". Lignin can be recovered from the resulting product, by alkali washing or solvent extraction and its molecular weight is lower than kraft lignin, while its solubility in alkali is higher. Some modifications of product stream include a reduction of β-O-4' linkages and increase of C-C bonds, resulting in a more condensed lignin [20, 22].

Processes resulting in native lignin: processes such as cellulolytic treatment or milling, consisting in an enzymatic degradation and wood grounded in a ball mill, respectively, followed by a solvent extraction; have been reported to give similar lignin products. These techniques are carried out normally at room temperature and pressure. The resulting lignins show a relatively high number of β-O-4' linkages and are structurally identical from each other, showing some carbohydrates residues. The final product resembles the previously described native lignin, also called protolignin [23, 24].

Other processes, e.g. pyrolysis, ionic liquid extraction or acidic hydrolysis, are not discussed, as their utilization is restricted, or not well developed [21].

The field that seeks for a better understanding of lignin properties is called lignin characterization; and comprises diverse analysis and laboratory techniques. Powerful imaging, spectroscopy, functional and chemical characterization methods have been developed with this purpose. The characteristics that have been studied include elemental analysis and empirical formula, determination of molecular weight, analysis of functional groups and frequencies of linkage types and functional groups in lignin. In addition, chemical and biochemical characterization and modification of lignin, including biodegradability and enzyme-based oxidation, have also been studied. The appropriate techniques to conduct this type of research varies, depending on the characteristic under study. For instance, gel permeation chromatography, light scattering, vapor-pressure osmometry and ultrafiltration can be used to determine the lignin molecular weight [3, 25]. Considering that no single method could stand alone as the supreme method for lignin characterization, techniques involving nuclear magnetic resonance (NMR), specially ^{13}C NMR, which provides structural and functional information with high sensitivity and precision; imaging; mass spectrometry;

and vibrational spectroscopy; have proven to be very valuable for lignin characterization [25].

1.4 The potential of lignin as a renewable feedstock

The depletion of fossil fuels and its involvement in environmental problems, e.g. greenhouse emissions, have led to a great public, scientific and governmental interest to find new renewable raw materials for production of energy, materials and chemicals. Fossil fuels reserves are limited and will be exhausted in the near future, though no exact date can be predicted for this event, it is thought that fossil fuel peak production will occur in 2025. Biomass represents one of the most attractive alternative for renewable energy production, and while it can generate greenhouse emissions, the resulting environmental impact would be significantly lower, since biomass needs CO_2 for growth, therefore, the use of biomass for production of fuels and chemicals would be carbon neutral. Currently, energy production form biomass represents the most important source of renewable energy, surpassing the total input from hydro, solar, wind and geothermal energy, combined [9, 26].

On the other hand, many valuable chemicals are fossil fuel-derived, therefore it is essential to find new raw materials to produce these chemicals in a sustainable way. While there are some other renewable sources for energy production, including wind or solar energy, the only renewable organic carbon resource in nature is biomass, making it the lone option available for value-added chemicals production in the long term [27]. Biomass can also be used to produce building blocks for the fabrication of new materials, including carbon fiber which could, in principle, be synthesised from lignin as a precursor [13]. The feasibility of obtention of fuels and chemicals from biomass has led to the emergence of biorefinery, defined as “the sustainable processing of biomass into a spectrum of marketable products and energy” [28]. This concept includes a wide range of technologies used to separate biomass resources into their building blocks, such as carbohydrates, proteins and triglycerides; which can be further converted into value added products, biofuels and chemicals [29].

The most abundant form of biomass is lignocellulose, which accounts for about 170 billion metric tons per year [30]; and unlike other sources of biomass, e.g. corn or starch, it is not edible, therefore it is not involved in the so-called "food vs. fuel" dispute, as it does not compete, in theory, for land, water, or other resources, with crops that should be primarily intended for supply of food. Lignocellulose comprises three different types of biopolymers, cellulose, hemicellulose and lignin, the latter constitutes from 10 to 35 % of the

total dry weight of lignocellulose, making it the second most abundant biopolymer on earth, only behind cellulose [9, 13]. Lignin availability is expected to increase in the future due to the development of the biorefinery aimed to replace fossil carbon sources for biofuel production. It has been estimated that about 225 million tons of lignin could be derived from lignocellulose material used to produce biofuels [31].

Lignin is different form the other two polymers found in biomass. On one hand, cellulose and hemicellulose composition is based in 5 or 6 carbon sugars, forming regular structures, which make them more prone to degradation than lignin, allowing their utilization in fuel and chemicals production [32-34]. On the other hand, the broad variability of linkages, the phenolic nature, the different functionalization and the intricate structure of lignin makes it a very recalcitrant material [35]. For this reason, despite its high carbon content and potential as a renewable feedstock, currently lignin represents only a waste stream in most pulping and biorefinery processes, whose main utility is restricted to provide energy and heat by direct combustion. A small fraction of lignin is used commercially as a fuel or concrete additive [36].

Finding an effective way to exploit lignin would greatly improve bio-based processes, for several reasons. Firstly, since lignin represents up to 35 % of total lignocellulose dry weight and up to 40% by energy, due to its high carbon / oxygen ratio [37], when lignin is available as feedstock, cost of production will be substantially reduced, improving the economic viability of the biorefinery [27]. Secondly, there is no other renewable source of aromatic compounds that can match lignin, due to its phenolic nature, so its depolymerization could yield a family of high-value phenolic chemicals such as cresols, catechols, quinones, guaiacols or vanillin, which are difficult to obtain form the classical petrochemical industry, making it the most promising material for aromatic chemicals production [3, 27]. Thirdly, in current processes employing biomass and lignocellulose as feedstock, lignin represents a major obstacle as it protects, to some extent, cellulose and hemicellulose from chemical and biochemical degradation, lowering the yields of released sugar and decreasing the overall efficiency of transformations, hence lignin degradation will allow an important improvement of these procedures. And fourthly, lignin waste streams represent a huge environmental problem for the pulping industry, as it produces approximately 7 tonnes of black liquor containing lignin per tonne of pulp. Lignin degradation and valorisation will solve this important environmental issue [27].

Although lignin can offer some interesting applications as a polymer, the cleavage of lignin into oligomers or aromatic monomers is the most important road to its sustainable

utilization. There is an active field of research focused on lignin valorisation, including chemical (acid/base catalysed depolymerization), physical (pyrolysis), biochemical (enzymatic oxidation), and mixed strategies; whose final goal is to find a cost-effective way for lignin depolymerization and degradation [9, 13, 27, 38].

1.5 Lignin biodegradation

Several strategies have been proposed for lignin degradation, mainly based on thermochemical treatments involving high temperatures and extreme pH conditions. These methods require a high energy input and generate an important environmental impact, while giving relatively low yields and low purity of products due to undesirable by-product formation. The huge interest in lignin valorisation has driven several fields of research to find and develop new methods for breaking-down lignin, among them, biological degradation has been proposed as an efficient alternative, since these transformations take place under mild conditions, present high specificity and are usually environmentally friendly [39, 40].

In nature, lignocellulose can be degraded by a range of organisms, including bacteria, brown-rot and white-rot fungi, oomycetes, shipworms, termites and lignocellulose-consuming animals through mutualism with gut microflora [40]. A narrower range of organisms can achieve lignin degradation. White-rot fungi are the only organisms able to breakdown lignin on their own. Brown-rot fungi can efficiently degrade lignocellulose, but they are able only to modify lignin. It has been reported that some soil bacteria could play a role in lignin degradation or modification, especially members of the phylum actinobacteria, α-Proteobacteria or γ-Proteobacteria, which have also been reported in termite guts and wood-boring insects, though they may need a microbial consortium to accomplish this goal efficiently [40-45].

1.5.1 Fungal lignin degradation

There are four main groups of enzymes involved in fungal lignin degradation: laccases (EC 1.10.3.2), lignin peroxidases (EC 1.11.1.14) (LiP), manganese peroxidases (EC 1.11.1.13) (MnP) and versatile peroxidases (EC 1.11.1.16) (VP) [44, 46]. Laccases had been described since 1883 in plants [47], and more recently in fungi and insects, where they had been related with diverse functions including pigment synthesis, fruit-body morphogenesis, and detoxification [48]. Laccases were reported to be produced as a unique characteristic of white-rot fungi in solid media, and their involvement in lignin degradation was not clear, as these enzymes showed a low redox potential activity, implying that these enzymes would be

able to oxidize only lignin phenolic units, which usually represents only about 10 %, of the total lignin units. However, the interest in laccases for biotechnology applications and their role in lignin biodegradation was reconsidered when it was discovered that laccases can oxidize high redox potential compounds in presence of mediators, which are small molecules that can change their redox state and serve as electron shuttle between the enzyme and the substrate. Natural mediators involved in lignin degradation remain to be fully characterized, though some synthetic and natural mediators have proven to be efficient [49, 50]. Laccases and their role in lignin degradation will be discussed in more detail in sections: 1.6, Laccases: properties and structure; 1.7, Role of laccase in lignin degradation; and 1.8, Finding laccase-like multicopper oxidases in bacterial lignin degraders.

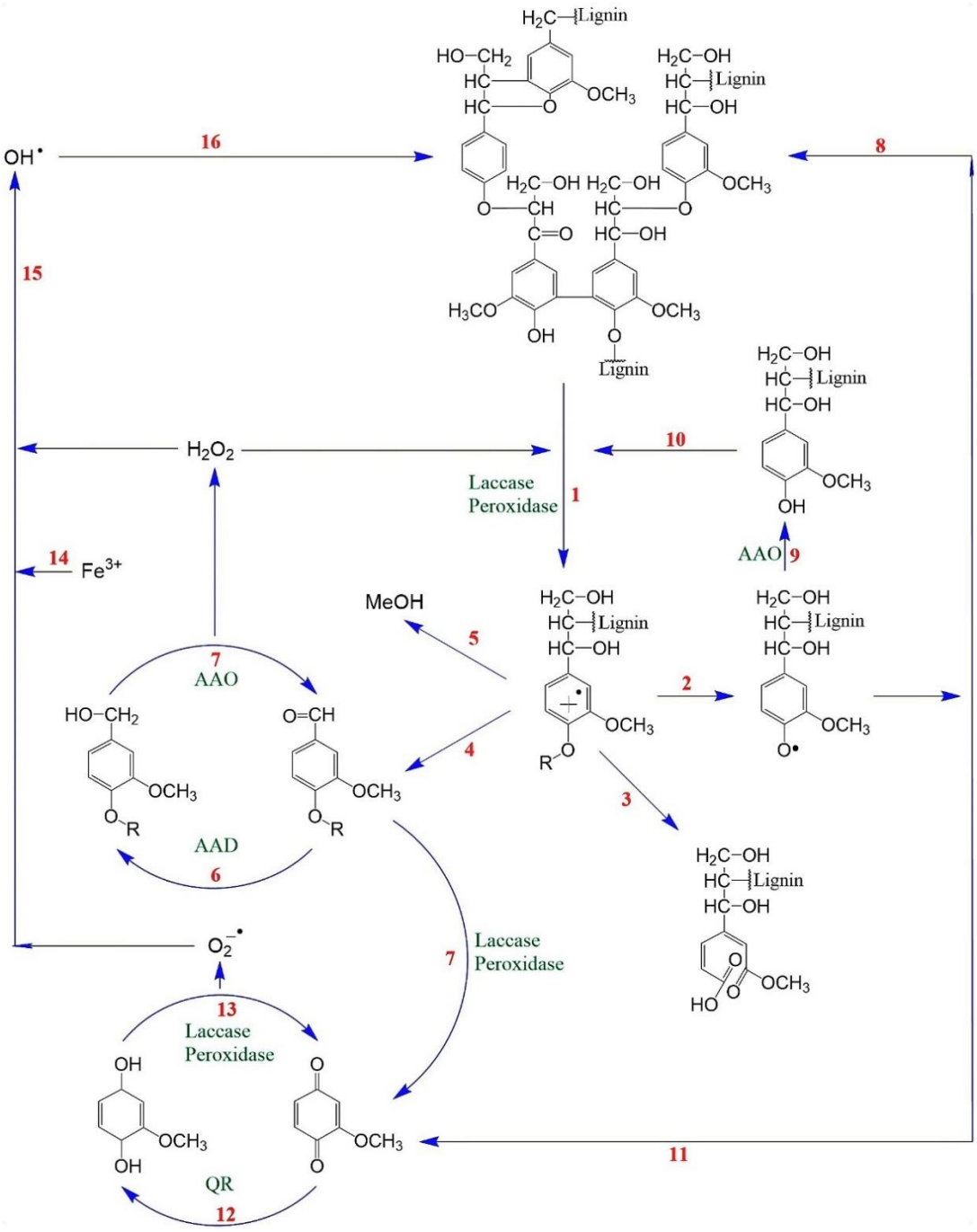

Figure 4. Scheme for fungal lignin biodegradation. (1) Ligninolytic enzymes oxidize the polymer generating aromatic radicals, which follow different non-enzymatic paths: (2) C4-ether breakdown, (3) aromatic ring cleavage, (4) Cα-Cβ breakdown, and (5) demethoxylation. Aromatic aldehydes from (4) or (6, 7) serve as substrate for H_2O_2 generation. Phenoxy radicals from (2) can undergo to a repolymerization (8) if they are not first reduced by oxidases to phenolic compounds (9). The phenolic compounds formed can be re-oxidized by laccases or peroxidases (10). Phenoxy radicals can also be subjected to Cα-Cβ breakdown (11), yielding p-quinones. Quinones from (7) or (11) contribute to oxygen activation in redox cycling reactions involving quinone reductase (QR), laccases, and peroxidases (12, 13). This results in reduction of the ferric iron present in wood (14), and its re-oxidation with the concomitant reduction of H_2O_2 to hydroxyl radical (OH·) (15), which is a very strong oxidizer that can initiate the attack on lignin (16) in the initial stages of wood decay. Adapted from [46].

LiP and MnP were described in the mid-1980s and were identified as lignin degrading enzymes due to their high redox potential. LiP can degrade non-phenolic units in lignin, while MnP can generate Mn^{3+}, a diffusible oxidizer which might play a role in early stage of lignin degradation, when cell wall is still compact, and enzymes cannot reach the substrate. The diffusivity of Mn^{3+} makes it able to oxidize secondary substrates at a distance, away from the active site of MnP. VP have been described as a third type of ligninolytic peroxidase that shown similar catalytic properties as LiP, MnP and plant/microbial peroxidases, oxidizing phenolic compounds [46, 51]. The characterization of accessory enzymes needed for lignin break-down, such as enzymes that can generate H_2O_2, an essential peroxidase co-substrate, is yet to be completed, though some enzymes have been proposed in this group, including aryl-alcohol oxidases (AAO), glyoxal oxidase, aryl-alcohol dehydrogenase (AAD), and quinone reductase (QR) [46, 52-55]. Recent studies have allowed the identification of new ligninolytic enzymes, including peroxidases with an intermediate catalytic behaviour between classic LiP and VP, and DyP and heme-thiolate superfamily peroxidases, which are under study and present interesting biotechnological applications [41, 56, 57]. **Figure 4** shows a summary with a proposed scheme for fungal lignin degradation [46]. Interestingly, it seems that the same type of enzymes involved in lignin biosynthesis in plants, laccases and peroxidases, are used by fungi with the opposite purpose, the depolymerization of lignin.

1.5.2 Bacterial lignin degradation

Fungal lignin degradation has been well studied since the 1980s, while the study of bacterial lignin degradation had been relegated, becoming an interesting field of research only in the recent years due to the identification of several organisms with lignin-degrading capabilities [58]. *Streptomyces viridosporus* T7A has been proved to produce an extracellular peroxidase enzyme to depolymerise lignin [59]; *Rhodococcus jostii* RHA1and *Pseudomonas putida* mt-2 showed lignin-degrading activity in absence of hydrogen peroxide, suggesting the presence of oxygen dependant enzymes, such as laccases, or the presence of extracellular enzymes able to generate hydrogen peroxide to trigger the activity of lignin peroxidases [60]. Lignin degradation activity has also been detected for *Microbacterium phyllosphaerae*, *Ochrobactrum sp*., *Rhodococcus erythropolis*, and *Sphingobacterium* [61]. DyP type peroxidases, lignin-modifying bacterial laccases, glutathione-dependent β-etherases, superoxide dismutases, catalase-peroxidases and bacterial dioxygenases have been identified as groups of enzymes involved in bacterial lignin degradation [42].

Homologues for fungal peroxidases enzymes LiP, MnP or VP have not been found either in biochemical studies, or in bacterial proteomes or genomes, suggesting that fungi and bacteria may tackle lignin depolymerization in a different way [62, 63].

DyP type peroxidases (EC 1.11.1.19) are abundant in bacterial lignin degraders and they are structurally unrelated with fungal peroxidases. These enzymes have been identified in *Thermobifida fusca* YX*, Rhodococcus jostii* RHA1, *Streptomyces viridosporus* T7A, *Streptomyces coelicolor* A3, *Amycolatopsis sp.* 75iv2, *Pseudomonas fluorescens* Pf-5, *Pseudomonas putida* A514, among others [42, 64-66]. These heme-containing peroxidases show a molecular weight ranging from 40 to 60 kDa, they require hydrogen peroxide as electron acceptor to catalyse the substrate oxidation, and their biological function is unknow, though they have been reported as ubiquitous proteins found in prokaryote and eukaryote cells [67]. Bacterial DyPs consists in a dimeric ferredoxin-like fold (four-stranded antiparallel β-sheet surrounded by α-helices) and the conserved motif GXXDG with a proximal histidine, which is involved in heme iron attachment. Even so, in the catalytic context, DyPs show a similar behaviour than fungal peroxidases, as these enzymes are active with a wide range of high redox potential substrates, such as synthetic dyes, monophenolic compounds, and lignin related compounds, including veratryl alcohol and the lignin model compounds guaiacylglycerol-β-guaiacol ether and veratrylglycerol-β-guaiacol. In addition, some DyPs seem to be extracellular proteins exported by the TAT (twin-arginine translocation) protein translocation system [42, 68]. Based on their sequence, DyPs have been divided into four classes: A, B, C and D. The latter belongs to fungal DyPs, while classes A to C are mainly found in bacteria. DyPs of the class A usually include a TAT signal on their sequences, hence they are thought to be extracellular proteins; while classes B and C seem to be intracellular proteins. However, it has been reported some DyP class B enzymes with activity for lignin-related compounds, suggesting that these class of DyPs could be extracellular, though secreted by a different translocation system, potentially through encapsulation [65, 67, 69-71].

Glutathione-dependent β-etherases have shown activity breaking β-ether bonds of lignin related compounds, and their role in lignin degradation might be at the level of small lignin oligomer degradation, as these proteins need NAD^+ as co-substrate, an intracellular metabolite, implying that these proteins would be located inside the cell. In *Sphingobium sp*.SYK-6, this system comprises three different proteins; Lig D (Cα-dehydrogenase), Lig F (a β-etherase) and Lig G (glutathione lyase), and they can cleave the β-aryl ethers of model lignin compounds. Lig D causes the oxidation of the α carbon, by using NAD^+ as co-substrate;

then Lig F attaches glutathione at the β carbon position, causing the cleavage of the molecule, and finally Lig G oxidizes the glutathione and releases the final product (**Figure 5**). There are two other glutathione reductases named Lig E and Lig P, whose catalytic activity is similar than Lig F, but they show enantioselectivity, catalysing the opposite enantiomer of the carbonyl compound formed by the reaction of the substrate with Lig D [42, 72, 73]. Another enzyme, the manganese dependent superoxide dismutase (Mn-SODs) from *Sphingobacterium* sp. T2, have also revealed lignin modification activity [74]. Ms-SOD2 common function is related with oxidative stress protection, by deprotonation of the anion superoxide into molecular oxygen and hydrogen peroxide. Two enzymes, Mn-SOD 1 and 2, from *Sphingobacterium sp*. T2, showed activity towards lignin model compounds, organosolv and kraft lignin, giving products released from aryl-Cα and Cα-Cβ cleavage and O-demethylation reactions [42, 74].

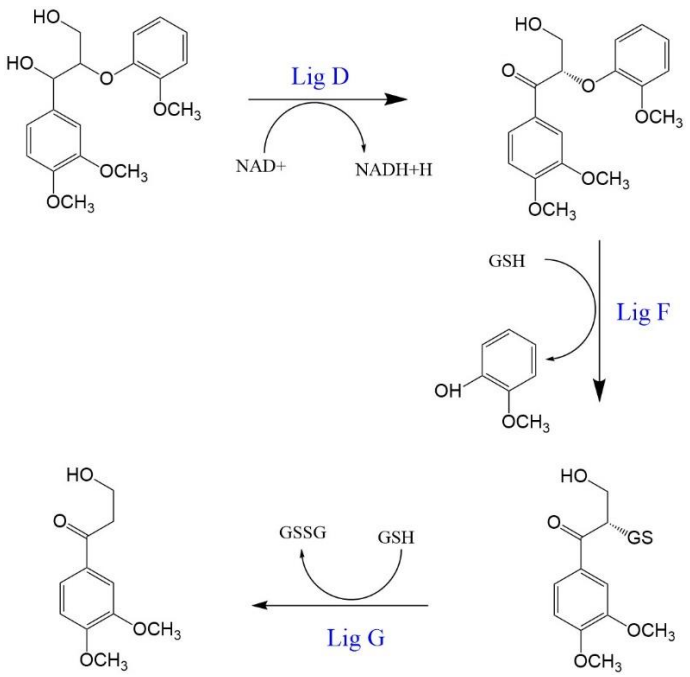

Figure 5. Lignin-related compound (guaiacylglycerol-β-guaiacyl) degradation by glutathione-dependent β-etherases Lig D, F and G. Lig D catalyse the oxidation at the α carbon position, the Lig F facilitate the addition of glutathione at the β carbon, and finally Lig G catalyse the oxidation of glutathione. Adapted from [42].

Other bacterial enzymes involved in lignin degradation include the catalase-peroxidases, dioxygenases and the very important group of laccases [42]. Nowadays, there is a great interest in laccases for their potential applications in research and industry, due to their catalytic properties, being named as perfect green catalysts [75]. For these reasons, laccases will be discussed in more detail in the following sections.

1.6 Laccases: properties and structure

Laccases (EC 1.10.3.2) are the most important and largest subgroup of the superfamily of proteins called multicopper oxidases (MCOs), which also include the subgroups: ascorbate oxidase (EC 1.10.3.3), ferroxidase (EC 1.16.3.1) nitrite reductase (EC 1.7.2.1) and ceruloplasmin (EC 1.16.3.1). Laccases were first discovered in the sap of the Japanese lacquer (hence its name) tree *Rhus vernicifera*, and they are widespread in nature, having been identified in higher plants, insects, lichens, oysters, fungi, metagenomic libraries of bovine rumen, and recently they have been reported in bacteria [48, 76-79]. Yet, fungal laccases are the type of laccases most widely studied by far. The biological function of laccases varies; in fungi these enzymes have been reported in almost all wood degraders, where they have been related with morphogenesis, pathogen-host interaction, stress defence, and lignin degradation; while in plants, laccases seem to be involved in lignin biosynthesis; in bacteria, laccases appear to be involved in morphogenesis, pigmentation, oxidative protection and copper homeostasis; and in insects, they play a role in sclerotization of the cuticle [79-81].

Laccases use the redox ability of copper ions to catalyse the oxidation of a wide range of substrates, by coupling this reaction with the reduction of molecular oxygen into water. There are more than 200 types of oxidases and oxygenases, but only six of them can perform this kind of reaction: laccases, bilirubin oxidases, ceruloplasmin, phenoxazinone synthase, cytochrome-c oxidase and L-ascorbate oxidase [81]. Laccases comprises normally three domains, although two-domain laccases have also been reported; and they contain four copper ions named as type 1 copper (T1), type 2 copper (T2), and a binuclear type 3 copper (T3). The T1 copper is located in domain 3, while the other three ions of copper are located in the interface between the domain 1 and 3 (**Figure 6**) [81-83].

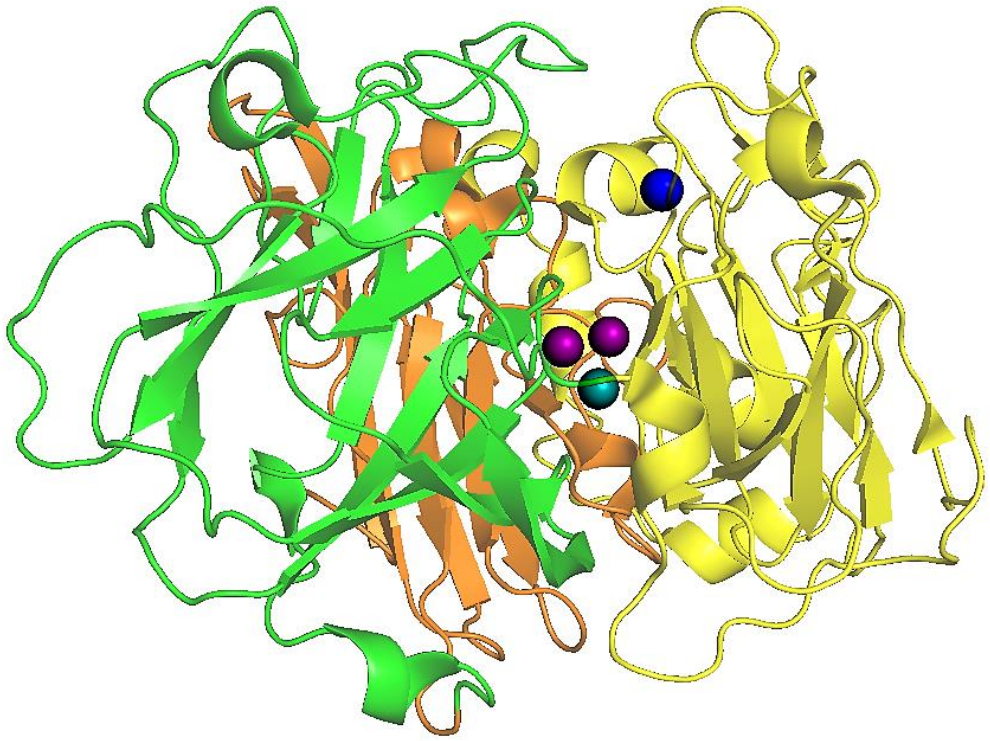

Figure 6. Laccase typical structure consisting of three domains and four ions of copper. Domain 1, 2 and 3 are coloured in orange, green and yellow, respectively; while copper ions type 1, 2 and 3 are represented as blue, teal, and purple spheres, respectively. Graphic generated by the software PyMOL, using *Trametes versicolor* laccase (TvL), PDB code 1GYC.

The copper ions classification into different types relates to distinct spectral properties and differences in the surrounding amino acids. The type 1 copper, in an oxidized state, show an intense absorbance at ≈610 nm due to a S(Cys)π →Cu(II) charge transfer transition, because of covalent nature of the Cu-S(Cys) bond and is responsible for conferring a characteristic blue colour to these proteins. In laccases, this copper ion shows a planar triangular coordination sphere with a cysteine (sulphur atom) and two histidines (Nδ1 nitrogen); while in most MCOs there is fourth ligand involved in T1 copper attachment, a methionine (sulphur atom), resulting in a tetrahedral geometry, being this bond longer and weaker than the other three ligand bonds. In laccases, this methionine residue is replaced by a hydrophobic phenylalanine or leucine, both unable to make a bond with T1 copper [84]. T2 and T3 copper ions are arranged in a trinuclear cluster (TNC), at about 13 Å from the T1 copper. The TNC is coordinated by a total of eight histidine residues, each T3 copper is coordinated by three histidine residues; while the T2 copper is coordinated by two histidine residues and one external hydroxo ligand forming a square planar geometry. When oxidized, T3 copper forms a bridge ligand with μ2-OH, giving a trigonal bipyramidal geometry. The T1 copper centre and the TNC are connected by a His-Cys-His conserved sequence, which

enables electron flow. The two histidine residues are ligands of the T3 copper, while the cysteine residue is a ligand of the T1 copper (**Figure 7**) [81, 84].

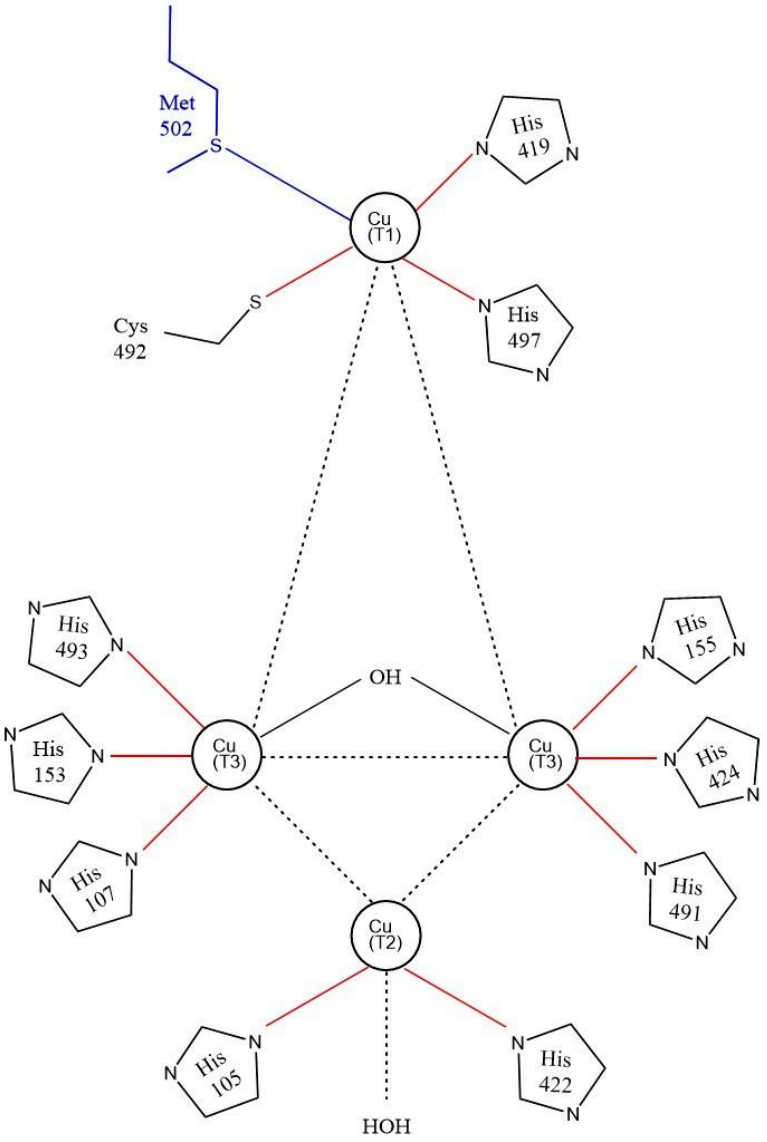

Figure 7. Schematic representation of copper ions arrangement and ligating-residues in the bacterial laccase CotA, from *Bacillus subtilis*. The axial ligand methionine (Met502) is coloured in blue. Adapted from [85].

The copper ions play a pivotal role in the substrate oxidation, performing a four-electron reduction of dioxygen into water. At the mononuclear copper centre T1, which is near the surface of the protein and it is located at the laccase active site, the substrate is oxidised by transferring one electron to the T1 copper, then the electrons are passed to the TNC by the His-Cys-His electron path, where reduction of oxygen into water takes place (**Figure 8**).

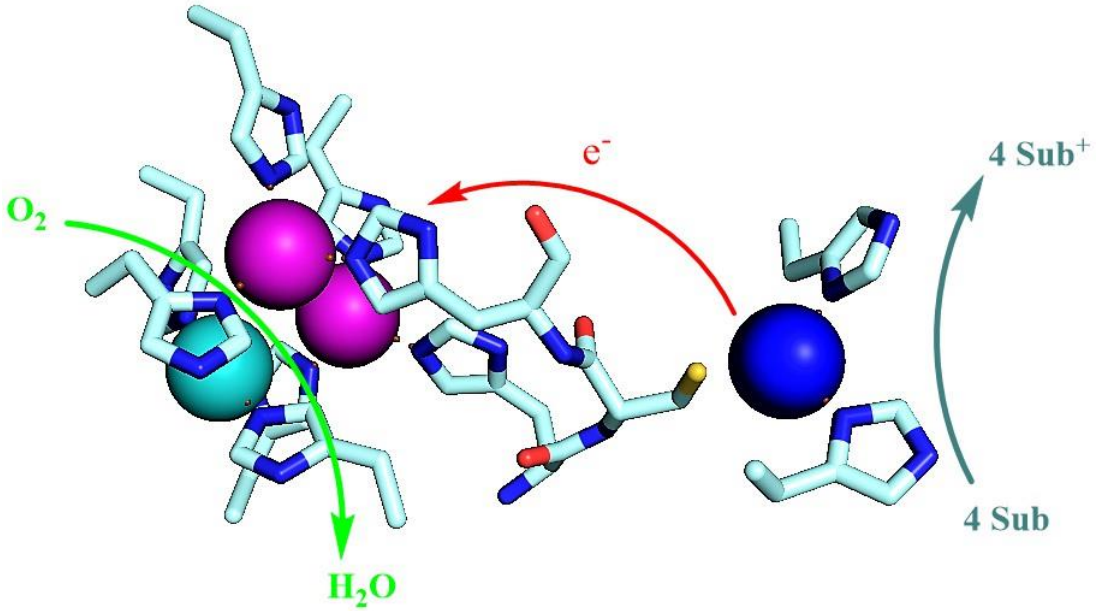

Figure 8. Substrate oxidation, electron flow and oxygen reduction in laccases. Copper ions type 1, 2 and 3 are represented as blue, teal, and purple spheres, respectively. Graphic generated by the software PyMOL, using *Trametes versicolor* laccase (TvL), PDB code 1GYC. Adapted from [86].

Electron transfer (ET) between the T1 copper and the substrate can be described by the Marcus theory [87], which provides the ET rate constant, k_{ET}, as a function of several factors, being the most influential in an intermolecular ET, the reorganization energy (energy required for rearrangement of ligand and solvent, before and after an ET occurs), λ; and the electronic driving force, ΔG°. It has been reported that λ is minimal for laccases, meaning that there are minor changes in the T1 copper between its reduced and oxidized state [88, 89]. The driving force, represented by the free energy difference, ΔG°, derives from the reduction potentials of T1 copper site, E°, which ranges in laccases from about 370 to 800 mV versus normal hydrogen electrode. This characteristic has been used as a measurement of the catalytic power of laccases, resulting in three different groups, high (720 to 800 mV), medium (470 to 710 mV) and low (370 to 460 mV) redox potential laccases [84, 90]. It is not clear which factors can affect the redox potential of the T1 copper in laccases, though hydrophobicity of neighbouring residues, hydrogen bonding to the sulphur atom of cysteine, and electrostatic interactions in the protein backbone have been suggested. Many approaches have been evaluated in order to increase the catalytic power of the T1 copper, and some studies have demonstrated that the presence of the methionine as a fourth axial ligand, common in bacterial laccases, can decrease the T1 copper redox potential. For instance, when the axial ligand Met502 of the bacterial laccase CotA, from *Bacillus subtilis*,

was changed into the non-ligating Phe (M502F) or Leu (M502L), the redox potentials of these mutants increased from 455 mV, to 548 and 515 mV, respectively. Conversely, when the fungal laccase from *Trametes villosa* laccase (TviL) was engineered to replace its native non-ligating F463 for a methionine, its redox potential decreased from 790 to 680 mV. Nevertheless, it should be noted that different redox potential values have been determined for several laccases, even with the same ligand structure [84, 91, 92]. In addition, interactions between the substrate and the protein active site can also affect the ET rate constant. A one-electron Cu(II)/Cu(I) pair is used for substrate oxidation in T1, through an outer sphere electron transfer, while an inner sphere electron transfer is used in the TNC for reduction of dioxygen. Because of the outer-sphere mechanism reaction in T1, the substrate specificity is defined by the nature of the substrate docking/oxidation site coupled with T1, which means that some of these proteins can catalyse a broad range of substrates. Some studies have concluded that the outer-sphere ET from the substrate to the T1 copper is the rate-limiting step in laccase turnover [84, 86, 93]. The oxygen reduction in the TNC begins with the enzyme in a fully reduced state, followed by a $2e^-$ step to reduce oxygen into water, generating an intermediate enzyme in a fully oxidized state. Then, the enzyme is regenerated to its reduced state in the catalytic cycle, instead of an enzyme returning to its resting oxidize state. The exact mechanism by which the oxygen is reduced in the TNC is unknown but is evident that a fully reduced TNC is required for this reaction, and four electrons are needed for this purpose. The order by which copper are reduced might vary depending on enzyme conditions [84].

Fungal laccases are normally extracellular and monomeric proteins, with a molecular weight ranging from 60 to 70 kDa, showing an acidic isoelectric point and normally glycosylated, with different degrees of glycosylation from 22% to 45% [94, 95]. The definition of a laccase is challenging and controversial, and there is no general consensus about the distinguished characteristics that could identify an enzyme as a "true laccase" [48, 96, 97]. Among MCOs, the homology of sequences is low; even so the copper binding motifs are very well conserved. The amino acids involved in copper binding comprise two histidine residues and one cysteine residue forming a metallo-organic bond for the T1 copper; two histidine residues for the T2 copper and six histidine residues for the T3 copper. The copper ligands are arranged in the four highly conserved motifs, HXHG, HXH, HXXHXH and HCHXXXHXXXXM/L/F [96]. A definition for laccases based on the type of reaction, sequence homology or specificity may be insufficient; due to the low sequence homology showed among MCOs and the broad range of substrates that these enzymes can accept. For instance,

a reported bilirubin oxidase (a MCO protein different from laccases), showed a 98% sequence identity with a reported CotA-type laccase [98, 99]. Regarding substrate specificity, although syringaldazine has been reported as a substrate unique for laccases, coinciding oxidation activity has been also reported with bilirubin oxidase, pholyphenol oxidase and tyrosinase [96, 98, 100, 101]. This uncertainty has led to the apparition of a singular terminology for laccases and terms as true laccase, pseudo-laccase, laccase-like multicopper oxidase (LMCO), white laccase, and yellow laccase; have been used to name several enzymes showing characteristics related with laccases (**Table 1**) [96, 102-104]. Among them, the term laccase-like multicopper oxidase (LMCO) seems to be well accepted, as it has allowed less ambiguity while taking into account the potential diversity of these interesting proteins at the same time [16, 96, 105, 106].

Table 1. Classification of laccases based on different criteria.

Laccase type	Classification criteria	Characteristics	References
Blue laccase	Spectroscopy	Blue in solution, peak at ≈600 nm in a UV-Vis spectrum	[75, 107]
Yellow laccase	Spectroscopy	Yellow or yellow-brown in solution, no peaks in a UV-Vis spectrum	[103, 108]
White laccase	Spectroscopy	Colourless in solution, no peaks in a UV-Vis spectrum	[104, 109]
True laccase	Activity	No need for addition of exogenous copper ions for activity, commonly are fungal laccases	[110]
Pseudolaccase	Activity	Need for addition of exogenous copper ions for activity, commonly are bacterial laccases	[102, 111, 112]
Laccase-like MCO	Host organism	May or may not need addition of exogenous copper ions for activity, commonly are bacterial or plant laccases	[16, 96, 106, 113]
Laccase *sensu stricto*	Host organism	Do not need addition of exogenous copper ions for activity, commonly are fungal laccases	[105, 114]

1.7 Role of laccase in lignin degradation

The ability of laccases to attack, degrade and modify lignin have been reported and documented by several studies [39, 115, 116]. Evidence for lignin degradation by laccases is based mainly on fungal degradation of lignin. Most of the white-rot fungi secrete laccases when grown on lignin; while brown-rot fungi, which are unable to grow on lignin, do not secrete laccases extracellularly [116]. Laccase involvement in lignin degradation is also

supported by the ability of some of these enzymes to split both β-1' and β-O-4' lignin model compounds, by cleaving the Cα-Cβ bond or oxidizing the Cα, which leads to a cleavage of alkyl-aryl parts; the capacity of laccases to cleave aromatic rings; also their oxidizing activity for non-phenolic units in presence of a mediator; and their ability to generate Mn^{3+}, which can penetrate the cell walls of wood and trigger initial oxidations [116].

However, the role of laccases in lignin degradation has been questioned, due to apparently contradictory observations. On the one hand, the low redox potential of laccases make them unable to oxidize non-phenolic units, which correspond with the vast majority of units found in lignin, up to 80 %; and the existence of well-known lignin degraders which are unable to express laccases, such as *Phanerochaete chrysosporium*; or observations such as those for *Coriolus versicolor*, showing the ability to degrade milled wood lignin despite that its laccase had been inhibited by specific antibodies [6, 117]. On the other hand, there are also experimental evidence that support laccase involvement in lignin degradation. For instance, a comparison between a laccase-less mutant and a laccase-positive revertant mutant of *Sporotrichum pulverulentum* showed that, while the laccase-less mutant was unable to degrade wood or kraft lignin, the laccase-positive mutant recovered this ability, similar to the wild type strain. Additionally, the laccase-less mutant decreased its yield of xylanases and cellulases in presence of lignin, while the addition of external purified laccase enabled the normal production of endo-1,4-β-glucanase in presence of vanillic acid and kraft lignin, and also allowed the degradation of kraft lignin by this mutant [118]. There are many other studies providing more evidence supporting the capacity of laccase for lignin degradation, including but not limited to, observations on *Coriolus versicolor* laccase with activity towards phenolic lignin model compounds [115, 119], observations of increased laccase production in *Pleurotus ostreatus* upon induction with the lignin precursor, ferulic acid [120], evidence that show laccase oxidation of lignin under formation of phenoxy radicals [121], fungal genome analysis that revealed the existence of multigenetic families of MCOs, suggesting that one of them can play a role in lignin degradation [105], experiments on *Pycnoporus cinnabarinus*, a model organism for laccases role in lignin degradation since it does not secrete neither LiP nor MnP, that showed a greatly reduced ability to degrade DHP (dehydrogenative polymer) for a laccase-less mutant, while proving a recovered ability for DHP degradation when exogenous laccase was supplemented to the media [122], evidence for laccase involvement in plastic and lignocellulose degradation and phenolic detoxification [123], among others.

Despite the studies suggesting an important role of laccases in lignin degradation, so far there is no commercially available process for lignin depolymerization based on these enzymes. There are issues that have limited their utilization, including the inherent chemical complexity of lignin as substrate, which has meant that many of the results shown for laccase activity on lignin have been obtained from different treated lignins, lignin derivatives or model compounds, with different chemical properties. In addition, while the sequence homology for MCOs is low, fungal laccases tend to show a high sequence homology, however it is not clear why these enzymes show significative differences regarding their catalytic activity for lignin oxidation and redox potential [110]. Finally, there is some level of uncertainty introduced by the lack of standard methods for lignin quantification, and often it is not clear whether lignin is indeed being degraded, modified, depolymerized or polymerized. The current terminology for lignin transformations could also lead to some confusion, since terms such as "degradation", “delignification” or "depolymerization" are used indiscriminately and as synonyms, while they are different concepts and in some cases there is no real evidence that those processes indeed occurred [6]. It has been suggested that the main function of laccases is the generation of a reactive radical of lignin, by delocalizing one electron. Then, this radical could follow different paths, depending on the environmental conditions, compounds concentrations and accessory enzymes or substrates present in the reaction, which is yet to be fully understood. The transformation that can occur upon laccases activity on lignin could be broadly divided into: bond cleavage, lignin modification or polymerization [6, 124-126]. The different ways in which laccases could affect lignin are shown in **Figure 9**.

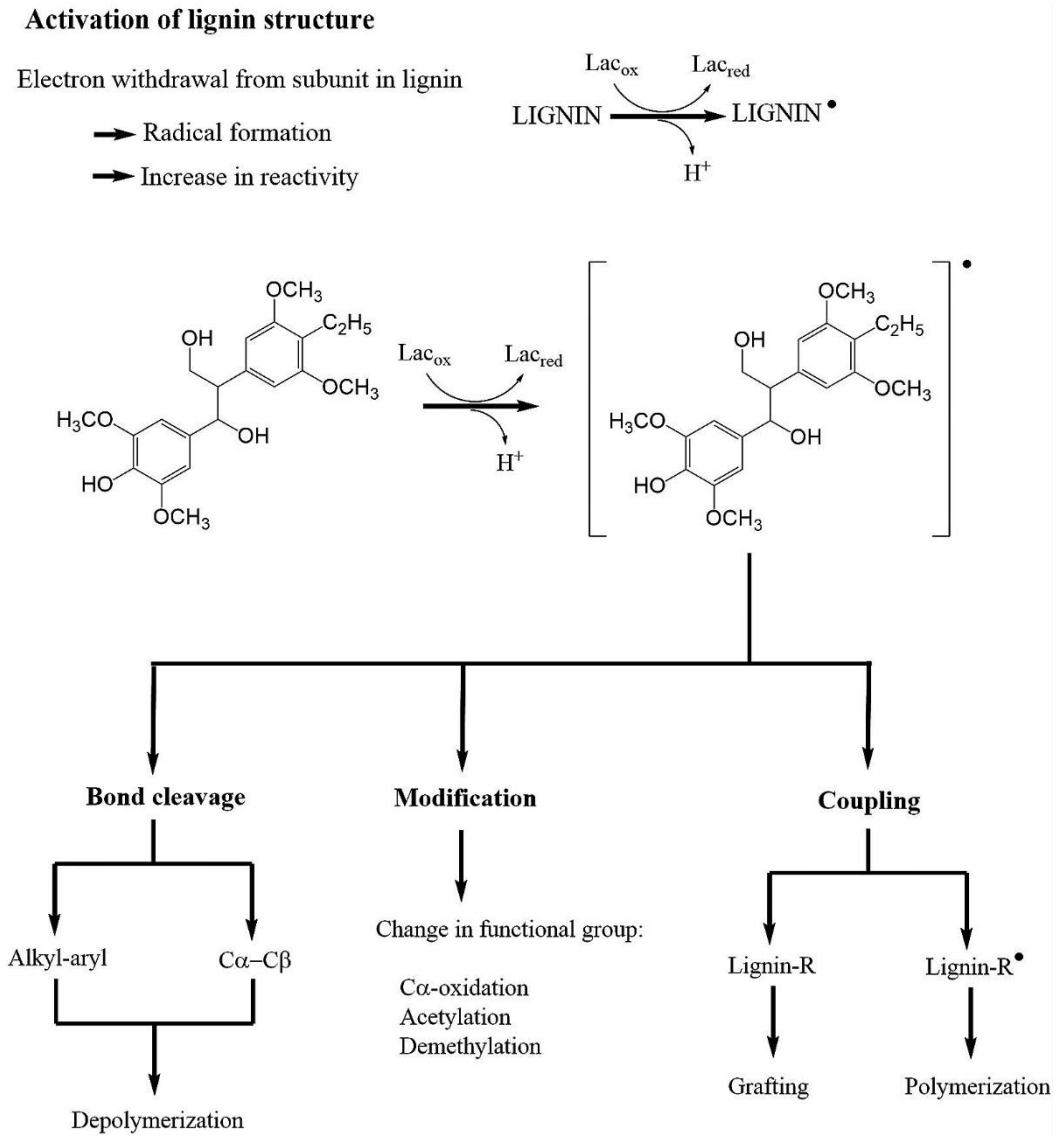

Figure 9. Schematic representation of possible changes on lignin by laccase activity. A phenolic model dimer is used as illustration. Adapted from [6].

A very important discovery showed that the redox potential of laccases can be modulated by molecules called mediators, which are small molecules that can change their redox state and serve as electron shuttle between the substrate and the enzyme active site. The first report about laccase-mediator systems (LMS) showed that *Trametes versicolor* laccase (TvL) was able to oxidize non-phenolic units in presence of 2,2'-azinobis(3-ethylbenzthiazoline-6-sulphonate) (ABTS) as mediator. In addition, TvL was able to catalyse the oxidation of the high redox potential substrate, veratryl alcohol, giving α-carbonyl derivatives as products. A β-1' lignin model dimer, was also cleaved by TvL in presence ABTS as mediator [49]. Since then, many other studies have been conducted to evaluate the effect of mediators on lignin depolymerization by laccases, and although some results have shown that the presence of a mediator could improve lignin depolymerization, there are

discrepancies with some results that show no effect or even the inverse reaction, polymerization, occurring in LMS [6, 39, 127-130]. These results could be explained by differences in the type of enzyme, mediator and lignin used for a given experiment. It has been suggested that after laccases have generated a lignin radical by electron withdrawal, competing reactions take place and their balance is affected by the surrounding conditions and the presence of mediators. This hypothesis would explain the inconsistent results about polymerization and depolymerization and it also would suggest that the type of mediator used is an important factor, although it is not yet well understood which and how these conditions could affect the course of LMS reactions on lignin [131-133].

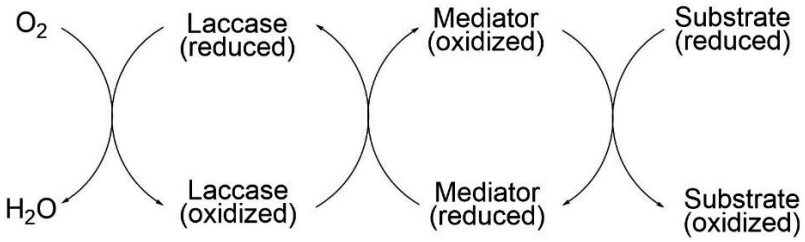

Figure 10. Schematic representation of the proposed mechanism of reaction in laccase mediator systems (LMS).

Therefore, a laccase mediator system becomes a stronger catalyst than laccase alone, by expanding the oxidation ability of the enzyme not only by overcoming the steric hindrance that may exist between the active site of laccases and a substrate with a size bigger than catalytic pocket, but also by providing an oxidized state of the mediator that could be a strong oxidizing intermediate, whose redox potential could exceed those of high redox potential substrates, such as non-phenolic lignin subunits [6, 39, 134]. The mediator is a small molecule that is continuously oxidized by the enzyme and reduced by the substrate (**Figure 10**). Mediators are commonly divided into natural (e.g. 4-hydroxybenzylic alcohol, p-cinnamic acid, sinapic acid) and synthetic (e.g. ABTS, 1-Hydroxybenzotriazole, syringaldazine) compounds and they ideally should be abundant, non-toxic, economic and stable in the oxidized and reduced states to ensure constant recycling, to maintain the cyclic redox enzymatic reaction [39]. Despite the issues discussed above, the capacity of lignin depolymerization by laccase-mediator systems is viewed as a potential “breakthrough” application for lignin valorisation [39].

1.7.1 Laccases: beyond lignin degradation

Laccases use a catalytic mechanism that is essentially different from the other mechanisms used by other groups of lignin-degrading enzymes, which usually need additional cofactors, such as hydrogen peroxide; while laccases require simply oxygen as electron acceptor and generate only water as by-product [6]. Their activity for a broad range of substrates and their capacity for generating a phenoxy radical, with the concomitant wide variety of reactions that can follow this radical formation, depending on the conditions and mediators used, give a huge versatility to laccases and make them suitable for many oxidation reactions. These facts give laccases an enormous potential for industrial application in so many fields, beyond lignin degradation, and would allow more sustainable processes [48]. For instance, a laccase has been used to improve ethanol production by the yeast *Saccharomyces cerevisiae*. Since some phenolic compounds present in lignocellulosic lysates are known to be fermentation inhibitors, the *Trametes versicolor* laccase (TvL) was expressed in this yeast, causing a more rapid consumption of inhibitors by the laccase-producing transformant, showing a benefit for the overall process [135]. Laccases have also been used for the creation of biosensors, for example to distinguish morphine from codeine, also for determination of polyphenol index in wine, and catechols in tea [136-138]. In bioremediation, laccases have been investigated to remove aromatic recalcitrant pollutants and dyes, including phenols, halogenated phenols, aromatic amines, trinitrotoluene, hydroxy-indols, herbicides, polycyclic aromatic hydrocarbons, chlorinated hydroxy biphenyls, bisphenol, pesticides and insecticides [109]. Given the ability of laccase to catalyse coupling reactions, these enzymes also have been used in organic synthesis to produce complex polymers and medical agents, flavonoids, textile dyes, cosmetic pigments, aromatic aldehydes, pesticides, and heterocyclic compounds [139]. In summary, these enzymes have proven to be very valuable for current and future technologies, hence the importance to look for new laccases or to engineer them, which could lead to the discovery of new laccases with novel and interesting functions and properties that can be applied not only in lignin degradation processes, but also in biocatalysis and bioanalytical applications.

1.8 Finding laccase-like multicopper oxidases in bacterial lignin degraders

1.8.1 Fungal versus bacterial Laccases

Commonly, fungal laccases tend to be extracellular proteins showing high catalytic activity, as they show high redox potential, when compared with bacterial laccases. However, their applications have been limited due to several drawbacks related with their production and manipulation, including low yields of protein expression; need for post-translational modification (glycosylation); intricate genetic manipulation and limited molecular tools for protein engineering. Besides, fungal laccases usually are less stable to pH and temperature than their bacterial counterparts; and attempts to produce fungal laccases in native hosts have led to problems related with scaling-up and poor development in non-conventional media, restraining their utilization in industrial and environmental applications; yet bacterial laccases (either, as cell-free protein or in bacterial expression systems) may overcome or complement these practical issues [39, 58, 140-142].

Despite the wide range of substrates that laccases can accept, diverse properties and low sequence homology among bacterial and fungal laccases, their molecular structure is similar for all multicopper oxidases, which normally include three cupredoxin-like domains, and the already mentioned conserved motifs: HXHG, HXH, HXXHXH and HCHXXXHXXXXM/L/F [141]. However, two distinctive characteristics have been reported that may distinguish fungal from bacterial laccases. Firstly, while most of the fungal laccases present a hydrophobic leucine or phenylalanine residue at the end of the fourth conserved motif, HCHXXXHXXXXM/L/F, which are unable to make a bond with the T1 copper ion; bacterial laccases usually present a methionine as an axial ligand at this position [83, 84, 143]. Secondly, bacterial laccases have shown the presence of a predicted α-helical loop near the T1 copper centre, which potentially could block or reduce the entrance of the substrate to the active site. Crystallography studies have been unable to expose this predicted region in some bacterial laccases, presumably because of its mobility; and its purpose is unknown, although a cysteine-rich region has been identified in this loop in some cases, and the suggested functions of this structure include metal binding, substrate specificity and interaction with other enzymes (**Figure 11**) [85, 144, 145].

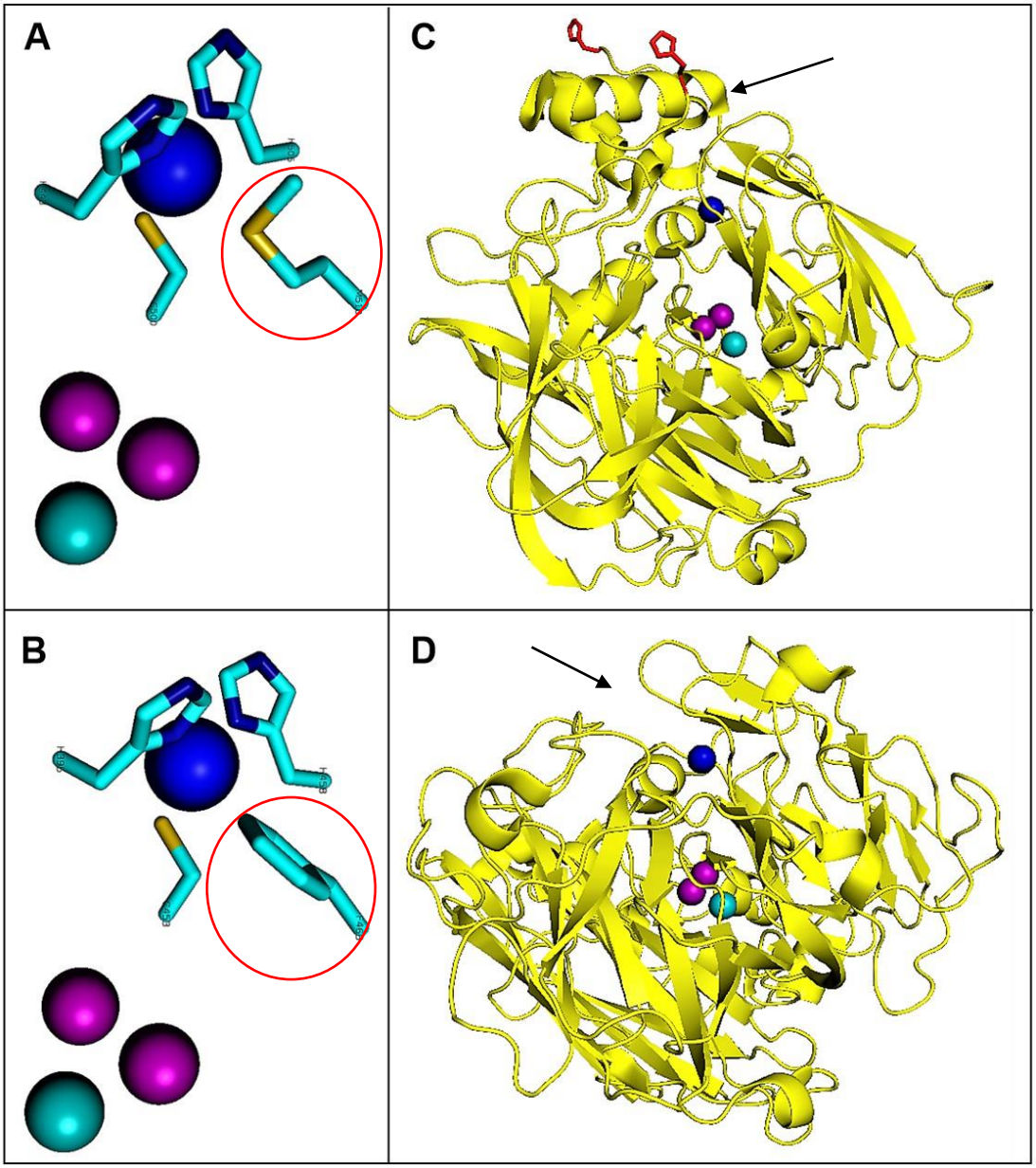

Figure 11. Structural differences between bacterial and fungal laccases. Copper ions type 1, 2 and 3 are represented as blue, teal, and purple spheres, respectively. The T1 copper shows a methionine (red circle) as an axial ligand, in bacterial laccases (A); while a non-ligating residue is located at this position in fungal laccases, in this case a phenylalanine (red circle) (B). The active site over the T1 copper is blocked by an α-helical loop (arrow) in bacterial laccases, and a segment is commonly missed in crystallography studies (initial and final residues of this segment are coloured in red) (C). The active site over the T1 copper (arrow) is exposed in fungal laccases (D). Graphic generated by the software PyMOL, using *Trametes versicolor* laccase (TvL), PDB code 1GYC; and *Escherichia coli* CueO, PDB code 4NER.

The most studied bacterial laccases (laccase-like multicopper oxidases, LMCO) are CopA from *Pseudomonas syringae*; PcoA from *Escherichia coli*; CotA from *Bacillus subtilis* and CueO from *Escherichia coli*. These proteins show motifs found in MCOs and are structurally homologous. Remarkably, all these proteins have been related with other biological

functions, e.g. copper resistance mechanisms and spore pigmentation [79, 146-149]. However, several factors, including substrate specificity, sequence homology, the existence of two- and three-domain laccases, with and without signal peptides for protein exportation, and the detection of LMCOs in anaerobic bacteria, suggest that the biological function of LMCOs is diverse and probably varies from one organism to another [113]. Despite the knowledge of occurrence of LMCOs in bacteria and their interesting properties, so far relatively few proteins have been purified and characterized, hence more research is needed in this field.

1.8.2 Laccase-like Multicopper oxidases in bacterial lignin degraders

As stated before, the role of LMCOs could vary depending on the host and environmental factors. An educated assumption could suggest that it is more likely to find LMCOs with activity towards lignin and lignin-related compounds, if the LMCOs in question come from a bacterial lignin degrader strain. Several of these organisms have been identified, including the Gram-negative bacteria *Pseudomonas putida* KT2440, *Pseudomonas fluorescens* Pf-5, *Ochrobactrum sp*., and *Burkholderia xenovorans* LB400; and the Gram-positive bacteria *Microbacterium phyllosphaerae*, *Arthrobacter sp*., and *Paenibacillus sp*. [58, 61, 65, 150, 151]. Genome analysis of these strains have revealed the presence of putative genes encoding LMCOs, two CopA-type proteins in *Pseudomonas putida* KT2440, one CopA-type in *Pseudomonas fluorescens*, one CueO-type protein in *Ochrobactrum sp*., and one polyphenol oxidase / laccase domain in *Paenibacillus sp*. In addition, these genes included a twin-arginine translocation (TAT) signal sequence, whose purpose is to translocate folded proteins across the lipid membrane to the periplasmic or extracellular space [152]. A multiple sequence alignment showed the presence of the conserved motifs in these proteins, except for the polyphenol oxidase / laccase domain in *Paenibacillus sp.*, which did not show a TAT signal sequence either.

Interestingly, the genome analysis found no LMCOs putative genes in the lignin degraders *Microbacterium phyllosphaerae*, *Arthrobacter sp*., nor in the aromatic degrdader *Burkholderia xenovorans* LB400; yet a new copper protein appeared, CopC-type protein. Two putative genes encoding CopC proteins were identified for *M. phyllosphaerae* and *B. xenovorans*, while one CopC was detected in *Arthrobacter sp*. In *Microbacterium phyllosphaerae* these two *copC* genes were named as *copC1032* and *copC886*, and they were found adjacent to putative genes encoding a DyP-A type peroxidase and a dihydrolipoamide dehydrogenase, respectively (**Figure 12**); both of these protein-types have been involved in

lignin degradation [71, 153], therefore a possible role of CopC in lignin degradation was suspected.

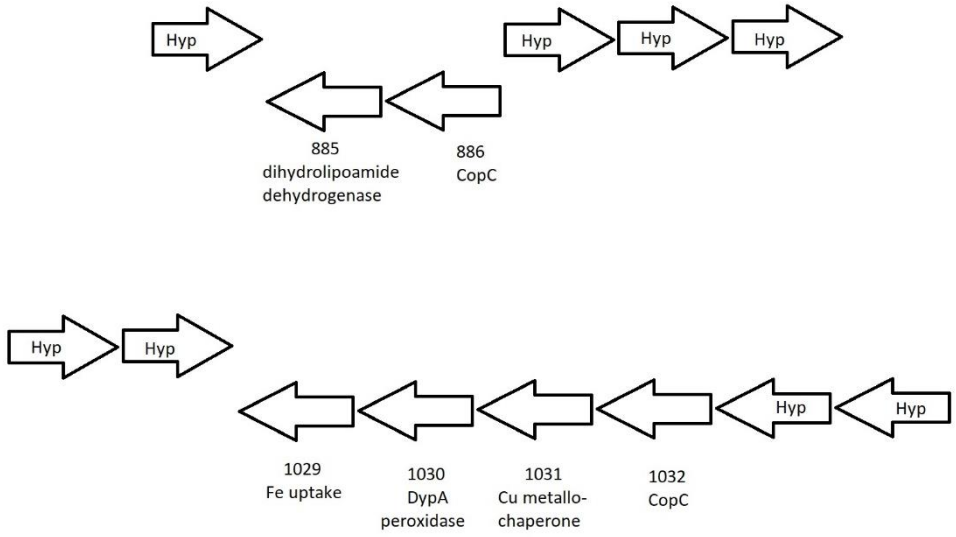

Figure 12. *copC*s gene clusters in *Microbacterium phyllosphaerae* genome. Hyp means hypothetical protein.

1.8.3 CopA, CueO and CopC: copper homeostasis or lignin degrading enzymes?

Copper is an essential trace element, used for defence against oxidative damage, as electron carrier and in redox enzymes. Nevertheless, copper is toxic at high concentrations, since it can compete for metal-sites in proteins with other metals; bind non-specifically to proteins, lipids and nucleic acids, or it could be involved in Fenton-type reactions that generate reactive hydroxyl radicals. Therefore, a highly regulated system to control copper homeostasis is essential for cells. For this purpose, cells have evolved several mechanisms to control copper concentrations, such as transmembrane pumps, copper chaperones, redox enzymes that can change the oxidation state of copper, and gene regulators [154]. Some of the mechanism that have been described for copper resistance include the Cue system, described in *Escherichia coli*, and the plasmid-borne copper resistance, described in *Pseudomonas syringae* pathovar tomato [155, 156]. The Cue system comprises a regulatory protein called CueR; an integral inner membrane protein that can pump copper (I) from the cytoplasm to the periplasmic space by using ATP, called CopA-ATPase (which should not be confused with the LMCO, CopA); and a periplasmic LMCO named CueO, whose function is thought to be oxidation of cooper (I) ions into copper (II) (**Figure 13**) [155, 157].

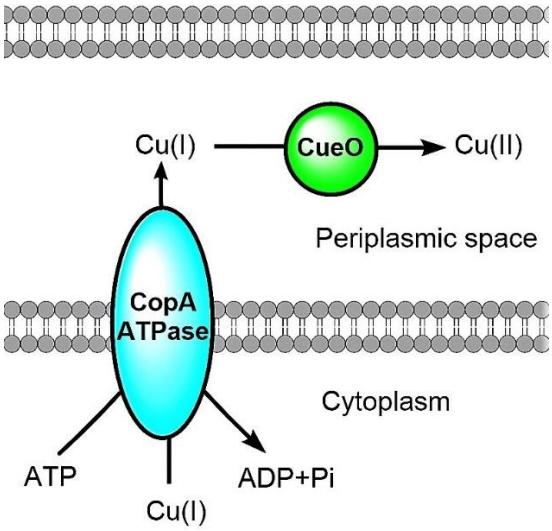

Figure 13. Model for Cue System in *E. coli*. The CopA-ATPase is a copper pump that translocate Cu(I) from the cytoplasm to the periplasmic space. The MCO CueO oxidises Cu(I) into Cu(II). Adapted from [154].

The plasmid-borne copper resistance described in *Pseudomonas syringae* pathovar tomato consists of an operon comprising four copper-resistance genes, *copA*, *copB*, *copC* and *copD*; which act under the control of a copper-inducible promoter that requires the regulatory genes *copR* and *copS* [156, 158]. The proteins encoded by *copA* and *copC* genes, correspond to the LMCO CopA (it should not be confused with CopA-ATPase enzyme), and the copper transporter CopC protein, respectively. Both proteins have been reported as periplasmic proteins, with a molecular weight of about 72 kDa for CopA, and 12 kDa for CopC, and it is thought that they play a role in sequestration of copper ions in the periplasmic space, preventing the entry of toxic copper ions into the cytoplasm (**Figure 14**) [156].

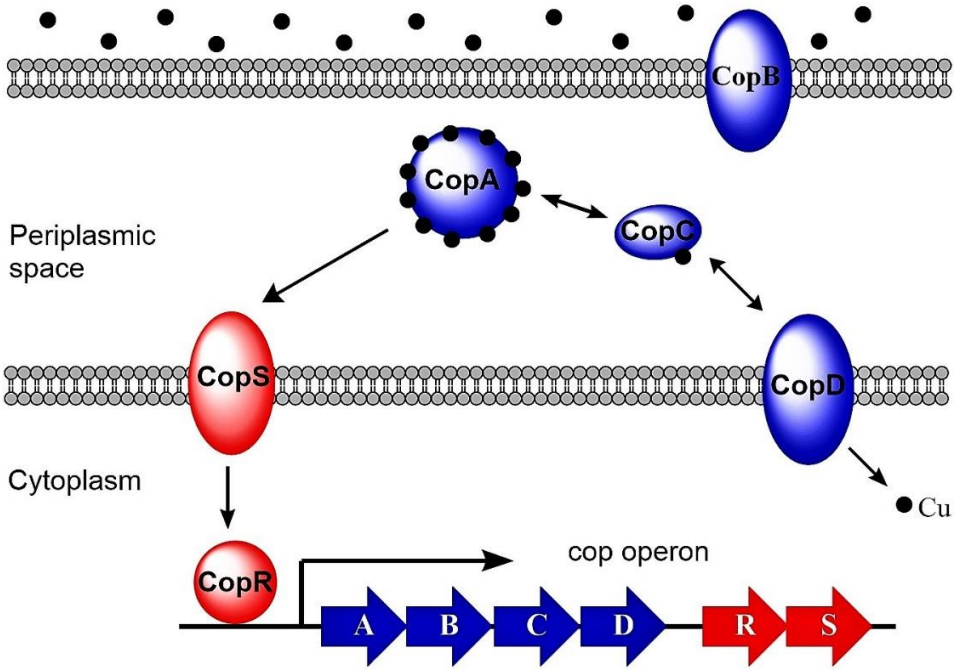

Figure 14. Model for plasmid-borne copper resistance in *P. syringae*. CopS senses copper accumulation and interact with CopR to induce the expression of the cop operon. CopA accumulates ions of copper, CopC can uptake and transport copper ions, and the function of CopD and CopB have not been fully elucidated. Adapted from [159].

The LMCO CueO from *E. coli* has shown laccase-like behaviour, though it may need addition of exogenous copper ions to enhance its oxidase activity [149]. There are no reports indicating that the LMCO CopA from *Pseudomonas syringae* pathovar tomato shows laccase activity, however it has been reported that a CopA protein from another species (probably *Pseudomonas stutzeri* ATCC 14405), not only shows laccase activity, but it could also be involved in lignin degradation [102]. This CopA protein was found by a biosensor responsive to lignin-related products commonly found during lignin degradation process. The biosensor in question, called PemrR-GFP biosensor, was responsive to vanillin, vanillate and p-coumarate; and consists in an *E. coli* strain containing the emrRAB promoter coupled with a fluorescent GFP signal, so that when the biosensor senses its substrate (lignin degradation products) it emits a fluorescent signal. When interrogated with bacterial metagenomic libraries sourced from coal beds, one of the selected clones expressed a product whose activity on lignin resulted in increased biosensor activation. A disruption of this mutant caused the its loss of lignin transformation activity. The product in question was a protein which had 100% and 80% amino acid sequence identity with CopA from *Pseudomonas stutzeri* ATCC 14405 and *Pseudomonas putida*, respectively. This protein was expressed and characterized, showing oxidase activity with ABTS, 2,6-Dimethoxyphenol (2,6-DMP), Syringol and industrially purified high-performance lignin [102].

CopC is a periplasmic protein expressed as part of the copper resistance operon in *Pseudomonas syringae* pathovar tomato. Its length is smaller than CopA and shows a Greek key beta-barrel fold constituted by two beta sheets which involves nine strands, two of them are parallel while the others are all antiparallel (**Figure 15**) [160], similar to cupredoxin-like folds found in individual domains of MCOs. No oxidase activity has been reported for these types of proteins, and their function has been related with copper uptake and transport [161]. CopC from *P. syringae* can bind two atoms of copper at different sites, each site shows a high affinity for a specific oxidation state of copper. The binding site for Cu(II) include the ligating-residues His-1, Glu-27, Asp-89, and His-91, while the Cu(I) site comprise the ligating-residues His-48 and three of the four Met residues (40, 43, 46, 51), which are clustered in a Met-rich region (**Figure 15**). Cu(I) and Cu(II) are separated for about 30 Å, and a change in the oxidation state of a Cu attached to one of these sites (either Cu(I) or Cu(II)), causes the movement of this copper from one site to the other with the corresponding affinity. This indicates that CopC can exchange copper between two sites activated by a redox switch [161].

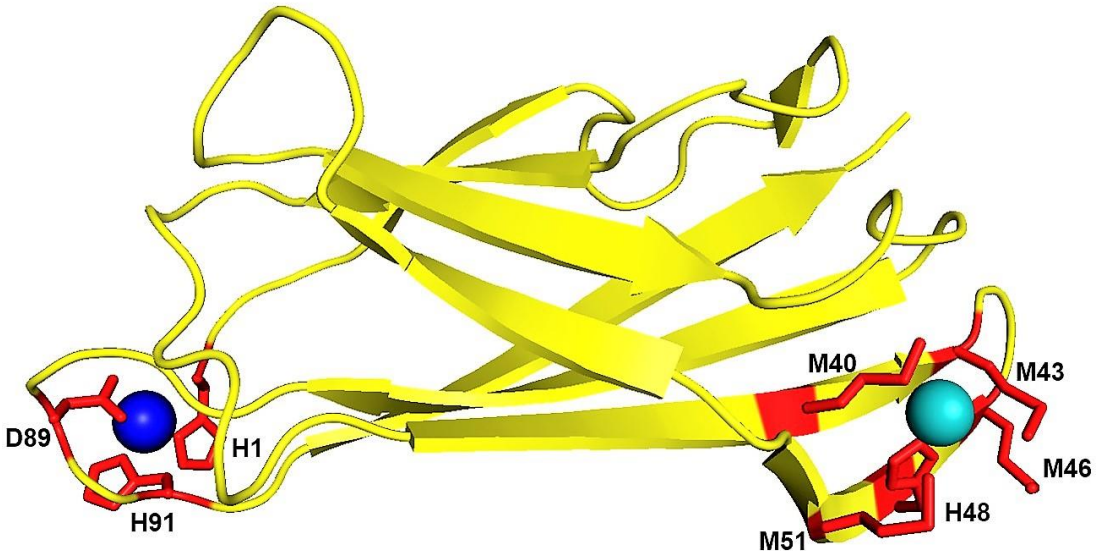

Figure 15. Structure of CopC from *Pseudomonas syringae*. Cu(II) and Cu(I) are depicted as blue and teal spheres, respectively. Ligating-residues and conserved rich methionine region are represented in red sticks. Graphic generated by the software PyMOL, using *Pseudomonas syringae* CopC, PDB code 2C9Q.

It must be noted that most of the studies involving CopC-type proteins have been focused on Cop or Pco systems involved in copper resistance, such as the well characterized CopC from *P. syringae*, described above. However, evidence suggest that CopC is a more widely distributed family of proteins, which often appear as a fusion protein with the inner

membrane protein, CopD [162]. In the lignin degradation context, when a genome analysis revealed the presence of CopA in *P. putida* and *P. fluorescens*, it was surprising that *P. fluorescens* did not include any encoding gene for CopC nearby CopA, while *P. putida* did not show any CopC gene at all in the whole genome. Moreover, the bacterial lignin degraders *M. phyllosphaerae*, *Arthrobacter sp*., and *B. xenovorans*; did not revealed the presence of any CopA at all, but putative genes for CopC were found in their genomes, and no other genes related with the plasmid-borne copper resistance operon were found nearby these genes. A multiple sequence alignment revealed that the CopCs found in these bacterial lignin degraders were indeed different from the well characterized CopC found in P. *syringae*; as these proteins lack the methionine-rich region involved in Cu(I) attachment (**Figure 16**). In addition, CopC has been described as a periplasmic protein in Gram-negative bacteria, yet *M. phyllosphaerae* and *Arthrobacter sp.* are Gram-positive bacteria, and this factor might have some influence on the structure or behaviour of their CopC proteins.

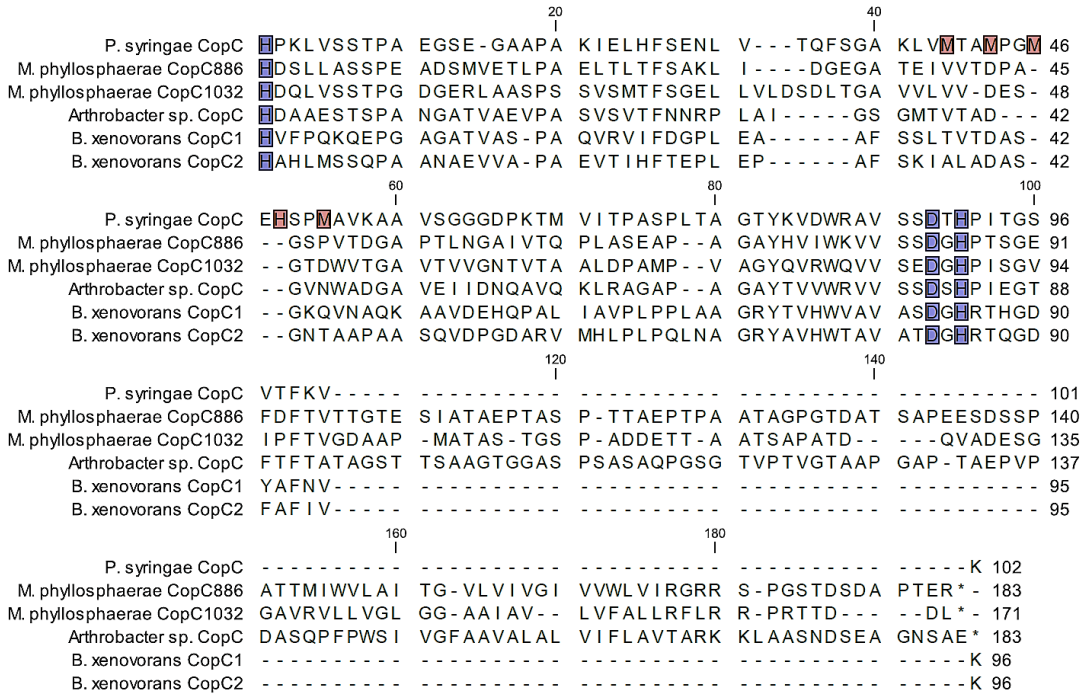

Figure 16. CopCs sequence alignment. Well characterized *P. syringae* CopC aligned with new CopC proteins from the bacterial lignin degraders *M. phyllosphaerae*, *Arthrobacter sp*., and *B. xenovorans*. Conserved ligating-residues for Cu(II) in blue background. Methionine-rich region with conserved ligating residues for C(I) in red background.

A deep study to understand the potential oxidase activity of the LMCO CopA and CueO, and the possible role of CopC proteins, sourced form bacterial lignin degraders, will improve the knowledge about bacterial multicopper oxidases and could increase the range of bacterial enzymes able to break down lignin and aromatic compounds.

1.9 Aims and Objectives

1.9.1 General objective:

- The aim of this project is to characterize the oxidase activity of some laccase-like multicopper oxidases and CopC proteins, towards lignin and aromatic compounds. Their annotated genes have been found in the genome of several bacterial lignin degraders. The LMCOs under study include CopA from *P. putida* (Pp-CopA) and *P. fluorescens* (Pf-CoPA), CueO from *Ochrobactrum sp*. (Oc-CueO), and a Laccase domain polyphenol oxidase from *Paenibacillus sp*. (Pae-Lac). The CopC proteins include two CopCs found in *M. phyllosphaerae* (CopC886 and CopC1032) and two CopCs found in *B. xenovorans* (C1-Bx and C2-Bx).

1.9.2 Specific objectives:

1. Construct strains able to express L MCOs and CopCs proteins, by using cloning and molecular biology techniques.
2. Establish a methodology to express and purify these proteins, and any other required process, such as His-tag removal or metal reconstitution, to obtain functional proteins.
3. Determine the catalytic activity of LMCOs and CopCs proteins, by using a range of aromatic compounds, lignin model compounds and polymeric lignin as substrates.
4. Characterize the biochemical properties of active enzymes, their products profiles, kinetics parameters and optimal pH values.
5. Investigate possible synergistic combinations of these proteins.
6. Perform structural studies, such as crystal structure and copper stoichiometry, to expand and confirm the knowledge about conserved motifs and protein folding of LMCO.

2 Protein expression of bacterial multicopper oxidases and CopC proteins

2.1 Introduction

Expressing and purifying recombinant fungal laccases in large quantities is a major issue that has limited their commercial availability, as their production usually implies long fermentation periods paired with low protein yields [58, 163]. Several studies have attempted to improve fungal laccase production, by using heterologous and homologous expression. Requirements for complex post-transcriptional modification of laccases, in some cases, may need for homologous expression systems, especially in the academic context, as these systems can generate products similar to native-proteins, whose study may give insights about their biological properties. However, in the industrial context, high product yields are required, which is unusual in homologous expression [164, 165]. Heterologous protein expression that use alternative fungal hosts can generate high yield of laccases, but commonly presents engineering problems, as fungal fermentations show non-Newtonian rheological behaviour and high viscosity, which leads to important limitations of transport phenomena in large scale, making industrial fermentation of fungi challenging [166]. To overcome these problems, heterologous production has been done using yeast as expression host, as these microorganisms can produce large amount of protein in a relatively short time [167, 168]. However, the complex post-transcriptional modifications needed by fungal laccases could lead to some protein modifications, including variation of the molecular weight, different rates of glycosylation or modification of some physical properties, e.g. optimum temperature. In addition, it has been reported that laccase production in yeast could result in low yields of protein [168-170]. Moreover, there are limited molecular biology techniques to manipulate and enhance protein production or activity when eukaryotic hosts are used, compared with their prokaryotic counterparts. Fungal laccases normally cannot be produced in bacterial hosts, as these organisms lack the biochemical machinery needed for post-translational modifications. Codon optimization of synthetic genes for expression in bacterial host might result in aggregates or inclusion body formation [171, 172]. Even so, protein expression in bacteria, especially in *Escherichia coli*, currently represents the most favoured expression system for recombinant proteins, so that using bacterial LMCOs instead

of fungal laccases, could constitute an interesting approach to solve some of the issues related with laccase production.

Several bacterial LMCOs have been heterologously expressed in *E. coli*, where the expression yields can be significantly enhanced by using high copy number plasmids with strong promoters, e.g. plasmids of the pET series, or codon optimization. Although higher yields of LMCOs have been achieved, some of these recombinant proteins are subjected to incomplete copper incorporation into their structure, and often they need addition of exogenous copper ions to enhance or trigger their catalytic activity. Copper is an essential element for LMCOs, yet its loading into the protein is poorly understood [85, 144, 173, 174]. Apparently, the presence of copper ions in the cytoplasm is needed for proper folding and incorporation of this element into LMCOs; however, *E. coli* has an inducible efflux system that prevents toxic copper accumulation in the cytoplasm [154, 155]. Evidence suggests that the copper incorporation in LMCOs expressed in *E. coli* is strongly dependent on copper and oxygen availability in the culture media. Production of the LMCOs CotA from *Bacillus subtilis* in *E. coli* showed that, in media supplemented with copper, a switch from aerobic to microaerobic conditions resulted in a complete incorporation of copper into CotA, while the maintenance of aerobic conditions gave copper-depleted proteins. Cells grown under microaerobic conditions accumulate up to 80-fold more copper in their cytoplasm than cells grown aerobically (2.5 mg Cu/g cell under microaerobic conditions versus ≈0.03 mg Cu/g cell under aerobic conditions), meaning that under low oxygen concentration, the inducible efflux system that prevents toxic copper entrance into the cytoplasm does not work at its normal level. The microaerobic condition was achieved simply by switching off the agitation once *E. coli* cultures were induced for protein expression. CotA *in vitro* copper reconstitution experiments revealed that this process follows a sequential order, in which the T1 copper is the first to be loaded into the protein, followed by the T2 copper and the T3 copper [175].

Before heterologous expression of LMCOs, the corresponding genes must first be identified. Although fungal laccases can show a high sequence homology among them, when compared with laccases from other organisms, the homology could be very low. It must be noted that there is no general consensus about the definition of what a laccase is, nor which characteristics could properly identify it as such. On the one hand, since the original laccase was found in the sap of lacquer tree of *Rhus vernicifera*, it has been suggested that this enzyme should be considered as a “true laccase” and consequently, only MCOs isolated in presence of the natural substrate urushiol (an unsaturated alkyl catechol) should be recognized as laccases [106]. On the other hand, it has been suggested that fungal laccases

should be considered as true laccases (or laccases *sensu stricto*), as the vast majority of studies regarding laccases have been conducted using these enzymes [81, 105]; besides, it is possible to segregate fungal laccases from other MCOs produced by fungi [105]. Regarding bacterial laccases, the term laccase-like multicopper oxidase (LMCO) is more widely used, as it can denote the great versatility of these enzymes without falling into the controversial definition of a "true laccase"; however, there is no direct way to find putative genes for these kinds of proteins based only on their sequence information. The discrimination of LMCOs from simply MCOs is unclear, and experimental evidence is often needed for their discovery, mostly based on sequence homology of the well-conserved residues involved in copper binding, common for all MCOs, complemented with some experiment proving some sort of phenol oxidase activity [96].

2.2 Protein expression of laccase-like multicopper oxidases (LMCOs)

2.2.1 Identification and genetic context of LMCOs genes

The genome sequences of several lignin-degraders were examined for the presence of genes encoding potential lignin oxidation enzymes, and biochemical pathways for aromatic compound metabolization that could degrade the oligomers products of lignin breakdown. Evidence for bacterial lignin depolymerization is supported by: the accumulation of vanillic acid and the generation of vanillin as metabolites of lignocellulose breakdown, the production of pyridine-dicarboxylic acids and the overexpression of genes of the β-ketoadipate pathway in presence of lignin, in a range of bacterial lignin-degraders [66, 176, 177]. Given that multicopper oxidase (MCO) cannot be automatically identified as a laccase-like multicopper oxidase (LMCO), as experimental evidence is needed for such a classification [96], initially the genome analysis was focused on finding MCO sequences.

Putative MCO genes were found in the genome of *Pseudomonas putida* KT2440 (GenBank accession number AE015451), *Pseudomonas fluorescens* PF-5 (GenBank accession number CP000076), *Ochrobactrum sp*. and *Paenibacillus sp*. The latter two strains were identified as lignin degraders, present in woodland soil and municipal waste soil samples [61, 178]. Their genome sequences were obtained by Illumina HiSeq 2500 system at the Brazilian Bioethanol Science and Technology Lab., Laboratory of Next Generation Sequencing (CTBE NGS), where it was estimated the genome sizes of 5.3 Mb and 7.2 Mb, for *Ochrobactrum sp*. and *Paenibacillus sp*. strains, respectively. The presence of typical bacterial marker genes

was performed by using Phyla-Amphora [179]. The resulting assembly has 87 scaffolds, with a total length of 5310057 bp, an N50 of 150153 bp and an average GC content of 56.2% for *Ochrobactrum sp*.; while the assembly for *Paenibacillus sp*. genome has 40 scaffolds, with a total length of 7187707 bp, an N50 of 353 719 bp and an average GC content of 43.5%. Gene prediction was done by using GeneMark and PROKKA Prokaryotic Genome Annotation Pipeline [180, 181]. For *Ochrobactrum sp*. a total of 5269 genes were identified, from which 5210 are protein-encoding genes, 3 rRNA genes, 54 tRNAs, and 1 tmRNA. A 16S rRNA analysis through EZBioCloud [182], revealed a 98.99% sequence similarity with *Ochrobactrum pecoris* O8RB2639 (T) and 98.13% with *Ochrobactrum rhizosphaerae* PR17(T). For *Paenibacillus sp*. a total of 6475 genes were identified, from which 6405 are protein-encoding genes, 1 rRNA gene, 68 tRNAs, and 1 tmRNA. The 16SrRNA analysis revealed a 99.45% sequence similarity with *Paenibacillus etheri* SH7 (T) and 98.66% with *Paenibacillus odorifer* DSM 15391(T) [183].

In the genome of *Pseudomonas putida* KT2440, a total of three MCOs genes were found, *copA-I*, *copA-II* and *cumA*, whose predicted proteins show the well-conserved motifs implicated in the four copper ions attachment. The gene *copA-I* was found located from nucleotide 2510006 to nucleotide 2511730 in the genome, adjacent to a putative *copB-I* gene. The gene *copA-II* was found located from nucleotide 6131843 to nucleotide 6133852 in the genome. Nearby *copA-II*, putative genes related with copper resistance mechanism were found, the plasmid-borne copper resistance operon (cop operon) genes *copB-II*, *copR-II* and *copS* [158]; and the copper and the silver efflux system (cus system) genes, *cusA*, *cusB* and *cusF* [184]. As stated before, no *copC* genes (part of the cop operon) were found in *P. putida* KT2440. The third MCO gene, *cumA*, was located from nucleotide 1180948 to nucleotide 1182354, and it has been involved in Mn^{2+} oxidation [185], so that attention was focused on *copA* genes, whose corresponding protein has been implicated in lignin degradation [102]. It was suspected that *copA-I* and *copA-II* would show relatively similar behaviour, and *copA-II* gene was chosen for protein expression. The protein encoded by this gene was named as Pp-CopA.

In the genome of *Pseudomonas fluorescens* PF-5, two MCO genes were found: a *cumA* gene (described above) and a lone putative *copA* gene, the latter was located from nucleotide 3237717 to nucleotide 3239456. A putative *copB* gene was found as the only gene related with plasmid-borne copper resistance operon (cop operon) located nearby *copA*. A putative *copC* gene was identified in *P. fluorescens* Pf-5, but it was located from nucleotide 2814512 to nucleotide 2814880 in the genome, away from *copA* and adjacent to a *copD*

gene. The gene *copA* was selected for cloning and expression, the resulting protein was named as Pf-CopA.

The *Ochrobactrum sp*. genome contained the MCO gene *cueO* (gene ID 4352, with 91.4% sequence identity to Uniprot E2GIP7_9RHIZ, an annotated laccase from *Ochrobactrum sp*. 531), and it was located immediately adjacent to a *sodC* gene encoding a Cu/Zn superoxide dismutase (SOD) protein. Two other SOD protein genes were found in the genome of *Ochrobactrum sp*.: the *sodF-773* and *sodF-4353* genes. Two extracellular manganese superoxide dismutase (Mn SOD) from *Sphingobacterium sp*. T2 have been implicated in bacterial lignin degradation [74], although neither of the *Ochrobactrum sp*. SOD genes contained signal sequences for protein export. In addition, a gene cluster (genes 4452 to 4463) encoding the β-ketoadipate pathway was found; five genes involved in the 4-hydroxyphenylacetate pathway (genes 96, 97, 104, 105, 1962 and 1964); and two genes for hydroquinone utilization (genes 2570–71). The *cueO* gene was selected for cloning and protein expression, the encoded protein was named as Oc-CueO.

Regarding the *Paenibacillus sp*. strain, a putative polyphenol oxidase annotated as a "laccase-domain" was found. The protein in question was the YlmD (gene ID 6155, named as *p-ppo*), with 41.4% sequence identity to Uniprot YLMD_BACSU, a polyphenol oxidase from *Bacillus subtilis* (strain 168), predicted by a BLAST analysis in Uniprot (http://www.uniprot.org/). In addition, the superoxide dismutase *sodM* (ID 6086) and *sodF* (ID 6093) genes were found in the genome, but neither gene contained a signal sequence for protein export. The gene cluster for β- ketoadipate pathways was absent in this strain. The gene annotated as putative laccase domain, *p-ppo*, was selected for cloning and protein expression, the produced protein was named as P-PPO.

Three out of four proteins selected for protein expression showed a molecular weight ranging from ≈55 to ≈70 kDa, a sequence length from 507 to 637 amino acid residues, a TAT signal sequence for protein exportation, and the well-conserved motifs of MCO: HXHG, HXH, HXXHXH and HCHXXXHXXXXM/L/F. The remaining protein, P-PPO, was smaller than the other proteins, it did not contain any signal sequence for protein exportation, and it did not include the conserved motifs involved in copper binding (**Figure 17**). **Table 2** shows a summary of these characteristics.

Table 2. Nucleotide and amino acid sequences characteristics of the MCO proteins under study. Tat signal sequences have been omitted in nucleotide and amino acid sequence length and in protein MW.

	Protein name			
	Pp-CopA	Pf-CopA	Oc-CueO	P-PPO
Organism	*Pseudomonas putida* KT2440	*Pseudomonas fluorescens* PF-5	*Ochrobactrum sp*.	*Paenibacillus sp*.
Nucleotide sequence length	2010 bp	1629 bp	1524 bp	858 bp
Amino acid sequence length	637 aa	542 aa	507 aa	285 aa
Predicted protein molecular weight	70.8 kDa	60.4 kDa	55.1 kDa	31.8 kDa
UniProt code	Q88C03	Q4KCN4	-	-
MCOs conserved motifs	Yes	Yes	Yes	-
Signal sequence for protein exportation	TAT	TAT	TAT	-

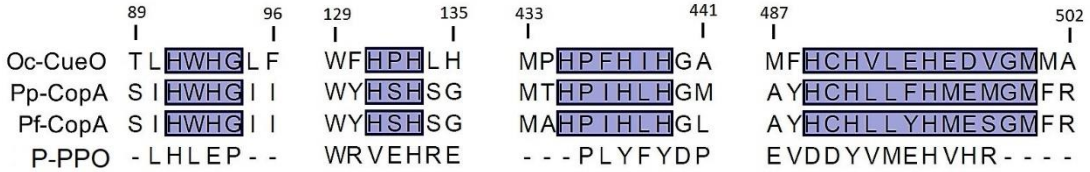

Figure 17. Amino acid sequence alignment showing the MCO well-conserved motifs (in blue background) found in the proteins under study. P-PPO does not contain these motifs. Numbering is based on Oc-CueO sequence as reference.

2.2.2 Cloning and protein expression of MCOs

Polymerase chain reaction (PCR) was used for amplification of the selected MCO genes. *Pseudomonas putida* KT2440, *Pseudomonas fluorescens* PF-5, *Ochrobactrum sp*. and *Paenibacillus sp*. were inoculated in 5 mL of Luria-Bertani broth (LB) and grown overnight. After cell harvesting, cells were used for genomic DNA extraction by using Wizard® Genomic DNA Purification Kit from Promega, following the manufacturer's protocol. The genomic DNA was used as template for PCR reactions, with Platinum Pfx-DNA polymerase, from Invitrogen. The sequences of the primers used are shown in **Table 3**. The resulting PCR products in their predicted size are shown in **Figure 18**. Each band corresponding to the desired PCR product was excised from the gel for purification, using the GeneJET Gel Extraction Kit, from Thermo Fisher Scientific, according to the manufacturer's protocol.

Table 3. List of primers used for PCR gene amplification of the MCOs under study.

Organism	Gene	Forward primer (5' to 3')	Reverse primer (5' to 3')
Ochrobactrum sp.	*cueO*	CACCCAGGACGCTCACCAG AAAATG	CTATACTGTTACGAACTG AGCCATC
Pseudomonas putida KT2440	*copA-II*	CACCGTGACCAGCCCTGGC CAACCG	TCATTCGTCCACGCGGAC TTC
Pseudomonas fluorescens PF-5	*copA*	CACCGTCAGCAGCCCGGGC CAG	TCAAGCTTCATGGTGGCG TTCCTC
Paenibacillus sp.	*p-ppo*	CACCATGGAACCGTTTGTG CAGGGGAAG	TCAACTCTCCTTTATTCC GATCCAG

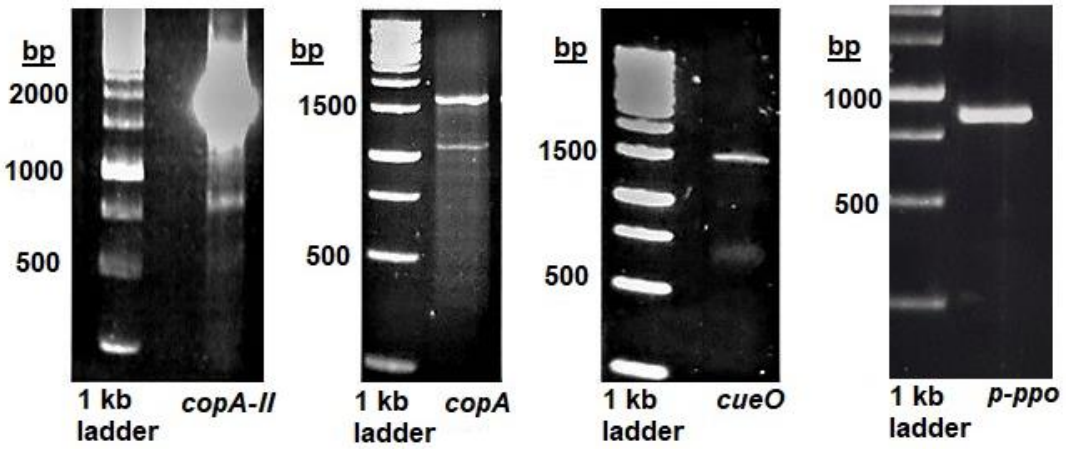

Figure 18. Agarose gel for PCR products of *copA-II*, *copA*, *cueO* and *p-ppo* genes.

The purified products were used for cloning into the expression vector pET151, by using the Champion™ Directional TOPO® Expression Kit, from Invitrogen. After ligation reaction, the vectors harbouring the desired gene were transformed into *E. coli* Top10 chemically competent cells. Several colonies were obtained, then a screening was performed by extracting the plasmid of four to six colonies, per each gene of interest, and these plasmids were sent for sequencing, to confirm the correct orientation of the fragments in the vector and the accuracy of their sequences. Based on sequencing results, the best plasmid whose sequence was in the correct orientation and did not contain any mutation, was selected for each gene of interest, and was transformed into *E. coli* BL21 chemically competent cells (Invitrogen), for protein expression.

E. coli BL21 cells harbouring the vector of interest, were inoculated in 10 mL of Luria-Bertani broth supplemented with ampicillin (100 µg/mL) and grown overnight. This culture was used for inoculation of 1 litre of Luria-Bertani broth supplemented with ampicillin (100 µg/mL), which was then incubated at 37 °C for 3 to 4 hours, then $CuSO_4$ was added to reach a final concentration of 80 µM, IPTG was added for induction at a final concentration of 1 mM, and the temperature was decreased to 18 °C. Finally, the culture was incubated for 16 hours for protein expression. After cell harvesting by centrifugation at 3200 x g, the cells

were lysed and disrupted by using high pressure, followed by centrifugation at 10300 x g for 35 minutes. Then the supernatant was loaded into a Ni-NTA resin column (HisTrap HP, 1 ml volume). The recombinant proteins were expressed as N-terminal His_6 fusion proteins, so they were purified by immobilized metal affinity chromatography (IMAC). The expressed recombinant proteins remained in the Ni-NTA resin due to the affinity between the His_6 fusion tag and the nickel present in the resin. Once the supernatant had passed through the column, resulting in a separation of the expressed protein from all other proteins present in the supernatant of the cell lysate, the column was washed twice with washing buffer (50 mM NaH_2PO_4, 20 mM imidazole, 300 mM NaCl, pH 8.0) and then the recombinant protein was finally eluted from the resin by using 7 mL of elution buffer with high imidazole concentration. The resulting protein was exchanged to a phosphate buffer (washing buffer), to perform a proteolytic digestion with TEV protease to remove the His_6 fusion tag. The ratio of recombinant protein to TEV protease, used for tag cleavage was of 1 mg of protease per 2 mg of expressed protein, and the reaction was incubated overnight at room temperature. Finally, the protein free of His_6 tag was further purified by a second IMAC, this time the flow-through was collected as it contained the untagged protein, and then it was buffer exchanged to 20 mM Hepes, 60 mM NaCl buffer, pH 7, to give recombinant proteins free of impurities. A small sample of the final protein solution was taken for SDS PAGE gel, which gave the expected protein bands (**Figure 19**, **Table 2**).

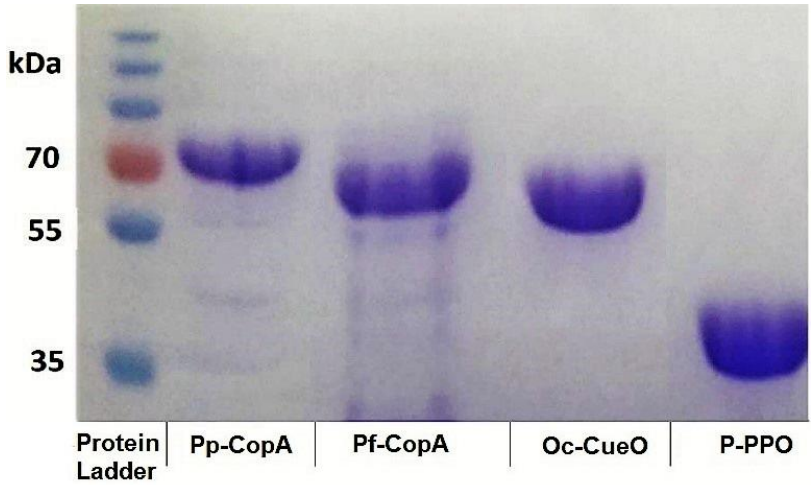

Figure 19. SDS PAGE of Pp-CopA, Pf-CopA, Oc-CueO and P-PPO proteins, expressed recombinantly in *E. coli* BL21, after IMAC purification and TEV cleavage.

The procedure for protein expression described above was used for production of protein intended for kinetic characterization experiments and assays of protein activity with lignin model compounds and polymeric lignin. However, for protein crystallisation

experiments, an additional step of purification was included, consisting of purification by size exclusion chromatography (Gel filtration column Superdex 75) in a Fast protein liquid chromatography (FPLC) equipment.

2.2.3 Copper reconstitution

Although 80 µM of $CuSO_4$ was added to the cultures during the induction phase, it was suspected that the produced proteins were in their apoprotein form. This suspicion was later confirmed by activity assays, the appearance of the protein solutions, and spectroscopy studies that showed the absence of copper in these proteins when they were produced under the conditions described above. Since P-PPO did not show the well-conserved motifs of MCOs, no copper attachment was expected for this protein and therefore P-PPO was omitted from the copper reconstitution experiments.

Laccases show an intense absorbance at ≈610 nm, due to the spectroscopic properties of T1 copper [84]. When a UV-Vis absorption spectroscopy scan was performed for Pp-CopA, Pf-CopA and Oc-CueO, the expected peak at ≈610 nm did not appear, suggesting an absence of T1 copper or a possible disturbance of the typical coordination sphere for this copper. A complementary experiment measuring the copper content besides other elements, including S, Fe, Zn and Ni, by inductively coupled plasma optical emission spectroscopy (ICP-OES), confirmed the absence of copper in Pp-CopA.

Two methods were assessed for copper reconstitution, based on *in vitro* and *in vivo* approaches. The *in vivo* method consisted of protein expression under microaerobic (limited oxygen) conditions. When MCOs are produced in *E. coli*, the addition of Cu^{2+} to the culture media can have a marginal effect on the copper loading into the recombinant protein, as *E. coli* inducible cus efflux system prevents the entrance of toxic Cu^{2+} into the cytoplasm, where the recombinant protein is produced. However, when oxygen is limited, this efflux system does not work at its normal level and copper ions can enter the cytoplasm, which leads to the generation of fully or partially copper loaded protein molecules [175]. The presence of a TAT (twin-arginine translocation) signal peptide sequences in some MCOs, including the proteins under study, suggest that these are folded as holoenzymes in their native hosts. It is generally accepted that the main role of the TAT system pathway is to translocate fully folded protein across the membrane, playing a vital role in redox proteins, which need to be translocated in their 3D conformation due to the acquisition of complex cofactors comprising multiple atoms, a process that takes place in the cytoplasm of bacteria [186]. Hence, recombinant MCOs that contain a TAT signal sequence, produced in *E. coli* under fully

aerated conditions could lead to the generation of proteins folded in their apoprotein form, as the copper needed for holoproteins generation would not be present in the cytoplasm. In addition, the presence of a TAT signal sequence may indicate that those proteins have extracellular functions. Pp-CopA, Pf-CopA and Oc-CueO were produced under microaerobic (limited oxygen) conditions, by switching off the agitation after induction with IPTG, and then incubating the cultures overnight, before cell harvesting. The resulting protein solutions showed some differences, including the appearance of blue colour in purified Oc-CueO solution and the expected peak at ≈610 nm in a UV-Vis absorption spectroscopy scan (**Figure 20**). Interestingly, Pp-CopA and Pf-CopA remained as colourless protein solutions, and their UV-Vis spectra did not show any peak at ≈610 nm (**Figure 20**). Additionally, the yield of protein achieved under microaerobic conditions was lower than the yield for proteins produced under fully aerated conditions (**Table 4**), and for this reason, most of the protein expression experiments were carried out by using normal agitation through the induction phase, while protein expression under microaerobic conditions was carried out only for production of protein intended for structural experiments.

Table 4. Approximate yield of protein achieved in protein expression experiments, under different oxygen conditions.

	Yield of expressed protein, per litre of culture.	
Protein	Fully aerated conditions (agitation, 180 rpm)	Microaerobic conditions (agitation switched off, 0 rpm)
Oc-CueO	≈20 mg	≈7 mg
Pp-CopA	≈25 mg	≈10 mg
Pf-CopA	≈3 mg	≈1 mg
P-PPO	≈60 mg	-

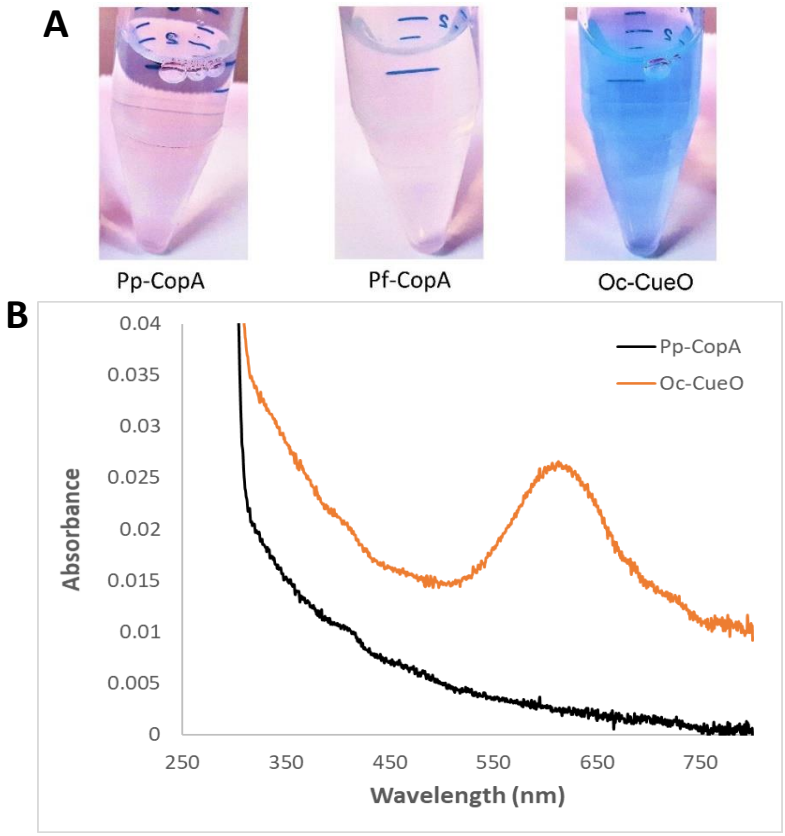

Figure 20. Copper content characterization of the expressed MCOs proteins, under microaerobic conditions. (A) Colour comparison of purified Pp-CopA, Pf-CopA and Oc-CueO protein solutions. (B) UV–Visible absorption spectra of purified recombinant Pp-CopA and Oc-CueO (0·5 mg/mL). λ_{max} for Oc-CueO at ≈610 nm.

On the other hand, *in vitro* copper reconstitution was carried out by adding a 400 mM $CuSO_4$ solution directly into concentrated solutions of Pp-CopA, Pf-CopA and Oc-CueO (in separate assays). These proteins were concentrated by centrifugation on 10 kDa Amicon centricon tubes. 3 µL of the $CuSO_4$ solution were added to 2 mL of concentrated protein (≈2 mg/mL), reaching a molar ratio between copper and protein of 8 to 1; since theoretically four ions of copper were needed per molecule of protein, and the reconstitution experiments required that the copper should be present in excess in the medium, to assure a fully loaded of this element into the proteins. Immediately after copper addition, Oc-CueO became blue, while Pp-CopA and Pf-CopA remained colorless. The mixture of Cu^{2+} and concentrated protein was incubated overnight, then the excess of copper was removed by buffer exchange in a PD-10 column, followed by an equilibration of the column with the intended buffer and the repetition of the buffer exchange step, in order to secure a total removal of the copper ions that were unable to bind to any protein. After copper reconstitution, a small sample volume was taken from each protein solution, for an inductively coupled plasma optical emission spectroscopy (ICP-OES) assay. Commercial standards of Cu (10020 ppm) and S

(9814 ppm) were used to prepare six different standards diluted in water, whose concentrations ranged from 0.2 to 5 ppm. Protein samples were diluted in water to reach two different concentrations of about 0.1 and 0.2 mg of protein / mL. The standards were measured, and their emission values were used to build calibration curves for Cu and S; which were then used to determine the concentration of copper and sulfur in the protein samples, and finally, knowing the number of sulfur atoms present in each protein molecule, their concentration and molar ratio with copper was accurately determined. The results are shown in **Table 5**.

Table 5. Molar ratio between copper and protein, measured by ICP-OES, after *in vitro* copper reconstitution.

Protein	mol of Cu per mol of protein	Standard deviation
Oc-CueO	4.7	± 0.8
Pp-CopA	9.1	± 1.5
Pf-CopA	8.7	± 1.3

Interestingly, while Oc-CueO shows approximately the expected ratio between copper and protein, Pp-CopA and Pf-CopA show higher values, even though their corresponding protein solutions are colorless, and the spectroscopy scans did not reveal any peak at ≈610 nm for these CopA proteins. The high copper content of CopA has been reported in *Pseudomonas syringae* pv. tomato, whose copper content obtained by atomic absorption spectrometry was 10.9 ± 1.2 ions of copper per CopA molecule, and for that reason its biological function has been related with copper accumulation in the periplasmic space to prevent the entrance of toxic copper ions into the cytoplasm [156]. The reported copper content of CopA agrees with the values found in this study. Pp-CopA and Pf-CopA reconstituted with copper were active in absence of copper addition, which is described in detail in the next chapter. Evidence suggesting the lack of T1 copper in Pp-CopA and Pf-CopA proteins, such as the absence of color in these protein solutions and the non appearance of the peak at ≈610 nm, even for copper reconstituted proteins, contrasts with the ICP-OES results showing an even higher copper content than common MCOs and their activity in absence of copper addition. This apparent contradiction is not well understood, maybe the T1 copper site is occupied after all, but there is a disturbance of the typical coordination sphere for this site due to axial ligand methionine and the α-helical loop nearby, which is larger in CopA proteins, however more research is needed to elucidate these peculiar observations.

2.3 Protein expression of CopC proteins

2.3.1 Identification and genetic context of copC genes

Several enzymes involved in lignin degradation have been identified, including Dyp-type peroxidases, superoxidase dismutases, glutathione-dependent β-etherases, catalase-peroxidases, bacterial dioxygenases, enzymes of the β-ketoadipate pathway, enzymes related with aromatic compounds degradation and laccase-like multicopper oxidases [71, 73, 74, 177]. Not all genes that encode these proteins are found together in the same genome, suggesting that each microorganism would use different strategies to metabolize lignin, or that the formation of a microbial consortium would be necessary for the degradation of lignin. Since bacterial lignin degradation has not been fully characterized, it is possible that there are more enzymes involved in lignin depolymerization yet to be discovered. In some bacterial lignin degraders strains whose genome did not contain genes for MCOs, other putative genes encoding a different type of copper protein were found, the *copC* genes.

In *Microbacterium phyllosphaerae* two different putative *copC* genes were found, identified as *copC886* and *copC1032*. The *copC886* gene was adjacent to a dihydrolipoamide dehydrogenase gene (885), while the copC1032 gene was adjacent to an A-type DyP peroxidase (1030) (**Figure 12**). In each case, there were no other *cop* genes nearby in the genome sequence. Both *copC* genes contained a signal peptide sequence, identified by Phobius (http://phobius.sbc.su.se/), and SignalP (http://www.cbs.dtu.dk/services/SignalP/) online tools, suggesting a possible extracellular function of their corresponding encoding proteins. However, these signal peptide sequences were not identified as TAT signals by the online tool TatP (http://www.cbs.dtu.dk/services/TatP/). Regarding the neighbouring enzymes, dihydrolipoamide dehydrogenase and DyP peroxidases, these have been identified as role players in lignin degradation. While it has been demonstrated that Dyp peroxidases can directly oxidise lignin, dihydrolipoamide dehydrogenase is thought to be an accessory enzyme, whose function would be to prevent the repolymerization of oxidized lignin radicals [71, 153]. Hence, a possible role of CopC proteins in lignin degradation was suspected.

CopC protein has been described as forming part of the plasmid borne copper resistant operon, whose function is to confer copper resistance to the Gram-negative bacteria *Pseudomonas syringae* pv. tomato [156]. The crystal structure of this protein has been elucidated and its function has been described as to be a copper transporter, comprising two different binding sites for this metal, each site having a strong preference for a defined redox state of the copper that it accepts [161]. However, a bioinformatic analysis

revealed that CopCs comprise a broader family of proteins which may present different properties and biological functions [162]. Indeed, a multiple sequence alignment of the predicted CopC proteins encoded by the putative genes found in the genome of bacterial lignin degraders showed differences with the canonical CopC from *P. syringae*, as they contained only one site for copper attachment, which could also imply a different function for these proteins. Moreover, no other putative genes of the plasmid borne copper resistance operon (cop operon) were found nearby these genes, instead some genes related with lignin degradation were found. Putative *copC* genes were also found in the genomes of *Arthrobacter sp*. and *Burkholderia xenovorans* LB400.

The two genes, *copC886* and *copC1032* were selected for cloning and protein expression experiments. Their encoded proteins were named as CopC886 and CopC1032. Other putative *copC* genes were found in two additional bacterial lignin degraders strains. One *copC* gene was found in *Arthrobacter sp*. strain (a lignin-degrading strain isolated by Dr. Fabio Squina, at the Brazilian Bioethanol Science and Technology Laboratory, CTBE), and two *copC* genes were found in *Burkholderia xenovorans* LB400, a known aromatic degrader [58, 187]. These two latter genes were named as *copC-bx1* and *copC-bx2* and were selected for cloning and protein expression experiments as well. No other *cop* genes (genes from the plasmid borne copper resistance operon) were found nearby these genes, except a putative *copD* gene located adjacent to the *copC-bx1* gene. Their encoded proteins were named as CopC-Bx1 and CopC-Bx2. **Table 6** shows a summary of the CopC predicted protein characteristics.

Table 6. Nucleotide and amino acid sequences characteristics of the CopC proteins under study. Signal sequences have been omitted in nucleotide and amino acid sequence length and in protein MW.

	Protein name			
	CopC886	CopC1032	CopC-Bx1	CopC-Bx2
Organism	*Microbacterium phyllosphaerae*	*Microbacterium phyllosphaerae*	*Burkholderia xenovorans*	*Burkholderia xenovorans*
Nucleotide sequence length	549 bp	513 bp	288 bp	288 bp
Amino acid sequence length	183 aa	171 aa	96 aa	96 aa
Predicted protein molecular weight	18.4 kDa	17.2 kDa	10.05 kDa	10.053 kDa
Peptide signal sequence	Yes (undefined)	Yes (undefined)	Yes (undefined)	Yes (undefined)

2.3.2 Cloning and protein expression of CopCs

For protein expression of CopC886 and CopC1032, two different approaches were assessed. In the first place, an expression system based on *E. coli* was used. The methodology employed was the same used for MCOs genes cloning and protein expression, described above. *copC886* and *copC1032* genes were amplified by PCR from chromosomal DNA. The sequences of the primers used are shown in **Table 7**. The resulting PCR products showing the bands in their predicted size are shown in **Figure 21**, **A**. The bands corresponding to the desired PCR products were excised from the gel for further purification, by using the GeneJET Gel Extraction Kit, and were used for cloning into the expression vector pET151, by using the Champion™ Directional TOPO® Expression Kit, from Invitrogen. After transformation into *E. coli* Top10 chemically competent cells, a plasmid extraction was carried out, which were then sequenced, and their results confirmed the presence of the genes in the correct orientation in the pET151 vector and the absence of mutations.

For protein expression, the vectors harbouring the desired genes were transformed into *E. coli* BL21 chemically competent cells. Protein expression was carried out by the same methodology described above, using Luria-Bertani broth supplemented with ampicillin, $CuSO_4$ and induced with IPTG. After cell harvesting and protein purification by IMAC, an SDS PAGE gel did not shown any band at the expected protein size, neither for CopC886 nor for CopC1032. A protein concentration measurement did not show the presence any significant level of overexpressed protein. Several attempts were carried out to express these proteins, including but not limited to, adding different concentrations of IPTG, in presence and in absence of copper, including and excluding their signal peptide sequences, different incubations times during the induction phase, among others. Unfortunately, all of them were unsuccessful, meaning that despite that the molecular cloning of these genes into the expression vector pET151 was achieved, these proteins were not expressed in *E. coli*, under the conditions tested.

No previous reports were found about poor or none protein expression of CopC in *E. coli*. A possible incompatibility of the host organism was suspected, as these *copC* genes belong to a Gram-positive bacterium, *M. phyllosphaerae*; while their expression was performed in a Gram-negative bacterium, *E. coli*. Besides, the high GC content of these genes, 70% for *copC886* and 69% for *copC1032*, could also have played a role on this matter. For these reasons, a second approach to protein expression was performed by using the bacterium *Rhodococcus jostii* RHA1 as expression system. PCR was used to amplify these genes from chromosomal DNA, adding the restriction sites NdeI and HindIII in the forward

and reverse primers, respectively. In addition, overhang sequences were added to each primer, a sequence for TEV recognition cleavage site was included in the reverse primer and these primers were designed to exclude the predicted signal peptide from these genes (**Table 7**). The PCR products were visualized by an agarose gel 1% (**Figure 21**, **B**), and the amplicons were excised for further purification with the GeneJET Gel Extraction Kit.

Table 7. List of primers used for PCR gene amplification of copC genes from Microbacterium phyllosphaerae.

Expression system	*E. coli* BL21	
Vector	pET151	
Gene	copC886	copC1032
Forward primer (5' to 3')	CACCGTGAAAACCACAGCTCGCCGCC	CACCGTGAAAACCACAGCTCGC
Reverse primer (5' to 3')	CTATCGCTCCGTGGGGGCGTCG	CTATCGCTCCGTGGGGGCGTC
Forward primer (5' to 3') Excluding signal peptide	CACCCACGACAGCCTCCTCGCGTC	CACCCACGATCAGCTGGTCTCGAG
Reverse primer (5' to 3') Excluding signal peptide	CTATCGCTCCGTGGGGGCG	TCACAGATCGTCTGTCGTCC
Expression system	*R. jostii* RHA1	
Vector	pTipQC-II	
Gene	copC886	copC1032
Forward primer (5' to 3') Excluding signal peptide	TAAGCACATATGCACGACAGCCTCCTCGCGTC	TAAGCACATATGCACGATCAGCTGGTCTCGAGC
Reverse primer (5' to 3') Excluding signal peptide	TGCTTAAAGCTTTCCCTGAAAATACAGGTTTTCTCGCTCCGTGGGGGCGTCG	TGCTTAAAGCTTTCCCTGAAAATACAGGTTTTCCAGATCGTCTGTCGTCCGAGG

The purified products were used for ligation into the pTipQC-II expression vector, and after confirmation of the correct orientation and lack of mutations in these fragments, by plasmid sequencing, the vectors were used for transformation into *R. jostii* competent cells by electroporation. For protein expression, 1 L of Luria-Bertani broth (LB) supplemented with chloramphenicol were inoculated with *R. jostii* harbouring the expression vector for CopC886 and CopC1032 production (in separate experiments). This culture was incubated at 30 °C for 36 hours, then the inducer (thiostrepton 1 mg/mL) was added to give a final concentration of 1 µg/ml in the flask. The induced culture was incubated overnight, then the cells were harvested by centrifugation at 4000 x g for 15 minutes and disrupted by sonication in a lysis solution in presence of lysozyme. An additional step consisting in a pressure disruption was performed. The lysed solution was centrifuged at 10200 x g for 35 minutes, the supernatant was loaded into a NI-NTA resin column for IMAC purification, as the recombinant proteins were produced as N-terminal His_6 fusion proteins. After the protein purification step, an SDS PAGE gel did not show any band at the expected size (about 18 kDa),

though bands at a lower size appeared (about 10 kDa). However, these results were not reproducible and activity assays did not show any catalytic property for these solutions, giving inconclusive results about their expression in *R. jostii*.

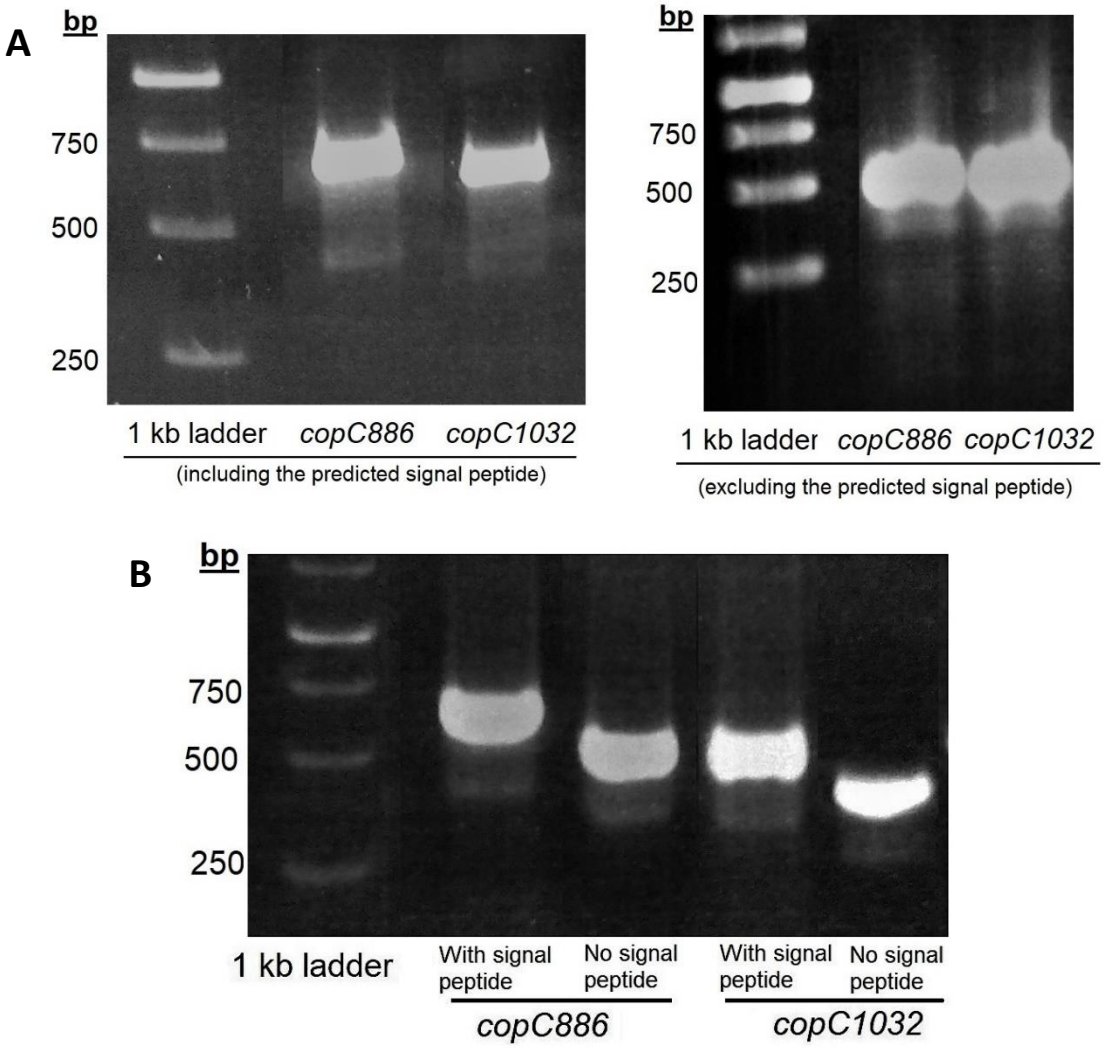

Figure 21. Agarose gel for PCR products of copC886 and copC1032, including and excluding their predicted peptide signal sequence. (A) PCR for E. coli based expression system. (B) PCR for R. Jostii based expression system.

Two new CopC proteins were selected for protein expression in *E. coli*, sourced from the Gram-negative bacterium, *B. xenovorans*. The proteins in question were named as CopC-Bx1 and CopC-Bx2. This time, a new approach was performed, by ordering synthetic genes codon optimized for expression in *E. coli* (GenScript). These genes were already cloned into the pET-28b(+) expression vector, which were transformed into chemically competent *E. coli* BL21 cells for protein expression. 1 litre of Luria Bertani media, supplemented with 80 µM $CuSO_4$ and 50 µg/mL of kanamycin, was used for recombinant protein expression and

induced with 1 mM IPTG. After cell harvesting, recombinant proteins were purified by immobilized metal ion chromatography (IMAC), which gave the expected protein bands at about 10 kDa for both CopC-Bx1 and CopC-Bx2 (**Figure 22**). Protein yields were low, ≈0.5 mg protein per litre of culture. Both proteins were subjected to TEV cleavage to remove the His_6 tag. The SDS gel showed two bands, one corresponding to the CopC-Bx1 at the expected ≈10 kDa size, whereas the band for CoPC-Bx2 showed a higher molecular weight, suggesting that the TEV reaction might have not worked for this protein. Unfortunately, not enough protein was expressed for copper content assays by ICP-OES or UV-Vis spectrum analysis.

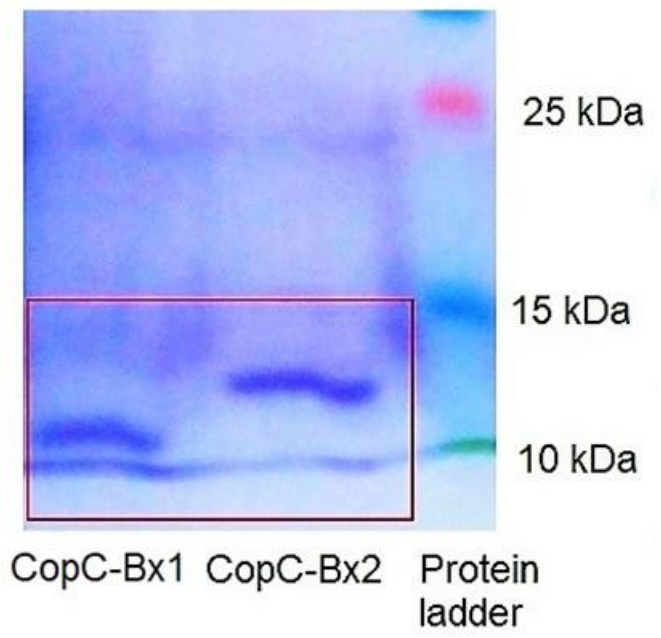

Figure 22. SDS PAGE of CopC-Bx1 and CopC-Bx2 proteins (red square), expressed recombinantly in *E. coli* BL21, after IMAC and TEV protease cleavage.

The identities of purified CopC-Bx1 and CopC-Bx2 were confirmed by protein analysis, using trypsin digestion. Samples of the proteins were sent to the Proteomics Research Technology Platform, School of Life Sciences, University of Warwick, for protein analysis. According to their report, the peptide data were used to interrogate the *E. coli* database and the two protein sequences Q13UF7 and I2IK44 (Uniprot), using uninterpreted MS/MS ions searches within MaxQuant software. Scaffold software was used to analyse and visualise the results from MaxQuant search (**Figure 23**). Both proteins of interest CopC-Bx1 (Q13UF7) and CopC-Bx2 (I2IK44) were identified in the samples. The protein CopC-Bx1 (Q13UF7) was identified with a coverage of 49%, whereas the protein CopC-Bx2 (I2IK44) was identified with a coverage of 68%.

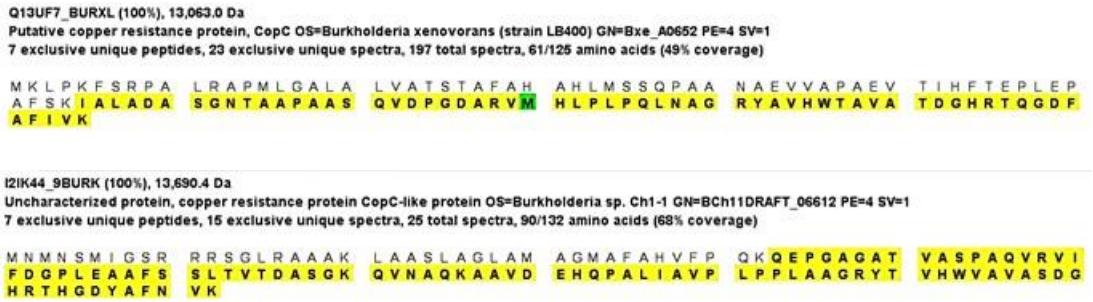

Figure 23. Mass spectrometry of CopC-Bx1 and CopC-Bx2 proteins, after trypsin digestion. Results generated by Scaffold software. The coverage of the sequence observed is shown highlighted in yellow. The native protein sequences include a signal peptide, so that the length shown is higher than the expected for the recombinant proteins (≈10 kDa).

3 Kinetic characterization of bacterial multicopper oxidases and CopC proteins

3.1 Introduction

Laccases and some multicopper oxidases (MCOs) can withdraw one electron from a substrate at the T1 copper site, then the subtracted electron is passed to the trinuclear cluster (TNC) by a Cys-His bridge, where four electrons are used to reduce oxygen into water. Laccases show oxidase activity; hence hydrogen peroxide is not needed for their activity. The reaction at the T1 site employs a one-electron Cu(II)-Cu(I) couple for the substrate oxidation by an outer sphere electron transfer, whereas an inner sphere electron transfer is used in the TNC for reduction of dioxygen [84, 86, 93, 163]. An outer sphere electron transfer (ET) takes place when the molecules that are exchanging electrons remain separate before, during and after the ET event (there is very weak or absence of electronic interaction between the molecules in the transition state), therefore the electron is forced to move through space from one redox centre to the other. Because of the outer sphere mechanism at the T1 site, substrate specificity is influenced by the nature of the docking/oxidation site formed between the substrate and the T1 copper site. The proteins performing this type of ET usually present a “moonlighting” behaviour, meaning that they have a broad specificity with many different substrates and they even may have multiple cellular functions [86]. This fact may explain the diverse biological functions assigned to LMCO, whereas acknowledging their function as oxidase enzymes at the same time.

Laccases can accept a wide range of substrates, including phenolic compounds, phenylpropanoids, azo dyes and indigo dyes [163]. The subtraction of a single electron from the substrate leads to the generation of a radical, which can follow different paths, subjected to the nature of the substrate, environmental conditions, the concentrations of the reactants and the presence of accessory enzymes. This is the basis of the reported versatility for laccases, as they can catalyse both cleavage (depolymerization) and coupling (polymerization) reactions and can perform other modification reactions as well [6, 48, 126, 163].

Normally, phenolic compounds are suitable substrates for laccase activity identification, especially methoxy-substituted compounds. ABTS (2,2'-azino-bis(3-ethylbenzothiazoline-6-sulphonic acid)), SGZ (syringaldazine), DMP (2,6-Di-methoxy phenol)

and guaiacol are among the most commonly used substrates for laccases, as their corresponding oxidised products show a colour change and can be easily detected by spectrophotometry assays. Laccases catalyse the oxidation of ABTS, SGZ, DMP and guaiacol; forming a stable cation radical, a quinone compound, and quinone dimers; which show a green, violet, yellow and brown colour, respectively [39, 188-193]. The reactions are shown in **Figure 24**.

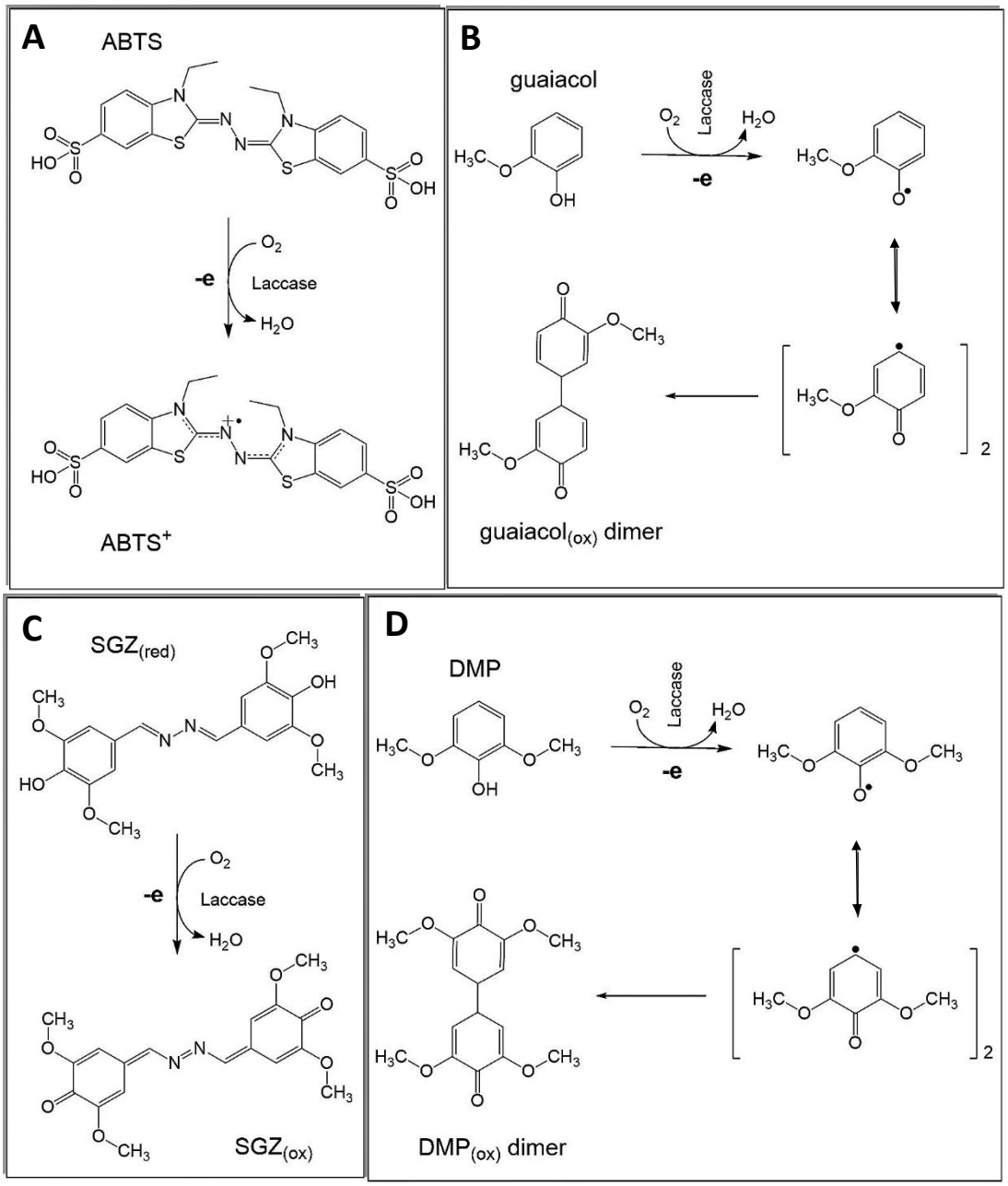

Figure 24. Proposed mechanism for the formation of coloured oxidation products, of common laccases substrates. (A) ABTS (2,2'-azino-bis(3-ethylbenzothiazoline-6-sulphonic acid)); (B) guaiacol (2-methoxyphenol); (C) SGZ (Syringaldazine or 4-Hydroxy-3,5-dimethoxybenzaldehyde azine); and (D) DMP (2,6-dimethoxyphenol).

In addition, these substrates have been used for the identification of laccase-producing strains, by using plates containing one of these compounds. After inoculation on these plates with the organism of interest, a colour change can indicate the presence of laccase activity [194]. The colorimetric method for detection of laccase activity is relatively easy, fast and cheaper when compared with other methods, such as the fluorometric or voltammetry methods [163], and it is commonly used for the quantitative determination of laccase activity. The measurement of activity under different conditions can give important information about the catalytic properties of an enzyme, including its stability, its optimum pH, and its kinetic parameters; these latter have been determined for several bacterial laccases and are shown in **Table 8**. The results suggest that there is a wide range of kinetic values for these enzymes, which support the idea that laccases can show different substrate preferences and even could play different biological roles, depending on the host, environmental conditions and reactant concentrations.

Table 8. Steady-state kinetic constants for several bacterial laccase-like multicopper oxidases (LMCOs). To allow comparison, some reported values were subjected to a change of units whenever was necessary. (*) Estimated from reported values.

Protein	Native organism	Substrate	Km [mM]	kcat [s^{-1}]	kcat/Km [s^{-1} M^{-1}]	Ref.
SmLac	*Stenotrophomonas maltophilia*	ABTS	0.16	1.18	7.38×10^3	[195]
		DMP	2.25	1.07	4.76×10^2	
CotA	*Bacillus licheniformis*	ABTS	0.0065	83	1.28×10^7 *	[196]
		SGZ	0.0043	100	2.33×10^7 *	
		DMP	0.0567	28	4.94×10^5 *	
CotA	*Bacillus subtilis*	ABTS	0.124	322	2.60×10^6 *	[175]
		SGZ	0.018	80	4.44×10^6 *	
		DMP	0.216	29	1.34×10^5 *	
MCO	*Klebsiella sp.* 601	ABTS	5.63	6640	1.18×10^6	[197]
		SGZ	0.023	11	4.78×10^5	
		DMP	0.487	1090	2.24×10^6	
Mrlac	*Meiothermus ruber* DSM 1279	ABTS	0.0273	5.42	1.98×10^5	[198]
		SGZ	0.0042	1.77	4.21×10^5	
		DMP	0.0031	1.92	6.18×10^5	
Tth-laccase	*Thermus thermophilus* HB27	ABTS	0.9	24.6	2.73×10^4 *	[199]
		SGZ	1.88	6.47	3.44×10^3 *	
LMCO	*Bacillus coagulans*	ABTS	0.031	69	2.23×10^6 *	[106]
		DMP	0.628	17	2.71×10^4 *	
LMCO	*Bacillus clausii*	ABTS	0.132	90	6.82×10^5 *	
		DMP	8.535	65	7.62×10^3 *	
CotA	*Bacillus pumilus*	ABTS	0.08	291	3.64×10^6 *	[99]
		DMP	0.68	11	1.62×10^4 *	

3.2 Kinetic characterization of laccase-like multicopper oxidases (LMCOs)

3.2.1 Enzymatic activity

All expressed proteins, Pp-CopA, Pf-CopA, Oc-CueO and P-PPO, were assayed for activity with common laccase substrates ABTS, SGZ, DMP, guaiacol and 2,4-dichlorophenol (DCP). Initially, a qualitative method was performed to determine the behaviour of these proteins, by evaluating the colour change of the reactions when incubated with the expressed LMCOs proteins after 5 minutes, in presence and in absence of copper ions (added in the form of $CuSO_4$) and hydrogen peroxide. The reaction mixture consisted of 1000 µL of 50 mM phosphate buffer (pH 7); 150 µL of protein solution at about 0.5 mg/mL; 150 µL of a 20 mM $CuSO_4$ solution; and 150 µL of a 10 mM substrate solution, except for SGZ whose concentration was 0.5 mM. In the case of DCP, addition of 4-amino antipyrine was needed (150 µL of a 10 mM solution) to make visible the colour change into purple. A qualitative approach (sight) was used to check colour changes. Results are shown in **Table 9**. Reactions containing Pp-CopA, Pf-CopA and Oc-CueO showed a colour change versus time, with all the assessed substrates, indicating that these proteins have catalytic activity. However, P-PPO was not active under any of the tested conditions. Two important features of the active proteins were found. Firstly, addition of hydrogen peroxide had no effect on the reaction, meaning that these proteins can perform an oxidase, and not a peroxidase, reaction [200]. Secondly, addition of exogenous copper ions was essential for their activity. As stated above, it was suspected that the expressed LMCOs proteins were generated as apoenzymes, which later was confirmed by spectroscopy and metal content analysis (section 2.2.3 Copper reconstitution). Therefore, addition of Cu^{2+} (in the form of $CuSO_4$) resulted in the formation of the holoenzyme, triggering their catalytic activity. However, when LMCOs were expressed under microaerobic conditions and after copper reconstitution, they did not need exogenous copper to be active, implying that under these conditions holoenzymes have been produced, though yield of expressed proteins decreased by approximately 70 % (**Table 4**) and the activity was also affected, since the final color change was not as intense as when exogenous Cu^{2+} was added. All experiments were carried out in triplicate, with a blank consisting in the addition of distilled water instead of protein solution. No significant delayed time was observed for the catalytic activity upon exogenous copper addition, as the change in colour

of the assayed substrates was found almost immediately after addition of copper, which could suggest a high affinity of these proteins for copper (II) ions.

Table 9. Qualitative activity of the expressed LMCOs, Pp-CopA, Pf-CopA, Oc-CueO and P-PPO. (+) means that the protein was active (colour change). (-) means that the protein was inactive (no colour change). (*) the colour change of the reaction containing guaiacol took longer time than reactions with other substrates, approximately 30 minutes.

		Proteins			
Substrate	Condition tested	Pp-CopA	Pf-CopA	Oc-CueO	P-PPO
ABTS	Neither $CuSO_4$ nor H_2O_2 added	-	-	-	-
	Only H_2O_2 added	-	-	-	-
	Only $CuSO_4$ added	+	+	+	-
	Both $CuSO_4$ and H_2O_2 added	+	+	+	-
SGZ	Neither $CuSO_4$ nor H_2O_2 added	-	-	-	-
	H_2O_2 added	-	-	-	-
	$CuSO_4$ added	+	+	+	-
	Both $CuSO_4$ and H_2O_2 added	+	+	+	-
DMP	Neither $CuSO_4$ nor H_2O_2 added	-	-	-	-
	H_2O_2 added	-	-	-	-
	$CuSO_4$ added	+	+	+	-
	Both $CuSO_4$ and H_2O_2 added	+	+	+	-
Guaiacol *	Neither $CuSO_4$ nor H_2O_2 added	-	-	-	-
	H_2O_2 added	-	-	-	-
	$CuSO_4$ added	+	+	+	-
	Both $CuSO_4$ and H_2O_2 added	+	+	+	-
DCP	Neither $CuSO_4$ nor H_2O_2 added	-	-	-	-
	H_2O_2 added	-	-	-	-
	$CuSO_4$ added	+	+	+	-
	Both $CuSO_4$ and H_2O_2 added	+	+	+	-

3.2.2 Effect of copper addition and pH

The active proteins, Pp-CopA, Pf-CopA and Oc-CueO were subjected to further biochemical and kinetic characterization. Most of the experiments performed with the active LMCOs were carried out with proteins expressed under fully aerated conditions, as the protein yields were higher, though apoenzymes were generated under these conditions. Hence, the addition of copper(II) was essential for activity, so that its influence on activity was investigated. A 10 mM solution of ABTS was used as substrate. The Pp-CopA, Pf-CopA and Oc-CueO protein solutions were at approximately the same concentration: 0.11 mg/mL, 0.14 mg/mL and 0.15 mg/mL, respectively. The reaction mixture consisted of 140 µL of acetate buffer at pH 4.1; 20 µL of protein solution; 20 µL of copper(II) solution ($CuSO_4$) at different concentrations; and 20 µL of ABTS substrate to give a final concentration of 1 mM. The reactions were measured continuously by a spectrophotometer at a wavelength of 420

nm. A total of 15 different copper standard solutions were prepared, with different concentrations from 0 to 15 mM, to give an effective copper concentration in the reaction that ranged from 0 to 1.43 mM. Results are shown in **Figure 25**.

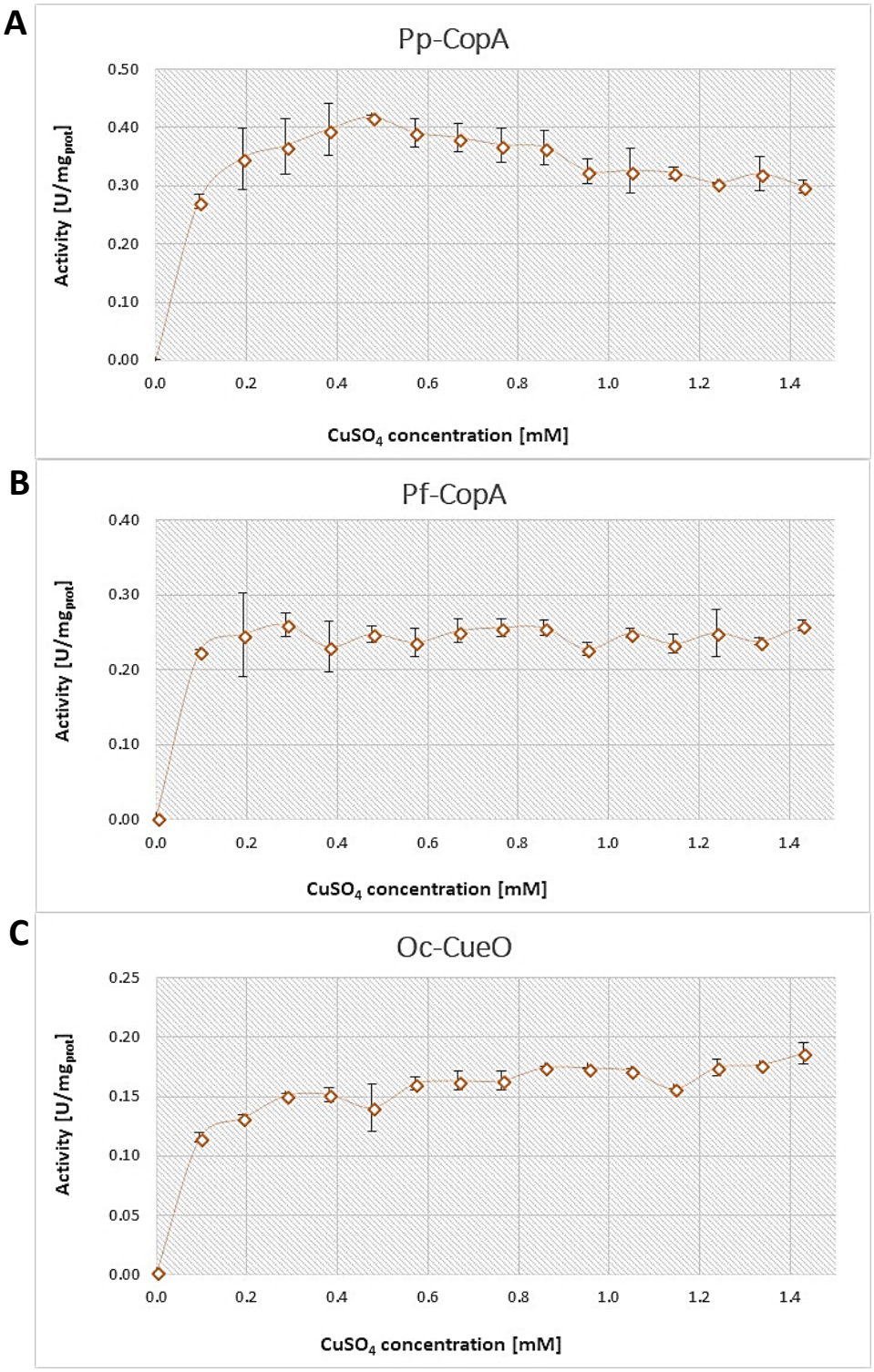

Figure 25. Effect of copper concentration on the activity of (A) Pp-CopA protein; (B) Pf-CopA protein; and (C) Oc-CueO protein. Activity has been represented as specific activity [U/mg$_{prot}$], using 1 mM ABTS as substrate.

A saturation behaviour was observed upon copper(II) addition. Activity increased as copper concentration increased, until a plateau was reached where the activity was not significantly affected by the increase of copper concentration anymore. Pp-CopA showed a slight decrease of activity when copper concentration surpassed 0.5 mM, while Oc-CueO showed a slight increase of its activity and Pf-CopA remained almost constant. Overall, the variations beyond the point of 0.5 mM were smaller than the variations observed before this point, indicating that the effect of copper concentration on enzyme activity is not significant at higher concentrations. Since the plateau (saturation) point was reached at copper concentrations as low as ≈0.2 mM, under the assayed conditions, it was expected that 0.5 mM copper (II) would ensure that the enzyme is fully active. Hence, 0.5 mM was established as the working copper concentration and it was used in all enzyme activity experiments. No significant inhibition was observed in the assayed range of concentrations, and though some differences were evidenced among LMCO proteins, the global behaviour was similar for all of them. Therefore, to investigate the effect of copper concentration in detail, only one protein was used, Pp-CopA. The copper effect on this protein was assessed by using ABTS as substrate and a lower range of copper concentrations. Results are shown in **Figure 26**. An increased enzyme activity was evidenced when either ABTS or copper concentration increased, which is typical of a double substrate kinetic behaviour. A plateau, common in saturation behaviour, was reached only at the highest value of substrate (ABTS) concentration, when copper concentration was above 2.3 µM (**Figure 26, A**). On the other hand, when copper was evaluated, the activity increased linearly, and the plateau was never reached (**Figure 26, B**), meaning that the saturation point for copper was not reached under these conditions, yet the protein was active even at copper concentration as low as 0.5 µM, indicating a micromolar affinity of this protein for copper.

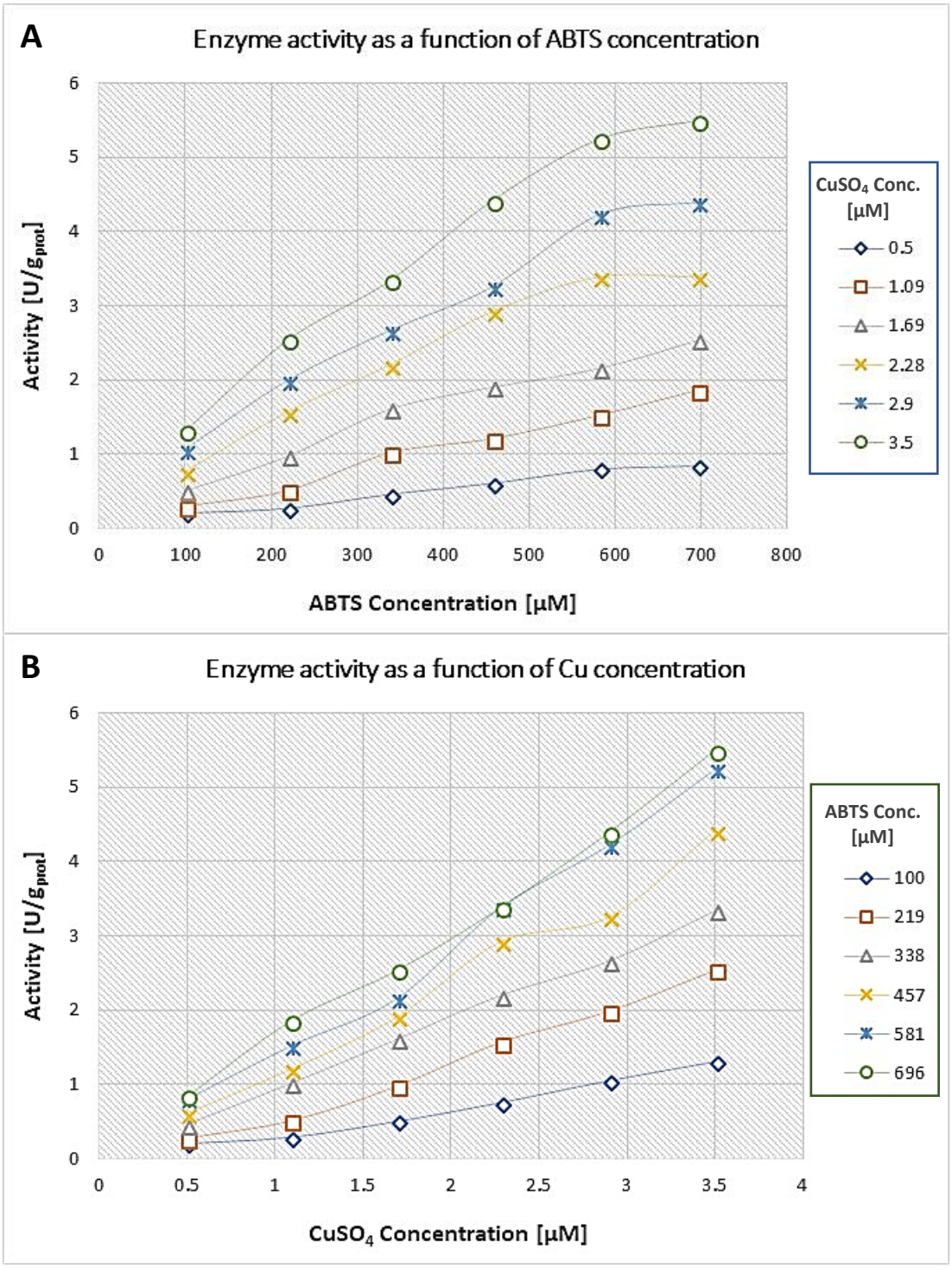

Figure 26. Effect of copper and substrate concentration on Pp-CopA activity. (A) Effect of substrate concentration on enzyme activity, at different concentrations of copper. (B) Effect of copper concentration on enzyme activity, at different concentrations of substrate (ABTS).

The conditions of the experiment were as follows: 150 µL of buffer acetate pH 4.1; 20 µL of Pp-CopA protein solution at a concentration of 0.3 mg/mL; and 20 µL of substrate and 20 µL of copper solution at different concentrations.

Once the copper dependence was established, another factor that can influence the enzyme activity was studied, the pH. SGZ and ABTS were used as substrates in a universal

Britton & Robinson buffer [201]. A total of 15 solutions of this buffer at different pH values were used, ranging from 1.75 to 11.3. The reaction mixture consisted of 150 µL of buffer; 20 µL of the substrate (either ABTS or SGZ); 20 µL protein solution and 20 µL of a 6 mM solution of $CuSO_4$. All experiments were performed by triplicate, and the concentrations of the protein solutions were 0.14 mg/mL, 0.11 mg/mL and 0.14 mg/mL, for Pf-CopA, Pp-CopA and Oc-CueO, respectively. Results are shown in **Figure 27**.

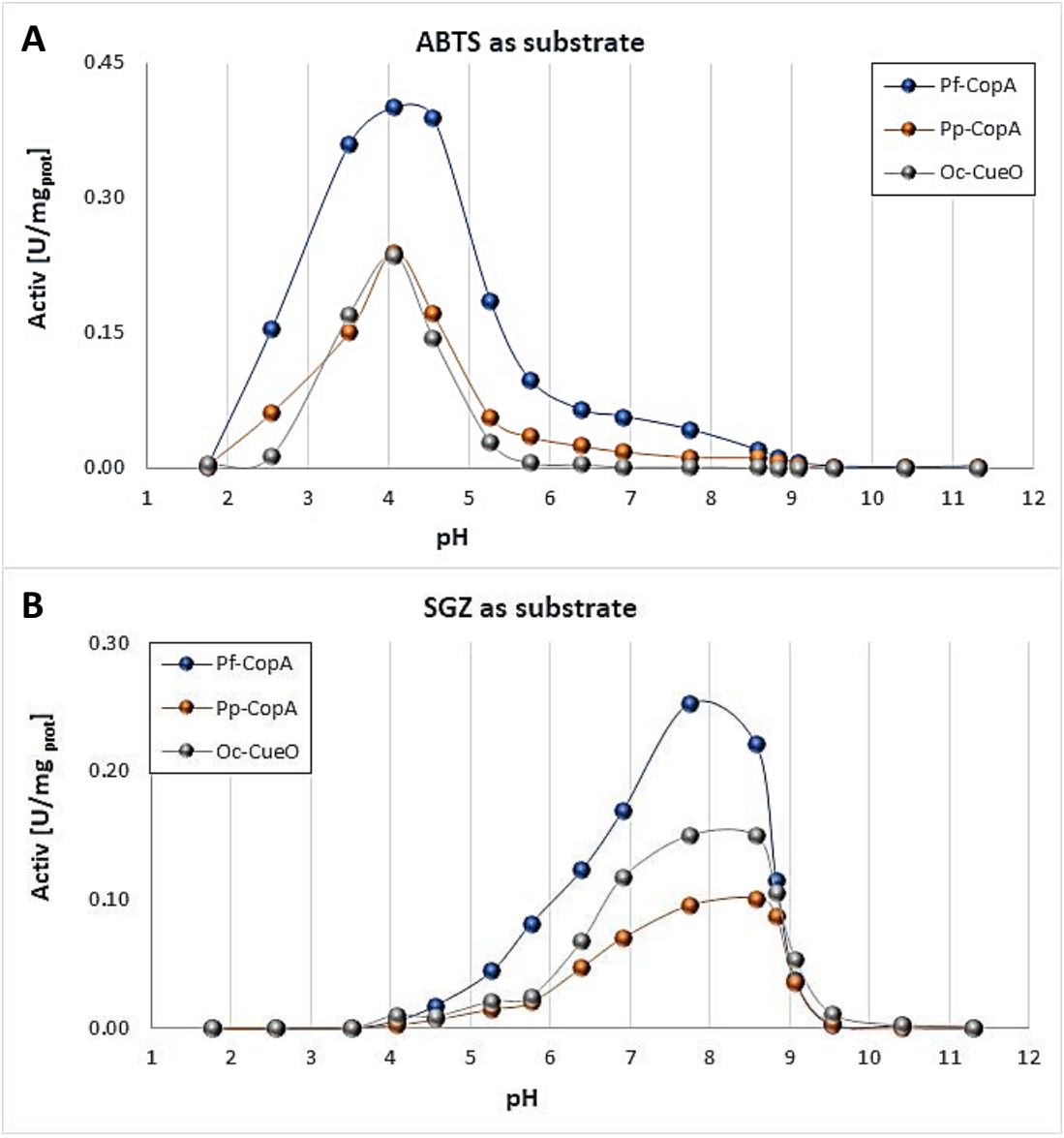

Figure 27. pH-activity profile of Pp-CopA, Pf-CopA and Oc-CueO with (A) ABTS and (B) SGZ.

The pH profile presented the typical shape for pH effect on enzyme activity, showing an optimal pH value that correspond to the maximum enzyme activity. pH values far from the optimal point resulted in moderate to complete loss of activity. Roughly speaking, these enzymes showed neither sensitivity nor stability for pH, as the range in which these enzymes were active varied ≈2 units of pH from the acidic to the basic side of the optimal pH value.

Considering that optimal pH value is an intrinsic characteristic of a couple enzyme-substrate, one optimal pH value was determined for ABTS and another for SGZ. For ABTS, an optimal pH of ≈4.1 was determined, while for SGZ, the optimal pH was ≈7.5. All three MCOs showed a similar pH profile, and the established optimal values agree with other reports that have identified similar optimal pH for bacterial laccases with ABTS and SGZ [196, 202, 203]. These reports have also found the optimal pH for DMP to be ≈7.0.

3.2.3 Steady state kinetic parameters

All active proteins, Pp-CopA, Pf-CopA and Oc-CueO, were assayed for activity with the common laccase substrates ABTS, SGZ and DMP, to determine their kinetic parameters. A total of eight standards at different concentration were prepared to measure the enzyme activity by spectrophotometry. For ABTS the standards concentrations ranged from 2.6 µM to 770 µM, while for DMP the standards concentrations ranged from 62 µM to 770 µM and for SGZ, from 3.1 µM to 77 µM. A wavelength of 410 nm (ε 36.8 L $mmol^{-1}cm^{-1}$), 530 nm (ε 65 $mmol^{-1}cm^{-1}$) and 468 nm (ε 49.6 $mmol^{-1}cm^{-1}$) were used for ABTS, SGZ and DMP, respectively. For ABTS, the reactions were carried out at a pH of 4.0, whereas a pH of 7.0 was used for SGZ and DMP. A copper(II) concentration of 0.5 mM was used in all experiments, and the concentration of protein solutions was ≈0.14 mg/mL. The reaction rate was plotted in relationship with the substrate concentration, then these data were linearized by using the Lineweaver-Burk and Eadie-Hofstee equations to determine the kinetic parameters. Results are shown in **Figure 28**. All experiments were performed in triplicate. Error bars represent the standard deviation and a summary of the results are shown in **Table 10** and in **Figure 29**. Linerizations can be seen in **Appendix 1**.

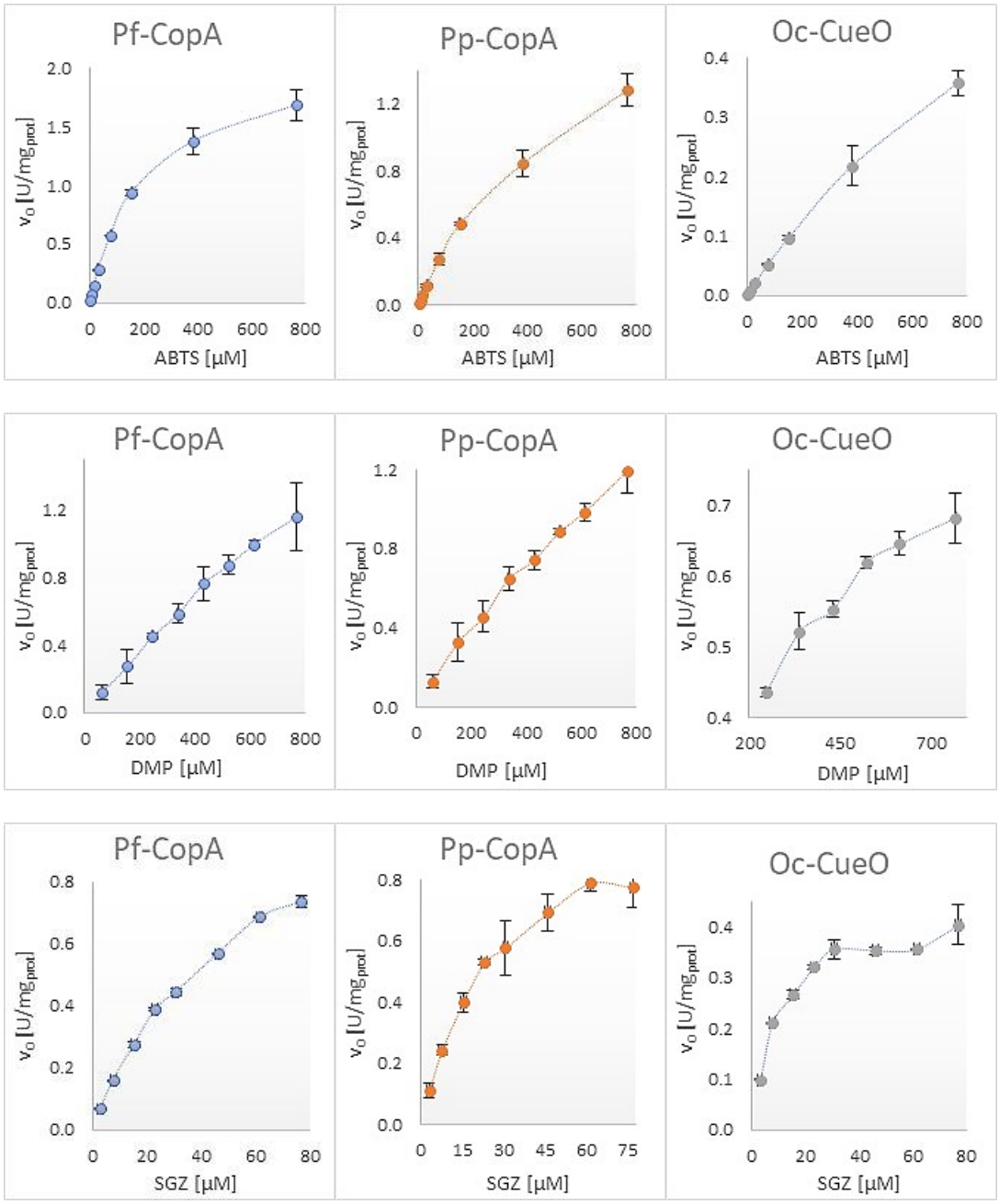

Figure 28. Steady state kinetic graphics of Pf-CopA (blue markers, in the left side), Pp-CopA (orange markers, in the centre) and Oc-CueO (grey markers, in the right side), with ABTS, DMP and SGZ. The substrate used is shown in the label of the "x" axis, in each graphic.

Table 10. Summary of Steady-state kinetic parameters for Pf-CopA, Pp-CopA and Oc-CueO, with ABTS, DMP and SGZ as substrates.

ABTS				
Enzyme	K_M [mM]	V_{max} [U mg_{prot}^{-1}]	k_{cat} [s^{-1}]	k_{cat}/K_M [s^{-1} M^{-1}]
Pf-CopA	0.214	2.18	2.19	$1.03 \times 10^4 \pm 163$
Pp-CopA	0.488	2.03	2.40	$4.91 \times 10^3 \pm 90$
Oc-CueO	1.463	1.02	0.93	$6.35 \times 10^2 \pm 34$
DMP				
Enzyme	K_M [mM]	V_{max} [U mg_{prot}^{-1}]	k_{cat} [s^{-1}]	k_{cat}/K_M [s^{-1} M^{-1}]
Pf-CopA	2.188	4.47	4.50	$2.06 \times 10^3 \pm 238$
Pp-CopA	1.459	3.37	3.97	$2.72 \times 10^3 \pm 132$
Oc-CueO	0.307	0.89	0.90	$2.93 \times 10^3 \pm 640$
SGZ				
Enzyme	K_M [mM]	V_{max} [U mg_{prot}^{-1}]	k_{cat} [s^{-1}]	k_{cat}/K_M [s^{-1} M^{-1}]
Pf-CopA	0.051	1.22	1.22	$2.40 \times 10^4 \pm 539$
Pp-CopA	0.026	1.09	1.28	$4.90 \times 10^4 \pm 2356$
Oc-CueO	0.004	0.51	0.46	$1.11 \times 10^5 \pm 3133$

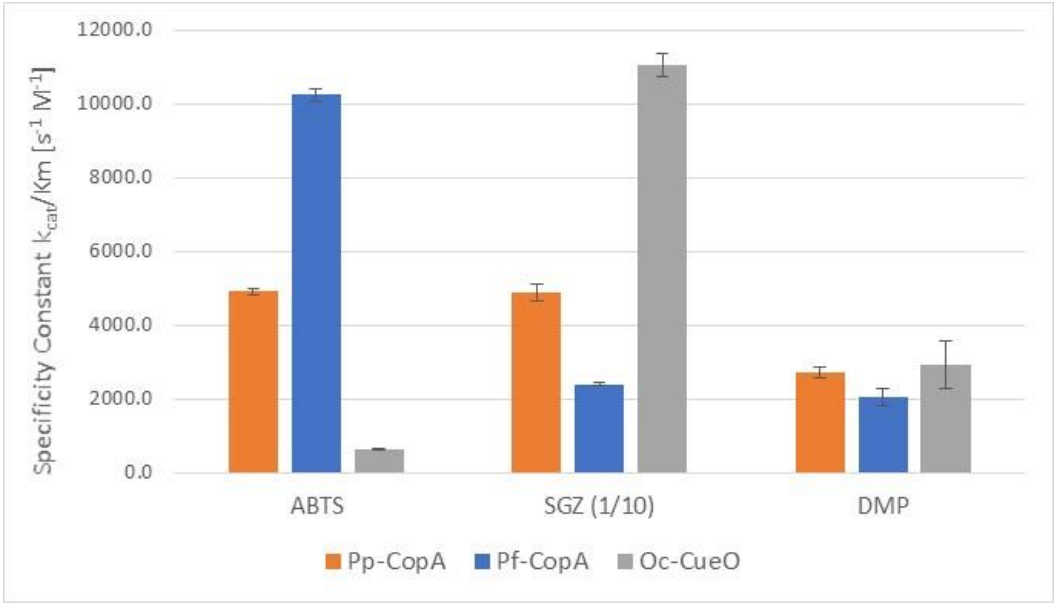

Figure 29. Specificity constants of Pf-CopA, Pp-CopA and Oc-CueO for ABTS, DMP and SGZ. Specificity constants for SGZ have been divided by 10 to allow its comparison in the same graphic.

The three enzymes showed broadly similar kinetic parameters, though Oc-CueO showed the lowest k_{cat} for all substrates; however, its specificity constant varied depending on the K_M value for each of them. For instance, Oc-CueO performed poorly towards ABTS, when compared with Pp-CopA and Pf-CopA, as its K_M was relatively high (1.463 mM);

whereas for SGZ it proved to be the most effective enzyme, as its specificity constant reached 1.11 x 10^5 s^{-1} M^{-1}, due to the low K_M value (only 0.004 mM), meaning a high affinity of Oc-CueO for SGZ. The CopA-type proteins, Pf-CopA and Pp-CopA, showed a similar behaviour, their kinetic parameters were very similar, specially k_{cat}, whose values were close to each other for all assayed substrates. The main kinetic difference between Pp-CopA and Pf-CopA was found in the K_M values, which made Pp-CopA more effective than Pf-CopA towards SGZ, while Pf-CopA proved to be more efficient with ABTS. Regarding DMP, the three enzymes presented similar specificity constants (**Figure 29**).

The specificity constant (k_{cat}/K_M), is a useful parameter for comparing the relative rates of an enzyme acting on different substrates [204]. In this context, the studied LMCOs showed similar performance with ABTS, SGZ and DMP, when compared with other bacterial laccases. For instance, SmLac from *Stenotrophomonas maltophilia* shows a specificity constant of 476 s^{-1} M^{-1} for DMP, while an MCO from *Klebsiella sp*. 601 shows a specificity constant of 1.18 x 10^6 s^{-1} M^{-1} for ABTS (**Table 8**). The specificity constants calculated for the LMCOs under study, ranged from 636 s^{-1} M^{-1} (Oc-CueO towards ABTS) to 1.11 x 10^5 s^{-1} M^{-1} (Oc-CueO towards SGZ) (**Table 10**), which is in the range of the reported values for bacterial laccases. However, the limitations of this method of comparison should be considered, since even if a given enzyme presenting a high specificity constant can catalyse a reaction faster than one with a lower specificity constant, the ratio of the two reaction rates is not a constant and depends on the value of $[S]/K_M$ [204]. In other words, for an accurate comparison between enzymes, they should be tested under the same conditions, especially the substrate concentration. Although the specificity constant is useful parameter for a broad comparison, there is a possibility that under different conditions a given enzyme with a low specificity constant can perform a reaction faster than another with a high specificity constant, depending on the enzyme and substrate concentrations.

3.2.4 Comparison with a commercial fungal laccase and thermal stability

Since the catalytic activity proved to be very similar between Pp-CopA and Pf-CopA and based on the availability of Pp-CopA due to its relatively high yield of protein expression, Pf-CopA was omitted in these experiments. Pp-CoPA and Oc-CueO were used to compare their thermal stability and their relative activity, with the commercial fungal laccase from *Trametes versicolor* (TvL). For thermal stability, only ABTS was used as substrate, and for enzyme activity, both ABTS and SGZ were used as substrates. A preliminary assay showed that TvL was the fastest enzyme when tested towards ABTS, and despite that the experiment

was meant to keep the same conditions for all enzymes, this was not possible for TvL due to its high reaction rate, so that the range of substrate concentrations was significantly lower (10 fold) for TvL than the range of concentrations used for Pp-CopA and Oc-CueO. An opposing effect was observed when the enzymes were tested towards SGZ, and in this case the concentration of Pp-CopA and Oc-CueO protein solutions were lower than the protein concentration of TvL. Hence, a relative comparison in terms of percentage was carried out, taking as 100 % the highest activity presented for any enzyme. Results are shown in **Figure 30**.

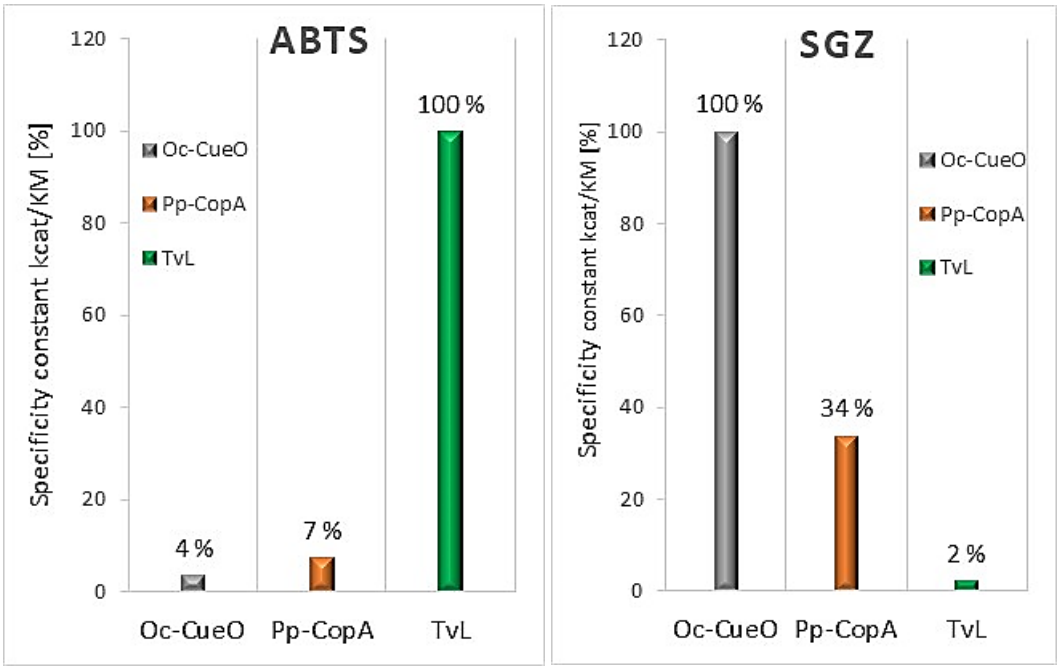

Figure 30. Relative comparison of the specificity constants of Oc-CueO and Pp-CopA with *Trametes versicolor* fungal laccase (TvL), with ABTS (left) and SGZ (right) as substrates.

The fungal laccase TvL was the fastest enzyme towards ABTS, its specificity constant surpassed the Oc-Cue and Pp-CopA constants by 25-fold and 14-fold, respectively. Similar catalytic performances have been reported [142], and it is commonly accepted that fungal laccases usually are more active than their bacterial counterparts [81, 90]. However, when SGZ was used as substrate, the best performance was achieved by Oc-CueO, followed by Pp-CopA, both exceeding the TvL catalytic efficiencies by 50-fold and 17-fold, respectively. This finding could suggest that, even if these proteins could be not very active with one substrate, they might perform extremely well with another substrate, so that they can be attractive for some specific applications. The reason for these preference for SGZ over ABTS is not known.

For stability, 100 % was considered as the activity presented at the beginning of the experiment. In this assay, all enzymes were incubated at 50 °C and after different intervals

of time, an aliquot of the incubated enzyme solution was taken and added to a reaction mixture at room temperature containing acetate buffer at pH 4.0, $CuSO_4$ at a concentration of 0.5 mM, and ABTS at 2 mM. Then the reaction was measured for absorbance changes by spectrophotometry. Results are shown in **Figure 31**.

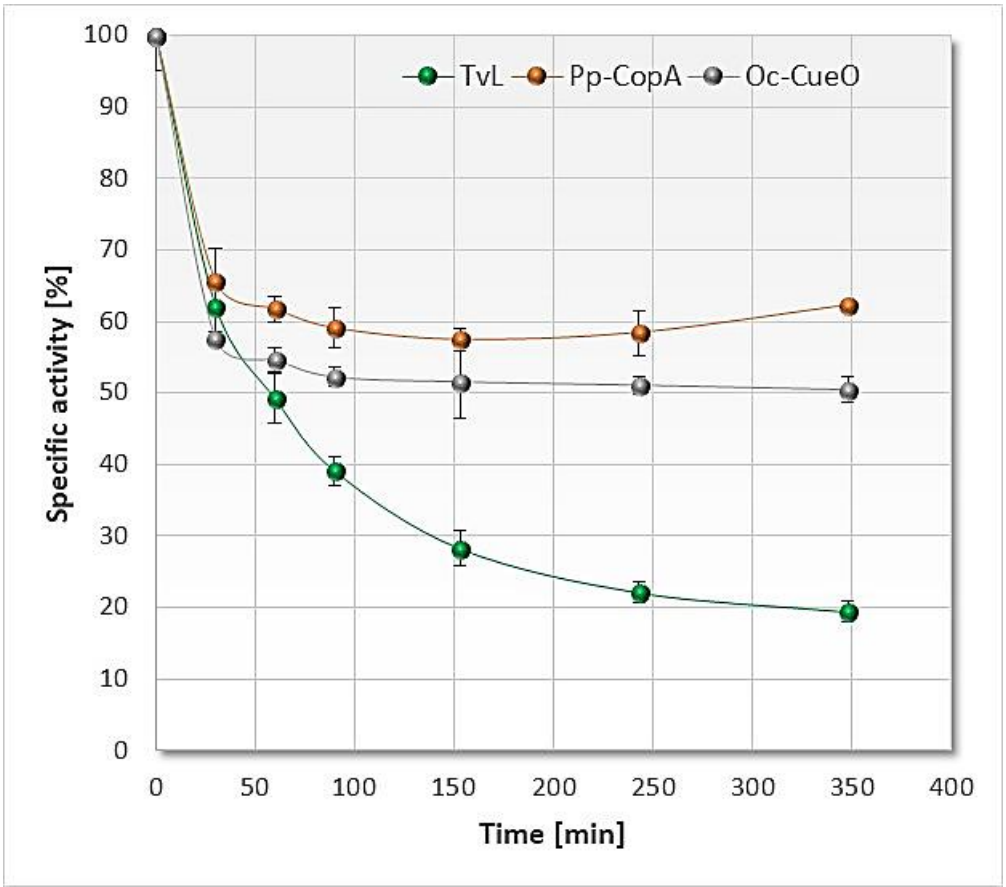

Figure 31. Stability comparison between bacterial laccases Oc-CueO and Pp-CopA with the commercial fungal laccase TvL, with ABTS as substrate. Error bars are SD, n = 3.

While it is commonly acknowledged that fungal laccases are more active than bacterial laccases, it has been also reported that bacterial laccases tend to be more stable, as they can tolerate extreme pH, temperature, and salinity conditions, making bacterial laccases very interesting for industrial applications [163]. The results shown in this section agree with those findings, and although the LMCOs under study have not performed extraordinarily well regarding pH-profile activity, Pp-CopA and Oc-CueO have proved to be more stable than the fungal laccase TvL. Moreover, these enzymes have shown a significant activity towards SGZ, being even more catalytically efficient towards this substrate than the

commercial TvL, suggesting that these enzymes could have some interesting applications, depending on the preferences shown for a given substrate.

3.2.5 Redox potential

Redox potential is an important feature of laccases, as it can determine the catalytic activity and the range of substrates that a given laccase can accept (Section 1.6, Laccases: properties and structure). Usually, fungal laccases present high redox potential, while bacterial laccases tend to be low redox potential enzymes [90]. Pp-CopA and Oc-CueO were used for redox potential analysis, with the collaboration of Dr Rachael Wilkinson, Research Fellow at Life Science Department in the University of Warwick. Some of the conditions tested include different buffers (Sodium acetate, pH 5, 5.5 and 6; sodium phosphate buffer, pH 4.1 and 4.5), platinum and gold working electrode, in solution and on electrode, varying scan rates, in the absence and in presence of $CuSO_4$ and the use of different concentrations of ABTS (0.2 or 1 mM) and with SGZ as an alternative mediator. Unfortunately, these approaches were unsuccessful, and no results were obtained as the data from cyclic voltammetry experiments was not satisfactory, the peak in cathodic current was observed only in the first scan, suggesting a loss of enzyme, while the peak in the anodic current was not clear. **Figure 32** shows the scans for Oc-CueO and Pp-CopA at lower scan rates.

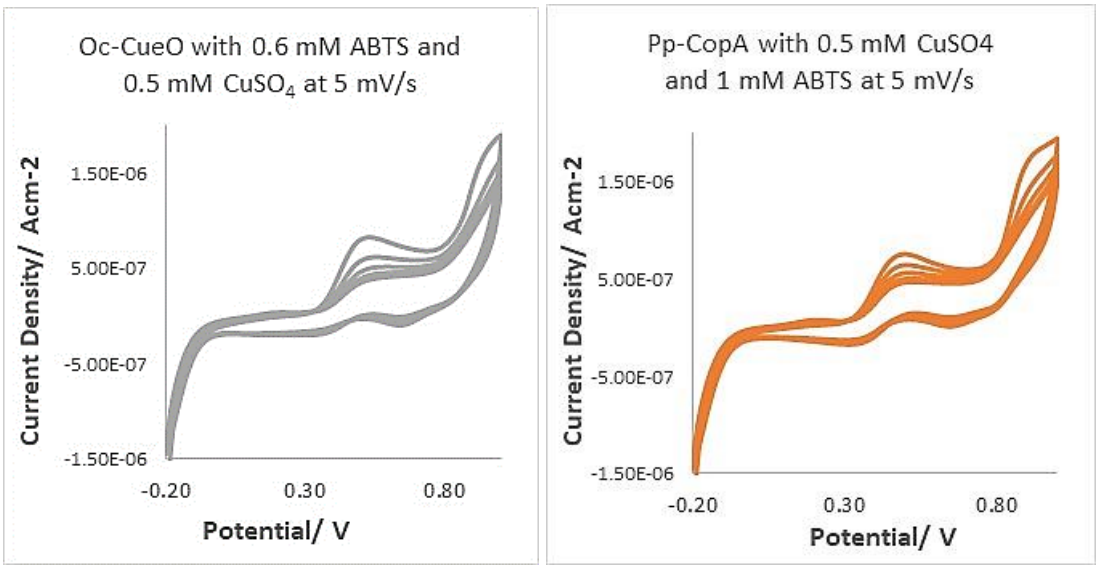

Figure 32. Cyclic voltammograms of Oc-CueO and Pp-CopA with ABTS.

Slower scan rates were assessed to improve definition of peaks. The method used to cover the electrode with enzyme however resulted in consistent loss of enzyme along the time, therefore the improvement in peak definition was reduced by the loss in signal from

the lower residual enzyme concentration. Anaerobic conditions could give better results (due to potential oxidation of the enzyme) but those experiments were not feasible to be carried out in Life Sciences.

3.3 Kinetic characterization of CopC-bx1 and CopC-bx2

The expressed CopC proteins were tested for activity, in the same way as LMCOs were assessed. Activity was assayed in presence and in absence of copper ($CuSO_4$) and hydrogen peroxide (H_2O_2), individually and together, due to the possibility of the formation of a protein complex or multiprotein. Since only one site was identified for copper attachment in these proteins, and two putative genes for CopC proteins were found in the native host, there was a possibility that the two polypeptide chains may have different functions and could form a multimer. ABTS, SGZ, DMP, guaiacol and 2,4-DCP were used as substrates. Results for ABTS, guaiacol and DCP are shown in **Figure 33**. As negative control, buffer was used instead of protein, and Pp-CopA was used for positive control.

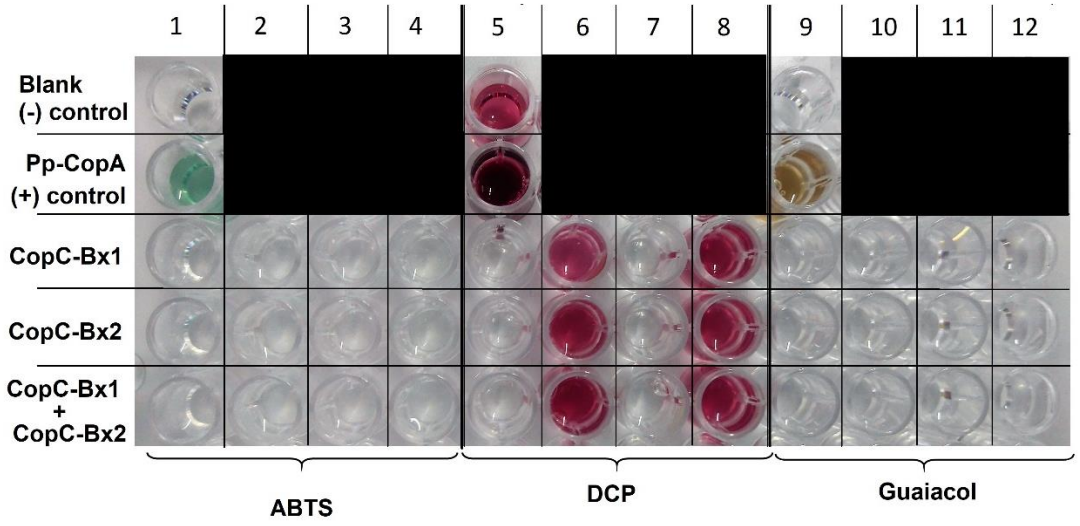

Figure 33. CopC-Bx1 and CopC-Bx2 activity with the common laccase substrates: ABTS, DCP and guaiacol. Negative and positive control are shown in 1st and 2nd row, and in columns 1, 5 and 9, for ABTS, DCP and guaiacol, respectively. For CopCs assays rows, conditions were as follows: columns 1, 5 and 9: no additives; columns 2, 6 and 10: $CuSO_4$ added; columns 3,7 and 8: H_2O_2 added; and columns 4, 8 and 9: $CuSO_4$ and H_2O_2 added.

Experiments were also carried out with and without cleavage of the His_6 fusion tag by Tev protease. Results showed that these proteins were not active towards common laccases substrates, under any of the conditions tested. The proteins were added later in combinations with LMCOs to see whether CopC proteins can accomplish functions as

accessory enzymes or not, which is detailed in the next chapter. However, those experiments did not show any activity for CopCs. These results may suggest that CopC proteins have no catalytic properties, and the previously reported involvement in copper traffic would remain as their only function. However, it should be considered that many problems were found during expression and the yields achieved were very low. Also, the CopC sequences of *B. xenovorans* were significantly smaller than other putative CopCs identified in other bacterial lignin degraders, hence those CopCs might show a different catalytic behaviour.

4 Activity of multicopper oxidases on lignin model compounds and polymeric lignin

4.1 Introduction

The role of laccases in lignin degradation is controversial, as both polymerization and depolymerization laccase catalysed reactions have been reported. As stated before, there are observations supporting the participation of laccases in lignin degradation and, conversely, there are indications suggesting that laccases are not essential for lignin degradation (Section 1.7, Role of laccase in lignin degradation). Laccases can generate reactive radicals from lignin, which depending on the environmental conditions, can be subjected to further reactions of modification, coupling or cleavage (**Figure 9**). The precise details of this are yet to be understood, and more than one enzyme, cofactor, or free radical could be involved. The relatively low redox potential of laccases has also been discussed as a potential barrier for lignin degradation, as most subunits present in native lignin are non-phenolic and their cleavage requires high redox potentials that laccases do not reach [6, 116]. However, the discovery of small molecules that can modulate laccase redox potential, called mediators, might overcome this issue [49]. Laccases can react with lignin, at least to some extent (e.g. catalysing polymerization or modification reactions), but the utilization of mediators could lead to novel and interesting reactions and products. Hence, the potential applications of laccase-mediator systems (LMS) in industrial processes utilizing lignocellulosic materials, have gained a lot of attention [6, 205]. A thorough knowledge about the mechanisms and the types of products generated by laccases, in the presence and absence of mediators, is of critical importance to understand the role of laccases in lignin degradation.

To understand the effect of laccases on lignin, polymeric lignin would be the obvious choice to be used as substrate in enzymatic assays. Nevertheless, the intricate structure of this material makes the underlaying mechanism of any possible transformation very challenging to elucidate. Therefore, the replacement of lignin as substrate with smaller molecules similar to lignin subunits or oligomers, called lignin-model compounds, represents a frequently accepted approach to test the catalytic properties of ligninolytic enzymes [6, 205]. Since phenolic compounds usually present low redox potential (0.5 to 1.0 V vs. normal hydrogen electrode), suitable for electron subtraction by laccases, several phenolic dimers have been used as lignin-model compounds, especially compounds representing the most

common bond within the lignin, the β-O-4' (**Figure 34**), are widely used in laccase and LMS experiments [6, 9, 205].

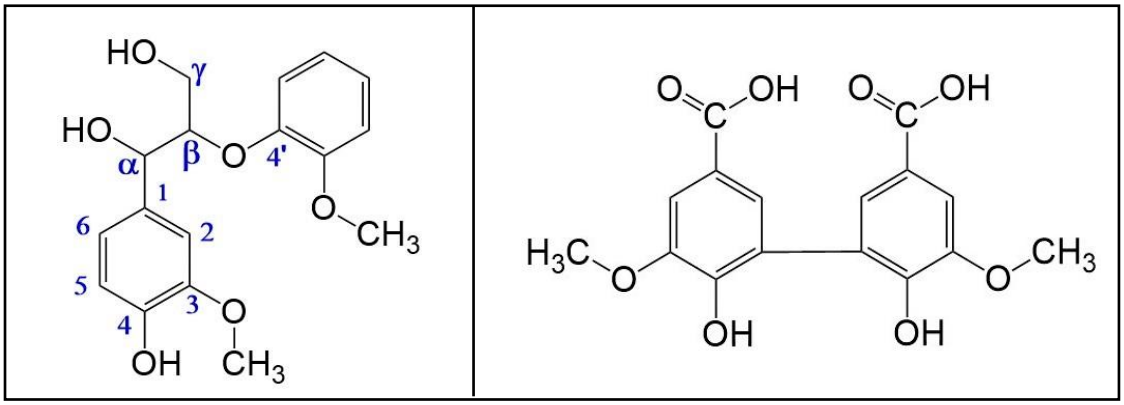

Figure 34. Lignin-model dimers used as substrates in ligninolytic enzymes assays. Left: Guaiacyl glycerol-β-guaiacyl ether, GGE, representing the common β-O-4' bond, found in lignin. Carbon positions are labelled in blue. Right: Biphenyl dimer 2,2'-dihydroxy-3,3'-dimethoxy-5,5'-dicarboxybiphenyl, DDVA, representing a carbon 5- carbon 5' bond.

In early studies, monomer subunits were used for this type of experiments, however in recently years, lignin-model compounds containing at least two aromatic rings are frequently used, and these compounds could be phenolic or non-phenolic [9]. In β-O-4' and β-1' phenolic lignin dimers, it has been reported that laccases can perform the following transformation shown in **Figure 35**: Cα-oxidation, which can lead to ketone (products 1 and 2) or aryl-Cα cleavage (product 6); cleavage at the Cα-Cβ (product 3); or cleavage of the Cα-C1 bond [116, 119, 125]. Results vary depending on the enzyme used, and often one enzyme can generate multiple products. Laccase-mediator systems (LMS) tend to favour the formation of smaller products, and even the aromatic ring cleavage of a non-phenolic lignin-model compound has been reported; while laccase alone might result in coupling reactions [6, 205, 206]. Regarding C-C bonds, model compounds representing a 5-5' and 5-α' bonds, in presence of laccase, have resulted in bond cleavage by oxidative side-chain reactions, yet the central C-C bond remained intact [207]. So far, there is no evidence demonstrating that laccase alone can break-down bonds in non-phenolic model compounds [6]. A summary of the products generated by laccase alone and by LMS, from β-O-4' lignin model compounds, is presented in **Figure 35**. A summary of the products generated from C-C lignin-model compounds is presented in **Figure 36**.

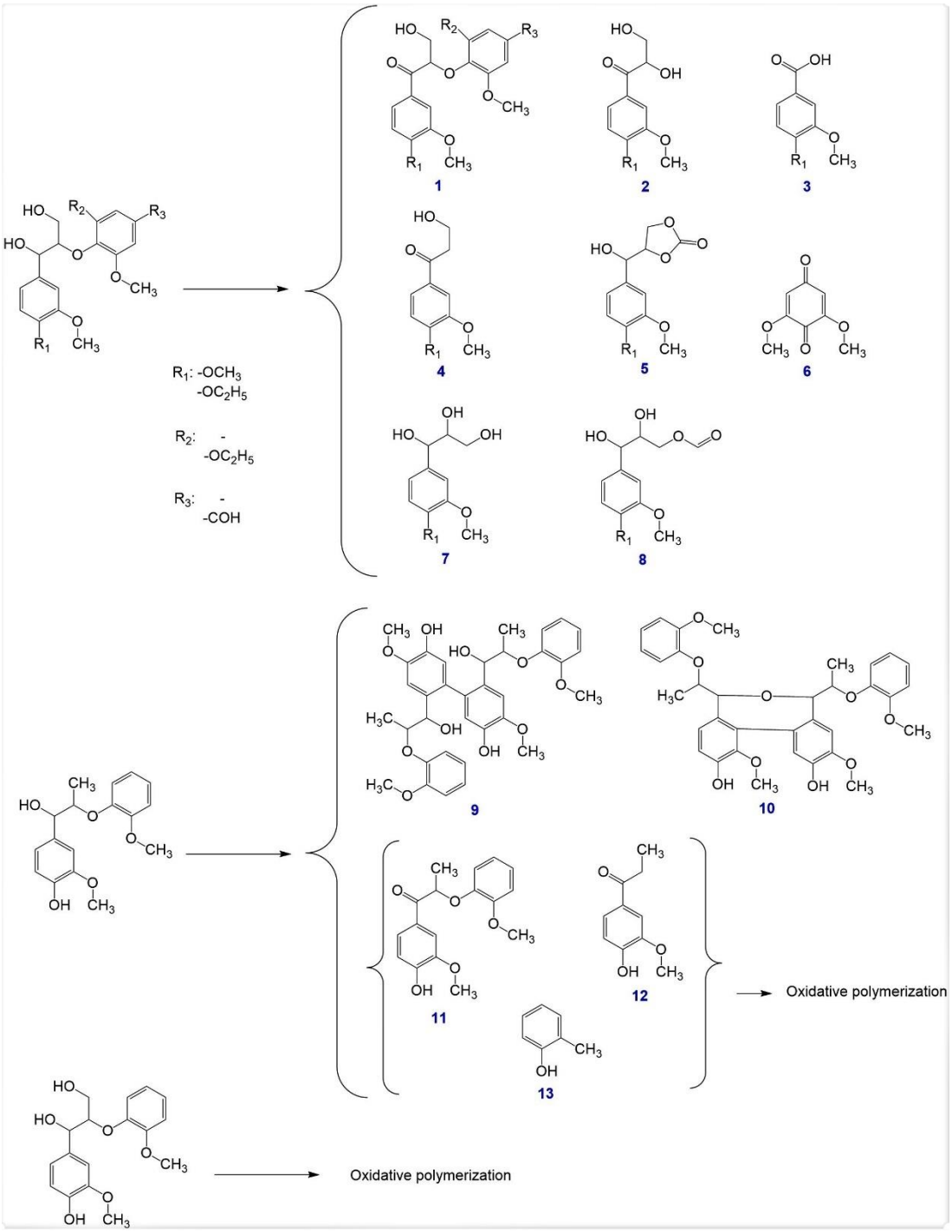

Figure 35. Summary of products obtained from lignin-model compounds representing the β-O-4' bond. Compounds 1 to 8 are arranged according to its reported frequency, from high (1) to low (8). These products were derived from non-phenolic lignin-model dimers under LMS conditions. Products 9 and 10 were obtained using laccases alone, while products 11, 12 and 13 were generated in LMS experiments. The products derived from phenolic lignin-model dimer lead to coupling reactions. Adapted from [205].

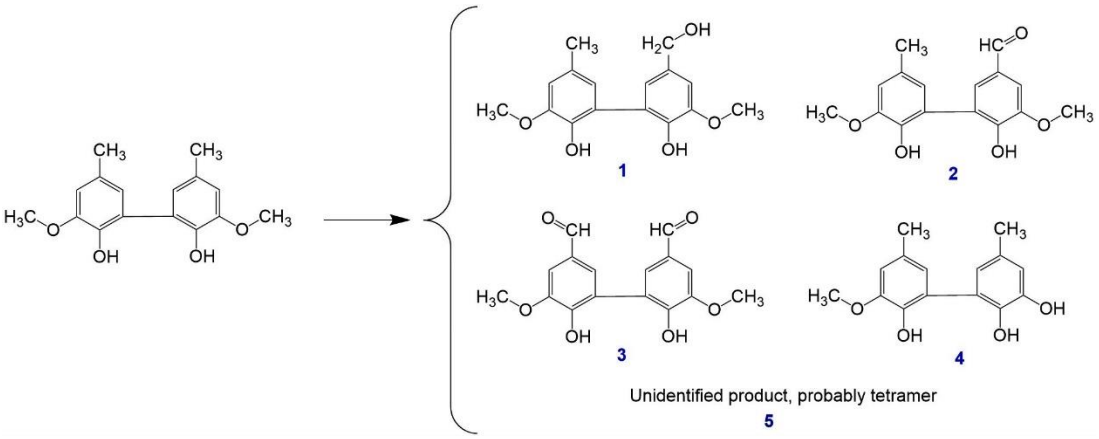

Figure 36. Summary of products obtained from lignin-model compounds representing a biphenyl (5-5') C-C bond. The presence of a mediator (either ABTS or HBT) did not significantly affect the product distribution. Adapted from [207].

A comparison of the type of products generated, based on the nature of the lignin-model compounds, reveals that the substitution of the phenolic rings influences the cleavability of the β-O-4' ether bond and modifies the range of products generated. Lignin-model dimers containing phenolic hydroxyl groups, such as GGE shown in **Figure 34** and **Figure 35**, leads to coupling reactions, regardless of whether a mediator is present or not. On the other hand, cleavage of the β-O-4' ether bond has been observed only in lignin-model compounds lacking phenolic hydroxyl groups, although the presence of a mediator is essential [205].

These kinds of experiments can provide valuable information about the reactions that laccases can perform on lignin-model compounds. However, most of these studies give only qualitative descriptions of the type of products formed, as a means to elucidate the biochemical pathways followed by laccases, but they often fail in determine the quantitative values of the reaction rates or the conversion yields, which tend to be low (less than 20% conversion) [208, 209]. Moreover, the results from these experiments might not be extrapolated to reactions with polymeric lignin, as lignin-model compounds only represent a very specific and narrow characteristic of a very complex and heterologous material. Therefore, it is important to confirm that the action of laccases with lignin-model compounds can also occur with polymeric lignin, the real substrate of interest.

Lignin reactivity is affected by the functional groups on its surface, which comprise phenolic hydroxyl, methoxyl, benzylic hydroxyl, benzyl alcohol, acyclic benzyl ether, and carbonyl groups. The most common linkage in lignin, the β-O-4' bond, can be oxidized to aromatic carbonyl compounds and carboxylic acids [210]. However, it must be noted that lignin is not a single type of molecule, but a heterogeneous material comprising different

characteristics (For more information, see section 1.3, Lignin sources and characterization). Lignosulfonate was one of the first types of lignins tested, as its relatively high molecular weight can be representative of real lignin, and it has a good water solubility. A study demonstrated that laccase activity on lignosulfonate involves both polymerization and depolymerization, depending on the molecular weight of the substrate [211]. It is currently widely accepted that the main effect of laccases alone on lignin is to catalyse polymerization reactions, whereas LMS can shift the activity of laccases towards lignin depolymerization, though the extent and efficiency of this shift varies. The effect of laccases could not be limited to these two types of reactions, as several modifications may also take place that can modified the physical and chemical properties of lignin, including its solubility and reactivity. Moreover, there is a chance for a possible synergistic effect when laccases are combined with other ligninolytic or accessory enzymes. However, these type of studies are difficult to carry out and so far there is not enough information on using combinations of enzymes [6, 205].

4.2 Enzyme activity of laccase-like multicopper oxidases (LMCOs) on lignin-model compounds

Pp-CopA, Pf-CopA and Oc-CueO were tested for activity with the lignin-model compounds GGE and DDVA (**Figure 34**), representing the β-O-4' and a 5-5' bonds, respectively. The reaction mixture consisted of buffer (100 mM acetate buffer, pH 4.0; or 20 mM Hepes with 80 mM NaCl buffer, pH 7.0); an enzyme solution (≈0.5 mg/mL); a 20 mM substrate solution (GGE was dissolved in methanol, while DDVA was dissolved in dimethyl sulfoxide (DMSO)); and a solution of $CuSO_4$ as copper supplement, in a final concentration of 0.5 mM. At first, only one protein was assayed, Pp-CopA, to determine the best conditions for the enzymatic reactions. Two different pH were evaluated (pH of 4 and 7), giving a pH of 7 as the pH that promote a higher product generation. The generation of product along the time was monitored by taking samples each 30 minutes, then the reaction was stopped with a 5 M HCl solution, and the product generation was measured by HPLC, monitoring by UV-Vis. Results showed the appearance of new peaks in the UV-Vis chromatogram, indicating that this protein was active towards these substrates. Once the activity was confirmed and the best conditions for the enzymatic reactions were established, all LMCOs, Pp-CopA, Pf-CopA and Oc-CueO, were tested for activity with these lignin-model compounds, in presence and in absence of mediators. SGZ and ABTS were used as mediators. The results in presence of ABTS as mediator and in absence of a mediator are shown in **Figure 37** for GGE and in

Figure 38 for DDVA. As negative controls, two different mixture compositions were used, one contained a buffer instead of the protein solution, while the other had all components listed for these reactions, including the protein solution, but they were performed in absence of copper. Both negative controls gave no product formation and confirmed the dependence of these protein for copper, when they are produced as apoenzymes.

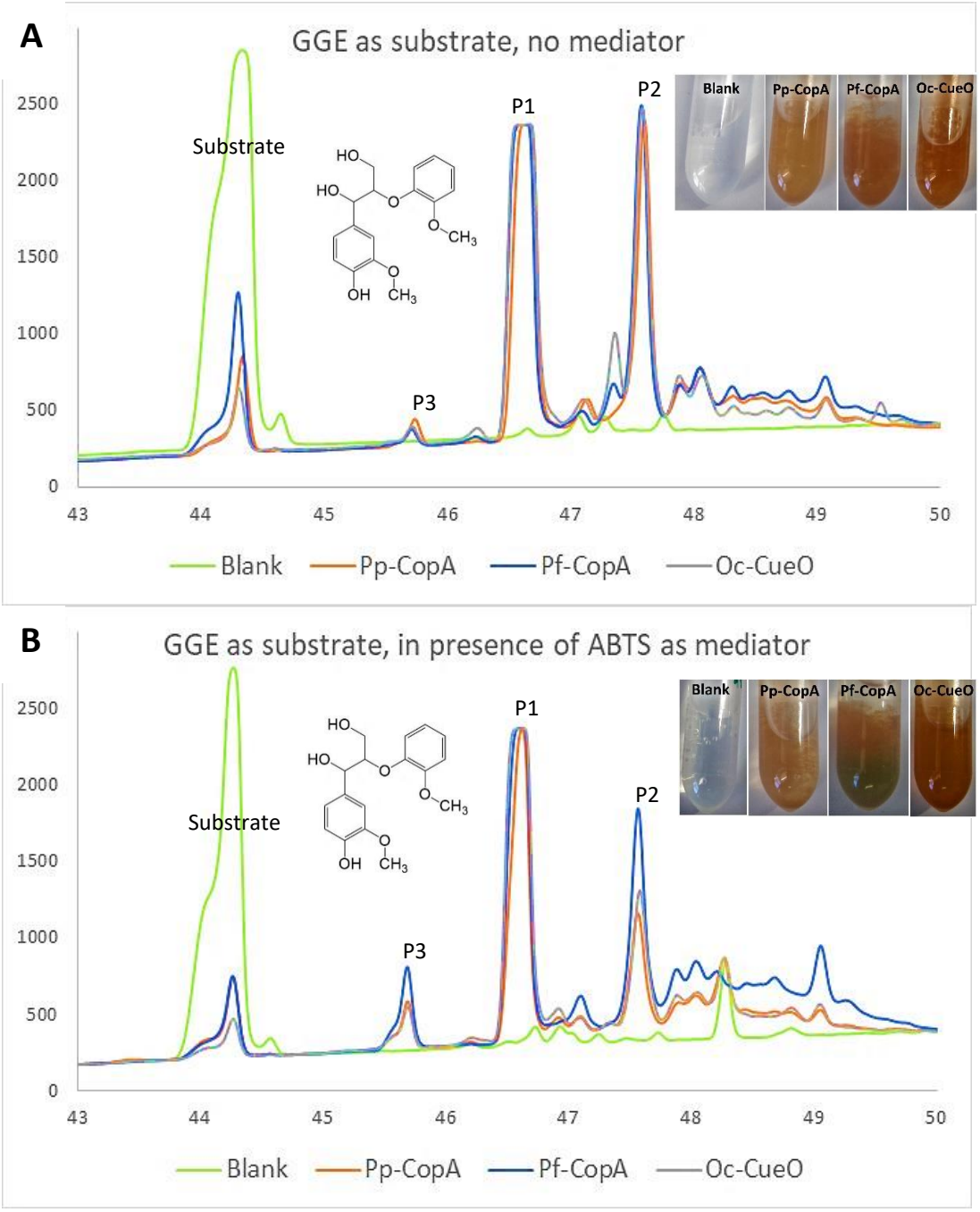

Figure 37. UV-Vis chromatograms showing products formation after reaction of the lignin-model compounds GGE, with Pp-CopA, Pf-CopA and Oc-CueO. In the right-upper side of each graphic, a photo shows the actual reaction after incubation of each enzyme with the substrate. (A) Reaction performed in absence of a mediator. (B) Reaction performed in presence of 1 mM ABTS as mediator.

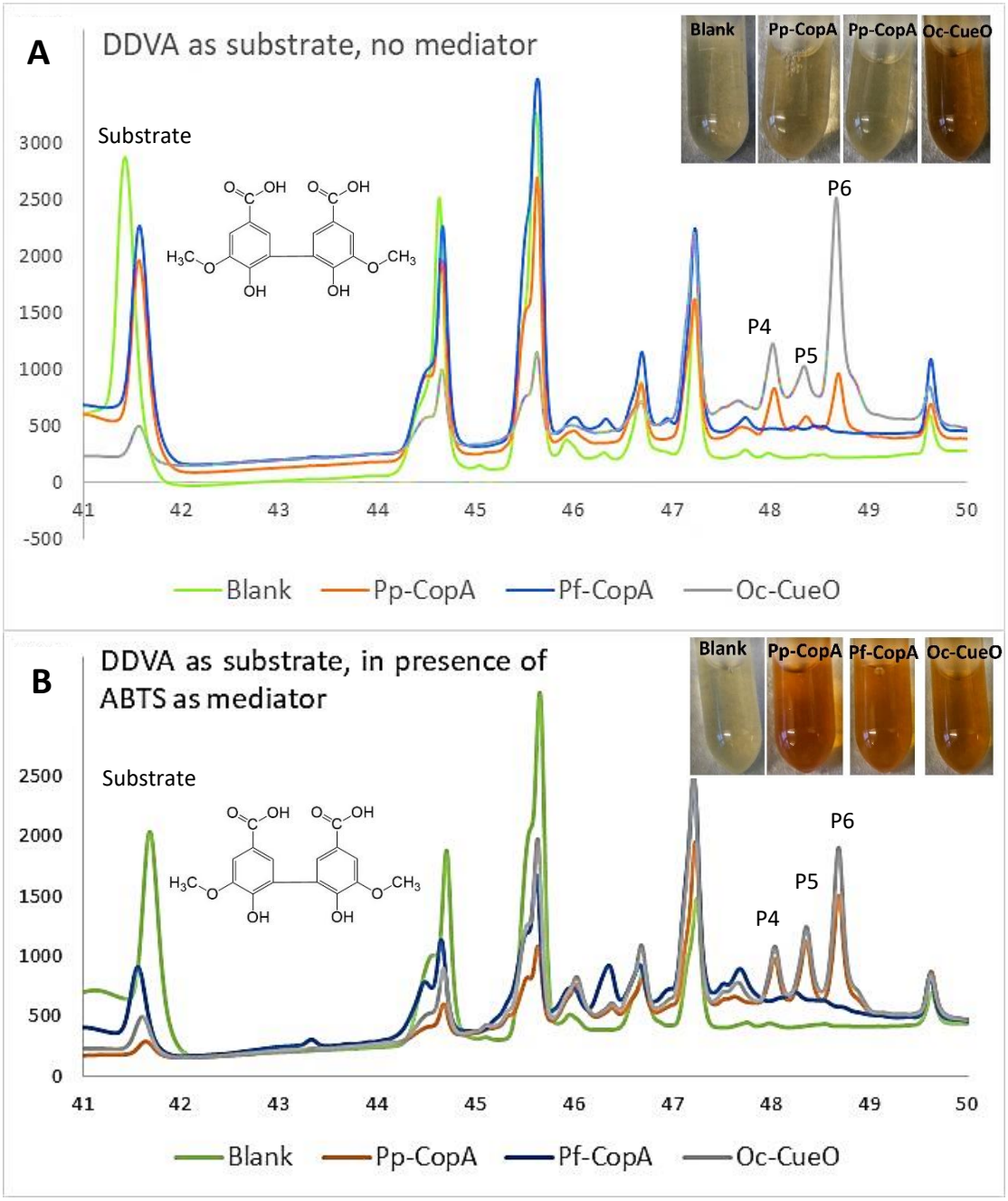

Figure 38. UV-Vis chromatograms showing products formation after reaction of the lignin-model compounds DDVA, with Pp-CopA, Pf-CopA and Oc-CueO. In the right-upper side of each graphic, a photo shows the actual reaction after incubation of each enzyme with the substrate. (A) Reaction performed in absence of a mediator. (B) Reaction performed in presence of 1 mM ABTS as mediator.

The results showed a different behaviour between GGE and DDVA. When GGE was used as substrate, the reactions showed a change into a brown darker colour, regardless the presence or absence of the mediator. On the other hand, when DDVA was used as substrate, in absence of the mediator, the change in colour only occurred when the Oc-CueO enzyme was used, whereas the colour changed for all assayed enzymes only if the mediator was

present. The change in colour suggested that the LMCOs enzymes had transformed these lignin-model compounds in some way. Moreover, the UV-Vis chromatogram revealed the appearance of new peaks, demonstrating the generation of new products because of the LMCO enzymatic activity. For GGE, as it can be seen in **Figure 37**, in absence of a mediator, two major peaks were formed in absence of the mediator (P1 and P2), at retention time 46.8 and 47.6 minutes; while a third minor peak (P3), appeared at 45.8 minutes. In presence of the mediator, peak P2 decreased, whereas peak P3 increased, suggesting that the presence of a mediator favoured to some extent the formation of product P3. All three enzymes performed the reaction with similar efficiency, as they gave the same peaks, though Pf-CopA seemed to be slightly more efficient, based on the height of the peaks generated. In the case of DDVA, in absence of the mediator only the enzyme Oc-CueO gave a change in colour and the formation of three new peaks (P4, P5 and P6), located at the retention time 48 - 49 minutes. Pp-CopA yielded a similar result, yet in a much lesser extent, as the change in colour and the peaks formation were less than observed with Oc-CueO. Pf-CopA gave no change in the absence of the mediator. In presence of the mediator, all LMCOs, Pp-CopA, Pf-CopA and Oc-CueO gave a change of colour, however the formation of the three peaks at the same retention times were detected only for Pp-CopA and Oc-CueO. Apparently, the presence of the mediator favoured the formation of peak P6, over the formation of the peak P5 (**Figure 38**).

Electrospray mass spectrometry was used to analyse peaks formation. For GGE, products P1, P2 and P3 showed higher molecular weight peaks with m/z 573.21, 697.66 and 479.22, respectively, compared with the substrate (320.13 Da for GGE). For DDVA, peaks P4, P5 and P6 also gave higher molecular weight peaks at m/z 621, 605 and 623, compared with the substrate (334.07 Da for DDVA). These results suggest that these proteins could catalyse an oxidative dimerization reaction, followed by additional modification reactions. **Table 11** summarizes the molecular weight (MW) of the products formed during LMCO reaction with GGE and DDVA.

Table 11. Mass spectrometry results of products generated from the substrates GGE and DDVA by LMCOs enzymatic activity. Whenever possible, two products are presented for each peak detected. Molecular formulas were predicted by high resolution mass spectrometry (HRMS), unless otherwise is indicated. (*) result from normal mass spectrometry. NA means not available.

	m/z ratio (MW) of products generated from GGE	Molecular formula		*m/z* ratio (MW) of products generated from DDVA	Molecular formula
GGE	320.126	$C_{17}H_{20}O_6$	DDVA	334.07	$C_{16}H_{14}O_8$
P1	573.2119 661.2272	$C_{33}H_{33}O_9$ $C_{36}H_{37}O_{12}$	P4	621.1228 643.1049	$C_{31}H_{25}O_{14}$ $C_{31}H_{24}NaO_{14}$
P2	697.658 675 (*)	NA $C_{34}H_{36}NaO_{13}$	P5	605.1271 663.1336	NA $C_{33}H_{27}O_{15}$
P3	479.22(*)	$C_{24}H_{24}O_9$	P6	623 663.1336	NA $C_{33}H_{27}O_{15}$

These results agree with the type of reaction catalyse by laccases with phenolic β-O-4' ether and C-C lignin-model dimers, which is mainly a polymerization (**Figure 35** and **Figure 36**). It is not well understood why apparently the absence of the hydroxyl group in the ring of β-O-4' ether model-dimers seems to be needed for its breakdown. In this study, a phenolic lignin-model dimer (GGE) has been used, which has proven to be resistant to breakdown, even by high redox potential laccases in presence of mediators [212-214]. Consequently, the main products generated by the LMCOs under study correspond with molecules with a higher molecular weight (MW) than the substrate. Even so, two distinctive features can be highlighted for the enzyme activity of these bacterial proteins. First, the LMCOs under study have proven to be active towards the two types of lignin-model compounds assayed, the a β-O-4' ether model dimer (GGE) and the 5-5' dimer (DDVA). Second, the type of polymerization followed for these bacterial LMCOs for the peak P3 from the reaction with the GGE (β-O-4' model dimer), does not correspond with a typical dimer formation, as the MW would suggest that a cleavage reaction followed by a coupling reaction have occurred. For P4, P5 and P6 products from the C-C dimer (DDVA) and the P1 and P2 from the β-O-4' model dimer (GGE), a dimerization may have occurred, followed by an unidentified modification. A high-resolution mass spectrometry (HRMS) was carried out to determine the exact MW of some of the products obtained, then these data were used to elaborate a probable molecular formula for the generated products (**Table 11**). In addition, a possible mechanism of reaction has been proposed by Prof. T.D.H. Bugg, for the products P1 and P4, generated from the substrates GGE and DDVA, respectively (**Figure 39**). However, to elucidate the exact mechanism for each product generated, a more detailed analysis is needed, which is out of the scope of the present study. The bacterial LMCOs under study have proven to be active towards the lignin-model compounds GGE and DDVA. The kind of

lignin-model dimers that have been used in this study (phenolic β-O-4' dimer and the DDVA dimer) seem to lead always to some sort of polymerization process in presence of laccases, no matter whether a high redox potential enzyme is used, nor if the reaction is carried out in the presence of a mediator [205, 212-214].

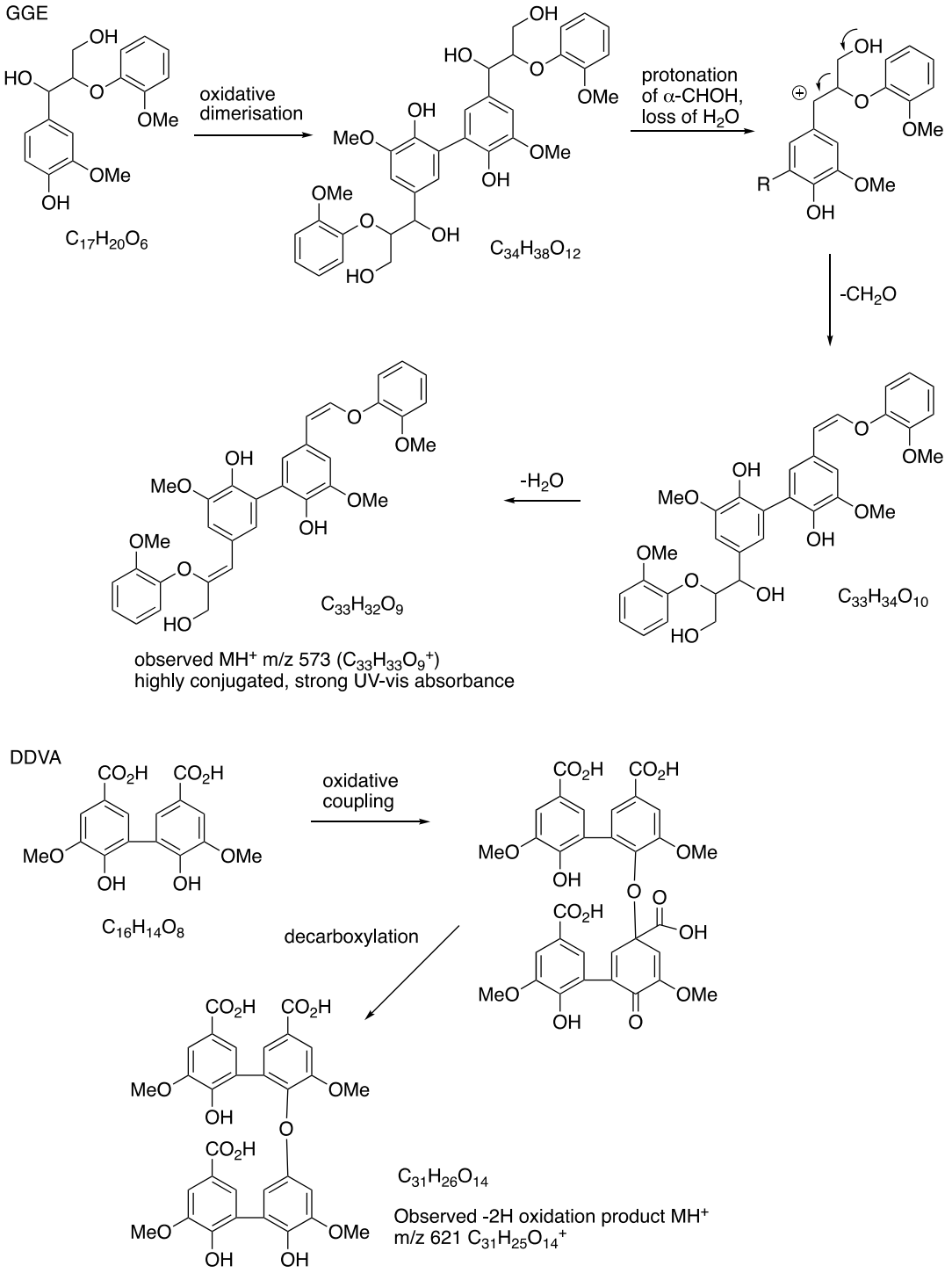

Figure 39. Proposed mechanism formation of products found in peaks P1 and P4, from GGE and DDVA reactions with bacterial LMCOs.

4.3 Enzyme activity of laccase-like multicopper oxidases (LMCOs) on polymeric lignin substrates

Pp-CopA, Pf-CopA and Oc-CueO were tested for activity with polymeric lignin substrates. The reaction consisted of 20 mM Hepes with 80 mM NaCl buffer, pH 7.0; enzyme solution (≈0.6 mg/mL); 0.5 mM of $CuSO_4$. The reaction was carried out in presence and in absence of a mediator (1 mM ABTS). The lignin substrate (5 mg) was directly added to the reaction. A total of eight different lignin preparations were used, some were soluble in aqueous buffer, while others were not. The lignins used are listed below:

Lignin 1: Poplar ammonia (percolation) organosolv (University of Glasgow)
Lignin 2: Wheat straw organosolv lignin (CIMV)
Lignin 3: Wheat straw protobind lignin (Green value)
Lignin 4: Alkali Kraft lignin (Sigma-Aldrich)
Lignin 5: Na-lignosulfonate softwood ultrafiltrated (Borregaard)
Lignin 6: Ca-lignosulfonate hardwood (Borregaard)
Lignin 7: Wheat straw alkali organosolv lignin (University of Glasgow)
Lignin 8: Wheat straw acid organosolv lignin (University of Glasgow)

Reactions were incubated overnight, and a solvent extraction with ethyl acetate was performed to collect the possible products formed. Product generation was determined by checking for new peaks formation by HPLC detecting by UV-Vis. In addition, from a qualitative analysis (sight), it was observed that the reactions containing the bacterial LMCOs enzymes changed into a darker brown colour. The change in colour of the reactions and UV-Vis chromatograms of the reactions carried out in presence of the mediator are shown in **Appendix 2**.

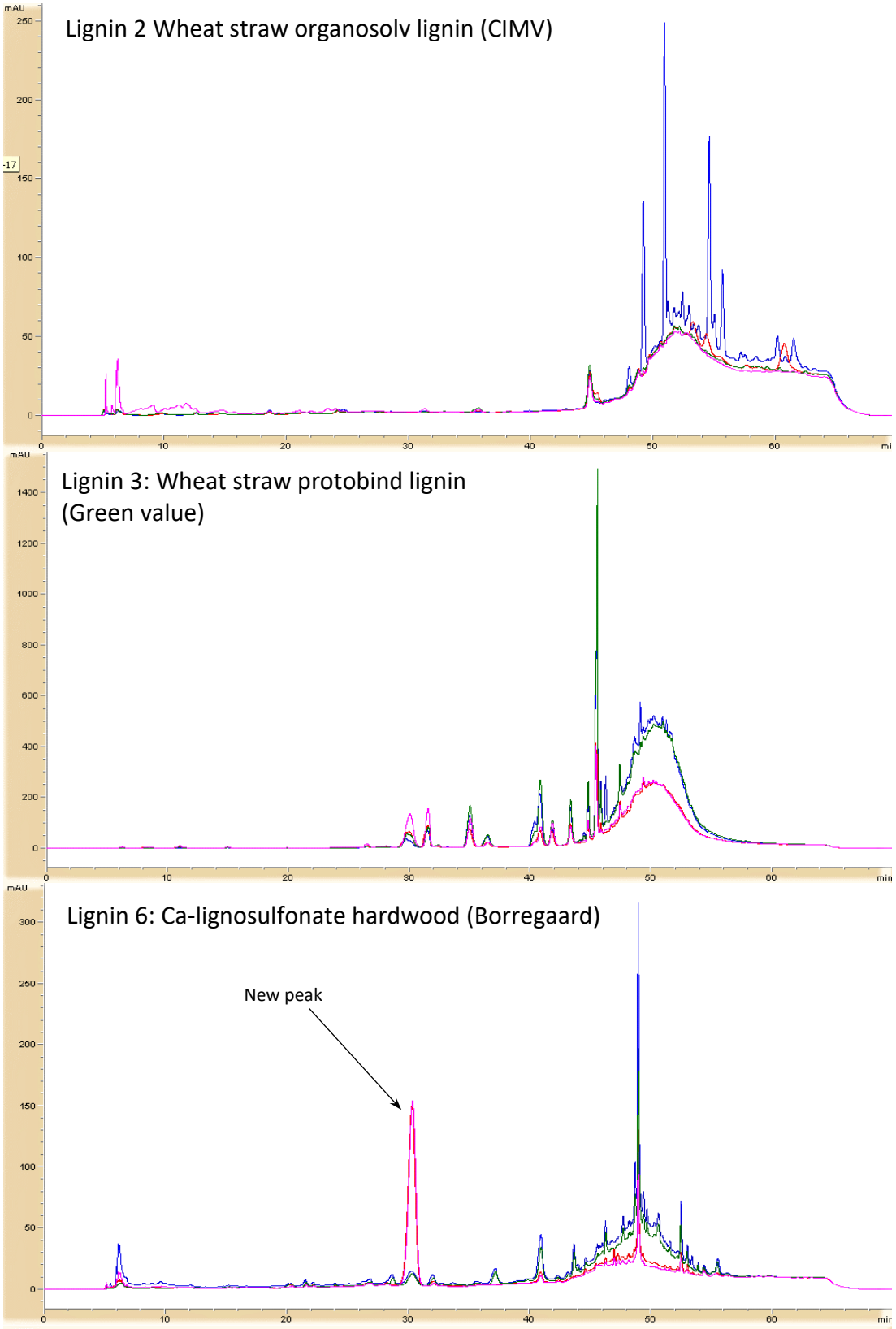

Figure 40. HPLC chromatograms for activity of LMCOs with polymeric lignins 2, 3 and 6, as substrates, in presence of ABTS as mediator. Blue line: blank/negative control. Red line: Pp-CopA. Green line: Pf-CopA. Pink line: Oc-CueO. Lignin 2 and lignin 3 showed chromatograms with decreased peaks compared with the blank. Lignin 6 gave the formation of a new peak.

The results showed that some of the peaks found in the blank (negative control) chromatograms appeared to have been diminished in presence of the enzymes, for example chromatograms with lignin 2 and lignin 3. With lignin 6, the Ca-lignosulfonate hardwood (Borregaard), a new peak was observed (**Figure 40**). A mass spectrometry analysis revealed that this peak matched with vanillic acid (m/z 169 MH+, 191 MNa+), a common product from lignin degradation [45, 215]. Remarkably, this product was generated by Pp-CopA even in absence of the mediator, though the mediator enhanced the formation of this peak with Pp-CopA and Oc-CueO. Apparently, Pf-CopA was unable to catalyse this reaction.

4.3.1 Activity of lignin 6 with Oc-CueO in combination with other enzymes

Once it was confirmed that Pp-CopA and Oc-CueO had an effect on the lignin 6 (Ca-lignosulfonate hardwood, Borregaard); a possible synergistic effect of the bacterial laccase Oc-CueO with other enzymes involved in lignin degradation, was investigated. Some enzymes have been identified as accessory enzymes in lignin depolymerization, such as a flavoprotein dihydrolipoamide dehydrogenase from *Thermobifida fusca*, which prevents the re-polymerization in lignin degradation processes [153]. Dr. Goran Rashid, in the TDHB research group, has recombinantly expressed a similar flavoprotein, dihydrolipoamide dehydrogenase (DhLDh) from *Sphingobacterium sp*., and another enzyme involved in lignin degradation, a glutathione S-transferase (LigE) from *Agrobacterium sp*. [216]. Dr. Rahman Rahmanpour, has expressed a Dyp-type peroxidase (Dyp1B) from *Pseudomonas fluorescens* Pf-5, whose activity on lignin has been proved [65]. These proteins have been cloned from bacterial lignin degraders. The enzymes were assayed individually and in combination with Oc-CueO, to determine whether a synergistic effect could emerge or not. Concentrations and the volumes used were carefully calculated, in order to assure the same protein and substrate concentrations for all reactions. External cofactors needed for these enzymes are listed as follows: ABTS (mediator) and $CuSO_4$ as copper supplementation, for Oc-CueO; hydrogen peroxide, for Dyp1B; NADH, for DhLDh; and glutathione (GSH), for LigE. **Table 12** summarise the enzymes combinations performed, and the results are shown in **Figure 41**.

Table 12. Combinations of enzymes assayed for activity with lignin 6.

Assay	Combinations	Assay	Combinations
1	Oc-CueO	10	DhLDh + LigE
2	Dyp1B	11	Oc-CueO + Dyp1B + DhLDh
3	DhLDh	12	Oc-CueO + DhLDh + LigE
4	LigE	13	Oc-CueO + Dyp1B + LigE
5	Oc-CueO + Dyp1B	14	Dyp1B + DhLDh + LigE
6	Oc-CueO + DhLDh	15	Oc-CueO + Dyp1B + DhLDh + LigE
7	Oc-CueO + LigE	B1	Blank1: no enzymes, no cofactors added
8	Dyp1B + DhLDh	B2	Blank2: no enzymes, cofactors added
9	Dyp1B + LigE		

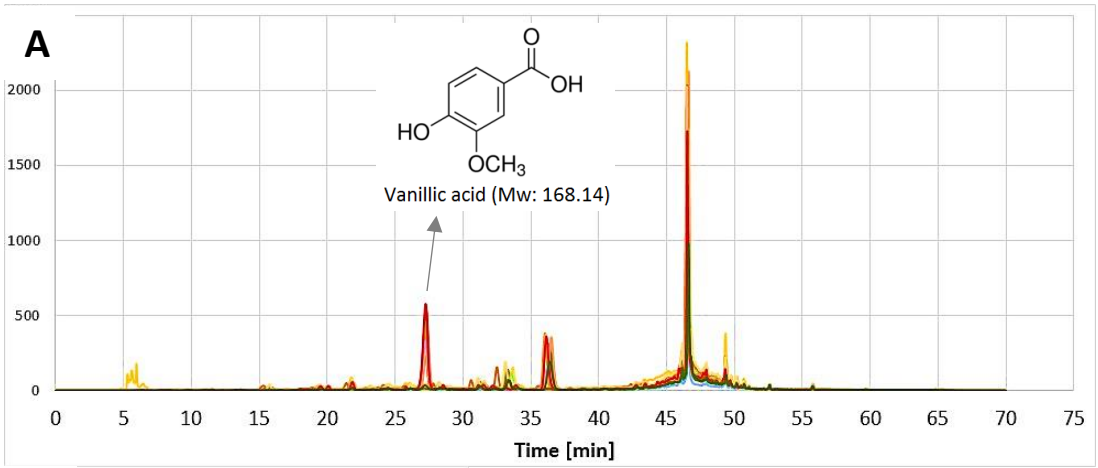

Sample	Peak height [mAu]
Blank 1	20
Blank 2	49
1	302
6	537
11	437
15	578

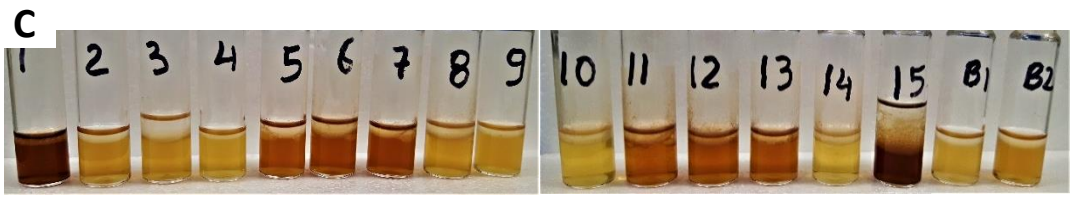

Figure 41. activity of enzyme combinations towards lignin 6, Ca-lignosulfonate hardwood, Borregaard. (A) HPLC chromatograms showing the formation of the 27 minute peak corresponding with vanillic acid. (B) Left: Amplification of the peak corresponding with vanillic acid formation. Right: table showing the height of each peak for the samples shown in graphic on the left. (C) Actual reactions performed, showing a change in colour. To identify the enzyme combination for each experiment, see **Table 12**.

Results showed that only those reactions containing Oc-CueO were able to generate vanillic acid. However, the addition of DhLDh, LigE and Dyp1B had an effect on the product generation, as the height of the peak increased when Oc-CueO was combined with one or more of these proteins, reaching a maximum when all proteins were present in the reaction. The combination of Oc-CueO with the dihydrolipoamide dehydrogenase (DhLDh) from *Sphingobacterium sp*., gave the second highest peak, which would confirm the observation made for dihydrolipoamide dehydrogenase about its role in preventing lignin repolymerization [153]. These results suggest that laccases could potentially be synergistic with other lignin-degrading enzymes.

5 Structural study of the laccase-like multicopper oxidase Oc-CueO, from *Ochrobactrum sp*.

5.1 Introduction

As it has been stated before (section 1.6, Laccases: properties and structure; and section 2.1, Introduction), there is no general consensus about the definition of laccases. Among the more accepted proposals that have been suggested, three main groups can be identified. Firstly, it has been suggested that only enzymes related with the original laccase isolated from the sap of the tree *Rhus vernicifera*, this is MCOs isolated from plant saps, in presence of the natural substrate urushiol, should be regarded as a "true laccases" [96, 106]. A second point of view states that since most studies have been carried out by using fungal laccases, only these enzymes should be considered as laccases, and they have been referred as "laccase *sensu stricto*" [105, 217]. Finally, a more flexible point of view states that any multicopper oxidase showing phenol oxidase activity by using oxygen as electron acceptor, should be considered as a laccase; yet, to avoid confusions the term "laccase-like multicopper oxidases" has been proposed for these enzymes, and this term would include the bacterial laccases [96]. In this study, the third point of view is accepted, as the main goal is to describe new catalysts that could be potentially useful for industrial applications. Therefore, as it has been proved that bacterial laccase-like proteins can catalyse the same reactions as "well-described" fungal laccases, such as the *Trametes versicolor* laccase (TvL), then the questions that arise are why and how fungal and bacterial laccases are different? To partially solve these questions, a structural analysis of bacterial laccases and comparison with their fungal counterparts can provide useful information to increase the current knowledge on these questions.

Laccases are globular proteins, usually with a molecular weight of 60 to 70 kDa, and fungal laccases are glycosylated [94]. All laccases are part of a bigger and diverse group of proteins, called multicopper oxidases (MCOs). The MCOs share four very well conserved motifs in their amino acid sequence: HXHG, HXH, HXXHXH and HCHXXXHXXXXM/L/F, and these regions contain the ligands of the four copper ions, usually found in MCOs [96, 218]. It is difficult to differentiate a laccase from another subgroup of MCO, as the sequence homology tends to be low among MCOs, and often experimental evidence is needed to prove

laccase activity. So far, no amino acid sequence motif suitable for laccase identification has been found, that can be used in a concise way [96]. However, sequence homology among fungal laccases tends to be higher, and the identification of four ungapped regions, L1 to L4, has been proposed to identify "laccases *sensu stricto*" from the broader class of multicopper oxidases, though this approach would be valid only for fungal laccases. A multiple sequence alignment of more than 100 fungal laccases gave as result the appearance of four conserved regions, which contain the 12 resides involved as copper ligands. L2 and L4 seem to be in line with the copper signature of MCOs, while L1 and L3 are distinctive to fungal laccases (**Figure 42**, **A**) [95]. Moreover, four loops have been identified as regions involved in substrate binding in laccases, by the analysis of structural superposition (**Figure 42, B**) [219].

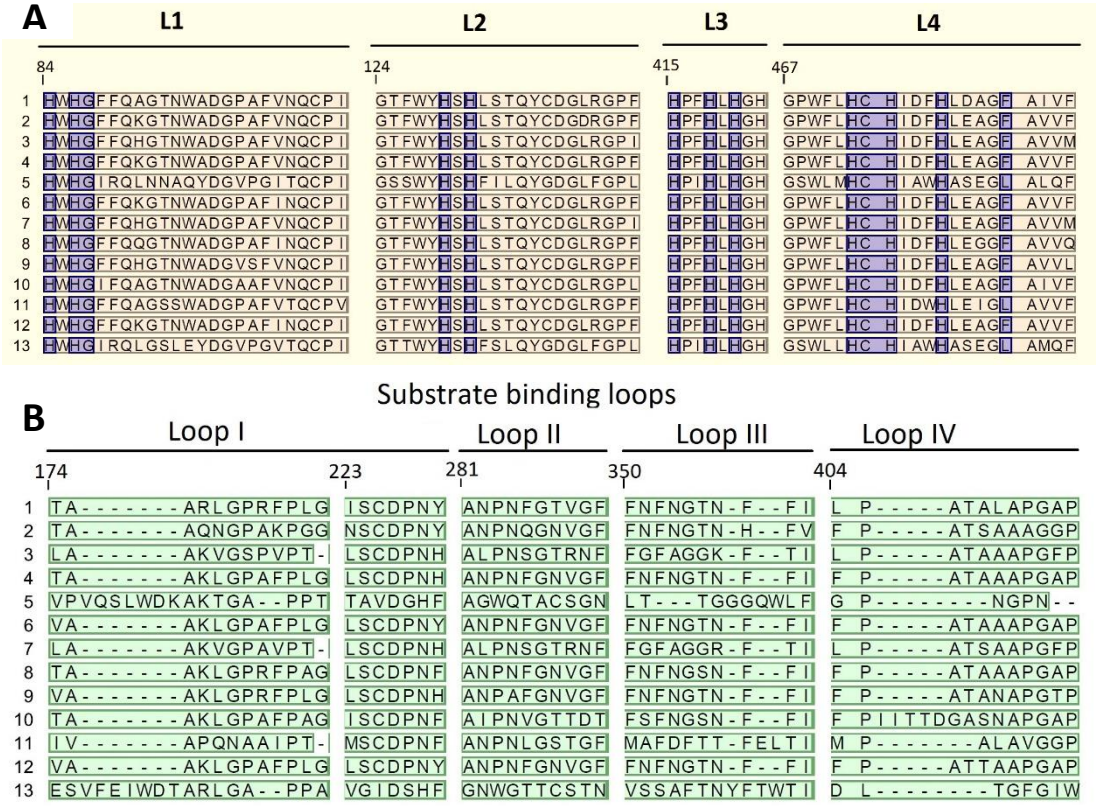

Figure 42. Multiple sequence alignment of different fungal laccases. Numbering is based on the sequence of enzyme 1, as reference. (A) Laccase signature sequences. MCOs well-conserved residues are coloured in blue. (B) Possible substrate binding loops based on 3-D structure of enzyme 1. Enzymes and PDB (*) or Uniprot codes used for alignment: 1: 1GYC*, *Trametes versicolor*; 2: 2HZH*, *Trametes ochracea*; 3: 2HRH*, *Coriolopsis trogii*; 4: Q02497, *Trametes hirsute*; 5: Q12570, *Botryotinia fuckeliana*; 6: Q99044, *Trametes villosa*; 7: Q12571, *Basidiomycete PM1*; 8: D0VWU3, *Cerrena maxima*; 9: O59896, *Pycnoporus cinnabarinus*; 10: Q8TG93, *Trametes pubescens*; 11: Q12739, *Pleurotus ostreatus*; 12: Q8TG94, *Trametes pubescens*; 13: H8ZRU2, *Botrytis aclada*. Adapted from [81]. Alignment generated by CLC Workbench software (https://www.qiagenbioinformatics.com/).

Although bacterial laccases usually contain the well-conserved motifs of MCOs, there is a low homology when their sequences are compared with the corresponding four regions, L1 to L4, found in fungal laccases. Nevertheless, despite the low sequence homology, wide taxonomic distribution and broad range of substrates accepted, the molecular architecture of laccases is common for all multicopper oxidases [141]. These proteins are commonly composed of three domains, each domain is sequentially arranged in a cupredoxin-like fold, comprising a β-barrel (Greek key motif) topology, formed by β-sheets and β-strands, disposed in sandwich configuration. Four ions of copper are contained in these proteins, and they are arranged in two copper centres. One copper centre is formed by a single copper ion, named as type 1 copper (T1), and it is in the domain 3. The second copper centre is a trinuclear cluster (TNC), which is formed by one type 2 copper (T2) and one binuclear type 3 copper (T3), embedded between domains 1 and 3, with both domains containing residues for copper coordination [81, 83, 141]. A detailed analysis revealed several differences between fungal and bacterial laccases 3-D structures [141], listed as follows:

- The domain 1 is distorted to some extent in bacterial laccases, when compared with domain 1 in fungal laccases (**Figure 43, A**).
- Domain 1 and domain 2 are connected by a coiled section in bacterial laccases, absent in fungal laccases (**Figure 43, B**). The function of this section has been suggested as packaging between these domains [85].
- Domain 2 and Domain 3 are connected by a large loop segment in bacterial laccases, through an external connection that wraps around the protein; whereas a short internal helical region connects domains 2 and 3 in fungal laccases (**Figure 43, C**).
- As stated before, domain 3 contains the T1 copper, contributes to the formation of the TNC site, and includes the putative substrate binding site (active site of the enzyme). The active site is located at the surface of the protein, close to the T1 copper. This region is open and accessible to the substrate in fungal laccases, whereas in bacterial laccases a loop and an α-helix form a lid-like structure over the substrate binding site, which might hinder the entrance of the substrate to the active site (**Figure 43, D**) [85, 220].
- The fourth conserved motif of MCOs, comprises the following sequence: HCHXXXHXXXXM/L/F. Fungal laccases contain a phenylalanine (F) or a leucine (L) as the last residue of this motif, while bacterial laccases contain a methionine residue (M), instead. This residue is not coordinated with the T1 copper in fungal laccases,

whereas in bacterial laccase the methionine can be coordinated with the T1 copper (**Figure 43, E**) [85, 91].

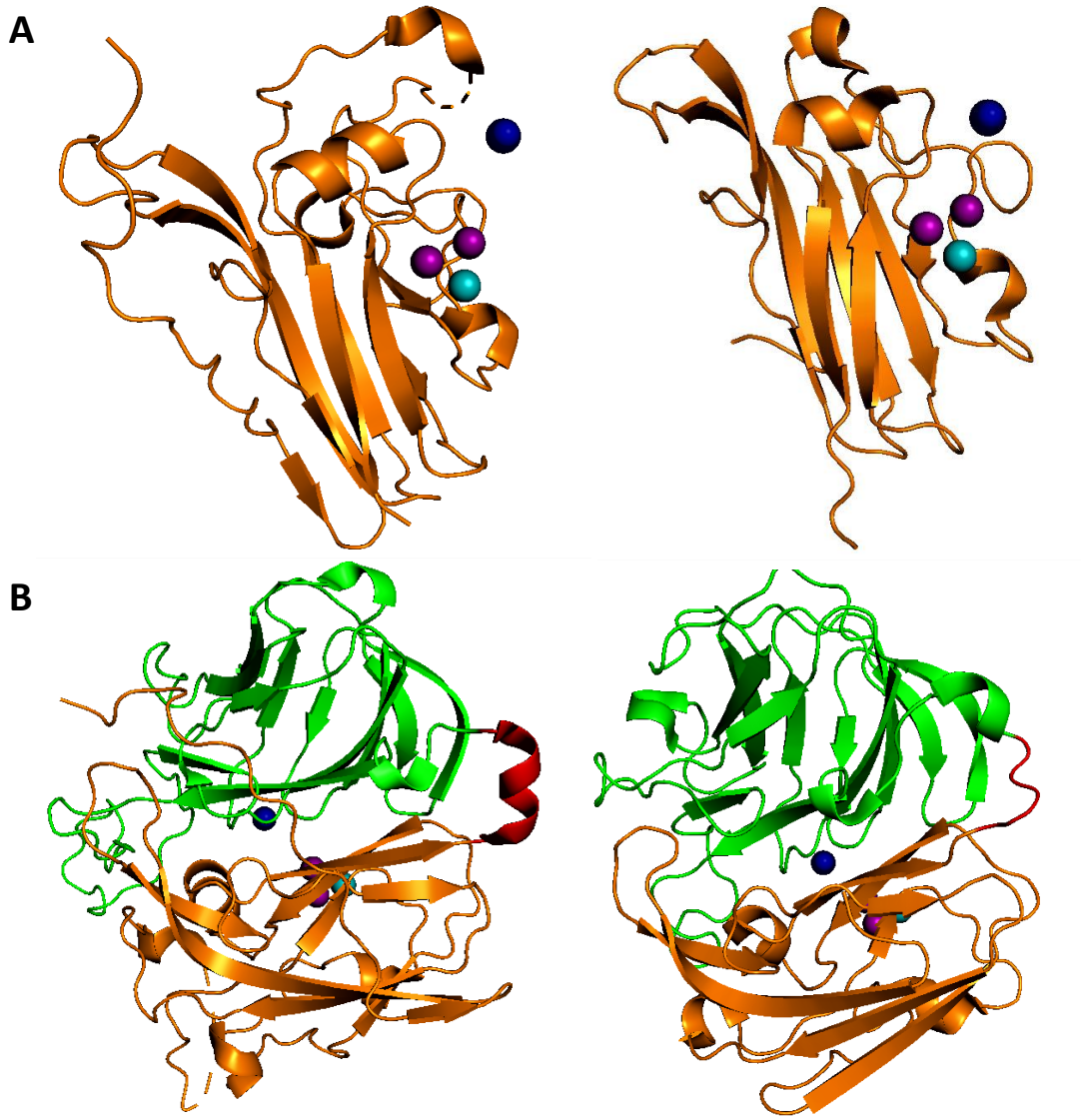

Figure 43. 3-D structural differences between fungal and bacterial laccases. Domain 1, 2 and 3 are coloured in orange, green and yellow, respectively. Copper ions type 1, 2 and 3 are depicted as blue, teal, and purple spheres, respectively. On the left side: CotA bacterial laccase. On the right side: TvL fungal laccase. (A) Distorted Domain 1 in bacterial laccases. (B) Connection between domain 1 and domain 2, shown in red colour. (C) Connection between domain 2 and domain 3, shown in red colour. (D) Lid-like structure over the active site (shown in red), presented in bacterial laccases. (E) Methionine as axial ligand of copper T1, in bacterial laccases. Graphic generated by the software PyMOL, using *Trametes versicolor laccase* (TvL), PDB code 1GYC; and CotA laccase from *Bacillus subtilis*, PDB code 4Q89 (Continued in the next page).

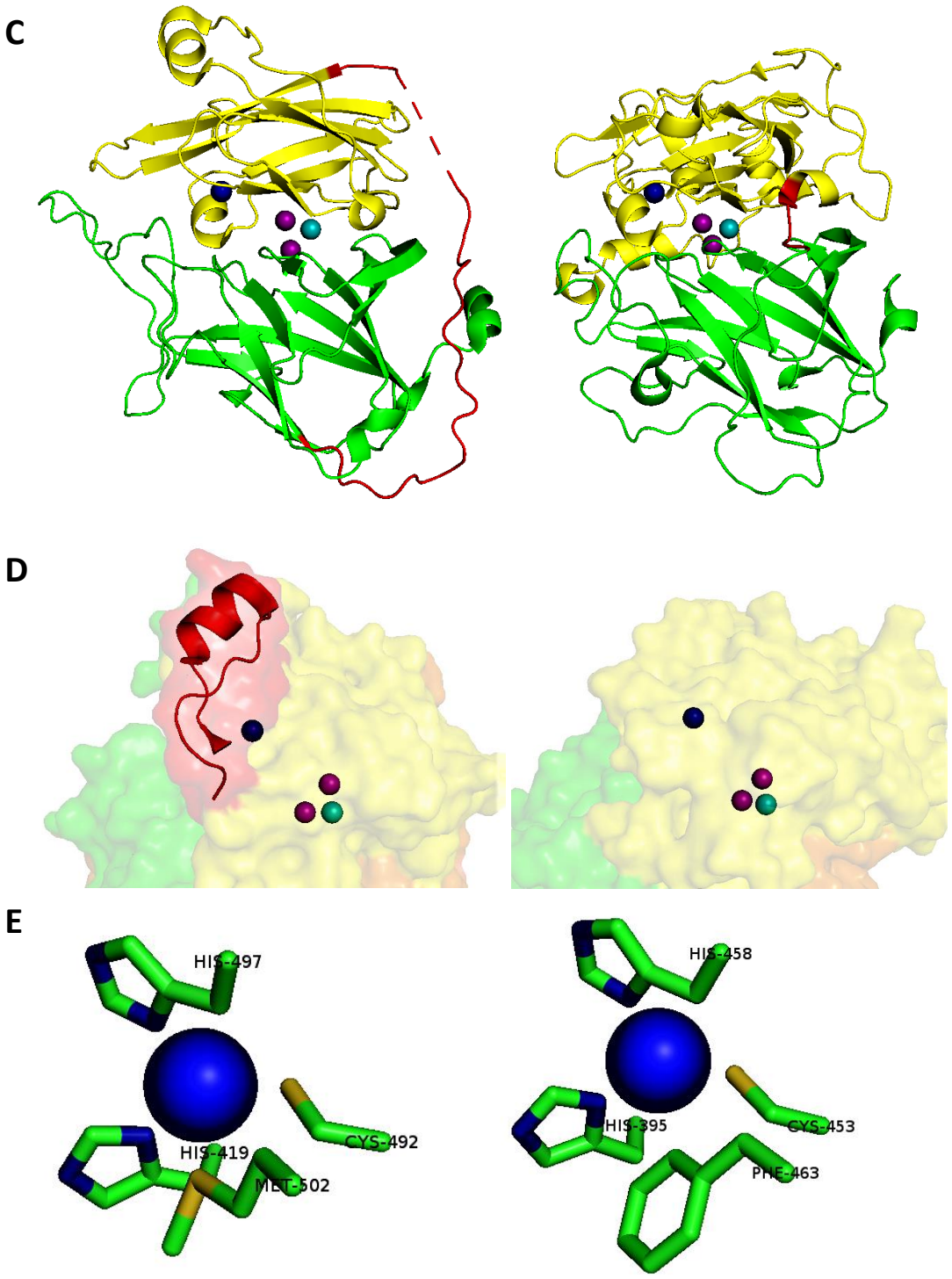

Figure 43. 3-D structural differences between fungal and bacterial laccases. Domain 1, 2 and 3 are coloured in orange, green and yellow, respectively. Copper ions type 1, 2 and 3 are depicted as blue, teal, and purple spheres, respectively. On the left side: CotA bacterial laccase. On the right side: TvL fungal laccase. (A) Distorted Domain 1 in bacterial laccases. (B) Connection between domain 1 and domain 2, shown in red colour. (C) Connection between domain 2 and domain 3, shown in red colour. (D) Lid-like structure over the active site (shown in red), presented in bacterial laccases. (E) Methionine as axial ligand of copper T1, in bacterial laccases. Graphic generated by the software PyMOL, using *Trametes versicolor* laccase (TvL), PDB code 1GYC; and CotA laccase from *Bacillus subtilis*, PDB code 4Q89 (Continued from the previous page).

Some of the differences found between fungal and bacterial laccases might explain their biochemical properties. For instance, it has been suggested that the coiled region connecting domains 1 and 2, and the long loop that connects domains 2 and 3 and wraps around the protein, could play a role in the thermal high stability observed for bacterial laccases. On the other hand, the lid-like helical-loop region found over the active site in bacterial laccases has been proposed as one of the many possible reasons for the limited range of substrates that some bacterial laccases can accept. This structure represents a distinctive signature of bacterial laccases, and so far, the crystallography studies have been unable to show this region fully, due to the low electron density in this area. Its function is still unknown, though a binding role with the substrate or other molecules is suspected, since this region seems to be very flexible [85]. This lid-like helical loop has also been described as a methionine rich region, playing a role in copper attachment and even a site for copper(I) ions has been identified in this region, which confers a cuprous oxidase activity to the MCO CueO, from *E. coli*. A mutant of this protein whose helical loop was removed, showed a that the scaffold, metal binding sites, high thermostability, and the spectroscopy and magnetic properties due to the presence of the four ions of copper, were conserved in this truncated mutant. On the other hand, the truncation led to a decreased cuprous oxidase activity, from 187 to 21 U/mg, whereas the activity for ABTS increased by 30 times, and a newly emerged activity for syringaldazine (SGZ) was observed, though the mutant was still inactive towards guaiacol, 2,6-dimethoxyphenol (DMP) and catechol [220]. These results may suggest that the lid-like helical loop observed in bacterial laccases might be not essential for their oxidase activity, on the contrary it could block the free entrance of the substrate limiting their catalytic potential, and its role could be rather related with some sort of supplementary biological function, often attributed to MCO bacterial proteins, such as copper homeostasis.

Another feature distinctive of bacterial laccases is the presence of a methionine as an axial ligand, near to the T1 copper, whereas in fungal laccases a phenylalanine (F) or a leucine (L) are commonly found in this site, and they do not interact with the T1 copper. It has been proved that this residue can affect the redox potential of a laccase, as its mutation in the CotA bacterial laccases into F and L, gave an increase of the redox potential from 455 mV, to 548 and 515 mV, respectively. However, it seems that the axial methionine residue is essential to keep the integrity of the T1 coordination sphere [91]. Regarding the domain 2, it has been stated that its main function is related with scaffolding, acting as a bridge between domain 1 and domain 3 [93, 141]. The distinctive regions found for fungal laccases, L1 and

L3 (**Figure 42, A**), are all contained in domain 1 and domain 3, supporting their importance for catalytic activity.

5.2 Oc-CueO crystal structure

The LMCOs Pp-CopA, Pf-CopA and Oc-CueO were used for protein crystallization trials. Protein expression and purification was carried out by me, whereas the protein crystallization, data analysis and protein modelling were carried out by Dr Rachael Wilkinson, Research Fellow at the School of Life Science, University of Warwick, under the supervision of Professor Vilmos Fulop, School of Life Sciences, University of Warwick.

The previously described method for protein purification was used. Detailed information can be seen in sections: 2.2.2, Cloning and protein expression of MCOs; and 8.1, General procedures. After TEV cleavage and a second IMAC, the protein solutions were subjected to a further step of purification, by using a size exclusion chromatography column (Gel filtration column Superdex 75) in a Fast protein liquid chromatography (FPLC) equipment. Fractions were collected, and their purity were evaluated by SDS-PAGE. Then, the collected fractions were pooled, concentrated by a 10 kDa Amicon centricon device, and buffer exchanged by using PD-10 columns, followed by a copper reconstitution (See section 2.2.3, Copper reconstitution). Finally, the excess of copper was removed by buffer exchanging the protein solutions in a PD-10 column, twice.

Final purified protein solutions reached a concentration of about 20 mg/mL and were transported on ice to the School of Life Science, at the University of Warwick, for protein crystallization assays, which were performed by Dr Rachael Wilkinson. Neither Pp-CopA nor Pf-CopA were able to produce any crystals under the tested conditions. However, it was possible to obtain crystals of Oc-CueO by using the following procedure. Pure recombinant Oc-CueO (10 mg/mL) in 20 mM sodium phosphate buffer and 100 mM NaCl, pH 8, was subjected to crystallization screening using a Mosquito liquid handling robot (TTP Labtech, Melbourn, UK). 200 nL of protein solution was mixed with 200 nL of crystallization solution from screens in MRC 96-well 2-drop crystallization plates. Plates were sealed and incubated at 22 °C. After 6 to 8 weeks, crystals appeared in several different conditions. Crystals grown in condition B5 of the PactPremier crystallization screen (0.1 M MIB buffer pH 8, 25% PEG 1500), were removed, cryoprotected and flash-frozen in liquid nitrogen. X-ray diffraction data to a resolution of 1.1 Å were collected at 100 K at the beam line I03 at the Diamond Light Source, UK, using a Pilatus 6M detector. All data were indexed, integrated, and scaled using the XDS package [221]. Further data handling was carried out using the CCP4

software package [222]. The structure was solved by molecular replacement, using the automated pipeline by BALBES [223]. Further analysis can be found in [183].

5.2.1 Overview of Oc-CueO crystal structure

The crystal structure of Oc-CueO was determined at 1.1 Å resolution and the 3-D structure was submitted and approved by the crystallographic database "Protein Data Bank" (PDB), under the accession code 6EVG. The asymmetric unit of the crystal contained one molecule with the space group P21. The 3-D structure revealed that Oc-CueO is a monomer showing the common molecular architecture of all MCOs, comprising three different domains [81, 224]. Domain one comprises from residue 22 to residue 160; domain two from residue 161 to residue 318; and domain three from residue 319 to residue 507 (**Figure 44**). These domains show the typical cupredoxin-like fold, containing a β-barrel (Greek key motif) topology, formed by β-sheets and β-strands, arranged in sandwich configuration, an architecture also observed in azurin and plastocyanin [141, 224, 225]. Data collection and refinement statistics are given in **Table 13**.

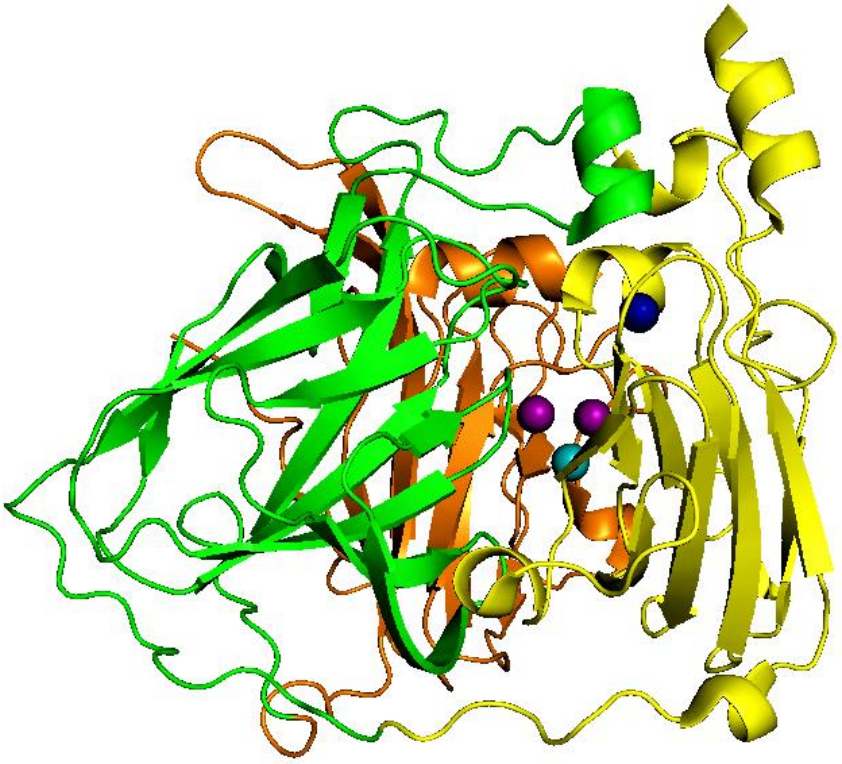

Figure 44. Oc-CueO crystal structure (PDB: 6EVG). Domain 1, 2 and 3 are coloured in orange, green and yellow, respectively. Copper ions type 1, 2 and 3 are depicted as blue, teal, and purple spheres, respectively. Only copper T1 was present in the crystal structure of Oc-CueO. T2 and T3 coppers were generated by a superposition of Oc-CueO with the *Escherichia col*i CueO (PDB: 4E9Q) which shared highest sequence similarity. Graphic generated by the software PyMOL.

Table 13. Summary of crystallographic data collection and refinement statistics

Data collection	
Wavelength (Å)	0.8
Unit cell (*a, b, c*) (Å), (β) (°)	47.33, 48.31, 88.85, 93.78
Space group	$P2_1$
Resolution (Å)	89 - 1.1 (1.16-1.1)
Observations	602 426
Unique reflections	161 992
$I/\sigma(I)$	12.2 (2.1)
R_{sym}[a]	0.056 (0.584)
Completeness (%)	99.9 (99.7)
$CC_{1/2}$[b]	0.999 (0.748)
Refinement	
Non-hydrogen atoms	3918 (including Cu^{2+}, 2 ethylene glycol & 477 water molecules)
R_{cryst}[c]	0.125 (0.242)
Reflections used	155 475 (11 395)
R_{free}[d]	0.149 (0.246)
Reflections used	6517 (493)
R_{cryst} (all data)[b]	0.126
Average temperature factors (Å^2)	
All atoms	14.1
Protein	12.4
Water	23.5
From Wilson plot	9.1
Rmsds from ideal values	
Bonds (Å)	0.019
Angles (°)	1.8
DPI coordinate error (Å)[e]	0.02
Ramachandran Plot (%)	
Most favoured	97
Additional allowed	3
Outliers	0
wwPDB code	6EVG

Numbers in parentheses refer to values in the highest resolution shell. [a]$R_{sym} = \sum_j\sum_h|I_{h,j} - \langle I_h\rangle|/\sum_j\sum_h\langle I_h\rangle$ where $I_{h,j}$ is the jth observation of reflection h, and $\langle I_h\rangle$ is the mean intensity of that reflection. [b]$CC_{1/2}$ is the correlation coefficient of the mean intensities between two random half-sets of data. [c]$R_{cryst} = \sum||F_{obs}|-|F_{calc}||/\sum|F_{obs}|$ where F_{obs} and F_{calc} are the observed and calculated structure factor amplitudes, respectively. [d]R_{free} is equivalent to R_{cryst} for a 4% subset of reflections not used in the refinement. [e]DPI refers to the diffraction component precision index [Cruckshank]

5.2.2 Structure of mononuclear copper centre and α-helical loop

Regarding the mononuclear copper centre (T1 copper), the 3-D structure showed that this ion is located within domain 3 and ligated with four different residues: His495, His434, and Cys490 with Met500 as an axial ligand, in a trigonal pyramidal coordination shape (**Figure 45, A**), the same as that observed in other bacterial laccases, such as *E. coli*

CueO (**Figure 45, B**). The presence of methionine as an axial ligand has been previously reported as a common feature of bacterial laccases, whereas in fungal laccases a phenylalanine or a leucine is found at this position, such as the phenylalanine found in the fungal laccase from *T. versicolor* (TvL) (PDB: 1GYC), whose T1 coordination shows a trigonal coplanar shape (**Figure 45, C**). It has been proved that the redox potential of a laccase can be affected by this residue, and that the presence of a methionine usually corresponds with a low redox potential value [85, 91, 92], as it has been previously stated in section 5.1, Introduction.

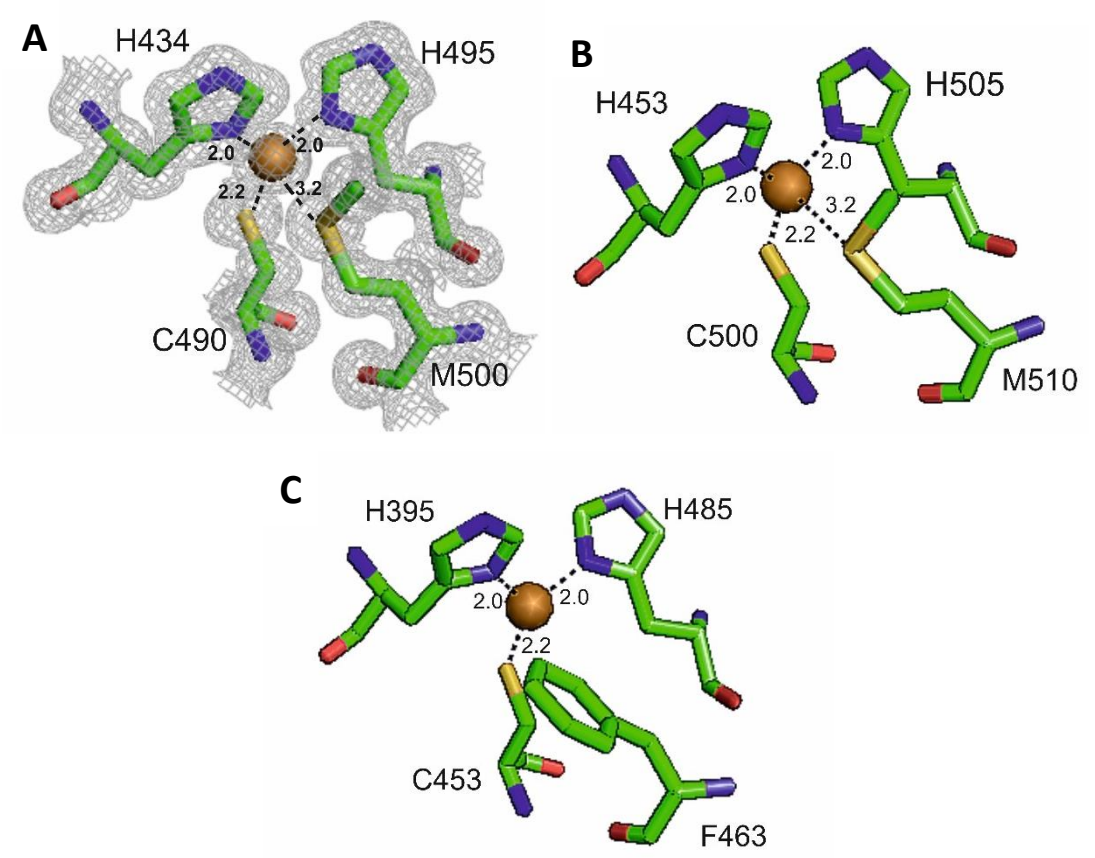

Figure 45. Comparison of the T1 copper centre. Copper-ligating residues are presented as green sticks. The distances between coordination residues and the copper ion (orange sphere) are depicted as dashed black lines. (A) Ochrobactrum sp. CueO (Oc-CueO, PDB: 6EVG), with the trigonal pyramidal coordination of the copper ion. The 2Fo - FC electron density map (1.5 σ level) is represented as gray mesh. (B) Escherichia coli CueO (Ec-CueO, PDB: 1KV7), with the trigonal pyramidal coordination of the copper ion. (C) Trametes versicolor laccase (TvL, PDB: 1GYC), with the trigonal coplanar co-ordination of the copper ion. Graphic generated in the software PyMOL, by Dr Rachael Wilkinson, and taken from [183].

The α-helical loop structure located close to the active site, reported for bacterial laccases, was also observed in Oc-CueO, comprising from residue 339 to residue 401. The T1

site is buried and the putative active site is partially blocked by this structure. Results of the crystal structure were unable to show residues 350 to 391, which are part of the α-helical loop, maybe due to its suspected flexibility (**Figure 46**). Similar observations have been reported for other bacterial laccases, including the *E. coli* CueO (Ec-CueO), whose residues 380 – 403 were not observed [144]. The sequence of the α-helical loop includes a total of 63 residues in Oc-CueO, being 11 methionine residues. The high methionine content of this structure has been reported for Ec-CueO, where 14 residues are methionine, out of 49 residues that comprise this structure, and its function has been proposed to be involved in copper attachment [220].

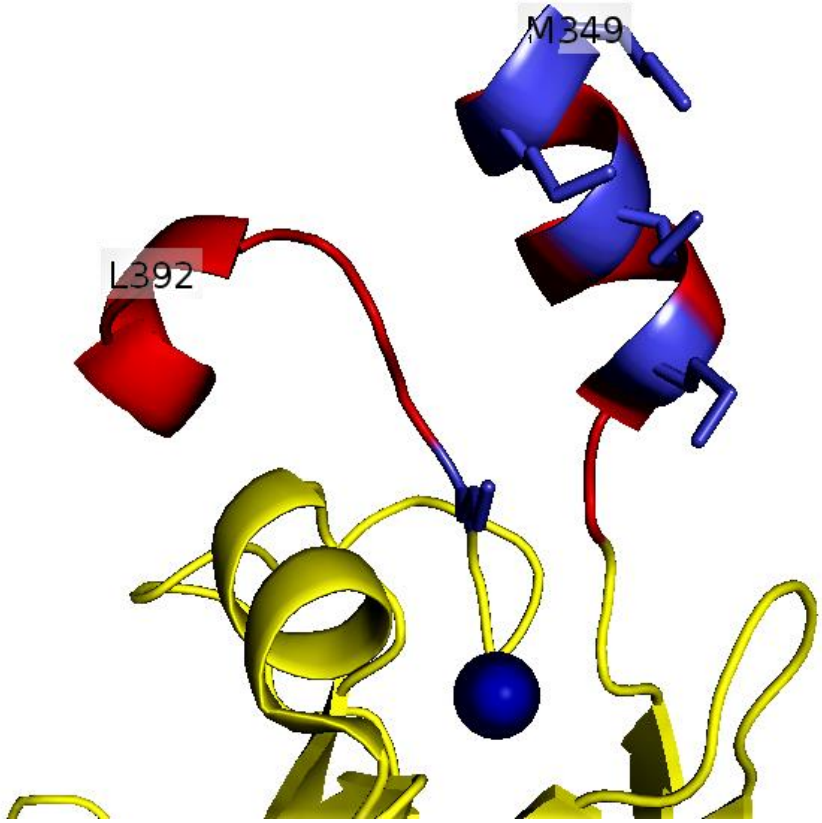

Figure 46. Oc-CueO α-helical loop over T1 copper. The α-helical loop is shown in red colour; T1 copper ion is depicted as a blue sphere; and methionine residues contained within the α-helical loop are represented as slate sticks. Residues 350 to 391 were unable to be traced in the structure, the missing fragment contains 6 additional methionine residues. Graphic generated by the software PyMOL, with Oc-CueO (PDB: 6EVG).

5.2.3 Structure of the trinuclear copper centre (TNC)

In bacterial and fungal laccases, the trinuclear copper site (TNC) is embedded between domain 1 and domain 3, however, no clear electron density was observed in the structure of Oc-CueO in this region, though all copper ligating-residues are present and the

overall typical surrounding configuration of the TNC is preserved (**Figure 47, A**). A possible damage induced by X-ray was considered as the possible cause of the lack of copper at this site. A detailed analysis of the Oc-CueO dataset using wedges of data showed no electron density for the T1 and T3 copper ions from the first wedge of data onwards. This evidence suggests that copper ions were missing from the crystals, which were grown aerobically. The difficulty to express laccases fully loaded with copper ions has previously been reported in literature [144, 173]. The T2 and T3 copper ions located at the TNC are coordinated by a total of eight well-conserved histidine residues [83, 141, 143], which are present in the crystal structure of Oc-CueO. Copper ions were modelled into the Oc-CueO structure using coordinates from the structurally similar *E. coli* CueO (Ec-CueO) structure (PDB: 3NSF) to confirm the positioning of the T2/3 site (**Figure 47, B**) [183]. A superposition of the Oc-CueO TNC site with that from the fully copper loaded *E. coli* CueO (PDB: 4E9Q [220]), showed that histidine residues 131 and 93 are in a different conformation (**Figure 47, C**), suggesting that these residues may have a key role in the coordination of T2 copper. Minor alterations were also found for the histidine residues 133, 439 and 91. On the other hand, histidine residues 491 and 489 were found to be almost identical to their *E. coli* CueO counterparts. The Oc-CueO sequence was used to generate a ModBase model [226], which produced a TNC site near identical in conformation to that observed for the fully copper loaded *E. coli* CueO (PDB: 4E9Q) TNC site [183].

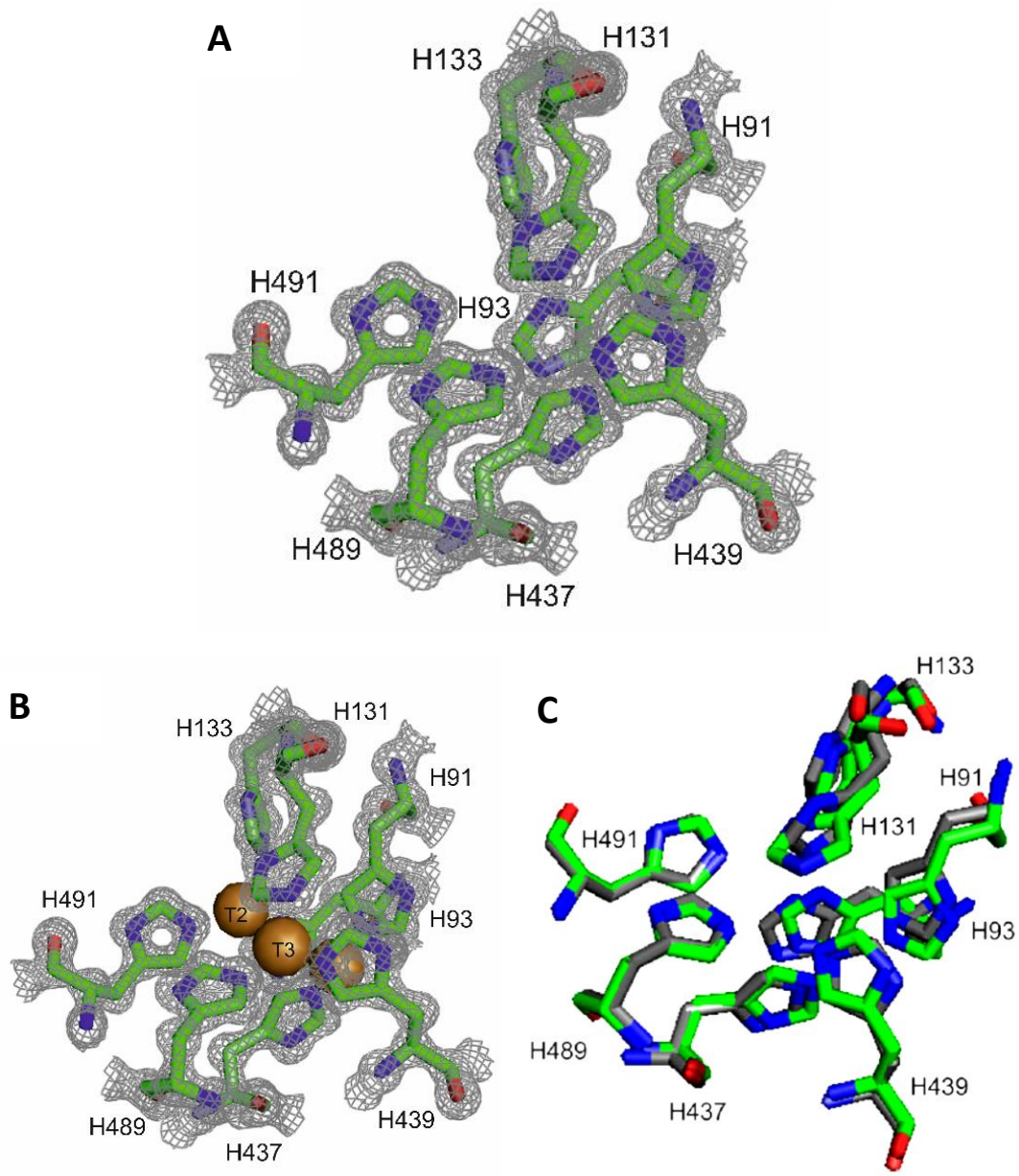

Figure 47. Oc-CueO trinuclear copper site (TNC). Oc-CueO conserved histidine residues are depicted as green sticks. The 2Fo – Fc electron density map (1.5 σ level) around conserved histidines is represented as gray mesh. Coper ions are represented as orange spheres. (A) Oc-CueO TNC site, without copper ions. (B) Oc-CueO TNC site with modelled copper ions based on coordinates from *Escherichia coli* CueO (PDB: 3NSF). (C) Superposition of the E. *coli CueO* (PDB: 1KV7) TNC site with the conserved histidines depicted as gray sticks, onto the apo Oc-CueO TNC (PDB 6EVG). Labels of residues are referred to the Oc-CueO sequence. Graphic generated in the software PyMOL, by Dr Rachael Wilkinson, and taken from [183].

5.2.4 Oc-CueO tunnels

Tunnels are accessible paths that can connect the interior of a molecule with the surrounding solvent environment, while channels are void spaces that can pass through the protein structure, with both endings opened to the surrounding solvent. These structures

are very important for protein functionality and enzyme activity, as their role can be related with molecules diffusion and substrate access [227]. In laccases, it is known that the entrance of oxygen is needed from the surrounding environment into the trinuclear cluster site (TNC), as oxygen is the last electron acceptor. Once oxygen reaches the TNC, it is reduced to water [75, 81, 84], which upon reaction completion would need to diffuse outside of the enzyme, to prevent water accumulation in the TNC. Tunnels connecting the surrounding environment of laccases with the TNC have been identified and described in both, fungal and bacterial laccases [83, 85, 144, 228, 229], though neither their function nor their detailed structure have been fully characterized. In *E. coli* CueO, a residue (Glu106) located at the entrance of a tunnel was proposed as the cause of the loosing of the T2 copper from the laccase, as the corresponding residue in non-copper dependant laccases is a hydrophobic residue (Ph), which might prevent T2 copper from exchange with solvent [144].

In Oc-CueO, three solvent tunnels leading to the TNC were identified using CAVER 3.0 [230]. The residues involved in tunnels formation are listed in table **Table 14**. Two tunnels would end at the T3 copper ion and are located between domains one and two. Each channel includes their own solvent entrance, then they converge in a single shared access to the TNC site (**Figure 48, A**). Another putative solvent tunnel was identified, which would originate from the T2 copper ion (**Figure 48, B**). This differs slightly from tunnels identified in other laccases, such as *Melanocarpus albomyces* [231] and *Lentinus tigrinus* [229] laccases, where only two tunnels were described, one ending at the T2 copper ion, whereas the other ended at the T3 copper ion. Tunnel 1 and 2 are located between domain 1 and 2, whereas tunnel 3 is located between domains 1, 2 and 3 (**Figure 48, C**). These channels ending at the TNC are important in enabling the access of oxygen and release of water molecules [229].

Table 14. Characteristics of solvent channels calculated for Oc-CueO. Throughput – denotes ease with which compounds could pass through the tunnel; Cost – the cost function denotes how likely a tunnel is with short direct paths 'cheap' and long complicated paths 'expensive'; Curvature – is the length of the tunnel divided by the shortest distance of the origin to the tunnel end point; Bottleneck radius – the radius for the smallest part of the tunnel. Table generated by Dr Rachael Wilkinson, and taken from [183].

Putative Solvent Tunnel	Throughput	Cost	Length/ Å	Curvature	Bottleneck radius	Bottleneck residues
1	0.44	0.82	25	1.34	1.35	H131, L493, H491, T138, P132, E496, H133, W129, H489, A142, H93
2	0.27	1.31	30.82	1.5	0.93	V186, F198, R179, V180, H143, Y187, R178, E188
3	0.68	0.38	12.6	1.2	1.4	H91, W92, H93, G94, L95, D102, H437, I438, H439, G440, D462, R478

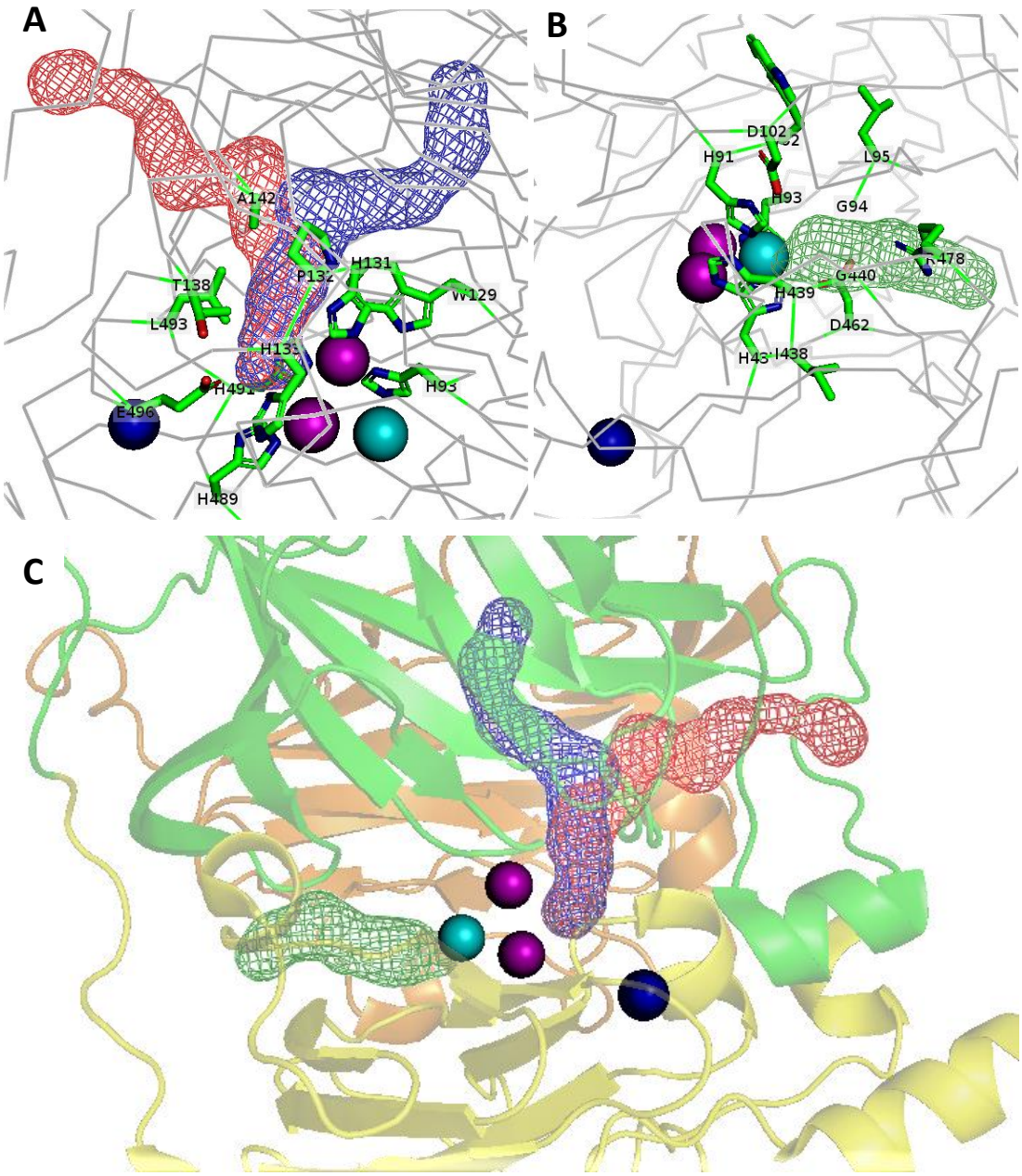

Figure 48. Oc-Cue tunnels identified by CAVER [230]. Oc-CueO is represented as a ribbon diagram and T1, T2 and T3 copper ions are depicted as blue, teal, and purple spheres, respectively. T2 and T3 coppers were generated by a superposition of Oc-CueO with the Escherichia coli CueO (PDB: 4E9Q), hence their location respecting to the tunnel is only approximated. (A) Tunnel 1 and tunnel 2 are presented in blue and red mesh, respectively, both ending in the TNC, close to where it would be one of the T3 copper ions. Bottleneck residues of the tunnel 1, in the surroundings of the TNC, are depicted as green sticks. (B) Tunnel 3 is presented in green mesh. This tunnel ends where it would be located the T2 copper. Bottleneck residues are depicted as green sticks. (C) Position of tunnels 1, 2 and 3 (blue, red and green mesh, respectively) in respect to their location in the protein. Domain 1, 2 and 3 are coloured in orange, green and yellow, respectively. Graphic generated by the software PyMOL, with Oc-CueO (PDB: 6EVG).

5.3 Oc-CueO site directed mutagenesis

The functional differences between bacterial and fungal laccases are yet to be understood. As stated before, the sequence homology between bacterial and fungal multicopper oxidases is low, though between fungal laccases, this homology is relatively high. For instance, the bacterial laccase CotA from *Bacillus subtilis* has a sequence identity of only 21% compared with the fungal laccase from *Trametes versicolor* (TvL), whereas the identity reaches 79% between the fungal laccases from *Trametes versicolor* (TvL) and *Cerrena maxima*. However, there are four motifs that are very well conserved in all MCOs: HXHG, HXH, HXXHXH, and HCHXXXHXXXXM/L/F, and these motifs contain the copper-ligating residues [95, 106, 113]. It is not clear how bacterial laccases can perform the same reactions and share the same molecular architecture as fungal laccases, with such a low sequence homology. Several distinguishing features have been identified for bacterial laccases, although neither their function nor their underlying evolutionary purpose have been elucidated. It is known that bacterial laccases usually present lower redox potentials than fungal laccases, and that they are usually easier to clone and express with relatively high yields [106, 175], whereas fungal laccases tend to accept a broader range of substrates due to their commonly high redox potentials [142]. Understanding how and why bacterial and fungal laccases are different could lead to the design of novel and interesting laccases for industrial applications.

5.3.1 Multiple sequence alignment of bacterial and fungal laccases

To acquire a deeper insight into the structural differences between fungal and bacterial laccases, a multiple sequence alignment was performed with 32 fungal laccases and 33 putative bacterial laccases or multicopper oxidases sequences. A protein sequence search was carried out in Uniprot (http://www.uniprot.org/) and NCBI (https://www.ncbi.nlm.nih.gov/protein/) databases. Where possible, reviewed (Swiss Prot) sequences were selected, which were usually available for fungal laccases, especially high redox potential laccases. Conversely, bacterial laccases sequences were commonly only predicted or putative sequences without experimental verification. The multiple sequence alignment was performed using the CLC workbench software (https://www.qiagenbioinformatics.com/). The aim of the alignment was, firstly, try to identify well-conserved residues among fungal and bacterial laccases, other than the already reported motifs present in all MCOs; and secondly, try to identify motifs conserved in high-

redox potential fungal laccases, that are not found in bacterial laccases. A partial amino acid sequence alignment can be seen in **Figure 49**, while the full alignment with all the sequences used for this analysis is presented in **Appendix 3**.

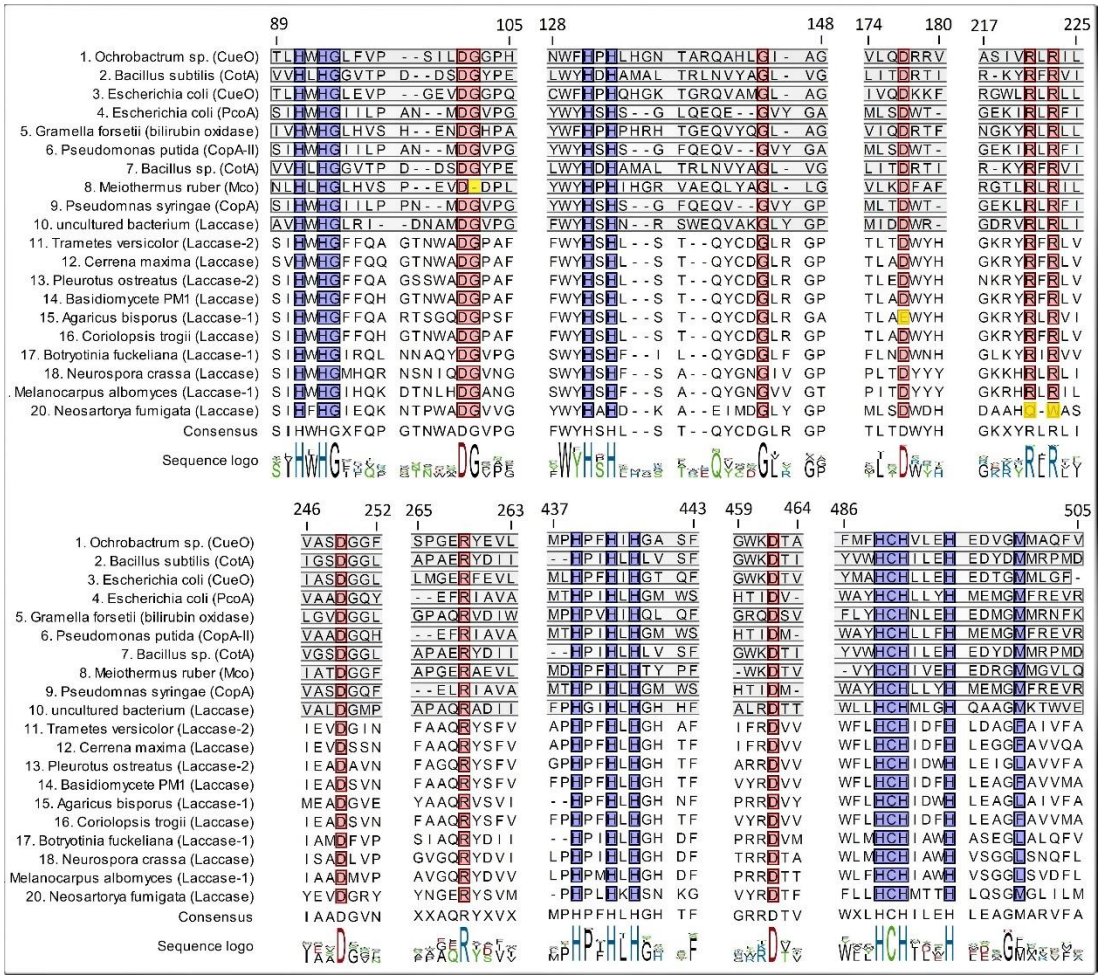

Figure 49. Partial amino acid sequence alignment, showing 10 bacterial laccase-like multicopper oxidases (in gray background) and 10 fungal laccases. Metal-binding residues are coloured in blue; other conserved residues are coloured in red (**Table 15**), while mismatches are highlighted in yellow. Numbering is based on Oc-CueO sequence as reference. Uniprot or GenBank accession codes as follows: 2, P07788; 3, P36649; 4, A0A0E0XT94; 5, (GB) WP_011709064.1; 6, Q88C03; 7, B9W2C5; 8, (GB) WP_013012601.1; 9, P12374; 10, E1ACR6; 11, Q12718; 12, D0VWU3; 13, Q12739; 14, Q12571; 15, Q12541; 16, Q9HDQ0; 17, Q12570; 18, P06811; 19, Q70KY3; and 20, E9RBR0. Adapted from [183].

From this analysis, two groups of amino acid residues were identified: Group 1 contained amino acid residues that are found in > 90% of fungal and bacterial sequences, representing well-conserved residues found among fungal and bacterial laccases; whereas Group 2 contained amino acid residues near to the copper ions, that are well-conserved only in high redox potential laccases (HRPL) but are not found in bacterial laccases (**Table 15**).

Table 15. Well-conserved residues among bacterial and fungal laccases (Group 1) and well-conserved residues in HRPL near to copper ions and absent in bacterial laccases (Group 2). Taken from [183].

Group 1: Well-conserved residues among bacterial and fungal laccases		Group 2: Well-conserved residues in HRPL near to copper ions and absent in bacterial laccases	
Oc-CueO location	Alignment hit percentage among fungal and bacterial laccases (%)	Oc-CueO location	Well-conserved HRPL sequence
D (102)	100%	K (482), S (483) H (484) and F (486)	NPGXW
G (103)	94%		
R (221)	91%		
R (223)	97%		
D (249)	94%	I (109), A (110), A (111) and G (112)	QCPI
R (269)	92%		
D (462)	95%		
G (145)	100%		
D (177)	97%		

Once these residues were identified, a 3-D structure analysis was carried out to determine their location in the protein using both, a fungal laccase (TvL laccase, PDB: 1GYC) and a bacterial laccase (Oc-CueO, PDB: 6EVG).

5.3.2 Group 1: well-conserved residues among fungal and bacterial laccases

Remarkably, 5 out of 9 well-conserved residues identified for group 1 were found in domain 2 (from residue 161 to residue 318), a domain whose role in laccases has commonly been seen as mere scaffolding, with no obvious function in enzyme activity [93, 141]. The fact that most of these well-conserved residues are in domain 2 may suggest that this domain could play a functional role in laccases, beyond its traditional structural role. Except for D102 and G103, which are just behind the T2 copper ion, neither of the residues of Group 1 are close to any of the copper centres, though most of them are more proximal to the TNC than to the T1 copper. The locations of these residues for bacterial (Oc-CueO) and fungal (TvL) laccases are shown in **Figure 50, A and B**. Based on their location, it was clear that these residues would not be involved in copper electron transfer, and although their function might be related with scaffolding, the location of most of these residues in an apparent cluster behind the TNC and their high conservancy suggests another possible role in laccases. A tunnel analysis was carried out by CAVER [230], using PyMOL software, and results showed that these residues are forming part of tunnels in bacterial and fungal laccases (**Figure 50, C and D**).

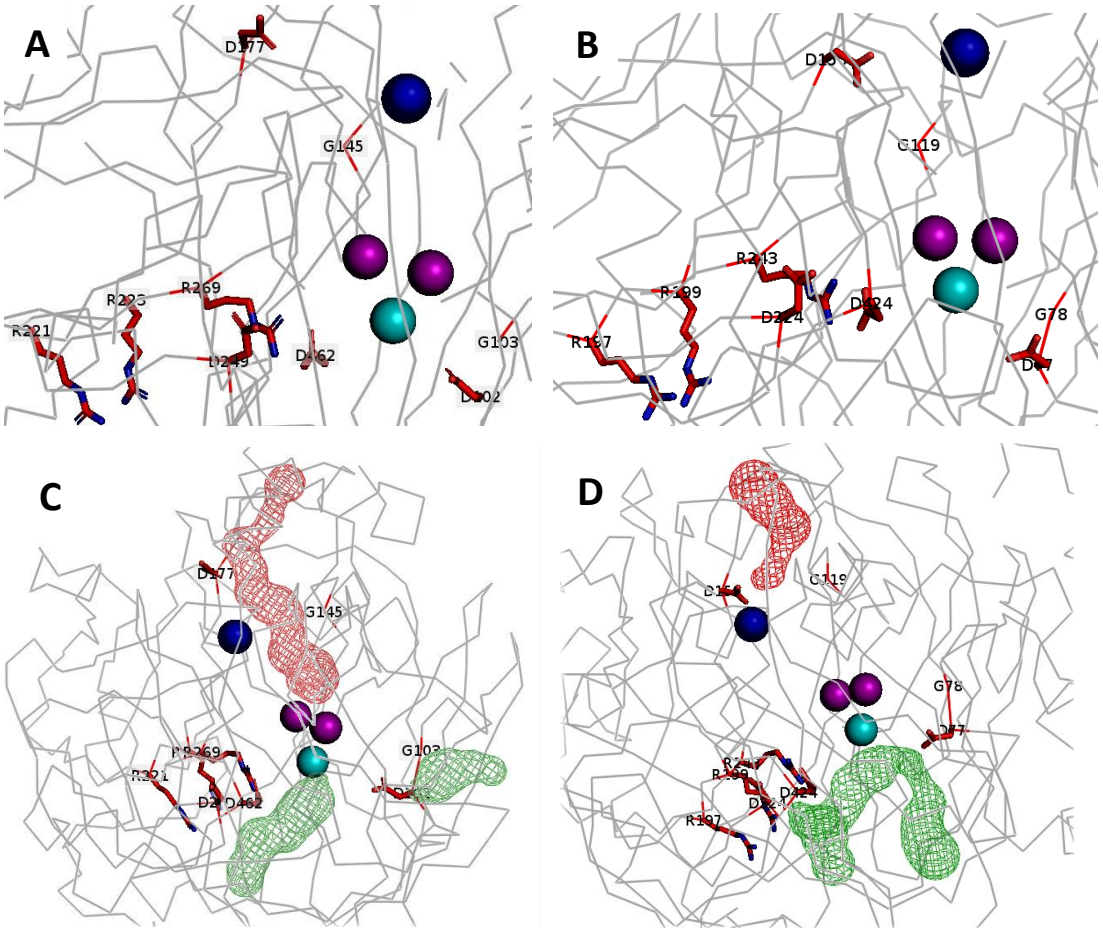

Figure 50. Group 1: well conserved residues among fungal and bacterial laccases. 3-D location of Group 1 residues in the protein structure of: (A) bacterial laccase Oc-CueO; and (B) fungal laccase TvL. Identification of tunnels associated with well-conserved residues and its location in the 3-D structure of (C) bacterial laccase Oc-CueO; and (D) fungal laccase TvL. Proteins are presented as gray ribbon, T1, T2 and T3 copper ions are depicted as blue, teal, and purple spheres, respectively. T2 and T3 coppers of Oc-CueO were generated by a superposition of Oc-CueO with the *Escherichia coli* CueO (PDB: 4E9Q). Graphic generated by the software PyMOL, with Oc-CueO (PDB: 6EVG) and Trametes versicolor laccase (TvL, PDB: 1GYC).

In the fungal laccase from *Trametes versicolor* (TvL), the corresponding well conserved residues are forming a channel in an inverted "U" shape that begin in the surface of the protein, pass through the TNC, connects the T2 copper, and ends at the surface of the protein in a different point (**Figure 50, D**; channel shown in green mesh). In Oc-CueO, two different tunnels were identified, one includes an entrance at the surface of the protein and ends in the T2 copper (the already described tunnel 3). This tunnel is short and straight, which might influence the loss of T2 and T3 coppers ions in the 3-D structure of Oc-CueO and could also be the reason for the dependence of this protein for addition of exogenous copper ions to trigger enzyme activity, while the fungal laccase TvL shows a more buried TNC. A

second tunnel was identified, connecting the well-conserved residues D102 and G103 with the surface of the protein, and it could be related with water diffusion from the TNC. In the bacterial laccase Oc-CueO, these tunnels are not connected (**Figure 50, C**; tunnels shown in green mesh).

The well-conserved double arginine (R221 and R223 in Oc-CueO) residues found among fungal and bacterial laccases do not form part of any tunnel, instead they are on the surface of the protein, very close to the entrance of the tunnels formed by the other well-conserved residues (**Figure 51**), which might also suggest an active role in molecule transportation. The positive charge of arginine might form a hydrogen bond with oxygen atoms at the surface of the protein, locating them close to the entrance of the tunnels connecting the surface of the protein with the T2 copper, hence facilitating their diffusion into the TNC.

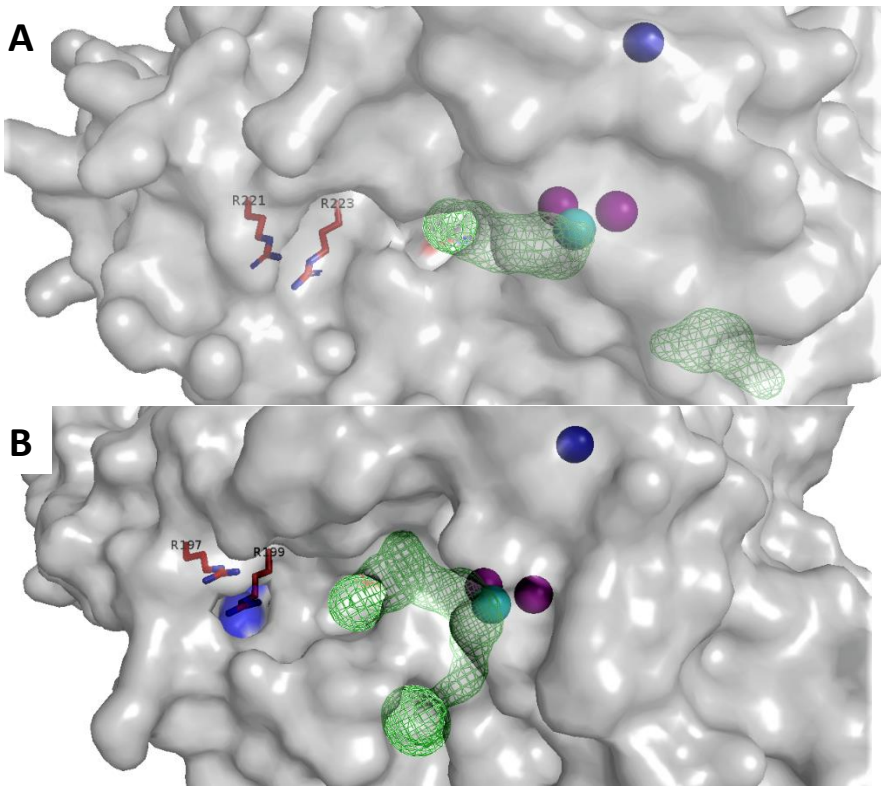

Figure 51. Conserved residues R221 and R223 are not forming part of tunnels. They are located at the surface of the protein, close to the entrance of the tunnel connecting the surrounding environment of the protein with the T2 at the TNC. (A) Bacterial laccase Oc-CueO. (B) Corresponding residues in the fungal laccase, TvL. T1, T2 and T3 copper ions are depicted as blue, teal, and purple spheres, respectively. T2 and T3 coppers of Oc-CueO were generated by a superposition of Oc-CueO with the *Escherichia coli* CueO (PDB: 4E9Q). Graphic generated by the software PyMOL, with Oc-CueO (PDB: 6EVG) and *Trametes versicolor* laccase (TvL, PDB: 1GYC).

In bacterial laccases, it was found that both G145 and D177 are forming part of the tunnels previously described as tunnel 2. The corresponding residues in fungal laccases are forming part of a smaller tunnel with no obvious function and not connected with any copper ion. From the analysis of tunnels in fungal (TvL) and bacterial (Oc-CueO) laccases, it seems that the fungal laccase uses the inverted "U" shape tunnel for oxygen entrance and water exit, while the bacterial laccase would use the channel behind T2 copper for entrance of oxygen, and the tunnel 1 or tunnel 2 for water exit. It is interesting that most of these newly identified well-conserved residues seem to be somehow connected with the TNC, whereas no additional residue was found related with the T1 copper, the centre that is commonly seen as the most important copper in laccases. Since the catalytic electron transfer is performed in the TNC, this would explain that several nearby residues must be conserved to enable laccase activity, while the T1 copper can be adaptative to the environment and to different substrates, so that its surrounding molecular environment can change depending on the needs of the host organism. More studies would be needed to confirm these suggestions.

5.3.3 Group 2: Well-conserved residues in high redox potential fungal laccases (HRPL) near to copper ions and absent in bacterial laccases

The sequence alignment of high redox potential fungal laccases (HRPL) showed a high similarity among these enzymes, hence the identification of conserved sequences that could play a pivotal role in enzyme activity was not clear. As selection criteria, conserved regions that could have an important function in catalysis should be always present in HRPL; whereas they should be completely missing in bacterial laccases. **Figure 52** shows the partial alignment. Only two short sequences met the selection criteria: QCPI and NPGXW (**Table 15**). Interestingly, both of these sequences have been previously described as signature features of fungal laccases [95], being QCPI located at the end of L1 region, and NPGXW partially included at the beginning of L4 region, both described in the section: 5.1, Introduction. In HRPL, these sequences were not involved in any tunnel or channel (**Figure 53, B**); while in the bacterial laccases Oc-CueO, the corresponding residues to the NPGXW sequence (K482, S483, H484 and F486) are forming part of the channel behind the TNC (**Figure 53, A**), so that it was suspected that the distorted tunnel observed in bacterial laccase might be related with this change.

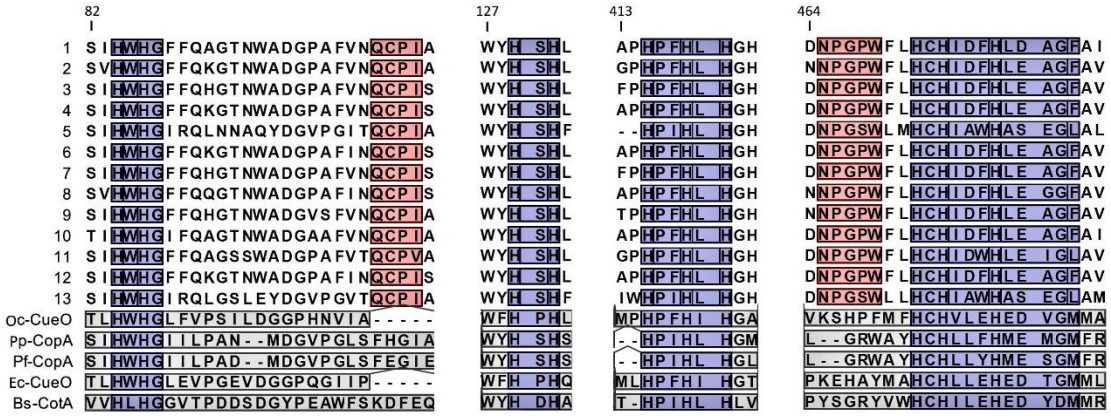

Figure 52. Partial sequence alignment of HRPL fungal laccases with some bacterial laccases (in gray background). MCOs conserved motifs are coloured in blue. Group 2 residues conserved in HRPL but absent in bacterial laccases (**Table 15)** are coloured in red. Fungal laccases Numbering is based on the sequence of enzyme 1, as reference. Enzymes and PDB (*) or Uniprot codes used for alignment: 1: 1GYC*, *Trametes versicolor*; 2: 2HZH*, *Trametes ochracea*; 3: 2HRH*, *Coriolopsis trogii*; 4: Q02497, *Trametes hirsuta*; 5: Q12570, *Botryotinia fuckeliana*; 6: Q99044, *Trametes villosa*; 7: Q12571, *Basidiomycete* PM1; 8: D0VWU3, *Cerrena maxima*; 9: O59896, *Pycnoporus cinnabarinus*; 10: Q8TG93, *Trametes pubescens*; 11: Q12739, *Pleurotus ostreatus*; 12: Q8TG94, *Trametes pubescens*; 13: H8ZRU2, *Botrytis aclada*. Oc-CueO: N/A; Pp-CopA: Q88C03; Pf-CopA: Q4KCN4; Ec-CueO: P36649; Bs-CotA: P07788. Alignment generated by CLC Workbench software (https://www.qiagenbioinformatics.com/).

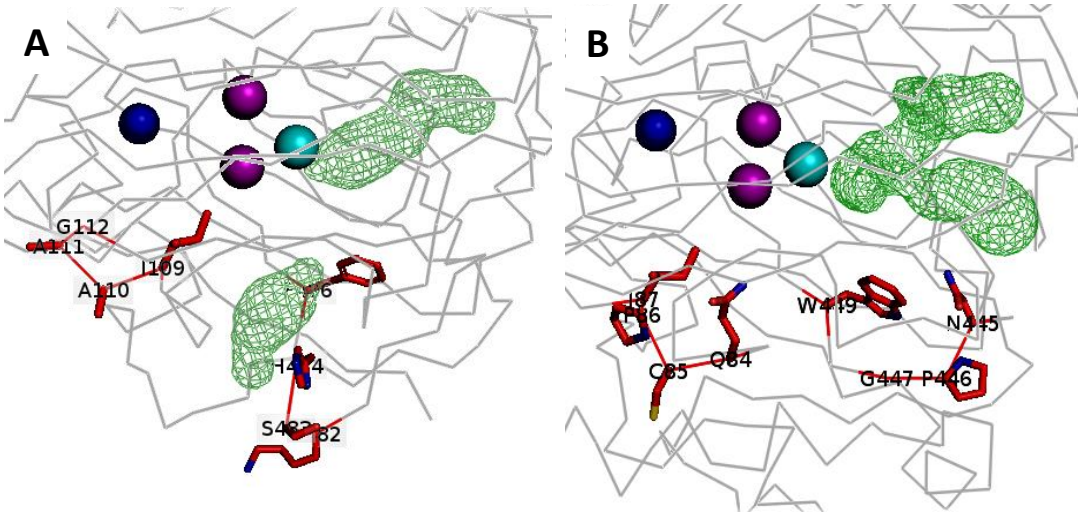

Figure 53. Group 2: well conserved residues in HRPL, absent in bacterial laccases. 3-D location of Group 2 residues in the protein structure of: (A) bacterial laccase Oc-CueO; and (B) fungal laccase TvL. Proteins are presented as gray ribbon, T1, T2 and T3 copper ions are depicted as blue, teal, and purple spheres, respectively. T2 and T3 coppers of Oc-CueO were generated by a superposition of Oc-CueO with the *Escherichia coli* CueO (PDB: 4E9Q). Graphic generated by the software PyMOL, with Oc-CueO (PDB: 6EVG) and *Trametes versicolor* laccase (TvL, PDB: 1GYC).

5.3.4 Oc-CueO site directed mutagenesis

A site directed mutagenesis approach was used to partially elucidate some of the possible influences in Oc-CueO activity of the conserved residues found by the multiple sequence alignment, sorted into Group 1 and Group 2. A total of 8 different mutants were designed, some residues were converted into alanine only to demonstrate their importance in enzyme activity, while other mutants were changed into the corresponding residue found in high redox potential laccases (HRPL) as an attempt to increase the Oc-CueO activity. The 8 mutants are listed as follows:

- Mutant 1: change of the well-conserved residue D462, and the adjacent residue K461 into alanine, to disturb the cluster of residues forming the tunnel 3, behind the TNC. This change would also affect the nearby well-conserved residues D249 and R269. A possible loss of activity was expected.
- Mutant 2: change of the well-conserved residues R221 and R223 into alanine residues. The function of these double arginines is unknown, yet a possible oxygen channelling is suspected, so the change of these residues into the hydrophobic alanine might result in loss of activity.
- Mutant 3: change of the well-conserved residues D102 and G103 into alanine residues. These residues are located behind the T2 copper and might be forming part of the tunnel 3 located behind the TNC or they could be interacting with the histidine-ligating residues of T2. A loss of activity was expected.
- Mutant 4: change of S163, F164 and N165 into G, T and F, respectively. The three target residues are adjacent to the well conserved motif of MCOs, HXH, and are nearby the new well-conserved residues D249, R269 and D462, possibly forming part of the distorted tunnel 3, behind the TNC. The replacing residues, G, T and F, were chosen as these residues are commonly found in HRPL, as an attempt to modify the tunnel and increase Oc-CueO activity.
- Mutant 5: change of I109, A110 and A111 into Q, C, P, respectively. The targeted residues are the corresponding residues found in Oc-CueO, at the location of the Group 2 sequences found in HRPL, QCPI. The mutation was an attempt to improve Oc-CueO activity by imitating the well-conserved residues found in HRPL. The mutated residues are located just behind the well conserved residues D102 and G103.
- Mutant 6: change of F486 and M487 into W and L, respectively. The replacing residues are the corresponding residues found in HRPL, between the MCOs

conserved motif HCHXXXHXXXXM/L/F, and the sequence found in Group 2, NPGXW. The mutation was an attempt to improve Oc-CueO activity by imitating the well-conserved residues found in HRPL. The mutated residues are behind the TNC, nearby of the conserved residues D102 and G103.

- Mutant 7: change of K482, S483 and H484 into N, P and G, respectively. The targeted residues are the corresponding residues found in Oc-CueO, at the location of the Group 2 sequences found in HRPL, NPGXW. The mutation was an attempt to improve Oc-CueO activity by imitating the well-conserved residues found in HRPL.
- Mutant 8: Change K461 into R. The residue K461 is adjacent to the well-conserved residue D462, and nearby of the well-conserved residues D249 and R269. This residue seems to be forming part of the tunnel 3, behind the T2 of the TNC. The replacing residue, R, is the corresponding residue found in HRPL. The mutation was an attempt to improve Oc-CueO activity by imitating the well-conserved residues found in fungal HRPL. Since both K and R are positively charged, this mutation can also lead to a silent mutation, yet the presence of R is strongly dominant in fungal laccases.

The site directed mutagenesis (SDM) was carried out using the QuikChange II XL Site-Directed Mutagenesis Kit (Agilent Technologies, Craven Arms, UK), following the instructions provided by the manufacturer. The oligonucleotide primers used, and a summary of the mutated residues can be found in **Table 16**. After PCR with designed primers was performed, the products were subjected to digestion with Dpn I enzyme, followed by transformation into competent cells and plating on LB agar plates, supplemented with ampicillin. A screening by sequencing was used to confirm that the desired mutation had occurred. Then the right plasmids were used for transformation into BL21 *E. coli* competent cells for protein expression. Expression and protein purification of each mutant protein was performed following the same procedure used for expression of wile type protein Oc-CueO. A summary of the yield of expressed mutant proteins is shown in **Table 17**. Once expressed, mutant proteins were tested for activity towards ABTS and SGZ, and their activity was compared with the activity of the Oc-CueO wild type. A detailed explanation of SDM procedures, protein expression and enzyme activity assays can be found in sections: 8.2, Specific procedures; and 8.1, General procedures.

Table 16. List of target mutations and primers used for SDM. Taken from [183].

Mutant	Original residues	Mutant residues	Forward and reverse primers 5' - 3'
Mutant 1	K, D (461, 462)	A, A	Fw cgcatcaatcgggatgggcggctaccgcattgatcgacg Rev cgtcgatcaatgcggtagccgcccatcccgattgatgcg
Mutant 2	R-R (221, 223)	A-A	Fw ccctgcatctatcgtcgctctggctatcttgaacggcgcc Rev ggcgccgttcaagatagccagagcgacgatagatgcaggg
Mutant 3	D, G (102, 103)	A, A	Fw gccgtcgatactcgctgccggaccccataatg Rev cattatggggtccggcagcgagtatcgacggc
Mutant 4	S, F, N (126-128)	G, T, F	Fw gaagtcaaaattcagcaaccggctgggaccttctggttccatccgcatttgcacgg Rev ccgtgcaaatgcggatggaaccagaaggtcccagccggttgctgaattttgacttc
Mutant 5	I, A, A (109-111)	Q, C, P	Fw gtcgatactcgatggcggaccccataatgttcagtgcccgggcgaggcttggaa Rev ttccaagcctcgcccgggcactgaacattatggggtccgccatcgagtatcgac
Mutant 6	F, M (486, 487)	W, L	Fw gtgaggcggtgaaaagccatccatggttgtttcattgccatgttctg Rev cagaacatggcaatgaaacaaccatggatggcttttcaccgcctcac
Mutant 7	K, S, H (482-484)	N, P, G	Fw ctggttcattttgaccgtgaggcggtgaatcccggtccatttatgtttcattgcca Rev tggcaatgaaacataaatggaccgggattcaccgcctcacggtcaaaatgaaccag
Mutant 8	K461	R	Fw gcgcatcaatcgggatggcgcgataccgcattgatcgac Rev gtcgatcaatgcggtatcgcgccatcccgattgatgcgc

Table 17. Protein yield of expressed mutant proteins and Oc-CueO wild type (wt), from 1 litre of culture. A volume of 7 mL of protein solution was achieved for each mutant, after protein purification.

Mutant	Protein Concentration (mg/mL)	Protein mass (mg)
Mutant 1	0.52	3.64
Mutant 2	0.65	4.55
Mutant 3	0.75	5.25
Mutant 4	0.75	5.25
Mutant 5	1.37	9.1
Mutant 6	2.31	16.2
Mutant 7	0.8	5.6
Mutant 8	0.7	4.9
O-CueO wt	2	14

Enzyme activity results showed that Mutants 1 and 2 lost completely their activity. A decrease in the enzyme activity was expected for both mutants, however such a strong response suggests that the well-conserved residue D462, and the double arginine residues, R221 and R223, can significantly affect the activity of Oc-CueO. Mutant 1 was designed to prove the importance of key charged residues in tunnel 3 (D462, D249 and R269), which connects the surface of the protein with the T2 copper at the TNC site. A disturbance of the molecular environment of this tunnel has blocked totally the activity of Oc-CueO. Regarding the conserved double arginine residue, R221 and R223, their function is still unknown,

although an involvement in oxygen channelling can be suggested. The high conservation of these residues in fungal and bacterial laccases, supported with the experimental evidence proving that an alteration of these residues can totally block the enzyme activity, suggest that no matter what their function, their presence is very important for laccase function.

Mutant 3 and mutant 8 decreased their activity significantly, over 80% compared with the wild type Oc-CueO. Mutant 3 was expected to do this, as the mutated residues are well conserved among fungal and bacterial laccases (D102 and G103). D102 residue is located just behind the T2 copper ion and might interact with the histidine-ligating residues of this atom, hence a stronger response was expected for this mutant. However, even though the activity was significantly lost, the resulting mutant was not completely inactive, showing that though important, these residues are not essential for Oc-CueO activity. On the other hand, mutant 8 was meant to increase the activity of Oc-CueO, or at least to produce a silent mutation, as both the target and the replacing residues, were positively charged amino acids (K and R). However, the mutation affected greatly the activity of Oc-CueO, showing that the surrounding region of the tunnel 3 is very sensitive to changes, therefore this tunnel could represent an interesting region for laccase optimization.

Mutants 4, 5, 6 and 7 were meant to increase the activity of Oc-CueO by imitating the residues found in high redox potential fungal laccases (HRPL). However, neither of these mutants were able to surpass the activity of the Oc-CueO wild type. A summary of the enzymatic assays results is shown in **Figure 54**. A summary with the steady state kinetic parameters of Oc-CueO mutants, for ABTS and SGZ, can be found in **Table 18**.

Table 18. Summary of Steady-state kinetic parameters for Oc-CueO wild type and Oc-CueO mutants generated by site directed mutagenesis (SDM), with ABTS and SGZ as substrates.

ABTS							
	Km [mM]	**V_{max} [U/mg_{prot}]**	**k_{cat} [s^{-1}]**	**Kinetic efficiency [S^{-1} M^{-1}]**	**Stnd. Dev.**	**Kinetic efficiency [%]**	**Stnd. Dev.**
M-1	0	0	0	0	0	0.0	0
M-2	0	0	0	0	0	0.0	0
M-3	0.56	0.015	0.02	27.2	1.1	18.9	0.7
M-4	5.72	0.445	0.44	76.2	11.5	52.8	8.0
M-5	1.05	0.111	0.11	104.1	8.7	72.1	6.0
M-6	12.70	0.852	0.84	66.4	2.8	46.0	2.0
M-7	1.87	0.142	0.14	75.6	4.6	52.4	3.2
M-8	1.42	0.037	0.04	25.7	2.3	17.8	1.6
Oc-CueO	5.88	0.864	0.85	144.3	7.7	100.0	5.3
SGZ							
	Km [mM]	**V_{max} [U/mg_{prot}]**	**k_{cat} [s^{-1}]**	**Kinetic efficiency [S^{-1} M^{-1}]**	**Stnd. Dev.**	**Kinetic efficiency [%]**	**Stnd. Dev.**
M-1	0	0	0	0	0	0.0	0
M-2	0	0	0	0	0	0.0	0
M-3	0.307	0.51	0.50	6561	219	4.7	0.2
M-4	0.032	1.51	1.48	45912	1069	33.1	0.8
M-5	0.013	0.36	0.35	30228	9805	21.8	7.1
M-6	0.005	0.24	0.23	42849	2362	30.9	1.7
M-7	0.014	0.15	0.14	10571	383	7.6	0.3
M-8	0.020	0.01	0.01	719	990	0.5	0.7
Oc-CueO	0.004	0.59	0.58	138751	15138	100.0	10.9

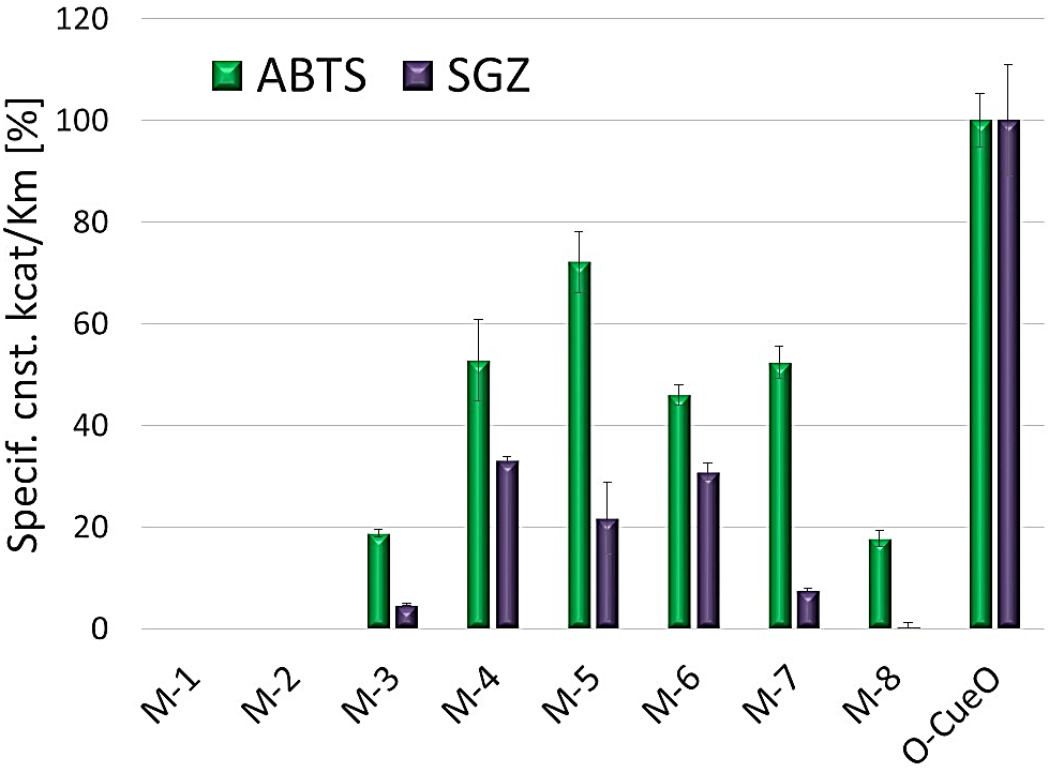

Figure 54. Kinetic activity of Oc-CueO mutants with ABTS and SGZ as substrates. Error bars are SD, n = 3. Mutant 1: K461 and D462 changed into A residues. Mutant 2: R221 and R223 changed into A residues. Mutant 3: D102 and G103 changed into A residues. Mutant 4: S126, F127 and N128 changed into G, T and F residues, respectively. Mutant 5: I109, A110 and A111 changed into Q, C and P residues, respectively. Mutant 6: F486 and M487 changed into W and L residues, respectively. Mutant 7: K482, S483 and H484 changed into N, P and G residues, respectively. Mutant 8: K461 changed into R residue.

6 Deletion of *copA* genes in *Pseudomonas putida* KT2440

6.1 Introduction

Biochemical studies on Pp-CopA and Pf-CopA have shown different properties of these proteins compared with Oc-CueO, such as the colour in solution, different UV-Vis spectrum profiles and differences in the copper content. These evidences could have suggested a different catalytic behaviour between Oc-CueO and the CopA-type proteins (Pp-CopA and Pf-CopA); however, the activity towards common laccases substrates, lignin-model compounds and even polymeric lignin proved to be very similar for the three bacterial LMCOs (see sections 3.2, 4.2 and 4.3). To elucidate to some extent these observations, a structural study was attempted by protein crystallization. Nevertheless, unlike Oc-CueO, CopAs did not form any crystals during crystallography assays, which limited these studies (see section 5.2). The biological function of CopA has been related with copper sequestration to confer copper resistance to *P. syringae* pv. tomato throughout the plasmid-borne copper resistance operon [156, 158]. On the other hand, a CopA-type protein was identified as a lignin degrading enzyme, detected by a specialized biosensor [102]. From these reports and the observations made in this study, it could be suggested that CopA proteins can potentially accomplish the two functions: be involved in copper resistance mechanisms and catalyse the oxidation of some phenolic compounds and maybe even lignin, which could challenge the canonical function assigned to this protein. To gain some understanding on this regard, a gene deletion experiment was conducted, to evaluate the growth of a strain lacking the *copA* genes, in a copper rich medium, and in presence of some phenolic compounds as sole carbon sources.

The host organism of Pp-CopA, *Pseudomonas putida* KT2440, was selected for gene deletion experiments, since genetic tools are available for this organism. *Pseudomonas putida* KT2440 is a Gram-negative, rod-shaped soil bacterium [232], and it is considered a microorganism with a great potential in environmental bioremediation and biotechnological applications, due to the astonishing capacities encoded in its genome, which provide it with huge metabolic versatility [233]. A revisited study of *P. putida* KT2440 genome revealed that, besides its well documented stress tolerance to adverse environmental conditions, this microorganism can also perform difficult redox reactions, making it a valuable platform microorganism for industrial biotechnology [234]. *P. putida* KT2440 contains the enzymatic

machinery needed for the metabolization of the following aromatic compounds: catechol, coniferyl-alcohol, protocatechuate, p-coumarate, caffeate, vanillate, p-hydroxybenzoate, ferulate, gallate, homogentisate, phenylacetate, benzoate, quinate, phenylalanine, tyrosine, nicotinate, and pyrimidine and purine nucleotides [234]; some of them are by-products or precursors of lignin. The *copA* genes have not been involved in any of these metabolic pathways.

6.2 Identification of copA genes and genetic context

The selected organism for gene deletion experiments, *Pseudomonas putida* KT2440, contains a powerful metabolic versatility; hence a possible loss of function due to a single gene deletion in a given metabolic pathway could potentially be restored by an alternative metabolic pathway, which would result in a silent mutant. To avoid this result, a Basic Local Alignment Search Tool (BLAST) was used to find putative *copA* or other multicopper oxidases genes contained in the genome of this strain. Results shown the presence of two putative genes encoding CopA proteins, and one gene encoding a multicopper oxidase protein, CumA. The details of these genes are shown in **Table 19**, whereas their genetic context can be seen in **Figure 55**. As the MCO CumA has been related in Mn^{2+} oxidation [185], and from its genetic context it does not appear to be involved in oxidation of phenolic compounds, the attention for gene deletion experiments was focused only on CopA encoding genes. More information regarding the genetic context of these genes in *Pseudomonas putida* KT2440 can be seen in section 2.2.1, Identification and genetic context of LMCOs genes.

Table 19. List of characteristics of *copA-I*, *copA-II* and *cumA* genes and their predicted proteins.

	Gene name		
	copA-I	*copA-II*	*cumA*
Location in the genome	2.510.006 bp to 2.511.730 bp	6.131.843 bp to 6.133.852 bp	1.180.948 bp to 1.182.354 bp
Length	1724 bp	2009 bp	1406 bp
Locus	PP_2205	PP_5380	PP_1034
Tat signal sequence	Yes	Yes	Yes
Most likely cleavage site of Tat sequence	52^53	73^74	47^48
Predicted protein	CopA	CopA (Pp-CopA) *	CumA
UniProt code	Q88KT4	Q88C03	Q88P19
Conserved MCOs motifs	Yes	Yes	Yes
(*) protein expressed and characterized in this study			

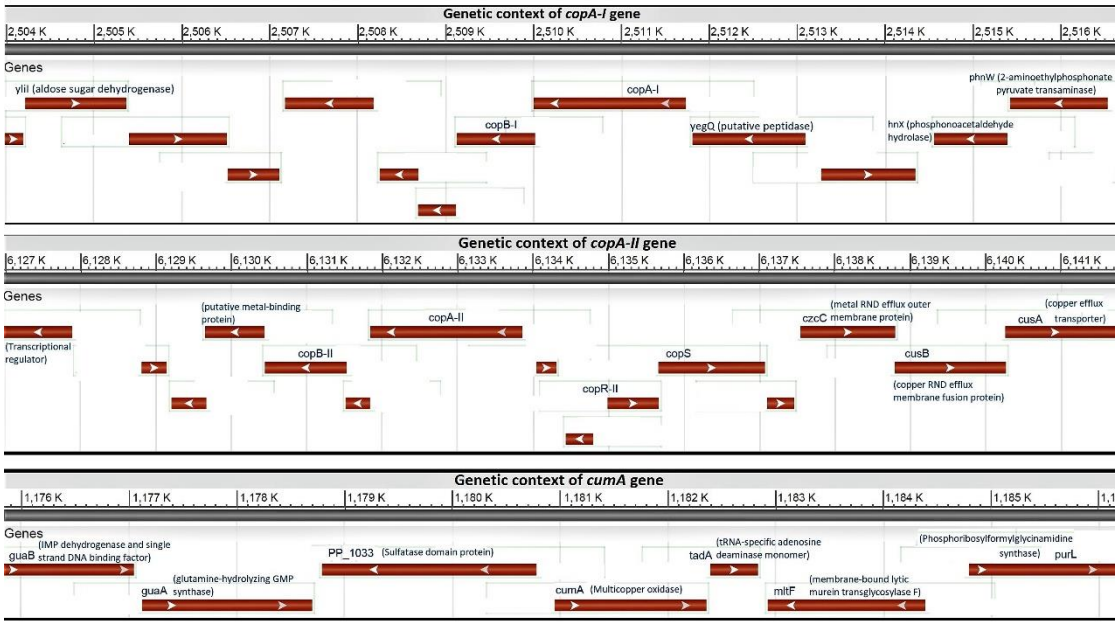

Figure 55. Genetic context of putative *copA-I*, *copA-II* and the multicopper oxidase *cumA* genes in *Pseudomonas putida* KT2440 genome. Unlabelled genes correspond with genes with unknown function.

6.3 Deletion of *copA-I* and *copA-II* genes

For gene deletion in *Pseudomonas putida* KT2440, an adapted method described for gene deletion in *P. aeruginosa* was used [235]. The method is based on homologous recombination to create unmarked deletion mutants. Briefly, the allelic exchange constructs for gene deletion were generated by ligation of PCR products of the flanking regions of each targeted gene into the vector pK18mobSacB ("suicide vector" for *Pseudomonas* sp.). After selection and screening of the mutants that have incorporated the vector in the bacterial chromosome, a counterselection approach based on sucrose was used to obtain the unmarked mutants. A schematic representation of this process is shown in **Figure 56**.

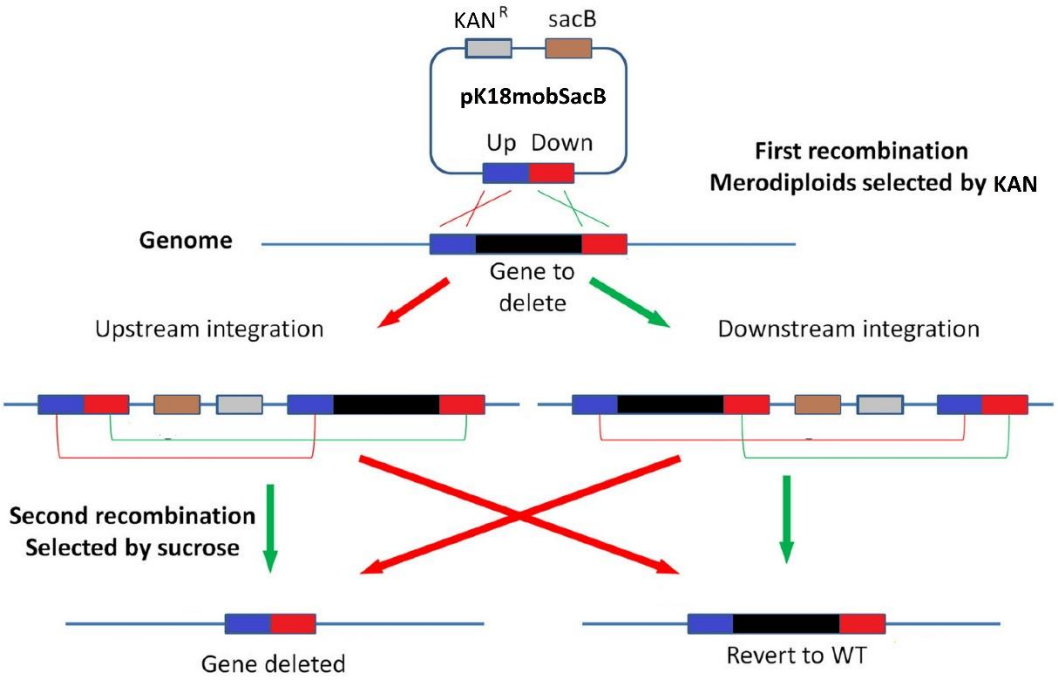

Figure 56. Schematic representation of gene deletion in Pseudomonas putida, via homologous recombination. Adapted from [235].

6.3.1 Amplification of the upstream and downstream sequences (flanking regions) of copA-I and copA-II genes

Sequence information was obtained from the genome of *Pseudomonas putida* KT2440 (GenBank accession number AE015451). Primers were designed to amplify the upstream and downstream regions for both genes, *copA-I* and *copA-II*. The length of the flanking regions used was ≈1000 bp. The details of the primers used are shown in **Table 20**. A Phusion high-fidelity DNA polymerase M0530 was used for PCR. The PCR product was meant to be blunt end for the following step. The Tm of each primer was calculated by the online tool (https://tmcalculator.neb.com/#!/). The detailed protocol for this enzyme can be found in section: 8.2, Specific procedures, and is available at this site: https://www.neb.com/protocols/1/01/01/pcr-protocol-m0530.

Table 20. List of primers used for amplification of upstream and downstream regions of genes targeted for deletion. Hangover and restriction sequence bases are shown in lower case.

Gene	Location	Primer type	Restriction enzyme sequence	Primers (5' - 3')
copA-I	Upstream	Forward	EcoRI	taagcagaattcTGTCGCTGGACGAAATCGAGGAAA
		Reverse	BamHI	tgcttaggatccTGTCAGGTAGCTGAGGTGCACATT AC
	Downstream	Forward	BamHI	taagcaggatccTGCTGACCTTGCTCGCCAGTGAAC
		Reverse	HindIII	taagcaaagcttTTGCAGCAGCCGCAGTTGGGGTC
copA-II	Upstream	Forward	XbaI	taagcatctagaACGCCTGCCGTTATCGGTAGCAATG
		Reverse	SalI	tgcttagtcgacTGCCGTAGTGTCCAGTCAGTCAGATAA
	Downstream	Forward	SalI	taagcagtcgacGAGATCCAAGATGAGCAAACCAATGA
		Reverse	PstI	taagcactgcagGAACGCCCATACAGAAGCTGCAA

A two-step PCR was performed (the annealing and extension steps were carried out at the same temperature). The PCR condition comprised an initial denaturation at 98 °C for 30 seconds, followed by 32 cycles of denaturation (98 °C for 10 seconds) and annealing (72 °C for 30 seconds), and a final extension at 72 °C for 10 minutes. PCR products were analysed in a 1% agarose gel (**Figure 57**), then the bands were excised from the gel and purified.

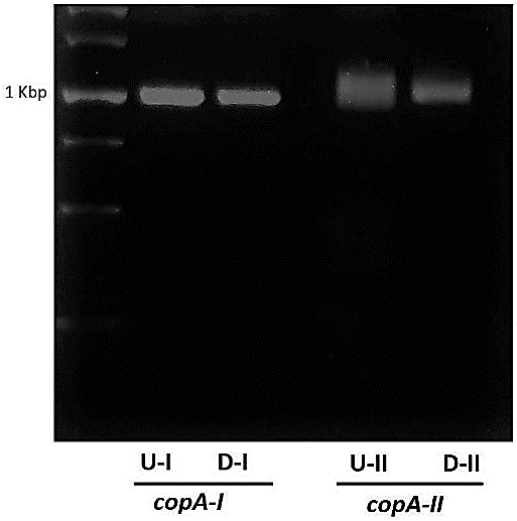

Figure 57. Agarose gel of PCR products (≈1000 bp) from the amplification of upstream and downstream DNA fragments of *copA-I* and *copA-II* genes. "U" lanes stand for upstream fragments, while "D" lanes stand for downstream fragments.

The purified PCR products were cloned into the pJET1.2/blunt vector for maintenance, by using the CloneJET PCR Cloning Kit (Thermo Scientific™), following the manufacturer instructions. Then, the vectors harbouring the fragments of interest were transformed into chemically competent Top10 *E. coli* cells, by heat shock, and the reaction was spread in ampicillin plates. Correctness of insertion was analysed by a double digestion of the vector with the corresponding restriction enzymes. The final products of this stage

were four different *E. coli* mutants with the pJET1.2/blunt vector harbouring the four fragments of interest: upstream fragment of *copA-I* (U-I), downstream fragment of *copA-I* (D-I), upstream fragment of *copA-II* (U-II), and downstream fragment of *copA-II* (D-II).

6.3.2 Construction of allelic exchange vectors

To construct the allelic exchange vector, both upstream and downstream regions previously amplified by PCR were joined together into the suicide vector for *Pseudomonas putida,* pK18mobSacB. To enable this joint, a restriction enzyme digestion with the proper enzyme was performed to generate fragments with overlapping sequences that can be ligated. A schematic representation of this step is shown in **Figure 58**. For *copA-I,* pJET1.2/blunt vectors, the vector containing the upstream fragment was digested with EcoRI and BamHI; while the vector with downstream fragment was digested with BamHI and HindIII; and pK18mobSacB plasmid was digested with EcoRI and HindIII. For *copA-II*, pJET1.2/blunt vectors, the vector containing the upstream fragment was digested with XbaI and SalI; while the vector with downstream fragment was digested with SalI and PstI; and pK18mobSacB plasmid was digested with XbaI and PstI. After restriction digestion, the resulting products were analysed in a 1% agarose gel and the bands were excised from the gel and were purified. Then, the purified products were used to set up a ligation reaction consisting in the upstream and downstream fragments and the digested pK18mobSacB vector, for each gene (either *copA-I* or *copA-II*), in presence of T4 DNA ligase. The reaction was incubated overnight at 4 °C, and 5 µL were used to transform 50 µL of chemically competent Top10 *E. coli* cells, by heat shock. The reaction was spread on plates supplemented with kanamycin. The resulting mutants were screened by restriction digestion to confirm the correct structure of the construct. The vector harbouring *copA-I* flanking regions was digested with EcoRI and HindIII, while the vector containing *copA-II* flanking regions was digested with XbaI and PstI. As two regions of ≈1000 bp were joined in one vector, the expected size of the fragments was 2000 bp, which was confirmed by a 1% agarose gel (**Figure 59**).

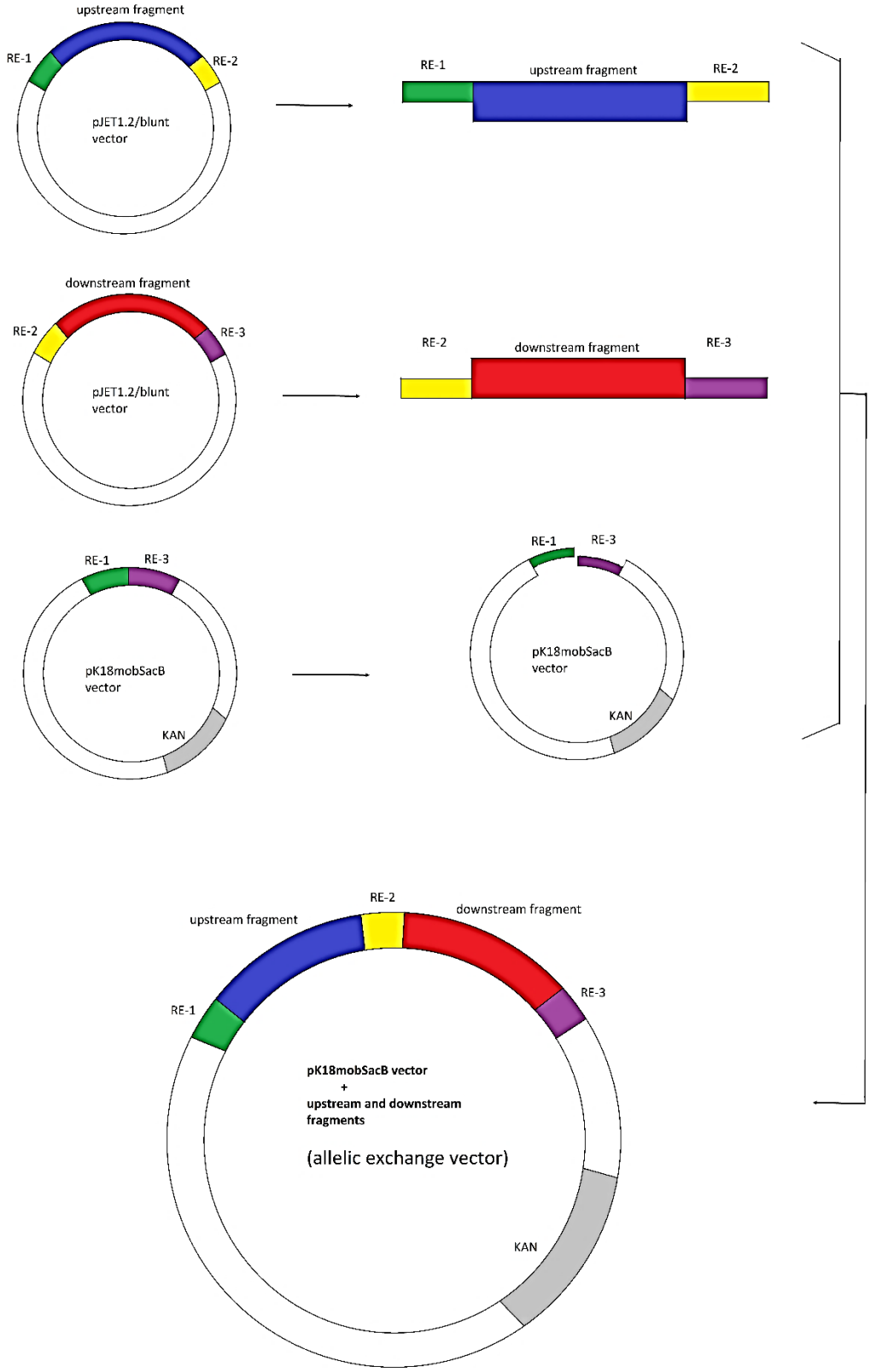

Figure 58. Schematic representation of the construction of allelic exchange vector. Top, right side are the products of the digestions with the corresponding restriction enzymes (RE). Final vector is made by ligation of the restriction digestion products with T4 DNA ligase.

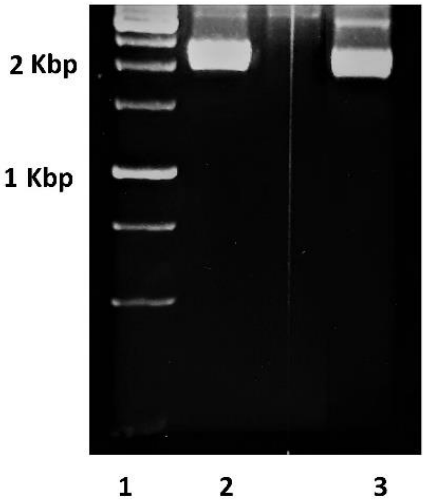

Figure 59. Agarose gel of products generated after a double restricted digestion of the allelic exchange vectors. Lane 1: DNA 1 Kbp ladder. Lane 2: Digestion of pK18mobSacB vector containing flanking regions of *copA-I*, with EcoRI and HindIII. Lane 3: Digestion of pK18mobSacB vector containing flanking regions of *copA-II*, with XbaI and PstI.

6.3.3 Generation of unmarked deleted mutants by homologous recombination

From the previous steps, two different allelic exchange vectors were generated, one containing the flanking regions of *copA-I* gene, and another containing the flanking regions of *copA-II* gene. These vectors were created by using the suicide vector pK18mobSacB, which is unable to replicate in *Pseudomonas putida* [236, 237], which means that if the vector is not integrated into the bacterial chromosome, then the bacteria would be unable to grow on a medium supplemented with the antibiotic kanamycin (a marker gene included in pK18mobSacB vector). This process occurs via homologous recombination, with the aid of the flanking regions contained in each vector that promotes the recombination event. A schematic representation of this process is shown in **Figure 56**.

The exchange vectors created for each *copA* gene were used to transform competent *Pseudomonas putida* KT2440 cells by electroporation. A detailed description of the methodology followed for the generation of *P. putida* competent cells and the transformation process can be seen in section 8.2, Specific procedures. After electroporation, the reaction was placed in a sterile Eppendorf tube and 500 µL of SOC media was added, then it was incubated at 30 °C for 1.5 hours, and after incubation, the reaction was plated in kanamycin plates and incubated overnight. After this step, several colonies were obtained (for each target gene), which indicated that the first event of recombination had occurred and therefore the vector had successfully integrated into the bacterial chromosome. From this plate, a single colony was re-cultured in a 10 % sucrose medium, as counter-selection. A second event of recombination would cause the loss of the targeted

gene, or the reversion to the wild type, and allow the survival of the cell, since the integrated vector would cause the death of the cell due to its sensitivity to sucrose. Several colonies were able to grow in these sucrose plates. Finally a PCR-based screening was performed to confirm the gene deletion. A new set of primers was designed with this aim, the forward primer was located about 100 bp upstream of the 3' end of the upstream flanking region, while the reverse primer was located about 100 bp downstream of the 3' end of the downstream flanking region (outside of the construct). Hence, if the targeted gene was deleted, a fragment of about 1000 bp was expected as a product of this PCR amplification, whereas if the genome was reverted to the wild type, a longer fragment of about 2800 (for *copA-I*) to 3000 (for *copA-II*) bp was expected, as the PCR amplicon would include the wild type gene plus the downstream fragment of ≈1000 bp. The primers used for gene deletion confirmation were, for *copA-I* deletion, Fw TCGACTACGGCCTGCTGAT, and Rev CTCATGTTTGGCTCGACG; and for *copA-II* deletion, Fw CCACTGTGACTTGCGCTTTC, and Rev ACCAAAAGCTCCCCATGTCT. The PCR conditions included a first denaturation at 95 °C for 5 minutes, 32 cycles of denaturation, annealing and extension at 95 °C for 1 minute, 60 °C for 2 minutes and 72 °C for 3 minutes, respectively; and a final extension at 72 °C for 5 minutes. For the creation of a double mutant (*copA-I* and *copA-II* deleted), essentially the same steps were followed as the required for the creation of single mutants. The only difference was that the allelic exchange vector containing the construct to delete the *copA-I* gene was used to transform *P. putida* competent cells that had already lost the *copA-II* gene. A 1% agarose gel was used to analyse the PCR products (**Figure 60**). Additionally, amplicons were sequenced to confirm the deletion of each gene. Results confirmed the obtention of three *P. putida* KT2440 mutants, one mutant with *copA-I* gene deleted (*ΔcopA-I*), another with *copA-II* deleted (*ΔcopA-II*), and a third mutant with both *copA-I* and *copA-II* deleted (*ΔcopA-I-II*).

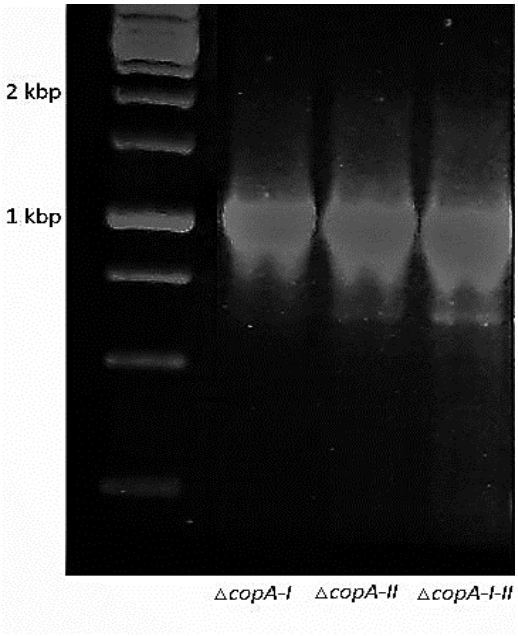

Figure 60. Agarose gel of PCR amplifications for *P. putida* KT2440 *ΔcopA-I*, *ΔcopA-II*, and *ΔcopA-I-II* mutants.

6.4 Growth experiment of gene-deleted mutants

As stated before, CopA is a protein that forms part of the plasmid borne copper resistance mechanism in *P. syringae* pv. tomato [156, 158]. However, its catalytic properties have been documented [102] and proved in this study, though its copper content and spectroscopy characteristics are uncommon for a multicopper oxidase, which might suggest an alternative biological function for this protein. To evaluate the possible biological involvement of this protein in the catalytic context, the generated gene-deleted mutants were grown on different carbon sources. In addition, the traditional copper resistance function was also tested. To assess the effect of *copA* genes in *P. putida* growth, four different substrate compounds were used:

- The first group was aimed to confirm the involvement of CopA in copper resistance, so that the deleted mutants were inoculated on LB media supplemented with different concentrations of $CuSO_4$, ranging from 0 mM to 4 mM.
- The second group comprised the utilization the well-known laccase substrates ABTS and SGZ in LB agar plates, to evaluate the possible apparition of coloured halos in colonies surroundings, which would indicate the presence of enzymes able to oxidize these substrates, and depending on the size of the halo generated, would also indicate the level of expression of such enzymes.
- The third group consisted in the utilization of small aromatic compounds as sole carbon source in minimal media (M9). The substrates used were mostly compounds

related with lignin degradation. The main objective was to assess the possible involvement of CopA as an accessory oxidative enzyme in some of the biocatalytic pathways, already described for these compounds.

- Finally, the fourth group comprised the utilization of polymeric lignin as sole carbon source, in minimal media (M9). The aim was to evaluate the possible involvement of CopA as an accessory oxidative enzyme in lignin degradation.

The whole plasmid borne copper resistance operon has been described to be copper inducible [158], which could indicate that CopA protein would be produced only if needed by the cell, when the concentration of copper became somehow toxic. Therefore, for growth assays of the second, third and fourth groups, a whole new set of experiments were carried out, which included the addition of 0.5 mM of $CuSO_4$ that would promote the expression of CopA. Cells growth was qualitatively measured, and the results are summarized in **Table 21**.

Table 21. Qualitative growth of deleted mutants *ΔcopA-I*, *ΔcopA-II*, *ΔcopA-I-II* and wild type *Pseudomonas putida* KT2440, on different media ('+' means growth, the more '+' signs, the more growth was achieved. '-'means no growth was achieved).

Group 1: Copper concentration on LB media						
Copper concentration		**0 mM**	**0.5 mM**	**1 mM**	**1.5 mM**	**4 mM**
Copper effect	WT	+++++	+++++	+++++	+++++	++++
	ΔcopA-I	+++++	+++++	++++	+++++	++
	ΔcopA-II	+++++	+++++	+++	+++	+
	ΔcopA-I-II	+++++	++++	++	+	-

Group 2: LB media supplemented with ABTS and SGZ							
		No copper added	**Copper added**			**No copper added**	**Copper added**
ABTS	WT	+++++	+++	**SGZ**	WT	+++++	+++++
	ΔcopA-I	+++++	+++		*ΔcopA-I*	+++++	+++++
	ΔcopA-II	+++++	+++		*ΔcopA-II*	+++++	+++++
	ΔcopA-I-II	+++++	+++		*ΔcopA-I-II*	+++++	++++

Group 3: M9 media with small aromatic compounds as sole carbon source							
		No copper added	**Copper added**			**No copper added**	**Copper added**
Vanillin	WT	+++	++	**Vanillic acid**	WT	+++++	+++++
	ΔcopA-I	+++	++		*ΔcopA-I*	+++++	++++
	ΔcopA-II	+++	++		*ΔcopA-II*	+++++	++++
	ΔcopA-I-II	+++	-		*ΔcopA-I-II*	+++++	+
p-coumaric acid	WT	+++++	+++++	**p-hydroxy-benzoic acid**	WT	+++++	+++++
	ΔcopA-I	+++++	++++		*ΔcopA-I*	+++++	++++
	ΔcopA-II	+++++	++++		*ΔcopA-II*	+++++	++++
	ΔcopA-I-II	+++++	++		*ΔcopA-I-II*	+++++	++
ferulic acid	WT	+++++	+++++	**phenol**	WT	-	-
	ΔcopA-I	+++++	++++		*ΔcopA-I*	-	-
	ΔcopA-II	+++++	++++		*ΔcopA-II*	-	-
	ΔcopA-I-II	+++++	++		*ΔcopA-I-II*	-	-

Group 4: M9 media with polymeric lignin as sole carbon source							
		No copper added	**Copper added**			No copper added	Copper added
Ca-lignosulfonate	WT	-	-	**Organosolv lignin (CIMV)**	WT	-	-
	ΔcopA-I	-	-		*ΔcopA-I*	-	-
	ΔcopA-II	-	-		*ΔcopA-II*	-	-
	ΔcopA-I-II	-	-		*ΔcopA-I-II*	-	-

From a broad point of view, the results showed no significant differences in bacterial growth between the mutants *ΔcopA-I* and *ΔcopA-II*, under any condition. Such was the case that if *ΔcopA-I* mutant showed none, low, medium or high growth; *ΔcopA-II* showed about

the same corresponding behaviour, indicating that these two genes encode proteins with very similar functions. The results were as follows:

6.4.1 Response to C(II) ions

Regarding the first group, the concentrations of $CuSO_4$ used were 0, 0.5, 1, 1.5 and 4 mM. For the lower concentrations of $CuSO_4$, wild type and mutants showed no difference in growing at 0 mM; while for 0.5, the wild type and single mutants showed no difference, though a slight diminished growth was observed for the *ΔcopA-I-II* double mutant. For $CuSO_4$ concentrations of 1 and 1.5, the wild type showed a better growing than the mutants, being the *ΔcopA-I-II* double mutant the most affected by $CuSO_4$. The wild type strain was able to grow normally even at the highest concentration of $CuSO_4$ (4 mM), while both *ΔcopA-I* and *ΔcopA-II* mutants showed a diminished growth, and the double mutant *ΔcopA-I-II,* lacking both *copA* genes, lost entirely its ability to grow at this $CuSO_4$ concentration (**Figure 61**). These results confirmed the important role of CopA proteins in copper resistance in *P. putida*.

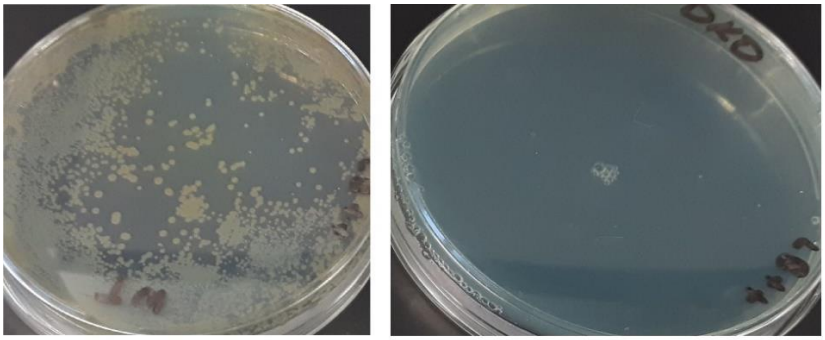

Figure 61. Growth of wild type and *ΔcopA-I-II* double mutant of *P. putida* Kt2440, on LB media supplemented with $CuSO_4$ (4 mM).

6.4.2 Oxidation of ABTS and SGZ

For group two, a faded green halo was observed in the colonies surroundings under all conditions for ABTS (**Figure 62**), which could suggest that CopA is not the only enzyme, nor the most important either, able to oxidase this compound and secreted by *P. putida* KT2440. Moreover, the addition of copper in the form of $CuSO_4$ caused a decrease of about 50 % in growth and did not produce any enhancement in the halo formation, suggesting a low level of expression of CopA. Plates supplemented with SGZ showed no halo formation and no differences in colonies growing was observed.

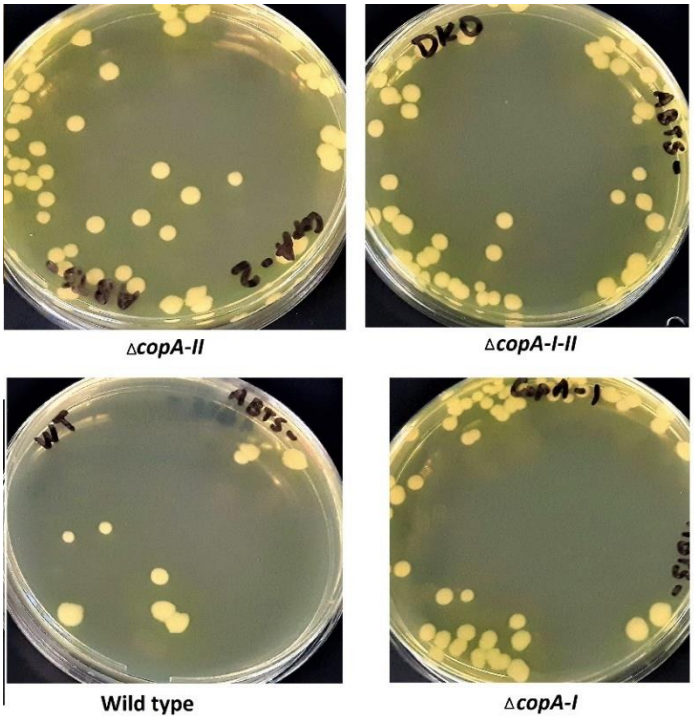

Figure 62. Growth of wild type, and *ΔcopA-I*, *ΔcopA-II* and *ΔcopA-I-II* mutants of *P. putida* Kt2440, on LB media supplemented with ABTS (1 mM). Green halos were formed in the surrounding of colonies.

6.4.3 Growth on aromatic carbon sources

For the third group, vanillin, vanillic acid, p-coumaric acid, p-hydroxybenzoic acid, ferulic acid and phenol were used as sole carbon source at 0.1 % concentration. *P. putida* was inoculated in plates supplemented and not supplemented with $CuSO_4$ (0.5 mM). The wild type strain and all *copA* deleted mutants were able to grow normally on these substrates, as long as $CuSO_4$ was not added into the medium. The only exception was when phenol was used as carbon source, as no growth was observed under any condition for this substrate. On the other hand, when copper was added in the form of $CuSO_4$, the inoculum used for these plates needed to be three orders of magnitude more concentrated than the ones used for plates without $CuSO_4$ addition. Interestingly, for plates supplemented with $CuSO_4$, a diminished growth was observed only for the double deleted mutant, *ΔcopA-I-II*, grown on vanillic acid, p-coumaric acid, p-hydroxybenzoic acid and ferulic acid, as carbon source. No growth at all was observed for *ΔcopA-I-II* growing on vanillin as carbon source (**Figure 63**). From these results, a possible involvement of CopA in the oxidation of low molecular weight aromatic compounds could be suggested, though this role would be valid only in presence of copper(II) ions. It is not clear whether this role is due to a direct oxidation

of the aromatic compounds by CopA, or if it plays an indirect role by sequestering copper(II) ions that would inhibit the action of other enzymes involved in this process.

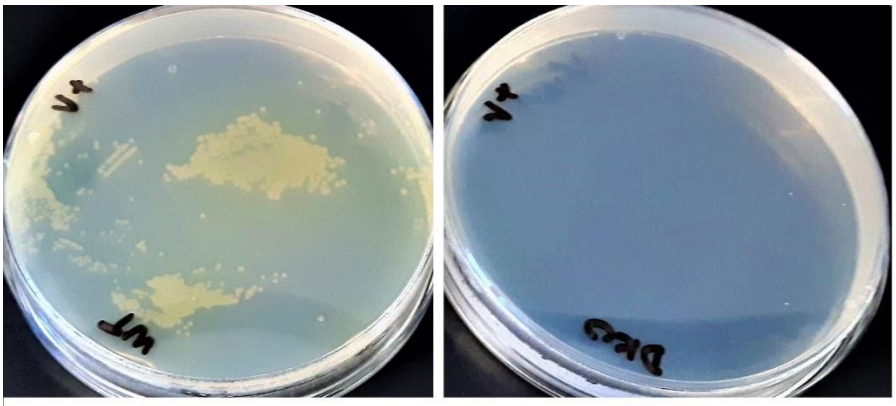

Figure 63. Growth of wild type and *ΔcopA-I-II* double mutant of *P. putida* Kt2440, on M9 media with vanillin as sole carbon source. Plates were supplemented with $CuSO_4$ (0.5 mM).

6.4.4 Growth on lignin carbon sources

Finally, when polymeric lignin was used as sole carbon source at 0.2 % concentration, no growth was observed by either P. putida wild type, nor the *copA* deleted mutants. *P. putida* KT2440 showed to be unable to grow on hardwood Ca-lignosulfonate (Borregaard) or organosolv lignin (CIMV). However, when glucose was supplemented to the media (at 0.1 % concentration), a modest growth was achieved for the wild type strain and *copA* mutants, though no significant differences were observed among them, under these conditions.

From these results, it can be concluded that the main role of CopA in *P. putida* Kt2440 is to participate in copper resistance mechanisms in this bacterium. CopA was not strictly required to oxidize small aromatic compounds, which was expected as the metabolic pathways for the degradation of some of these compounds have been well documented [234, 238], without the need of a multicopper oxidase such as CopA. However, CopA proved to be important for the oxidation of small aromatic compounds when copper ($CuSO_4$) was present in the media, at a moderate concentration (0.5 mM). These results could be explained either by the presence of copper ions causing stress to the cells, maybe by the inhibition of some enzymes involved in aromatic degradation pathways (e.g. oxygenases), which would lead to a diminished growth and lack of energy; or by the direct biochemical involvement of CopA in aromatic oxidation. In either case, the results shown in this work demonstrate the participation of CopA in copper resistance mechanisms and in the oxidation of aromatic compounds, which would suggest a double function of this interesting protein.

7 Discussion and Conclusions

7.1 Introduction

The huge potential of lignin as a renewable feedstock for production of energy, materials and chemical commodities can only be fully exploited if a complete and efficient process for its depolymerization is developed. Currently, chemical and physical methods available to depolymerize lignin usually provide a heterogeneous mixture of compounds, containing aromatic, contaminating and unidentified species, with variable yields and different profiles, due to the complex composition and structure of lignin. A heterogenous mixture of compounds is commonly acceptable as fuel, therefore, lignin has been mainly used for direct combustion to produce energy. However, the production of chemical commodities requires purity and high yields, hence this heterogeneity becomes a major challenge to be solved, mainly due to the costly and difficult task to separate valuable compounds from this matrix in an economical way [239, 240]. Lignin valorization through biological strategies represents a promising approach to overcome this problem. Lignin biodegradation involves the utilization of enzymes, which in principle could lead to the formation of defined products. However, the enzymes involved in this process are yet to be fully characterized, and considerable research is needed to completely elucidate how lignin biodegradation occurs. Additionally, substantial efforts will be required to develop microbial catalysts optimized for both the feed stream and targeted products [240]. Therefore, basic research to find and characterize new biocatalysts with novel properties and determine their role in lignin degradation is an ongoing task, which needs to be investigated and developed to unleash the fully potential of lignin as a renewable feedstock.

Biological full lignin degradation mainly involves the action of four groups of enzymes [44, 46], with laccases being the group that has drawn more attention from the scientific community, since laccases can catalyse redox reactions without the need for an additional cofactor and generating water as the only by-product [81]. The interest to find and develop enhanced laccases reaches beyond lignin degradation, as these enzymes could potentially be used in several other fields (e.g. bioremediation, bleaching, development of biosensors, food industry, organic synthesis, among others) [109, 137, 139]. It is clear that the obtention of powerful and robust laccases with enhanced properties, available at low prices, can represent a game-changing factor in myriads of industrial applications, especially in the

production of chemicals and materials [90]. Most commercially available laccases are derived from fungal sources as they can show high redox potentials [81, 110], however their utilization is restricted due to issues related with their production and manipulation. The recently discovered bacterial laccases might overcome or complement some of the shortcomings of their fungal counterparts, as these proteins have proven to be commonly more stable to pH and temperature, they could reach higher yields of expressed protein and they can be optimized more easily, due to the more extensive availability of molecular biology tools [58, 140, 142]. Despite their properties, so far only few bacterial laccases have been purified and characterized, making patent the necessity and importance to expand our current knowledge of these catalysts. Therefore, in this study a biochemical and structural characterization of bacterial laccases (laccase-like multicopper oxidases, LMCO) and CopC proteins from bacterial lignin degraders has been performed.

7.2 Protein expression and activity of CopC proteins

Based on genomic analysis of bacterial lignin degraders, putative genes encoding multicopper oxidases and CopC proteins were selected for cloning and protein expression. In *Microbacterium phyllosphaerae*, two putative *copC* genes were found and these genes were close to putative genes encoding the enzymes dihydrolipoamide dehydrogenase and A-type DyP peroxidase (**Figure 12**), both enzymes having been shown to be involved in lignin degradation [71, 153]. A detailed analysis of the CopC sequences from bacterial lignin degraders showed that these proteins contain a signal peptide for protein exportation, suggesting an extracellular function, and also revealed a difference with the canonical CopC proteins, such as the well described CopC protein from the plasmid-borne copper resistant operon found in *P. syringae* pv tomato [158, 161], consisting in a lack of a methionine-rich region usually involved as copper(I) ion ligands (**Figure 16**). These evidences, supported by the fact that while some bacterial lignin degraders contain putative multicopper oxidases genes but not *copC* genes, and vice versa, suggested a potential role for these proteins in lignin degradation. Although these proteins are short (≈ 10 to 15 kDa), and they could bind only a single copper ion, it was suspected that these proteins would utilize the redox properties of copper to perform oxidative reactions, whether as single proteins or by forming multimeric proteins with more than one copper ion. There is a precedent for this assumption, as it has been reported the occurrence of shorter laccases comprising only 2 domains (domain 1 and domain 3, while domain 2 is missing). In order to bind the four copper ions needed for its catalytic activity, these proteins form trimers and the trinuclear cluster lies

between domains 1 and 2 of each pair of neighbour chains [241]. A similar behaviour was thought for these short CopC proteins that might bind only one copper ion. Besides, a bioinformatic analysis revealed that CopC proteins comprise a much larger and diverse family of proteins than previously believed, expanding their potential functions [162]. Considering this evidence, putative genes found in *Microbacterium phyllosphaerae*, *copC886* and *copC1032*, were selected for cloning and protein expression. In first instance, *E. coli* was used as expression host with the plasmid pET151, and the signal peptide from their sequences was included and excluded (giving a total of 4 different recombinant proteins), ending up with no protein expression under the tested conditions. Some variations were assayed, such as varying inductor (IPTG) concentration, copper ($CuSO_4$) concentration and induction temperature. After cell harvesting and disruption, the protein was searched in soluble and insoluble fractions without success. Since *Microbacterium phyllosphaerae* is a Gram-positive bacterium and *E. coli* is a Gram-negative bacterium, it was suspected that this could be the reason behind the negative results for protein expression, due to the periplasmic location absent in the native host, the formation of inclusion bodies or problems related with mRNA processing due to different codon preferences between the native and expression system host [242]. Therefore, two different approaches were evaluated to express these proteins: the first one consisting in the use of a Gram-positive host, *Rhodococcus jostii* RHA1, with the vector pTipQC-II; and the second one was the use of synthetic genes with codons optimized for expression in *E. coli*. Neither was successful in production of the recombinant proteins. Then, a new set of CopC protein were used, CopC-Bx1 and CopC-Bx2, found in the genome of the aromatic degrader *Burkholderia xenovorans* LB400. These proteins were shorter compared with the CopC proteins found in *Microbacterium phyllosphaerae*, and though they were expressed, their yields were very low (reaching a maximum of ≈0.5 mg per litre of culture), which limited the number of assays for their biochemical characterization. An identity confirmation was needed for these proteins, due to the low yields produced, which was carried out by trypsin digestion and whose results showed that these proteins indeed had been expressed. However, since the amount of protein was limited, only activity assays were performed by using common laccase and peroxidase substrates (ABTS, SGZ, DMP, 2,4-DCP and guaiacol), in presence and in absence of hydrogen peroxide, and with and without copper ($CuSO_4$) supplementation. In addition, their possible role as an accessory enzyme was explored, in combination with the enzymes Dyp1B peroxidase and Oc-CueO laccase. Result showed no activity for any of these proteins under the tested conditions. From all of this evidence, it is concluded that these proteins do not have catalytic properties, and their only

role might be related with copper ion transportation, as it has been described for the canonical CopC proteins. However, since evidence such as the genomic context and sequence analysis of these proteins may indicate a possible oxidative function, and considering that in this study the expression of the primary target CopC proteins (CopC886 and CopC1032 from *Microbacterium phyllosphaerae*) failed, and that the proteins used (CopC-Bx1 and CopC-Bx2) were only expressed at low yields, which constrained the observations and conditions tested; a further study is recommended to confirm or discard the possible catalytic role of CopC proteins.

7.3 Protein expression and activity of laccase-like multicopper oxidases (LMCOs)

Based on genome analysis, genes encoding the multicopper oxidases Pp-CopA, Pf-CopA, Oc-CueO and P-PPO from *Pseudomonas putida* KT2440, *Pseudomonas fluorescens* Pf-5, *Ochrobactrum sp*., and *Paenibacillus sp*., respectively, were selected for cloning and protein expression. Genes were cloned from chromosomal DNA and the sequences were confirmed by agarose gel electrophoresis (**Figure 18**) and sequencing (GTAC Biotech Company). Protein expression was successful and recombinant proteins were expressed at relatively high yields (**Table 4**), with P-PPO being the protein that reached the maximum value (≈60 mg of protein produced from 1 litre of culture). A sequence analysis revealed that P-PPO was annotated as a laccase domain (not as a "complete" laccase) which does not contain neither the well-conserved residues used as copper ions ligands, nor a signal sequence for protein exportation (**Table 2**, **Figure 17**). A preliminary activity assay showed that P-PPO was inactive towards common laccases substrates, regardless of the presence of hydrogen peroxide or $CuSO_4$, and also in assays as an accessory enzyme in combination with Oc-CueO or Dyp1B peroxidase, so that despite the fact that P-PPO reached the highest yield of expressed protein, this protein was not further investigated. The reason for its inactivity could lie in the lack of the residues needed for copper ions ligation, which is essential for laccases activity.

Regarding the remaining proteins, they were expressed as N-terminal His_6 fusion proteins. An additional step after an initial IMAC purification was performed to remove the His_6 tag, by using TEV protease, so that untagged native-like proteins were produced. The resulting protein solutions for Pp-CopA, Pf-CopA and Oc-CueO, showed to be colourless, though a bluish colour was expected, which has been described as a characteristic property of laccases [75, 107]. A metal content analysis by ICP-OES and UV-Vis absorption

spectroscopy assays revealed that these proteins had been produced as apoenzymes, with no copper ions bound to any of them, even when cultures were supplemented with a copper salt ($CuSO_4$). This peculiarity has been reported for other bacterial multicopper oxidases expressed in *E. coli* [85, 175, 202], yet the problem seems not to be related with protein generation or folding, but instead with the host (*E. coli*) used for protein expression. The availability of copper ions when the protein is being formed could be essential to generate fully loaded proteins with this metal, however it is known that *E. coli* displays an elaborate homeostasis mechanism (Cu-efflux and Cu-sensing systems) to maintain copper ions concentration within a narrow range. Copper homeostasis in *E. coli* is dependent on oxygen availability, and under anaerobic growth conditions an intracellular accumulation of copper occurs [243], which ultimately could led to the formation of holoenzymes fully loaded with copper ions [175]. This approach was assayed in order to obtain recombinant proteins with copper ions bound to the LMCOs under study. After protein expression in microaerobic conditions, achieved simply by turning off the agitation (agitation 0 rpm), it was observed that only Oc-CueO protein solution changed its colour into blue. Moreover, the characteristic peak of laccases at ≈610 nm in a UV-Vis spectrum was observed for Oc-CueO, suggesting that a fully copper loaded protein had been produced under microaerobic conditions. However, both Pp-CopA and Pf-CopA remained as colourless protein solutions, and Pp-CopA did not present the classical spectra reported for laccases (**Figure 20**). Then, an *in vitro* copper reconstitution was performed by incubating these protein solutions with a $CuSO_4$ solution overnight, followed by two consecutive washings in PD10 columns to remove the excess of copper. Oc-CueO was again the only protein solution that changed its colour into blue. Surpinsingly, after a metal content analysis by ICP-OES, results showed that whereas Oc-CueO contained 4 copper ions per protein molecule (expected for a multicopper oxidase), Pp-CopA and Pf-CopA showed an even greater stoichiometry for metal content, reaching about 9 copper ions per protein molecule. CopA protein has been involved in copper resistance mechanisms, with a sequestering role of toxic copper ions in the periplasmic space that prevent the entrance of this ions into the cytoplasm. Hence, a high copper-protein stoichiometry has been associated with this protein in *P. syringae* (≈11 copper ions per molecule of protein) [156], which agrees whit the results found in this study. It is remarkable that despite having such a high metal content, these proteins (Pp-CopA and Pf-CopA) were colourless in solution and did not show the characteristic peak at ≈610 nm in spectroscopy assays, yet in preliminary studies they showed catalytic activity towards ABTS as substrate without any need for exogenous copper ions. The characteristic blue colour of laccases and

the peak at ≈610 nm have been attributed to a S(Cys)π →Cu(II) charge transfer transition, because of covalent nature of the Cu-S(Cys) bond in the T1 copper [84]. Therefore, a lack of these characteristics could have suggested an absence of copper ion in this position, however the catalytic activity of these proteins in absence of exogenous copper and the metal content analysis contradicts this conclusion. An alternative explanation can indicate that this position is not empty after all, and that a copper ion is occupying this place, however the lack of colour and peak at ≈610 nm may indicate that this position is distorted, albeit more studies would be needed to elucidate what is really happening with the T1 copper in these interesting proteins. Since the expression of LMCOs under microaerobic conditions decreased the yield by about 65 % (**Table 4**) and that addition of exogenous copper ions enhanced the activity of these enzymes, unless otherwise is stated, all experiments of protein expression were carried out under fully aerated conditions, whereas for catalytic activity experiments, exogenous copper ions were added as $CuSO_4$.

The LMCOs were assayed for catalytic activity using common laccase substrates, lignin model dimers and polymeric lignin. Pp-CopA, Pf-CopA and Oc-CueO showed oxidase activity with these substrates. In first instance, a preliminary catalytic assay was carried out to find out whether these proteins show oxidase activity or peroxidase activity, by performing the reaction in presence and in absence of hydrogen peroxide. Besides, the reactions were carried out in presence and in absence of exogenous copper ions, in the form of $CuSO_4$, and ABTS, SGZ, DMP, guaiacol and DCP were used as substrates. Neither of these proteins required hydrogen peroxide for its activity, therefore it was concluded that these proteins are oxidase enzymes (laccases), and not peroxidases [200]. On the other hand, the presence of exogenous copper ions was essential for their activity (**Table 9**), which has been reported previously for other bacterial laccases [106, 144, 148]. However, it was concluded that the dependence for exogenous copper ions is not a characteristic feature of bacterial laccases, but it is a consequence of the expression system (*E. coli*) and its cultivation under fully aerated conditions, resulting in the generation of apoenzymes, depleted of copper, as it was explained above.

Since most of the experiments were carried out using protein expressed as apoenzymes, the addition of copper ions was crucial for their activity, so that copper concertation and its relationship with activity was investigated. It was observed that the rate of reaction increased as copper ions concentration increases, until a plateau is reached where the activity is almost independent of copper concentration, and no important inhibition was observed in the range of copper concertation assayed. From these values, the

concentration that ensured an excess of this metal in the reaction mixture to avoid a limitation by copper, without interfering or disturbing the reaction mixture with unnecessarily high copper concentrations that could interfere with the catalytic measurements, was determined to be 0.5 mM (**Figure 25**). Once the copper working concentration was determined, a pH-activity profile was elucidated for ABTS and SGZ as substrates. Pp-CopA, Pf-CopA and Oc-CueO showed analogous pH profiles, giving optimal pH values of ≈4.1 for ABTS, and ≈7.5 for SGZ (**Figure 27**). Similar optimal pH values have been reported previously for other laccases with the same substrates [196, 202, 203]. To the best of our knowledge, an explanation for this observation has not been made, and many hypotheses could be suggested (different active site, different residues interacting with the substrate, a direct effect of the pH in the substrate or some consequence of the outer sphere mechanism used for catalysis), though it would be difficult to reach a final conclusion without any further evidences. A crystallography study including these substrates is recommended, which might show the residues involved in binding of each substrate.

The steady state kinetic parameters were obtained for Pp-CopA, Pf-CopA and Oc-CueO with ABTS, SGZ and DMP as substrates (**Table 10**). From a general point of view, these three enzymes exhibited similar kinetic parameters, albeit Oc-CueO presented the lowest k_{cat} for all of the tested substrates. As mean of comparison, the specificity constant (k_{cat}/K_M) was used to evaluate the efficiency of these enzymes. K_M was the kinetic parameter that mostly influenced the enzyme efficiency, since this value presented more variation. For instance, despite that similar k_{cat} were determined for Pp-CopA and Pf-CopA (2.4 and 2.19 s^{-1}, respectively) with ABTS as substrate, their performance varied significantly, since the Pf-CopA specificity constant was twofold larger than the specificity constant of Pp-CopA, a difference caused by the values of K_M obtained for these enzymes. Oc-CueO proved to be the most efficient enzyme towards SGZ and DMP, while Pf-CopA was the most efficient enzyme with ABTS. The observations suggest that, though the kinetic parameters were similar among these LMCOs, these enzymes could be of particular interest for certain specific applications, depending of each enzyme and their own substrate preferences. This conclusion was supported by the results obtained when the activity of Pp-CopA and Oc-CueO was compared with the activity of the commercially available fungal laccase from *Trametes versicolor* (TvL), by using ABTS and SGZ as substrate. Interestingly, while TvL exceeded greatly the catalytic capacity of Oc-CueO and Pp-CopA when ABTS was used as substrate (TvL activity was 25-fold and 14-fold higher than Oc-CueO and Pp-CopA, respectively); the opposite occurred when SGZ was used as substrate, being the activity of Oc-CueO 50-fold, and Pp-CopA 17-fold higher

than TvL activity (**Figure 30**). Furthermore, thermal stability assays comparing these bacterial laccases with TvL showed that Pp-CopA and Oc-CueO were more stable than its fungal counterpart (**Figure 31**), which has been reported for other bacterial laccases [163], and highlight the importance of these enzymes and their potential applications.

The activity of these enzymes towards the lignin model dimers GGE, representing a β-O-4' bond, and DDVA, representing a carbon-carbon bond, were assayed. The reactions were carried out in presence and in absence of a mediator (ABTS or SGZ). Pp-CopA, Pf-CopA and Oc-CueO showed oxidase activity with GGE, in presence and in absence of ABTS as mediator, and the formation of dimeric products were confirmed by LC-MS. Three new peaks were identified in the chromatogram upon reaction of LMCOs with GGE, and they were named as P1, P2 and P3. The only difference observed in presence of a mediator was that the formation of P3 was favoured to some extent. When DDVA was used as substrate, only Oc-CueO was active in absence of a mediator, whereas Oc-CueO, Pf-CopA and Pp-CopA were able to oxidase this compound in presence of a mediator. Formation of dimeric products were confirmed by LC-MS and three new peaks were identified in the chromatograms of Oc-CueO and Pp-CopA, named as P4, P5 and P6 (**Table 11**). These results agree with previous reports for catalytic activity of laccases towards phenolic β-O-4' ether and C-C lignin-model dimers, which is mainly a polymerization. Apparently, the absence of the hydroxyl group in the ring of β-O-4' ether model-dimers seems to be essential for their breakdown, though the reason for this is not clear. GGE is a phenolic lignin-model dimer, which has proven to be resistant to breakdown, even by high redox potential laccases (fungal laccases), regardless the presence or absence of a mediator [212-214]. Then, the activity of LMCOs was assayed with polymeric lignin, in presence and in absence of a mediator. A total of 8 different lignins were used as substrate, all of them showed a change into a darker colour upon reaction with the LMCOs under study (**Appendix 2**), and some chromatograms displayed decreased or disappearing peaks after the reaction, suggesting that the low molecular compound found in these materials had been polymerized. This conclusion is supported by the formation of precipitates in the test tubes after reaction. Only one lignin, Ca-lignosulfonate (Borregaard) gave a low molecular product identified as vanillic acid by LC-MS, upon reaction with Pp-CopA and Oc-CueO (**Figure 40**). A further experiment was carried out by using this lignin as substrate with Oc-CueO in combination with other enzymes, to test possible synergistic effects. The peroxidase enzymes Dyp1B was used, whose activity has been proved in lignin substrates [65]. In addition, a dihydrolipoamide dehydrogenase (DhLDh) from *Sphingobacterium sp*., and another enzyme involved in lignin degradation, a glutathione S-

transferase (LigE) from *Agrobacterium sp*. were used. These proteins were cloned by Dr. Rahman Rahmanpour and Dr. Goran Rashid, in the TDHB research group. The chromatogram analysis showed that vanillic acid was generated only when the bacterial laccase Oc-CueO was present in the reaction, so that this product can be identified as a specific product released by a laccase activity from this substrate. No significative synergistic effect was observed, though the addition of all enzymes, especially the dihydrolipoamide dehydrogenase (DhLDh) helped to some extent to the formation of vanillic acid **Figure 41**. This enzyme has been involved in lignin degradation as an accessory enzyme that prevents repolymerization once a lignin radical is formed [153], which may explain the observation made. As a final remark, it was surprising and interesting to observe that despite the spectroscopy and metal content differences found between Oc-CueO and the CopA-type proteins (Pp-CopA and Pf-CopA), these LMCOS were able to perform analogous catalytic reactions with a relative similar efficiency, over the diverse substrate compounds tested in this study. To elucidate to some extent how these dissimilar proteins in the spectroscopy and metal content context can show similar catalytic properties, structural and functional studies were conducted.

7.4 Structural and functional analysis of Oc-CueO and Pp-CopA

7.4.1 Crystal structure and site directed mutagenesis of Oc-CueO

The crystal structure for Oc-CueO was solved at a resolution of 1.1 Å (PDB accession code 6EVG), however despite several attempts neither Pp-CopA nor Pf-CopA formed crystals, so their crystal structures were not able to be generated, for now. Oc-CueO was identified as three domain laccase, and presented the same characteristic structural features that have been described for other bacterial laccases, including: a distorted domain 1; the presence of a methionine residue (Met500) as an axial ligand of the T1 copper; a connection between domain 2 and domain 3 by a large loop segment that wraps the protein; the presence of an α-helix loop that forms a lid-like structure over the substrate binding site; the presence of a methionine as the last residue in the well-conserved motif found in all multicopper oxidases, HCHXXXHXXXXM/L/F [96, 218]. However, a connection by between domain 1 and domain 2 by a coiled section, described for CotA laccase found in *Bacillus subtilis* [85], was not found in this crystal structure and a loop was present instead. The α-helix loop over the active site comprises from residue 339 to residue 401, albeit residues 350 to 391 were not shown in the crystal structure due to a diminished electron density in this region. Similar observations have been reported for other bacterial laccases [144], and the biological function of this

structure is unknown, yet it seem that it is not essential for the catalytic properties of bacterial laccases, conversely, it can hinder the entrance of the substrate into the active site [220]. A hypothesis for its possible role has involved this region with a methionine-rich region that could bind toxic copper ions, sequestering this metal, thus helping in copper defence mechanism. This region would be movable, which may also explain the low electron density obtained in this region [220]. The site for the trinuclear cluster copper ions was found to be empty, however the ligating residues and the three-dimensional structure was intact, so that these ions were modelled using coordinates from the structurally similar *E. coli* CueO (Ec-CueO) structure (PDB: 3NSF) to confirm the positioning of the T2/3 site [183]. Only minor alterations were found, confirming the preservation of this site and suggesting that the copper ions have been lost before crystallization, perhaps when the protein was expressed under microaerobic conditions, the availability of copper was not enough to form fully copper-loaded proteins.

Then a site directed mutagenesis study was performed. In first instance, a sequence alignment of bacterial and fungal laccases was made, and from these results, two groups were determined: the first group contained well-conserved residues among fungal and bacterial sequences that have not been previously reported; whereas the second group comprised well-conserved residues in high redox potential laccase, which would be absent in bacterial laccases. The main purpose of the second group was the generation of a mutant protein with enhanced activity, however, no mutant was able to surpass the wild type Oc-CueO activity. Most interesting were the result found for the first group (**Table 15**), as a total of 9 new conserved residues were found that were present in almost all analysed sequences (32 fungal and 33 bacterial laccases) that have not been previously reported. 5 out of the 9 residues are located in domain 2, a domain whose role has been associated simply as a scaffold structure in laccases; however, considering the relatively high number of well-conserved residues found in this region, a functional role can be suggested for this domain. When these amino acid residues were identified in the 3-D structure of Oc-CueO, they appeared to be forming part of some structure, as some of these residues were close to each other and surprisingly all of the were far from the T1 copper ion, whereas they seemed to be close to the TNC to some extent (**Figure 50**). After a tunnel analysis performed by CAVER [230], using PyMOL software, showed that these residues were forming part of tunnels, suggesting that these well-conserved residues could be involved in the formation of tunnels that transport oxygen and water between the TNC site and the outside of the protein. Furthermore, the only residues that were not found forming part of these tunnels, Arg221

and Arg223 in Oc-CueO, were located on the surface of the protein, very close the entrance of a tunnel connecting the surface of the protein and the T2 copper in the TNC site, so that it might be involved in oxygen diffusion. The positive charge of arginine might form a hydrogen bond with oxygen atoms on the surface of the protein, locating them close to the entrance of this tunnel and thus facilitating their diffusion into the TNC (**Figure 51**). Site directed mutagenesis experiments confirmed the importance of these residues, as mutants 1, 2 completely lost their activity, while mutant 3 showed a significant decrease of its activity. These mutants replaced one of the well conserved residues (Mutant 1: Asp62; Mutant 2: Arg221 and Arg223; and Mutant 3: Asp102, Gly103) by an alanine (**Figure 54**). The finding of these new conserved residues could prompt further investigations on their specific role, whereas their nearby residues and tunnel could be interesting regions for laccases enhancement and optimization.

7.4.2 Deletion of copA genes in Pseudomonas putida Kt2440

The biochemical characterization of LMCOs showed that while Oc-CueO and the CopA-type proteins (Pp-CopA and Pf-CopA) were able to catalyse the oxidation of several substrates with similar efficiency, their UV-Vis absorption spectrum profile, colour in solution and metal content, turned out to be different. While the biological function of CopA has been related with copper resistance mechanism in *Pseudomonas syringae* [156], a CopA-type protein was recently detected as a lignin-degrading enzyme by a specialized biosensor, from a bacterial metagenomic DNA sample [102]. From these reports and based on the observations made in this study, it was suspected that CopA proteins could present a moonlight behaviour and accomplish more than one function. There is no crystal structure reported so far for this type of proteins, which would be useful to see how copper ions are distributed, especially the T1 copper ion, and elucidate why they do not show the characteristic blue colour of laccases. Moreover, the α-helical loop located over the active site in bacterial laccases, is particularly long in CopA proteins, so that its crystal structure could help to gain some insights about its function. Since crystallization experiments for both Pp-CopA and Pf-CopA failed, this kind of analysis was not possible to be made. A new approach was assayed to shede some light on the role of these proteins in their native host. *Pseudomonas putida* KT2440 was selected for gene deletion experiments, to assess the phenotype of *copA* deleted mutants against high concentrations of copper, and the oxidation of aromatic compounds and lignin materials. Three different multicopper oxidases were found in *Pseudomonas putida* KT2440, *copA-I*, *copA-II* (whose product is the expressed

protein Pp-CopA) and *cumA*. Based on a genetic context analysis of these genes and knowing that the role of CumA has been associated with Mn^{2+} oxidation, only *copA-I* and *copA-II* were selected for gene deletion. Three different mutants were generated, a *copA-I* deleted mutant (*ΔcopA-I*), a *copA-II* deleted mutant (*ΔcopA-II*), and a double mutant with both genes, *copA-I and copA-II*, deleted (*ΔcopA-I-II*). Growth phenotype of each mutant was evaluated under four different conditions: 1. High copper concentration in LB media; 2. LB media supplemented with ABST and SGZ; 3. Growth on minimal media with small aromatic compounds as the only carbon source; and 4. Growth on minimal media with polymeric lignin as the only carbon source. Experiments for groups 2, 3 and 4 were performed in presence and in absence of copper (added as $CuSO_4$ at a concentration of 0.5 mM), as it is known that CopA expression is inducible by high concentrations of copper. A summary of results can be seen in **Table 21**. No significant differences were found between *ΔcopA-I* mutant and *ΔcopA-II* under any of the tested conditions. The reason for this behaviour was assumed to be a homologous function of the proteins encoded by these genes, so that if *P. putida* lack *copA-I* gene, the possible lost function was recovered by the homologous *copA-II* gene, and vice versa. However, differences were observed for the double mutant *ΔcopA-I-II*, under certain conditions. From the results obtained with the first group, a role of CopA proteins in copper defence mechanisms was confirmed, as the double mutant was unable to grow at a high copper concentration (4 mM), whereas the *P. putida* wild type was able to do so (**Figure 61**). The results from the second condition showed no difference between the wild type and the double mutant, though for growth on LB media supplemented with ABTS, the formation of green halos was observed surrounding the colonies (**Figure 62**), which suggest that *P. putida* does not need CopA proteins to oxidize this substrate and it can secrete other oxidoreductases that can accomplish this function, due to the huge metabolic versatility of this organism [233]. For the third condition, no differences were observed between the wild type *P. putida* and the double mutant *ΔcopA-I-II* when copper was absent, however significative differences were observed when copper was added (as $CuSO_4$ at 0.5 mM concentration) to the culture medium. A diminished growth was observed for the *ΔcopA-I-II* mutant, growing in minimal media supplemented with copper, when vanillic acid, p-coumaric acid, p-hydroxybenzoic acid and ferulic acid, were used as sole carbon source, whereas no growth at all was observed when vanillin was used as the sole carbon source (**Figure 63**). It is not clear whether this observation is due to a direct oxidation of the aromatic compounds by CopA proteins, or if they play an indirect role by sequestering the excess of copper (II) ions that would inhibit the action of other enzymes involved in the oxidative

process. Finally, for the fourth condition, no differences were observed between the wild type and the double mutant *ΔcopA-I-II*. Even the wild type strain was unable to grow on these substrates as sole carbon sources, so that the addition of a small amount of glucose (0.1 %) was needed to promote the formation of colonies. Nevertheless, when glucose was added the double mutant was able to grow as well, presumably due to the presence of glucose which ultimately led to the same pattern of growth observed for both the wild type strain and the mutant strain.

These results suggest that the main role of CopA in *P. putida* KT2440 is related with copper resistance mechanisms. CopA was not critical for the oxidation of small aromatic compounds in absence of copper ions, conversely its importance was significant when copper ions ($CuSO_4$) were present in the media. These observations could be explained either by the accumulation of copper ions when CopA is absent, which would subject the cells to a severe stress, or by the direct involvement of CopA in the oxidation of small aromatic compounds under these conditions. More research would be needed to confirm these assumptions. It can be concluded that CopA proteins can indeed accomplish two functions, they definitely play a role in copper resistance mechanisms, and the catalytic properties of these interesting proteins have also been demonstrated.

7.5 Future work

Due to the failed expression assays of CopC proteins from *Microbacterium phyllosphaerae*, it would be worth to keep trying to find a method to obtain these proteins. Having an efficient method to produce these CopC proteins would allow further investigations on their possible catalytic activity in lignin oxidation or as accessories enzymes. Positive results would turn CopC proteins into a whole new type of oxidative enzymes with several potential applications; otherwise, their action as copper transporters would be confirmed and, even so, these CopCs from *Microbacterium phyllosphaerae* would represent a novel type of proteins different from the canonical CopC, as they lack the binding site for Cu(I) ions, therefore their mode of action or biological role migth be different.

Based on activity assays, a more detailed investigation of the products generated by the action of Pp-CopA, Pf-CopA and Oc-CueO with lignin model dimers, would shed some light on their mode of action. The range of mediators used can be expanded and the utilization of a non-phenolic β-O-4' model dimer could lead to a bond cleavage, as it has been reported for other laccases. Moreover, new substrates can be assessed to widen the potential applications of these bacterial enzymes.

To elucidate the differences observed regarding the metal content and the spectroscopic properties between the CopA-type proteins (Pp-CopA and Pf-CopA) and Oc-CueO, the obtention of the 3-D structure of either Pp-CopA or Pf-CopA would be crucial. This information would allow the direct observation of the localization of the 9 copper ions measured for CopA, and also would show whether the T1 site is occupied or not by a copper ion. Besides, it would show how the T1 site surroundings amino acids are arranged in CopA. If the 3-D structure is able to show the full length of the α-helical loop located over the active site, which is particularly long in CopA proteins, a more general issue would be solved, common for all 3-D structure of bacterial laccases reported so far. A direct visualization of this structure could help us to understand what its function is, why it is located in this position and if it is or not essential for the catalytic activity of bacterial laccases.

The new conserved amino acid residues identified in all laccases could be used for deeper investigations about their possible role in catalytic activity. Furthermore, the effect of changes in the surrounding regions of these well-conserved residues on catalytic efficiency can be explored, not only in bacterial laccases, but also in fungal laccases. Such studies would determine if these regions are hot spots for laccases enhancement. In addition, Oc-CueO itself could be subjected to optimization as its crystal structure has been solved, thus rational methods could be used to identify potential targets for modification that would result in Oc-CueO enhancement. Two suggested approaches would include the mutation of Met500 into a leucine or phenylalanine (common residues in fungal laccases), or the elimination of the α-helical loop located over the active site, to enhance the substrate accessibility into the catalytic pocket.

Despite the progress made in this study, there is still much work to be done to increase the current knowledge and gain a deeper understanding of these proteins and the bacterial laccases in general.

8 Experimental and Methods

8.1 General procedures

8.1.1 Primer Design, PCR and agarose gel:

Unless otherwise is stated, the following procedures were used for primer design, polymerase chain reaction (PCR) and agarose gel. The Oligonucleotide Properties Calculator (OligoCalc) tool, available at http://biotools.nubic.northwestern.edu/OligoCalc.html, and Primer3Plus - Bioinformatics tool, available at http://www.bioinformatics.nl/cgi-bin/primer3plus/primer3plus.cgi, were used for primer design and primer check. PCR reactions were carried using an Eppendorf Master cycler and Platinum Pfx- DNA polymerase. Primers, dNTPS and enzyme concentration were according to Pfx Invitrogen protocol for PCR, as is indicated in the following table:

PCR Compound	Volume per reaction [µL]
Water	37.1 (could vary)
Pf 10x buffer reaction	5
50 mM MgSO4	1.5
10 mM dNTPs	1.5
10 µM Fw Primer	1.5
10 µM Rev Primer	1.5
Platinum Pfx- DNA polymerase	0.4
DNA sample	1.5
Total volume	**50**

Agarose gels were prepared at 1% (w/v) of concentration in 1x TBE buffer and mixed with 5 µL of GelRed dye. A volume of 5 µL of samples were mixed with 1 µL of loading dye and then loaded in the gel. PCR Clean-Up System kit from Promega were used for general PCR cleaning.

8.1.2 DNA extraction, plasmid extraction and gel purification

DNA extraction

Genomic DNA extractions were performed by the Wizard® Genomic DNA Purification Kit from Promega, briefly summarized in the following steps:

- 10 mL of a culture incubated overnight were centrifuged for 10 minutes at 4000 x g.
- Cells were lysed with Nuclei Lysis Solution and RNA was degraded by adding RNase Solution.
- Proteins were precipitated with Protein Precipitation Solution and centrifuged at 11200 x g for 3 minutes.
- DNA was precipitated with isopropanol to the supernatant, then it was centrifuged and washed with 70% ethanol twice. The pellet was air-dried, and the DNA pellet was rehydrated with Rehydration Solution.

Plasmid extraction

Plasmid extractions were performed by the GeneJET Plasmid Extraction Kit from Thermo Scientific. The manufacturer's instructions were followed. The protocol is briefly summarized as follows:

- Cell resuspension, Lysis and neutralization: Pelleted cells were resuspended in 250 µL of Resuspension Solution. Then 250 µL of Lysis Solution were added and mixed thoroughly by inverting the tube. 350 µL of the Neutralization Solution were added and mixed immediately and thoroughly by inverting the tube 4-6 times. Next, cells were centrifuged at 11000 x g for 5 min to pellet cell debris and chromosomal DNA.
- Bind plasmid DNA: supernatant was transferred to the supplied GeneJET spin column by pipetting and centrifuged at 11000 x g for 1 min, the flow-through was discarded and the column was placed back into the same collection tube. Tubes were washed twice with 500 µL of Wash Solution. The tubes were centrifuged an additional minute to remove residual Wash Solution.
- Elute purified plasmid DNA: the GeneJET spin column was transferred into a fresh 1.5 mL microcentrifuge tube. 50 µL of the Elution Buffer were added to the centre of GeneJET spin column membrane to elute the plasmid DNA. It was incubated for 2 min at room temperature and the centrifuged for 2 min.

Gel extraction

Gel extractions were carried out by using the GeneJET Gel Extraction Kit from Thermo Scientific. The Kit protocol was followed, which is summarized as follows:

- Gel extraction and DNA resuspension: the DNA band of interest was excised from the gel using a clean scalpel. It was cut as close to the DNA as possible to minimize gel volume. The gel slice was placed into a pre-weighed 1.5 ml tube and the weigh

was recorded. A 1:1 volume of Binding Buffer was added to the gel slice (volume: weight). The gel mixture was incubated at 50 - 60°C for 10 min. Then, the tube was mixed by inversion every few minutes to facilitate the melting process. When the gel was completely dissolved, the gel mixture was briefly vortex.

- Bind DNA and wash the column: up to 800 µL of the solubilized gel solution were transferred to the GeneJET purification column and it was centrifuged for 1 min. The flow-through was discarded and the column was placed back into the same collection tube. 700 µL of Wash Buffer were added to the GeneJET purification column. It was centrifuged for 1 min. The flow-through was discarded and the column was placed back into the same collection tube. The empty GeneJET purification column was centrifuged for an additional 1 min to completely remove residual wash buffer.
- Elute purified DNA: the GeneJET purification column was transferred into a clean 1.5 ml microcentrifuge tube. 50 µL of Elution Buffer were added to the centre of the purification column membrane. It was centrifuged for 1 min, the GeneJET purification column was discarded and the purified DNA was stored at -20°C.

8.1.3 Cloning methodology

Unless otherwise is stated, the cloning procedure was carried out by the Champion™ pET Directional TOPO® Expression Kit, from Invitrogen, according manufacturer's protocol. This procedure does not require the use of restriction endonucleases.

Ligation

Purified PCR product was added to the ampicillin resistance pET151/D-TOPO® vector in presence of water and salt solution, for ligation. As recommended, a 1 to 1 molar ratio of PCR product versus vector, was used. A volume of PCR product of 0.5 to 4 µL was mixed with 1 µL of salt solution, then sterile water was added to a volume of 5 µL; and finally, 1 µL of TOPO® vector was added to reach a final volume of 6 µL. The reaction was gently mixed and incubated for 30 to 60 minutes, at room temperature (22-23°C). The reaction was used for transformation into *E. coli* chemically competent cells.

Transforming One Shot® TOP10 *E. coli* competent cells

For vector maintenance: A volume of 3 µL of the TOPO® cloning reaction (Ligation reaction, from the previous step) were added into a vial of One Shot® TOP10 Chemically

Competent *E. coli* cells, and it was gently mixed while avoiding pipetting up and down. Then, the reaction was incubated on ice for 20 minutes, followed by a heat shock at 42°C for 30 seconds, without shaking; and then the vial was immediately transferred to ice. A volume of 250 µL of SOC or LB medium was added, at room temperature. The vial was capped tightly and shaken horizontally (200 rpm) at 37°C for 1 hour. Finally, 100 to 200 µL from the vial were spread on a pre-warmed selective petri plate (LB supplemented with 100 µg/mL of ampicillin), and incubated overnight at 37°C.

Transforming BL21 Star™(DE3) One Shot® *E. coli* competent Cells

For protein expression: One vial of BL21 Star™(DE3) One Shot® cells per transformation was thawed on ice. An amount of 5-10 ng plasmid DNA in a 1 to 5 µL volume, were added into each vial of BL21 Star™(DE3) One Shot® cells and mixed by stirring gently with the pipette tip, avoiding pipetting up and down. Then, the reaction was incubated on ice for 30 minutes, followed by a heat shock at 42°C for 30 seconds, without shaking. The tube was immediately transferred to ice and incubated for 5 minutes. A volume of 250 µL of SOC or LB medium was added, at room temperature. The vial was capped tightly and shaken horizontally (200 rpm) at 37°C for 30 to 60 minutes. The entire transformation reaction was added to 10 ml of LB (liquid media or petri plate), supplemented with 100 µg/mL of ampicillin. Finally, cells were grown overnight at 37 °C with shaking.

Screening by colony PCR, sequencing and glycerol stocks

Once colonies were obtained from transformation reactions (previous step), the correct structure of the inserted fragment was checked by colony PCR and sequencing. For colony PCR, some colonies from the petri plates generated in the transformation step, were selected. Each colony was picked and transferred to a tube containing 20 µL of sterile water, then the cells were resuspended. Parallelly, a PCR reaction was set up for each colony, as previously described. A volume of 1 to 2 µL of DNA template (colonies previously resuspended in water) were added to a tube containing a master mix reaction for PCR, with the corresponding primers aimed to amplify the fragment of interest. The volume of water used for each PCR reaction was adjusted to reach a final volume of 50 µL. The PCR reaction was carried out, and results were analysed by agarose gel. If a band appeared in the right size, the band was excised from the gel and purified, then the product was sent for sequencing to the GATC Biotech company. After sequencing results were available, an alignment was performed with the CLC software (Qiagen) to check the correct structure of

the fragment. Correct mutants were selected and cultured overnight in LB medium supplemented with ampicillin, then 0.5 mL of sterile 50 % glycerol solution was mixed with 0.5 mL of the selected mutant culture (giving a 25 % final glycerol concentration), in a cryovial, which was then flash-freeze in liquid nitrogen and store at -80 °C.

8.1.4 Protein expression and protein purification

Protein expression

The following procedure describes the expression of a recombinant protein in 1 litre of culture. As starter culture, 10 mL of LB supplemented with ampicillin (100 µg/mL) was inoculated with 50 µL of the glycerol stock of the *E. coli* BL21 mutant expressing the desired protein. The starter culture was incubated overnight at 37 °C, under 180 rpm agitation. The starter culture was used to inoculate 1 L of LB supplemented with ampicillin (100 µg/mL), the culture was grown for 4 hours, at 37 °C, under 180 rpm agitation, until cells reached an O.D. of 0.6. Then, 1 mL of 1M IPTG and 0.2 mL of $CuSO_4$ 400 mM were added to the culture, which was then incubated at 18 °C overnight. In this point, two different approaches were assayed for protein expression. The first method consisted of the incubation at 180 rpm of agitation, to produce the protein in its apoenzyme form, whereas a second method involved the incubation at 0 rpm, to achieve microaerobic conditions. The second method was only used to express fully copper loaded proteins (holoenzymes).

Cells harvesting

To harvest the cells, the culture was centrifuged at 5000 x g for 15 minutes, and the supernatant was discarded. Cells were transferred to a 50 mL tube and washed with water, then the pelleted cells were subjected to proteins purification.

Protein purification

The protein purification method was based on the generation of His_6 tagged recombinant proteins. An ion affinity chromatography (IMAC) approach was used for protein purification. Buffers used are listed below:

- Lysis buffer: 50 mM NaH_2PO_4, 10 mM imidazole, 300 mM NaCl, pH to 8.0.
- Wash buffer: 50 mM NaH_2PO_4, 20 mM imidazole, 300 mM NaCl, pH 8.0.
- Elution buffer: 50 mM NaH_2PO_4, 250 mM imidazole, 300 mM NaCl, pH 8.0.

All chemical reagents were purchased from Sigma-Aldrich. Once cells were harvested, they were disrupted by the addition of 30 mL Lysis Buffer pH=8 to the tube, then the mixture was agitated by vortex until cells were completely resuspended. The resulting solution was loaded into cell disruptor (Constant Systems pneumatic cell disruptor at 20.1 kilo-pound per square inch, kpsi), to break down the cells by pressure. The resulting solution was centrifuged at maximum speed (11000 x g), for 35 minutes. The supernatant was used for immobilized ion affinity chromatography (IMAC) protein purification. 1 ml of Ni-NTA resin column (GE Healthcare) was equilibrated with 3 volumes of washing buffer. A solution containing the His_6 tagged recombinant protein was poured into the column, and the flow through was discarded. Then, the column was washed twice with washing buffer, and finally the protein trapped in the column was eluted with 5 mL of elution buffer. The flow-through was collected.

Buffer exchange

A PD-10 column (GE Healthcare) was used for buffer exchange. The column was first equilibrated with 3 volumes of the intended buffer. Then, 2.5 mL of protein solution were added to the column. The flow-through was discarded and then 3.5 mL of the intended buffer were loaded into the column, in this step the flow-through was collected. The PD-10 column was re-equilibrated. The process was repeated if it was needed. This method was used to buffer exchange the recombinant proteins expressed, in a 20 mM Hepes, 80 mM of NaCl buffer solution, pH 7.0, for storage.

TEV cleavage

Recombinant His6 tagged proteins contained a TEV recognition sequence that allowed the cleavage of the histidine tag. Firstly, TEV protease was expressed and purified following the same procedure described for recombinant LMCOs, except that the culture for protein expression did not contain copper ions ($CuSO_4$, Sigma-Aldrich). The reaction was carried out by mixing TEV protease solution with the target protein solution. The amount of TEV protease used for cleavage was 1 mg of TEV per each 3 mg of His_6 tagged protein. The reaction was incubated at 4°C for about 24 hours. Then, TEV protein was removed from the mixture by a second IMAC, as TEV would have cleavage the His_6 tag from the recombinant protein, and TEV protease itself contained a His_6 tag, the collected flow through in this case contained the target protein without the His6 tag.

8.1.5 Enzyme activity

Common laccases substrates

2,2'-azino-bis(3-ethylbenzothiazoline-6-sulphonic acid) (ABTS); syringaldazine (SGZ); guiacol; 2,6-Dimethoxyphenol (DMP) and 2,4-Dichlorophenol (DCP) were used as substrates (All substrates were purchased from Sigma-aldrich). Buffers: Acetate buffer (100 mM) was used for reactions that require an acidic (pH 4.0). 0.3% of acetic acid and 0.68% of sodium acetate trihydrate, were dissolved in water to a final volume of 100%. 20 mM Hepes (Sigma-aldrich) and 80 mM Na Cl buffer was used for reactions that require a neutral pH (pH 7.0). Reaction mixture and the wavelength used for spectroscopy measurement are shown in the table below.

Substrate	Wavelength [nm]	Buffer [mL]	Enzyme solution [mL]	$CuSO_4$ solution [mL]	Substrate solution [mL]	4-amino_ Antipyrine [mL]
Guaiacol	436	1	0.2	0.15	0.15	-
DMP	468	1	0.2	0.15	0.15	-
DCP	510	0.85	0.2	0.15	0.15	0.15
ABTS	420	1	0.2	0.15	0.15	
SGZ	530	1	0.2	0.15	0.15	

Substrate concentrations: all substrates solutions were prepared at a concentration of 10 mM, to give a final concentration of 1 mM in the reaction, except for SGZ which had a concentration of 0.5 mM, giving a final concentration of 0.05 mM. For the reaction with DCP, the addition of 4-amino antipyrine was needed to allow colorimetric measurement. Acetate buffer (pH 4.0) was used for ABTS and DMP, while Hepes buffer (pH 7.0) was used for guaiacol, SGZ and DCP. Protein solutions were adjusted to a concentration of ≈0.15 mg/mL. Copper sulphate solution ($CuSO_4$) had a concentration of 7 mM, giving a final concentration of 0.7 mM. All assays were performed by triplicate. The UV-Vis spectrum was followed continuously during the reaction, at the corresponding wavelength.

Polymeric lignin and lignin model compounds as substrate

The lignin model compounds guaiacylglycerol-beta-guaiacyl ether (GGE) and 2,2'-dihydroxy-3,3'-dimethoxy-5,5'-dicarboxybiphenyl (DDVA), were used as substrates (Both chemicals were synthesized in the Chemical Biology Research Facility). For HPLC analysis, reactions were carried out with acetate buffer (pH 4.0) and Hepes buffer (pH 7.0). For LC-MS

analysis, reactions were carried out with 20 mM Ammonium bicarbonate buffer (pH 7.0) was used for reactions.

GGE: Reaction mixture consisted of 1.4 mL of buffer (20 mM ammonium bicarbonate), 0.2 mL of protein solution (≈0.7 mg/mL); 0.1 mL of substrate (20 mM of GGE dissolved in methanol); 0.15 mL of 7 mM $CuSO_4$ and 0.15 mL of 10 mM ABTS 10 as mediator. Samples were purified by solvent extraction and then analysed by HPLC and LC-MS.

DDVA: reaction mixture consisted of 1.2 mL buffer (20 mM ammonium bicarbonate), 0.2 mL of protein solution (≈0.7 mg/mL), 0.05 mL of substrate (20 mM dissolved in DMSO), 0.15 mL of 7 mM $CuSO_4$ and 0.15 mL of 10 mM ABTS as mediator. Reactions were incubated for 4 hours. Samples were purified by solvent extraction and then analysed by HPLC and LC-MS. As DMSO should be avoided for HPLC and LC-MS analysis, in this experiment only 50µL of substrate were used (DDVA final concentration was about 0.67 mM). Solvent extraction was used before HPLC and LC-MS analysis.

Polymeric lignin substrates: Reaction mixture consisted of 1.2 mL of buffer (20 mM ammonium bicarbonate), 0.2 mL of protein solution (≈0.7 mg/mL), 5 mg of lignin, 0.15 mL of 7 mM $CuSO_4$ and 0.15 mL of 10 mM ABTS as mediator. Reactions were incubated overnight. Samples were centrifuged (4000 x g for 2 minutes) and then subjected to solvent extraction for HPLC and LC-MS analysis.

Solvent extraction

Solvent extraction was used for samples requiring HPLC and LC-MS analysis. Once reaction had occurred, product purification was carried out by adding of 1 to 2 volumes of ethyl acetate (Sigma-Aldrich) and 100 µL of 1 M HCl, to the reaction. After mixing by inverting the tubes 4 to 5 times, two phases were formed. The organic phase (upper phase) was carefully transferred to a new container and dried out by rotary evaporation. Finally, dried samples were resuspended in 200 µL of a 50 % methanol solution, which then was used as sample for HPLC or LC-MS analysis.

8.1.6 HPLC and LC-MS analysis

For HPLC and LC-MS analysis, water was used as solvent A and methanol was used as solvent B, containing both 0.1% of formic acid. Maximum pressure was set as 200 bar and the flow was 0.5 mL/min. Method details were as follows:

Time	% Solvent A (H2O)	% Solvent B (Methanol)
0	95	5
10	90	10
20	70	30
30	70	30
35	60	40
40	30	70
45	0	100
57	0	100
60	95	5
70	95	5

8.1.7 Copper effect

Copper effect on enzyme activity was investigated for Pp-CopA, Pf-CopA and Oc-CueO. Concentrations were calculated in an Excel spreadsheet. $CuSO_4$ (Sigma-Aldrich) concentrations in reaction were as follows (in mM): 0.000, 0.095, 0.190, 0.286, 0.381, 0.476, 0.571, 0.667, 0.762, 0.857, 0.952, 1.048, 1.143, 1.238, 1.333, 1.429. $CuSO_4$ standard concentrations ranged from 0 to 15 mM with steps of 1 mM. A main solution of $CuSO_4$ 50 mM was used to prepare 5mL of each standard, data are summarized in the next table:

50 mM $CuSO_4$ Volume	Standard Conc.	Conc. In reaction	50 mM $CuSO_4$ Volume	Standard Conc.	Conc. In reaction
0	0	0.000	0.8	8	0.762
0.1	1	0.095	0.9	9	0.857
0.2	2	0.190	1	10	0.952
0.3	3	0.286	1.1	11	1.048
0.4	4	0.381	1.2	12	1.143
0.5	5	0.476	1.3	13	1.238
0.6	6	0.571	1.4	14	1.333
0.7	7	0.667	1.5	15	1.429

A plate reader was used to perform this experiment; hence reaction volume was modified. The reaction mixture was as follows:

Compound	Volume (µL)	Observations
Buffer	150	Acetate buffer, pH 4.5
Protein	20	≈0.13 mg/mL
$CuSO_4$	20	different concentrations
Substrate	20	ABTS 10 mM

8.1.8 ICP-OES metal content analysis and copper reconstitution

Protein expression was carried out for Pp-CopA, Pf-CopA and Oc-CueO, as previously described. Microaerobic conditions were used to generate holoenzymes. Then, a copper reconstitution assay was performed for the purified proteins. 3 µL of sterile $CuSO_4$ 400 mM were added to each protein solution (≈1 mg/mL) and mixtures were incubated overnight at room temperature. Protein solutions were buffer exchanged to ammonium bicarbonate buffer 20 mM by PD10 column (GE Healthcare). This procedure was performed twice to completely remove the excess of copper(II) ions.

For metal content analysis, protein solutions were diluted to achieve a final concentration of ≈0.2 and ≈0.1 mg/mL. To prepare the standards, commercially available standards for Cu and S were used, with a concentration of 10020 ppm and S 9814 ppm, respectively. A 100 ppm solution was prepared containing 200 µL of each standard into a new plastic tube and adding water up to 20 mL. From this solution, a 10 ppm solution was made by adding 2 mL of it and adding 18 mL of water. The 10 ppm solution was used to prepare the standards as follows:

Standard	Concentration (ppm)	Vol. of 10 ppm Sol.	Vol. of water
1	0.2	200 µL	9.8 mL
2	0.5	500 µL	9.5 mL
3	0.7	700 µL	9.3 mL
4	1	1000 µL	9 mL
5	2	2000 µL	8 mL
6	5	5000 µL	5 mL

This procedure was carried out in a balance, and the weight of each volume added was recorded to obtain the exact amount of the added compounds, which was later used for an accurate calculation of each standard concentration.

The standards were used to generate calibration curves for Cu and S in an ICP-OES equipment. Then, protein samples were run, and the concentration of each element was obtained by interpolation of the standard curve.

8.1.9 pH activity profile

A Britton & Robinson Universal Buffer solution was prepared, by adding different volumes of sodium hydroxide solution(0.2 N) to 20 mL of a solution of mixed acids, containing phosphoric acid, boric acid and acetic acid (0.04 M each of them) (All chemicals were purchased from Sigma-Aldrich). The volumes of sodium hydroxide added were 1.5 mL; 3 mL; 4 mL; 5 mL; 6 mL; 7 mL; 7.5 mL; 8.5 mL; 9.5 mL; 10.5 mL;11.5 mL; 12 mL; 12.5 mL; 13.5 mL; 14.5 mL; 14.5 mL and 15.5 mL. As result, different solutions with final pH of 2.35; 2.95; 3.84; 4.38; 4.75; 5.26; 5.54; 6.29; 6.78; 7.3; 8.01; 8.48; 8.68; 9.16; 9.56 and 10.4, respectively, were obtained. A plate reader was used to conduct this experiment, so reaction volume was modified accordingly. The reaction mixture was as follows:

Compound	Volume (µL)	Observations
Buffer	150	Different pH buffer
Protein	20	(≈0.13 mg/mL, each protein)
$CuSO_4$	20	7 mM
Substrate	20	ABTS 10 mM

8.2 Specific procedures

8.2.1 Primer design and PCR conditions of LMCOs

Gene encoding sequences of Pp-CopA, Pf-CopA and Oc-CueO contained TAT signal sequences. For these proteins, the primers were designed to exclude the TAT sequence from the corresponding recombinant expressed protein. The primers used are shown in **Table 3**.

The PCR conditions were as follows: Initial denaturation at 95 °C for 5 minutes; cycle denaturation at 95 °C for 30 seconds; annealing at the temperature shown in the table below for 30 seconds; cycle extension at 72 °C for 1 minute per 1 kbp; and a final extension at 72 °C for 5 minutes. 32 cycles were used.

Gene (Protein)	Annealing temperature	Observations
copA-II (Pp-CopA)	61 °C	2.5 µL of enhancer was added to 50 µL of PCR reaction
copA (Pf-CopA)	65 °C	1.5 µL of DMSO was added to 50 µL of PCR reaction
cueO (Oc-CueO)	55 °C	No enhancer nor DMSO
p-ppo (P-PPO)	56 °C	No enhancer nor DMSO

8.2.2 CopC proteins, cloning and protein expression

Primer design and PCR

CopC proteins from *Microbacterium phyllosphaerae* were selected for cloning and protein expression. The corresponding genes contain a peptide signal identified by Phobius (http://phobius.sbc.su.se/), and SignalP (http://www.cbs.dtu.dk/services/SignalP/) online tools, which suggested a possible extracellular function of the encoding proteins. However, these sequences were not identified as TAT signals by the online tool TatP (http://www.cbs.dtu.dk/services/TatP/). Two expression systems were used for protein expression, *E. coli* BL21 cells with the pET151 vector (the same expression system used for the LMCOs, Champion™ pET Directional TOPO® Expression Kit, from Invitrogen); and *R. jostii* RHA1 with the pTipQC-II vector. Therefore, primers were designed accordingly and are shown in **Table 7**. The primers used for expression in *E. coli* system were designed to include and exclude the peptide signal sequence. The primers used for expression in *R. jostii* contained the restriction sites NdeI and HindIII in the forward and reverse primers, respectively. Additionally, the primers were designed to include a TEV recognition sequence in the PCR products.

PCR conditions were as follows: initial denaturation at 95 °C for 5 minutes; denaturation at 95 °C for 30 seconds; annealing at 64 °C for *copc886* and 62 °C for *copc1032*, for 30 seconds; extension at 72 °C for 1 minute per 1 kbp; and final extension at 72 °C for 5 minutes. A total of 32 cycles were used. PCR reaction: Primers, dNTPS and enzyme concentration were according to Pfx Invitrogen protocol for PCR, as mentioned previously.

Ligation, transformation and protein expression

The same ligation, transformation and protein expression methods used for LMCO proteins, were used for the amplified PCR products intended for expression of CopC886 and CopC1032 in *E. coli* BL21. Therefore, the methodology described below applies only for expression of these proteins in *R. jostii*. Once PCR products were generated, and the plasmid pTipQC-II was obtained by plasmid extraction (described above), a restriction digestion reaction was set up as follows:

	For plasmid (µL)	For PCR products (µL)
Water nuclease free	30	30
10x Fast digest buffer	4	10
DNA	4 (447 ng/µL)	50
Enzymes NdeI and HindIII	2 of each	5
Reaction	37 °C for 5 minutes	37 °C for 60 minutes

Then, the digested plasmid and PCR products were subjected to a purification with the QIAquick PCR Purification Kit, Qiagen. Purified fragments were used to set up the ligation reaction, as follows:

	copC1032 [µL]	*copC886* [µL]
PCR product	3	7
10 x buffer	2	2
T4 DNA ligase	1	1
Water DNA free	9	5
Vector (pTipQCII)	5	4

Purified fragments concentrations were as follows: digested vector pTipQC-II, 22 ng/µL; PCR *copC886*, 16.7 ng/µL; and PCR *copC1032*, 23.1 ng/µL.

Transformation in Top10 *E. coli* chemically competent cells and screening was carried out as previously described. 100 µL of ligation reaction were added to a pre-warmed LB plates, containing chloramphenicol (25 µg/mL). After incubation overnight, 20 colonies were screened per each mutant. A colony PCR was performed for screening, and then 3 positive mutants were selected for sequencing, by the GATC Biotech Company. After sequence analysis, the mutants with a correct structure (sequences without mutations, in frame and right orientation, including the His_6 tag and Tev signal sequence) were selected for plasmid extraction. Then, plasmids harbouring the fragment of interest were used for transformation into *Rhodococcus jostii* RHA1 competent cells. *R. jostii* competent cells were transformed by electroporation. 50 µL of cells were added in an electroporation cuvette and mixed with 6 µL of the previously extracted plasmids harbouring the gene of interest. An electric potential of 1.8 V for 5 seconds was used in a pulse electroporator. Then 200 µL of LB medium was added to the cuvette and the mixture was incubated for 4 hours at 30 °C and 180 rpm of agitation. The resulting culture was spread in a LB plate supplemented with chloramphenicol (25 µg/mL) and incubated for about 48 to 72 hours. Once colonies grew, a second colony PCR and sequence analysis confirmed the presence of the vector in the transformed *R. jostii*.

For protein expression, the same general procedure described above was used, with the following variations: the antibiotic used was chloramphenicol (25 µg/ml). Before induction, a temperature of 30 °C was used for incubation, for 36 hours. For induction, thiostrepton (1 mg/mL) was added to the culture giving a final concentration of 1 µg/ml. The induced culture was incubated overnight. The method used for protein purification was the same as the described for expression of LMCO proteins.

Protein expression of CopC proteins from *B. xenovorans*

The corresponding synthetic genes of *Burkholderia xenovorans* CopC proteins, CopC-Bx1 and CopC-Bx2, were ordered to Genscript Company. Since the first amino acid, a histidine residue, at the N-terminus of the CopC proteins sequence, has been described as a copper ligand, the synthetic genes were designed to include a His_6 tag at the C-terminus position. The synthetic genes were ordered to be contained in the expression vector pET28b+ with the restriction sites: NcoI at the 5' end, and XhoI at the 3' end. The gene sequences were as follows:

copC-Bx1

CCATGGGCCATGCGCATCTGATGAGCAGCCAACCGGCGGCGAACGCGGAAGTGGTTGCG
CCGGCGGAAGTGACCATCCACTTCACCGAGCCGCTGGAACCGGCGTTTAGCAAGATTGCGCTGGC
GGACGCGAGCGGTAACACCGCGGCGCCGGCGGCGAGCCAGGTGGACCCGGGCGATGCGCGTGTT
ATGCACCTGCCGCTGCCGCAACTGAACGCGGGTCGTTACGCGGTGCATTGGACCGCGGTTGCGACC
GATGGTCACCGTACCCAGGGCGATTTCGCGTTTATCGTTAAAGAGAACCTGTATTTCCAAGGCCTCG
AG

copC-Bx2

CCATGGGCCACGTGTTTCCGCAGAAGCAAGAACCGGGTGCGGGTGCGACCGTTGCGAGC
CCGGCGCAAGTGCGTGTTATCTTCGACGGTCCGCTGGAAGCGGCGTTTAGCAGCCTGACCGTGACC
GATGCGAGCGGCAAGCAGGTGAACGCGCAAAAAGCGGCGGTTGATGAGCACCAACCGGCGCTGA
TTGCGGTGCCGCTGCCGCCGCTGGCGGCGGGTCGTTACACCGTTCATTGGGTGGCGGTTGCGAGC
GATGGTCACCGTACCCACGGCGATTACGCGTTCAACGTTAAAGAAAACCTGTATTTTCAGGGCCTC
GAG

Lyophilized plasmids containing the synthetic genes (4 µg) were resuspended in 40 µL of TB buffer, yielding a final solution with a concentration of 100 ng/µL. For maintenance, 50 µL Top10 *E. coli* competent cells were transformed with 3 µL of each synthetic gene solution; whereas for protein expression, 15 µL of chemically competent BL21 *E. coli* cells were mixed with 135 µL of $CaCl_2$ 0.1 M and 5 µL of the synthetic gene solution (100 ng/µL) on ice. For transformation and protein expression, the methods used were the same as previously described for transformation of LMCO proteins, with the following variation: Plates and liquid culture were supplemented with kanamycin (50 µg/ml).

8.2.3 Enzyme activity of CopC proteins from B. xenovorans

Activity of CopC-Bx1 and CopC-Bx2 was tested with ABTS, guaiacol and 2,4-DCP as substrates. A negative (blank) and positive (Pp-CopA) controls were used. The assayed enzyme solutions and their combinations are listed in the following table:

Negative control (blank)			
Positive control (Pp-CopA)			
CopC-Bx1	CopC-Bx1 + $CuSO_4$	CopC-Bx1 + H_2O_2	CopC-Bx1 + $CuSO_4$ + H_2O_2
CopC-Bx2	CopC-Bx2 + $CuSO_4$	CopC-Bx2 + H_2O_2	CopC-Bx2 + $CuSO_4$ + H_2O_2
CopC-Bx1 + CopC-Bx2	CopC-Bx1 + CopC-Bx2 + $CuSO_4$	CopC-Bx1 + CopC-Bx2 + H_2O_2	CopC-Bx1 + CopC-Bx2 + $CuSO_4$ + H_2O_2

The reaction consisted of:

Compound	Volume (µL)	Observations
Buffer	≈140	Adjusted to give a final volume of 200 µL
Protein	15	(≈0.8 mg/mL, each protein)
$CuSO_4$	15	7 mM
Substrate	15	10 mM, all used substrates
H_2O_2	15	62 mM

CopC proteins activity with polymeric lignin

Hardwood Ca-lignosulfonate (Borregaard), listed as lignin 6 in polymeric lignin assays (See section 4.3, Enzyme activity of laccase-like multicopper oxidases (LMCOs) on polymeric lignin substrates), was used as substrate. Enzymes used in this experiment included Pp-CopA, Dyp1B, CopC-Bx1 and CopC-Bx2. A 100 mM citrate buffer (pH 4.0) and a 20 mM Hepes buffer (pH 7.0) were used. Reaction mixture consisted of: 1.4 mL of buffer (adjusted to give a final reaction volume of 2 mL); 5 mg of polymeric lignin; 0.2 mL of 7 mM $CuSO_4$ solution; 30 µL of H_2O_2 65 mM (added only if Dyp1B was present); 0.2 mL of ABTS 10 mM as mediator and 0.1 mL of each protein solution. Protein combinations were as follows: Pp-CopA; Pp-CopA + Dyp1B; Pp-CopA + Dyp1B + CopC-Bx1; Pp-CopA + Dyp1B + CopC-Bx2; and Pp-CopA + Dyp1B + CopC-Bx1+ CopC-Bx2. Protein concentrations were adjusted to ≈ 1.2 mg/mL. Reactions were incubated overnight, and then subjected to solvent extraction, for HPLC analysis.

8.2.4 Site directed mutagenesis (SDM) of Oc-CueO

Site directed mutagenesis (SDM) of Oc-CueO was performed for selected amino acid residues by the QuikChange II XL Site-Directed Mutagenesis Kit (Agilent Technologies, Craven

Arms, UK) following the manufacturer's protocol. The list of target amino acid residues with their corresponding pair of primers, can be found in **Table 16**. For each intended mutant, the pair of primers was designed to contain the flanking regions of the mutation point. The primers were designed by the online tool provided in the kit protocol, available at: https://www.genomics.agilent.com/primerDesignProgram.jsp.

The methodology used for SDM consisted of three steps. 1. Mutant Strand Synthesis: A PCR was carried out to denature the DNA template, anneal mutagenic primers containing desired mutation and extend the primers with the DNA PfuUltra polymerase. 2. Dpn I Digestion: Digestion of parental methylated and hemimethylated DNA with Dpn I restriction enzyme, and 3. Transformation: Transformation of the mutated molecule into competent cells for nick repair.

A concentration of 120 ng per each primer was used for PCR, and the pET-151 vector harbouring the Oc-CueO encoding gene was used as DNA template at a concentration of 8.1 ng/ µL. PCR reaction was set up as follows: 5 µL of 10 x reaction buffer, 1 µL (≈10 ng) DNA (pET-151 Oc-CueO vector), 1.5 µL (≈125 ng) Fw and Rev primers, 1 µL of dNTP mix, 3 µL of quick solution, 37 µL of water and 1 µL of Pfu Ultra polymerase. PCR conditions were as follows: initial denaturation at 95 °C for 1 min, denaturation at 95 °C for 50 seconds, annealing at 60 °C for 50 seconds, extension at 68 °C for 8 min (1 min/kbp), and a final extension at 68 °C for 8 min. a total of 12 cycles were carried out. After PCR, Dpn I digestion of amplified products was performed for 1 h at 37 °C, and XL 10 gold *E. coli* ultracompetent cells were used for transformation as indicated in the kit manual. As final step, the sequence of mutants generated were analysed by GATC biotech Company. For protein expression, a plasmid extraction for each mutant was carried out and then plasmids were transformed in in BL21 *E. coli* competent cells. Transformation of BL21 cells and protein expression was performed as previously described for LMCO proteins.

8.2.5 Deletion of copA genes in P. putida KT2440

Amplification of flanking regions of target genes by PCR

Phusion high-fidelity DNA polymerase M0530 was used for PCR. Generated products were blunt end. The primers used can be seen in **Table 20**. Tm for each primer was calculated by the online tool available at this site: https://tmcalculator.neb.com/#!/. Full protocol for this enzyme can be found in: https://www.neb.com/protocols/1/01/01/pcr-protocol-m0530. Reaction set up is shown in the table below.

PCR of flanking regions for *copA* genes, by Phusion high-fidelity DNA polymerase M0530

Compound	Vol (50 µL)	Final concentration
Water nuclease free	To 50 µL	
5x Phusion HF/GC buffer	10 µL	1x
10 mM dNTPs	1 µL	200 µM
10 µM Fw primer	2.5 µL	0.5 µM
10 µM Rev primer	2.5 µL	0.5 µM
DNA Template	Variable (1 µL)	50-200 ng
Phusion DNA polymerase	0.5 µL	1 U/50 µL PCR Rx

A two-step PCR was performed (the annealing and extension steps were carried out at the same temperature). The PCR condition comprised an initial denaturation at 98 °C for 30 seconds, followed by 32 cycles of denaturation (98 °C for 10 seconds) and annealing (72 °C for 30 seconds), and a final extension at 72 °C for 10 minutes. PCR products were analysed in a 1% agarose gel.

Ligation and transformation using the pJET1.2/blunt vector

PCR products were purified and ligated with CloneJET PCR Cloning Kit (Thermo Fisher Scientific). Full protocol is available at https://tools.thermofisher.com/content/sfs/manuals/MAN0012966_CloneJET_PCR_Cloning_40rxn_UG.pdf. 20 ng of each purified PCR product was used for ligation into the pJET1.2/blunt vector. The reaction was set up on ice, and it consisted of:

Ligation of PCR products into pJET1.2/blunt vector (maintenance vector)

Compound	Amount	Used (10 µL) *
2X reaction buffer	10 µL	5 µL
Purified **blunt end** DNA product	0.15 pmol / 50 ng (20 ng was used)	1 µL (per each PCR fragment)
pJET cloning vector (50 ng/ µL)	1 µL	0.5 µL
Water nuclease free	Up to 19 µL	3 µL
T4 DNA ligase	1 µL	0.5 µL

The reaction was incubated at room temperature for 30 minutes, and then 5 µL were used to transform 50 µL of Top10 *E. coli* competent cells, as previously described for LMCO proteins.

Generation of allelic exchange vectors for *copA-I* and *copA-II*

Three colonies were taken for upstream and downstream fragments of each gene. Colonies were plated and cultivated overnight in LB supplemented with ampicillin (100

µg/mL). After cells harvesting, a plasmid extraction (pJET1.2/blunt vector) was performed and the resulting plasmids were subjected to a double restriction digestion to confirm the presence of the fragment of interest. The enzymes used, and reaction set up are shown in the tables below. Results were analysed by 1% agarose gel.

Restriction enzymes used for double digestion of each flanking region fragment

copA-I		copA-II	
Upstream fragment	Downstream fragment	Upstream fragment	Downstream fragment
EcoRI	BamHI	XbaI	SalI
BamHI	HindIII	SalI	PstI

Reaction set up for double digestion of flanking regions inserted in the pJET1.2/blunt vector (protocol according Fast Digest – Thermo Fisher)

Compound	Double digestion
Water	13 µL
10x fast digestion buffer	2 µL
DNA plasmid	3 µL
Enzyme	1 µL (each enzyme)
Total volume	20 µL

The reaction was incubated at 37 °C for 30 minutes. Parallelly, a double digestion reaction was set up for suicide vector pK18mobSacB. The restriction enzymes used for the vector intended for construction of the exchange vector for *copA-I*, were EcoRI and HindIII, while for *copA-II* were XbaI and PstI. Reaction set up is shown in the table below.

Reaction set up for double digestion of suicide vector pK18mobSacB

Compound	Double digestion
Water	15 µL
10x fast digestion buffer	2 µL
DNA plasmid	1 µL (vector 487 ng/µL)
Enzyme	1 µL (each enzyme)
Total volume	20 µL

The reaction was incubated at 37 °C for 30 minutes. Product was cleaned by QIAgene PCR purification Kit. Then, the digested upstream and downstream fragments and the corresponding vector for copA-I and copA-II were ligated to generate the allelic exchange vector. Reaction set up for this ligation is shown below.

Ligation of digested flanking regions and suicide vector pK18mobSacB

Compound	*copA-I*	*copA-II*
Linear vector DNA	4 µL (4.6 ng/µL)	4 µL (4.5 ng/µL)
Insert DNA (Left – L)	3.5 µL (6 ng/µL)	5 µL (4 ng/µL)
Insert DNA (Right – R)	4.5 µL (4.3 ng/µL)	4 µL (4.4 ng/µL)
10xT4 DNA buffer	2 µL	2 µL
T4 DNA ligase	1 µL	1 µL
Water nuclease free	5 µL	-
Total volume	20 µL	20 µL

Reaction was incubated overnight at 4 °C. Then, 5 µL of ligation reaction was used to transform 50 50 µL of Top10 E. coli chemically competent cells. Transformation was performed as previously described for LMCO proteins. The only difference was that utilization of Kanamycin (50 µg/mL) instead of ampicillin. A screening was performed by double restriction digestion and sequencing, with the GATC Biotech Company to confirm the correct structure of the construct. These allelic exchange vectors were used to transform competent *P. putida* cells.

Generation of *Pseudomonas putida* competent cells and transformation

To generate competent *P. putida* cells, 20 mL LB media were inoculated with *P. putida*, wild type (not supplemented with any antibiotic), and incubated overnight at 30 °C. Cells were harvested by centrifugation at 3200 x g for 10 minutes. The supernatant was discarded, and cells were resuspended in 10 mL of a 10 % glycerol sterile solution. The resuspended solution was centrifuged at 3200 x g for 10minutes, the supernatant was discarded, and cells were resuspended in 1 mL of 10% glycerol solution and transfer to a 1.5 mL Eppendorf tube. The process was repeated, and cells were resuspended in 500 µL of 10% glycerol solution. The resulting solution was distributed into 100 µL aliquots and flash freeze by liquid nitrogen. Store at -70 C.

For transformation, 1 µL of plasmid harbouring the allelic exchange vector was mixed with 100 µL of competent *P. putida* cells. The reaction was incubated for 5 minutes on ice and the mixture was transferred to an electroporation cuvette. Then the cuvette was placed in electroporator, a voltage of 1.8 kV was set up and electroporation was carried out for 5 seconds. After electroporation, the reaction was placed in a sterile Eppendorf tube and 500 µL of LB media was added. Culture was incubated at 30 °C for 1.5 hours. Then, transformation reaction was plated in kanamycin plates and incubated overnight. Colonies able to grow on kanamycin plates were spread on 10% sucrose plates (counter selection marker), and plates were incubated at 30 °C for 24 hours. The resulting colonies were subjected to PCR to confirm

the deletion of the gene. The primers used for confirmation of gene deletion are shown in section 6.3.3, Generation of unmarked deleted mutants by homologous recombination. A sequence analysis by GATC Biotech Company was used to confirm the gene deletion.

9 References

1. Martone, P. T., Estevez, J. M., Lu, F., Ruel, K., Denny, M. W., Somerville, C. & Ralph, J. (2009) Discovery of lignin in seaweed reveals convergent evolution of cell-wall architecture, *Current Biology.* **19**, 169-175.

2. Chabannes, M., Ruel, K., Yoshinaga, A., Chabbert, B., Jauneau, A., Joseleau, J. P. & Boudet, A. M. (2001) In situ analysis of lignins in transgenic tobacco reveals a differential impact of individual transformations on the spatial patterns of lignin deposition at the cellular and subcellular levels, *The Plant Journal.* **28**, 271-282.

3. Calvo-Flores, F. G., Dobado, J. A., Isac-García, J. & Martín-Martínez, F. J. (2015) *Lignin and lignans as renewable raw materials: chemistry, technology and applications*, John Wiley & Sons.

4. Falkehag, S. I. (1975) Lignin in materials. *Appl Polym Symp.* **28**, 247-257

5. Boerjan, W., Ralph, J. & Baucher, M. (2003) Lignin biosynthesis, *Annual Review of Plant Biology.* **54**, 519-546.

6. Munk, L., Sitarz, A. K., Kalyani, D. C., Mikkelsen, J. D. & Meyer, A. S. (2015) Can laccases catalyze bond cleavage in lignin?, *Biotechnology Advances.* **33**, 13-24.

7. Djikanović, D., Simonović, J., Savić, A., Ristić, I., Bajuk-Bogdanović, D., Kalauzi, A., Cakić, S., Budinski-Simendić, J., Jeremić, M. & Radotić, K. (2012) Structural differences between lignin model polymers synthesized from various monomers, *Journal of Polymers and the Environment.* **20**, 607-617.

8. Buranov, A. U. & Mazza, G. (2008) Lignin in straw of herbaceous crops, *Industrial Crops and Products.* **28**, 237-259.

9. Zakzeski, J., Bruijnincx, P. C. A., Jongerius, A. L. & Weckhuysen, B. M. (2010) The Catalytic Valorization of Lignin for the Production of Renewable Chemicals, *Chemical Reviews.* **110**, 3552-3599.

10. Parthasarathi, R., Romero, R. A., Redondo, A. & Gnanakaran, S. (2011) Theoretical study of the remarkably diverse linkages in lignin, *The Journal of Physical Chemistry Letters.* **2**, 2660-2666.

11. Chakar, F. S. & Ragauskas, A. J. (2004) Review of current and future softwood kraft lignin process chemistry, *Industrial Crops and Products.* **20**, 131-141.

12. Samuels, A., Rensing, K., Douglas, C., Mansfield, S., Dharmawardhana, D. & Ellis, B. (2002) Cellular machinery of wood production: differentiation of secondary xylem in Pinus contorta var. latifolia, *Planta.* **216**, 72-82.

13. Ragauskas, A. J., Beckham, G. T., Biddy, M. J., Chandra, R., Chen, F., Davis, M. F., Davison, B. H., Dixon, R. A., Gilna, P., Keller, M., Langan, P., Naskar, A. K., Saddler, J. N., Tschaplinski, T. J., Tuskan, G. A. & Wyman, C. E. (2014) Lignin Valorization: Improving Lignin Processing in the Biorefinery, *Science.* **344**.

14. Steeves, V., Förster, H., Pommer, U. & Savidge, R. (2001) Coniferyl alcohol metabolism in conifers—I. Glucosidic turnover of cinnamyl aldehydes by UDPG: coniferyl alcohol glucosyltransferase from pine cambium, *Phytochemistry.* **57**, 1085-1093.

15. Vanholme, R., Demedts, B., Morreel, K., Ralph, J. & Boerjan, W. (2010) Lignin biosynthesis and structure, *Plant Physiology.* **153**, 895-905.

16. McCaig, B. C., Meagher, R. B. & Dean, J. F. (2005) Gene structure and molecular analysis of the laccase-like multicopper oxidase (LMCO) gene family in Arabidopsis thaliana, *Planta.* **221**, 619-636.

17. Sato, Y. & Whetten, R. W. (2006) Characterization of two laccases of loblolly pine (Pinus taeda) expressed in tobacco BY-2 cells, *Journal of Plant Research.* **119**, 581.

18. Ralph, J., Lundquist, K., Brunow, G., Lu, F., Kim, H., Schatz, P. F., Marita, J. M., Hatfield, R. D., Ralph, S. A. & Christensen, J. H. (2004) Lignins: natural polymers from oxidative coupling of 4-hydroxyphenyl-propanoids, *Phytochemistry Reviews.* **3**, 29-60.

19. Pereira, A., Hoeger, I. C., Ferrer, A., Rencoret, J., del Rio, J. C., Kruus, K., Rahikainen, J., Kellock, M., Gutiérrez, A. & Rojas, O. J. (2017) Lignin films from spruce, eucalyptus, and wheat straw studied with electroacoustic and optical sensors: Effect of composition and electrostatic screening on enzyme binding, *Biomacromolecules.* **18**, 1322-1332.

20. Decina, S. & Crestini, C. (2012) Conversion of lignin: chemical technologies and biotechnologies-oxidative strategies in lignin upgrade in *Biorefinery: From Biomass to Chemicals and Fuels* pp. 167-206, De Gruyter Berlin, Boston.

21. Vishtal, A. G. & Kraslawski, A. (2011) Challenges in industrial applications of technical lignins, *BioResources.* **6**, 3547-3568.

22. Li, J., Henriksson, G. & Gellerstedt, G. (2007) Lignin depolymerization/repolymerization and its critical role for delignification of aspen wood by steam explosion, *Bioresource Technology.* **98**, 3061-3068.

23. Ikeda, T., Holtman, K., Kadla, J. F., Chang, H.-m. & Jameel, H. (2002) Studies on the effect of ball milling on lignin structure using a modified DFRC method, *Journal of Agricultural and Food Chemistry.* **50**, 129-135.

24. Rinaldi, R., Jastrzebski, R., Clough, M. T., Ralph, J., Kennema, M., Bruijnincx, P. C. & Weckhuysen, B. M. (2016) Paving the way for lignin valorisation: recent advances in bioengineering, biorefining and catalysis, *Angewandte Chemie International Edition.* **55**, 8164-8215.

25. Lupoi, J. S., Singh, S., Parthasarathi, R., Simmons, B. A. & Henry, R. J. (2015) Recent innovations in analytical methods for the qualitative and quantitative assessment of lignin, *Renewable and Sustainable Energy Reviews.* **49**, 871-906.

26. Cheng, J. (2017) *Biomass to renewable energy processes*, CRC press.

27. Li, C., Zhao, X., Wang, A., Huber, G. W. & Zhang, T. (2015) Catalytic transformation of lignin for the production of chemicals and fuels, *Chem Rev.* **115**, 11559-11624.

28. Cherubini, F., Jungmeier, G., Mandl, M., Philips, C., Wellisch, M., Jrgensen, H., Skiadas, I., Boniface, L., Dohy, M. & Pouet, J.-C. (2007). IEA Bioenergy Task 42 on Biorefineries: Co-production of fuels, chemicals, power and materials from biomass. *IEA Bioenergy Task*.

29. Cherubini, F. (2010) The biorefinery concept: using biomass instead of oil for producing energy and chemicals, *Energy Conversion and Management.* **51**, 1412-1421.

30. Amidon, T. E. & Liu, S. (2009) Water-based woody biorefinery, *Biotechnology Advances.* **27**, 542-550.

31. Bozell, J., Holladay, J., Johnson, D. & White, J. (2007) Top value added chemicals from biomass, *Volume II: Results of Screening for Potential Candidates from Biorefinery Lignin Report PNNL-16983*.

32. Carpenter, D., Westover, T. L., Czernik, S. & Jablonski, W. (2014) Biomass feedstocks for renewable fuel production: a review of the impacts of feedstock and pretreatment on the yield and product distribution of fast pyrolysis bio-oils and vapors, *Green Chemistry.* **16**, 384-406.

33. Dutta, S., De, S., Saha, B. & Alam, M. I. (2012) Advances in conversion of hemicellulosic biomass to furfural and upgrading to biofuels, *Catalysis Science & Technology.* **2**, 2025-2036.

34. Bio, H. G. (2012) From Carbohydrates and Sugar Alcohols to Platform Chemicals Ruppert, Agnieszka M.; Weinberg, Kamil; Palkovits, Regina, *Angewandte Chemie, International Edition.* **51**, 2564-2601.

35. Achyuthan, K. E., Achyuthan, A. M., Adams, P. D., Dirk, S. M., Harper, J. C., Simmons, B. A. & Singh, A. K. (2010) Supramolecular self-assembled chaos: polyphenolic lignin's barrier to cost-effective lignocellulosic biofuels, *Molecules.* **15**, 8641-8688.

36. Doherty, W. O., Mousavioun, P. & Fellows, C. M. (2011) Value-adding to cellulosic ethanol: Lignin polymers, *Industrial Crops and Products.* **33**, 259-276.

37. Shrotri, A., Kobayashi, H. & Fukuoka, A. (2017) Catalytic Conversion of Structural Carbohydrates and Lignin to Chemicals in *Advances in Catalysis* pp. 59-123, Elsevier.

38. Calvo-Flores, F. G. & Dobado, J. A. (2010) Lignin as renewable raw material, *ChemSusChem.* **3**, 1227-1235.

39. Christopher, L. P., Yao, B. & Ji, Y. (2014) Lignin biodegradation with laccase-mediator systems, *Frontiers in Energy Research.* **2**, 12.

40. Cragg, S. M., Beckham, G. T., Bruce, N. C., Bugg, T. D., Distel, D. L., Dupree, P., Etxabe, A. G., Goodell, B. S., Jellison, J. & McGeehan, J. E. (2015) Lignocellulose degradation mechanisms across the Tree of Life, *Current Opinion in Chemical Biology.* **29**, 108-119.

41. Camarero, S., Martínez, M. J. & Martínez, A. T. (2014) Understanding lignin biodegradation for the improved utilization of plant biomass in modern biorefineries, *Biofuels, Bioproducts and Biorefining.* **8**, 615-625.

42. de Gonzalo, G., Colpa, D. I., Habib, M. H. & Fraaije, M. W. (2016) Bacterial enzymes involved in lignin degradation, *Journal of Biotechnology.* **236**, 110-119.

43. Brown, M. E. & Chang, M. C. (2014) Exploring bacterial lignin degradation, *Current Opinion in Chemical Biology.* **19**, 1-7.

44. Sánchez, C. (2009) Lignocellulosic residues: biodegradation and bioconversion by fungi, *Biotechnology Advances.* **27**, 185-194.

45. Bugg, T. D., Ahmad, M., Hardiman, E. M. & Rahmanpour, R. (2011) Pathways for degradation of lignin in bacteria and fungi, *Natural Product Reports.* **28**, 1883-1896.

46. Guillén, F., Martínez, M. J., Gutiérrez, A. & Del Rio, J. (2005) Biodegradation of lignocellulosics: microbial, chemical, and enzymatic aspects of the fungal attack of lignin, *International Microbiology.* **8**, 195-204.

47. Call, H. & Mücke, I. (1997) History, overview and applications of mediated lignolytic systems, especially laccase-mediator-systems (Lignozym®-process), *Journal of Biotechnology.* **53**, 163-202.

48. Mayer, A. M. & Staples, R. C. (2002) Laccase: new functions for an old enzyme, *Phytochemistry.* **60**, 551-565.

49. Bourbonnais, R. & Paice, M. G. (1990) Oxidation of non-phenolic substrates: an expanded role for laccase in lignin biodegradation, *FEBS Letters.* **267**, 99-102.

50. Camarero, S., Ibarra, D., Martínez, M. J. & Martínez, Á. T. (2005) Lignin-derived compounds as efficient laccase mediators for decolorization of different types of recalcitrant dyes, *Applied and Environmental Microbiology.* **71**, 1775-1784.

51. Banci, L., Ciofi-Baffoni, S. & Tien, M. (1999) Lignin and Mn peroxidase-catalyzed oxidation of phenolic lignin oligomers, *Biochemistry.* **38**, 3205-3210.

52. Guillén, F., Martínez, A. T. & Martínez, M. J. (1992) Substrate specificity and properties of the aryl-alcohol oxidase from the ligninolytic fungus Pleurotus eryngii, *The FEBS Journal.* **209**, 603-611.

53. Guillén, F., Martínez, M. a. J., Muñoz, C. & Martínez, A. T. (1997) Quinone redox cycling in the ligninolytic fungus pleurotus eryngiileading to extracellular production of superoxide anion radical, *Archives of Biochemistry and Biophysics.* **339**, 190-199.

54. Gutierrez, A., Caramelo, L., Prieto, A., Martínez, M. J. & Martinez, A. T. (1994) Anisaldehyde production and aryl-alcohol oxidase and dehydrogenase activities in ligninolytic fungi of the genus Pleurotus, *Applied and Environmental Microbiology.* **60**, 1783-1788.

55. Kersten, P. J. (1990) Glyoxal oxidase of Phanerochaete chrysosporium: its characterization and activation by lignin peroxidase, *Proceedings of the National Academy of Sciences.* **87**, 2936-2940.

56. Fernández-Fueyo, E., Ruiz-Dueñas, F. J., Miki, Y., Martínez, M. J., Hammel, K. E. & Martínez, A. T. (2012) Lignin-degrading peroxidases from genome of selective ligninolytic fungus Ceriporiopsis subvermispora, *Journal of Biological Chemistry.* **287**, 16903-16916.

57. Floudas, D., Binder, M., Riley, R., Barry, K., Blanchette, R. A., Henrissat, B., Martínez, A. T., Otillar, R., Spatafora, J. W. & Yadav, J. S. (2012) The Paleozoic origin of enzymatic lignin decomposition reconstructed from 31 fungal genomes, *Science.* **336**, 1715-1719.

58. Bugg, T. D. H., Ahmad, M., Hardiman, E. M. & Singh, R. (2011) The emerging role for bacteria in lignin degradation and bio-product formation, *Current Opinion in Biotechnology.* **22**, 394-400.

59. Ramachandra, M., Crawford, D. L. & Hertel, G. (1988) Characterization of an extracellular lignin peroxidase of the lignocellulolytic actinomycete Streptomyces viridosporus, *Applied and Environmental Microbiology.* **54**, 3057-3063.

60. Ahmad, M., Taylor, C. R., Pink, D., Burton, K., Eastwood, D., Bending, G. D. & Bugg, T. D. (2010) Development of novel assays for lignin degradation: comparative analysis of bacterial and fungal lignin degraders, *Molecular Biosystems.* **6**, 815-821.

61. Taylor, C. R., Hardiman, E. M., Ahmad, M., Sainsbury, P. D., Norris, P. R. & Bugg, T. D. H. (2012) Isolation of bacterial strains able to metabolize lignin from screening of environmental samples, *Journal of Applied Microbiology.* **113**, 521-530.

62. Davis, J. R., Goodwin, L., Teshima, H., Detter, C., Tapia, R., Han, C., Huntemann, M., Wei, C.-L., Han, J. & Chen, A. (2013) Genome sequence of Streptomyces viridosporus strain T7A ATCC 39115, a lignin-degrading actinomycete, *Genome Announcements.* **1**, e00416-13.

63. Brown, M. E., Walker, M. C., Nakashige, T. G., Iavarone, A. T. & Chang, M. C. (2011) Discovery and characterization of heme enzymes from unsequenced bacteria: application to microbial lignin degradation, *Journal of the American Chemical Society.* **133**, 18006-18009.

64. van Bloois, E., Pazmiño, D. E. T., Winter, R. T. & Fraaije, M. W. (2010) A robust and extracellular heme-containing peroxidase from Thermobifida fusca as prototype of a bacterial peroxidase superfamily, *Applied Microbiology and Biotechnology.* **86**, 1419-1430.

65. Rahmanpour, R. & Bugg, T. D. H. (2015) Characterisation of Dyp-type peroxidases from Pseudomonas fluorescens Pf-5: Oxidation of Mn(II) and polymeric lignin by Dyp1B, *Archives of Biochemistry and Biophysics.* **574**, 93-98.

66. Lin, L., Cheng, Y., Pu, Y., Sun, S., Li, X., Jin, M., Pierson, E. A., Gross, D. C., Dale, B. E. & Dai, S. Y. (2016) Systems biology-guided biodesign of consolidated lignin conversion, *Green Chemistry.* **18**, 5536-5547.

67. Colpa, D. I., Fraaije, M. W. & van Bloois, E. (2014) DyP-type peroxidases: a promising and versatile class of enzymes, *Journal of Industrial Microbiology & Biotechnology.* **41**, 1-7.

68. Liers, C., Aranda, E., Strittmatter, E., Piontek, K., Plattner, D. A., Zorn, H., Ullrich, R. & Hofrichter, M. (2014) Phenol oxidation by DyP-type peroxidases in comparison to fungal and plant peroxidases, *Journal of Molecular Catalysis B: Enzymatic.* **103**, 41-46.

69. Fawal, N., Li, Q., Savelli, B., Brette, M., Passaia, G., Fabre, M., Mathe, C. & Dunand, C. (2012) PeroxiBase: a database for large-scale evolutionary analysis of peroxidases, *Nucleic Acids Research.* **41**, D441-D444.

70. Yoshida, T. & Sugano, Y. (2015) A structural and functional perspective of DyP-type peroxidase family, *Archives of Biochemistry and Biophysics.* **574**, 49-55.

71. Ahmad, M., Roberts, J. N., Hardiman, E. M., Singh, R., Eltis, L. D. & Bugg, T. D. H. (2011) Identification of DypB from Rhodococcus jostii RHA1 as a Lignin Peroxidase, *Biochemistry.* **50**, 5096-5107.

72. Sato, Y., Moriuchi, H., Hishiyama, S., Otsuka, Y., Oshima, K., Kasai, D., Nakamura, M., Ohara, S., Katayama, Y. & Fukuda, M. (2009) Identification of three alcohol dehydrogenase genes involved in the stereospecific catabolism of arylglycerol-β-aryl ether by Sphingobium sp. strain SYK-6, *Applied and Environmental Microbiology.* **75**, 5195-5201.

73. Tanamura, K., Abe, T., Kamimura, N., Kasai, D., Hishiyama, S., Otsuka, Y., Nakamura, M., Kajita, S., Katayama, Y. & Fukuda, M. (2011) Characterization of the third glutathione S-transferase gene involved in enantioselective cleavage of the β-aryl ether by Sphingobium sp. strain SYK-6, *Bioscience, Biotechnology, and Biochemistry.* **75**, 2404-2407.

74. Rashid, G. M., Taylor, C. R., Liu, Y., Zhang, X., Rea, D., Fülöp, V. & Bugg, T. D. (2015) Identification of manganese superoxide dismutase from Sphingobacterium sp. T2 as a novel bacterial enzyme for lignin oxidation, *ACS Chemical Biology.* **10**, 2286-2294.

75. Riva, S. (2006) Laccases: blue enzymes for green chemistry, *TRENDS in Biotechnology.* **24**, 219-226.

76. Laufer, Z., Beckett, R. P., Minibayeva, F. V., Lüthje, S. & Böttger, M. (2009) Diversity of laccases from lichens in suborder Peltigerineae, *The Bryologist.* **112**, 418-426.

77. Lang, M., Kanost, M. R. & Gorman, M. J. (2012) Multicopper oxidase-3 is a laccase associated with the peritrophic matrix of Anopheles gambiae.

78. Luna-Acosta, A., Rosenfeld, E., Amari, M., Fruitier-Arnaudin, I., Bustamante, P. & Thomas-Guyon, H. (2010) First evidence of laccase activity in the Pacific oyster Crassostrea gigas, *Fish & Shellfish Immunology.* **28**, 719-726.

79. Sharma, P., Goel, R. & Capalash, N. (2007) Bacterial laccases, *World Journal of Microbiology and Biotechnology.* **23**, 823-832.

80. Bao, W., O'malley, D. M., Whetten, R. & Sederoff, R. R. (1993) A laccase associated with lignification in loblolly pine xylem, *Science.* **260**, 672-674.

81. Giardina, P., Faraco, V., Pezzella, C., Piscitelli, A., Vanhulle, S. & Sannia, G. (2010) Laccases: a never-ending story, *Cellular and Molecular Life Sciences.* **67**, 369-385.

82. Machczynski, M. C., Vijgenboom, E., Samyn, B. & Canters, G. W. (2004) Characterization of SLAC: a small laccase from Streptomyces coelicolor with unprecedented activity, *Protein Science.* **13**, 2388-2397.

83. Piontek, K., Antorini, M. & Choinowski, T. (2002) Crystal structure of a laccase from the fungusTrametes versicolor at 1.90-Å resolution containing a full complement of coppers, *Journal of Biological Chemistry.* **277**, 37663-37669.

84. Jones, S. M. & Solomon, E. I. (2015) Electron transfer and reaction mechanism of laccases, *Cellular and Molecular Life Sciences.* **72**, 869-883.

85. Enguita, F. J., Martins, L. O., Henriques, A. O. & Carrondo, M. A. (2003) Crystal Structure of a Bacterial Endospore Coat Component: A laccase with enhanced thermostability properties, *Journal of Biological Chemistry.* **278**, 19416-19425.

86. Xiao, Z. & Wedd, A. G. (2011) Metallo-oxidase enzymes: Design of their active sites, *Australian Journal of Chemistry.* **64**, 231-238.

87. Marcus, R. A. & Sutin, N. (1985) Electron transfers in chemistry and biology, *Biochimica et Biophysica Acta (BBA)-Reviews on Bioenergetics.* **811**, 265-322.

88. Olsson, M. H., Ryde, U. & Roos, B. O. (1998) Quantum chemical calculations of the reorganization energy of blue-copper proteins, *Protein Science.* **7**, 2659-2668.

89. Ryde, U. & Olsson, M. H. (2001) Structure, strain, and reorganization energy of blue copper models in the protein, *International Journal of Quantum Chemistry.* **81**, 335-347.

90. Mate, D. M. & Alcalde, M. (2015) Laccase engineering: From rational design to directed evolution, *Biotechnology Advances.* **33**, 25-40.

91. Durao, P., Bento, I., Fernandes, A. T., Melo, E. P., Lindley, P. F. & Martins, L. O. (2006) Perturbations of the T1 copper site in the CotA laccase from Bacillus subtilis: structural, biochemical, enzymatic and stability studies, *JBIC Journal of Biological Inorganic Chemistry.* **11**, 514.

92. Xu, F., Palmer, A. E., Yaver, D. S., Berka, R. M., Gambetta, G. A., Brown, S. H. & Solomon, E. I. (1999) Targeted mutations in a Trametes villosa laccase axial perturbations of the T1 copper, *Journal of Biological Chemistry.* **274**, 12372-12375.

93. Xu, F., Shin, W., Brown, S. H., Wahleithner, J. A., Sundaram, U. M. & Solomon, E. I. (1996) A study of a series of recombinant fungal laccases and bilirubin oxidase that exhibit significant differences in redox potential, substrate specificity, and stability, *Biochimica et Biophysica Acta (BBA)-Protein Structure and Molecular Enzymology.* **1292**, 303-311.

94. Shleev, S., Morozova, O., Nikitina, O., Gorshina, E., Rusinova, T., Serezhenkov, V., Burbaev, D., Gazaryan, I. & Yaropolov, A. (2004) Comparison of physico-chemical characteristics of four laccases from different basidiomycetes, *Biochimie.* **86**, 693-703.

95. Kumar, S., Phale, P. S., Durani, S. & Wangikar, P. P. (2003) Combined sequence and structure analysis of the fungal laccase family, *Biotechnology and Bioengineering.* **83**, 386-394.

96. Reiss, R., Ihssen, J., Richter, M., Eichhorn, E., Schilling, B. & Thöny-Meyer, L. (2013) Laccase versus laccase-like multi-copper oxidase: a comparative study of similar enzymes with diverse substrate spectra, *PloS One.* **8**, e65633.

97. Sakurai, T. & Kataoka, K. (2007) Basic and applied features of multicopper oxidases, CueO, bilirubin oxidase, and laccase, *The Chemical Record.* **7**, 220-229.

98. Durand, F., Kjaergaard, C. H., Suraniti, E., Gounel, S., Hadt, R. G., Solomon, E. I. & Mano, N. (2012) Bilirubin oxidase from Bacillus pumilus: A promising enzyme for the elaboration of efficient cathodes in biofuel cells, *Biosensors and Bioelectronics.* **35**, 140-146.

99. Reiss, R., Ihssen, J. & Thöny-Meyer, L. (2011) Bacillus pumilus laccase: a heat stable enzyme with a wide substrate spectrum, *BMC Biotechnology.* **11**, 1.

100. Madhavi, V. & Lele, S. (2009) Laccase: properties and applications, *BioResources.* **4**, 1694-1717.

101. Beloqui, A., Pita, M., Polaina, J., Martínez-Arias, A., Golyshina, O. V., Zumárraga, M., Yakimov, M. M., García-Arellano, H., Alcalde, M. & Fernández, V. M. (2006) Novel polyphenol oxidase mined from a metagenome expression library of bovine rumen biochemical properties, structural analysis, and phylogenetic relationships, *Journal of Biological Chemistry.* **281**, 22933-22942.

102. Strachan, C. R., Singh, R., VanInsberghe, D., Ievdokymenko, K., Budwill, K., Mohn, W. W., Eltis, L. D. & Hallam, S. J. Metagenomic scaffolds enable combinatorial lignin transformation, *Proceedings of the National Academy of Sciences.* **111**, 10143-10148.

103. Pozdnyakova, N., Rodakiewicz-Nowak, J. & Turkovskaya, O. (2004) Catalytic properties of yellow laccase from Pleurotus ostreatus D1, *Journal of Molecular Catalysis B: Enzymatic.* **30**, 19-24.

104. Palmieri, G., Giardina, P., Bianco, C., Scaloni, A., Capasso, A. & Sannia, G. (1997) A novel white laccase from Pleurotus ostreatus, *Journal of Biological Chemistry.* **272**, 31301-31307.

105. Hoegger, P. J., Kilaru, S., James, T. Y., Thacker, J. R. & Kües, U. (2006) Phylogenetic comparison and classification of laccase and related multicopper oxidase protein sequences, *FEBS Journal.* **273**, 2308-2326.

106. Ihssen, J., Reiss, R., Luchsinger, R., Thöny-Meyer, L. & Richter, M. (2015) Biochemical properties and yields of diverse bacterial laccase-like multicopper oxidases expressed in Escherichia coli, *Scientific Reports.* **5**.

107. Morozova, O. V., Shumakovich, G. P., Gorbacheva, M. A., Shleev, S. V. & Yaropolov, A. I. (2007) "Blue" laccases, *Biochemistry (Moscow).* **72**, 1136-1150.

108. Leontievsky, A. A., Vares, T., Lankinen, P., Shergill, J. K., Pozdnyakova, N. N., Myasoedova, N. M., Kalkkinen, N., Golovleva, L. A., Cammack, R. & Thurston, C. F. (1997) Blue and yellow laccases of ligninolytic fungi, *FEMS Microbiology Letters.* **156**, 9-14.

109. Strong, P. & Claus, H. (2011) Laccase: a review of its past and its future in bioremediation, *Critical Reviews in Environmental Science and Technology.* **41**, 373-434.

110. Baldrian, P. (2006) Fungal laccases–occurrence and properties, *FEMS Microbiology Reviews.* **30**, 215-242.

111. Ufarté, L., Potocki-Veronese, G., Cecchini, D., Tauzin, A. S., Rizzo, A., Morgavi, D. P., Cathala, B., Moreau, C., Cleret, M. & Robe, P. (2018) Highly promiscuous oxidases discovered in the bovine rumen microbiome, *Frontiers in Microbiology.* **9**.

112. Solano, F., Lucas-Elío, P., López-Serrano, D., Fernández, E. & Sanchez-Amat, A. (2001) Dimethoxyphenol oxidase activity of different microbial blue multicopper proteins, *FEMS Microbiology Letters.* **204**, 175-181.

113. Ausec, L., Zakrzewski, M., Goesmann, A., Schlüter, A. & Mandic-Mulec, I. (2011) Bioinformatic analysis reveals high diversity of bacterial genes for laccase-like enzymes, *PLoS One.* **6**, e25724.

114. Lundell, T. K., Mäkelä, M. R. & Hildén, K. (2010) Lignin-modifying enzymes in filamentous basidiomycetes–ecological, functional and phylogenetic review, *Journal of Basic Microbiology.* **50**, 5-20.

115. Leonowicz, A., Cho, N., Luterek, J., Wilkolazka, A., Wojtas-Wasilewska, M., Matuszewska, A., Hofrichter, M., Wesenberg, D. & Rogalski, J. (2001) Fungal laccase: properties and activity on lignin, *Journal of Basic Microbiology.* **41**, 185-227.

116. Youn, H. D., Hah, Y. C. & Kang, S. O. (1995) Role of laccase in lignin degradation by white-rot fungi, *FEMS Microbiology Letters.* **132**, 183-188.

117. Evans, C. S. (1985) Laccase activity in lignin degradation by Coriolus versicolor in vivo and in vitro studies, *FEMS Microbiology Letters.* **27**, 339-343.

118. Ander, P. & Eriksson, K.-E. (1976) The importance of phenol oxidase activity in lignin degradation by the white-rot fungus Sporotrichum pulverulentum, *Archives of Microbiology.* **109**, 1-8.

119. Kawai, S., Umezawa, T. & Higuchi, T. (1988) Degradation mechanisms of phenolic β-1 lignin substructure model compounds by laccase of Coriolus versicolor, *Archives of Biochemistry and Biophysics.* **262**, 99-110.

120. Kim, K.-J., Shin, K.-S. & Hong, S.-W. (1986) Induction of extracellular polyphenol oxidase from two white-rot fungi, *The Korean Journal of Mycology.* **14**, 43-47.

121. Grönqvist, S., Viikari, L., Niku-Paavola, M.-L., Orlandi, M., Canevali, C. & Buchert, J. (2005) Oxidation of milled wood lignin with laccase, tyrosinase and horseradish peroxidase, *Applied Microbiology and Biotechnology.* **67**, 489-494.

122. Eggert, C., Temp, U. & Eriksson, K.-E. L. (1997) Laccase is essential for lignin degradation by the white-rot fungus Pycnoporus Cinnabarinus, *Febs Letters.* **407**, 89-92.

123. Xie, N., Chapeland-Leclerc, F., Silar, P. & Ruprich-Robert, G. (2014) Systematic gene deletions evidences that laccases are involved in several stages of wood degradation in the filamentous fungus Podospora anserina, *Environmental Microbiology.* **16**, 141-161.

124. Hatakka, A. (1994) Lignin-modifying enzymes from selected white-rot fungi: production and role from in lignin degradation, *FEMS Microbiology Reviews.* **13**, 125-135.

125. Kawai, S., Nakagawa, M. & Ohashi, H. (2002) Degradation mechanisms of a nonphenolic β-O-4 lignin model dimer by Trametes versicolor laccase in the presence of 1-hydroxybenzotriazole, *Enzyme and Microbial Technology.* **30**, 482-489.

126. Suurnäkki, A., Oksanen, T., Orlandi, M., Zoia, L., Canevali, C. & Viikari, L. (2010) Factors affecting the activation of pulps with laccase, *Enzyme and Microbial Technology.* **46**, 153-158.

127. Eggert, C., Temp, U., Dean, J. F. & Eriksson, K.-E. L. (1996) A fungal metabolite mediates degradation of non-phenolic lignin structures and synthetic lignin by laccase, *Febs Letters.* **391**, 144-148.

128. Gouveia, S., Fernández-Costas, C., Sanromán, M. & Moldes, D. (2012) Enzymatic polymerisation and effect of fractionation of dissolved lignin from Eucalyptus globulus Kraft liquor, *Bioresource Technology.* **121**, 131-138.

129. Moya, R., Saastamoinen, P., Hernández, M., Suurnäkki, A., Arias, E. & Mattinen, M.-L. (2011) Reactivity of bacterial and fungal laccases with lignin under alkaline conditions, *Bioresource Technology.* **102**, 10006-10012.

130. Shleev, S., Persson, P., Shumakovich, G., Mazhugo, Y., Yaropolov, A., Ruzgas, T. & Gorton, L. (2006) Interaction of fungal laccases and laccase-mediator systems with lignin, *Enzyme and Microbial Technology.* **39**, 841-847.

131. Crestini, C., Jurasek, L. & Argyropoulos, D. S. (2003) On the mechanism of the laccase–mediator system in the oxidation of lignin, *Chemistry-A European Journal.* **9**, 5371-5378.

132. Barneto, A. G., Aracri, E., Andreu, G. & Vidal, T. (2012) Investigating the structure–effect relationships of various natural phenols used as laccase mediators in the biobleaching of kenaf and sisal pulps, *Bioresource Technology.* **112**, 327-335.

133. Moldes, D., Díaz, M., Tzanov, T. & Vidal, T. (2008) Comparative study of the efficiency of synthetic and natural mediators in laccase-assisted bleaching of eucalyptus kraft pulp, *Bioresource Technology.* **99**, 7959-7965.

134. Rochefort, D., Leech, D. & Bourbonnais, R. (2004) Electron transfer mediator systems for bleaching of paper pulp, *Green Chemistry.* **6**, 14-24.

135. Larsson, S., Cassland, P. & Jönsson, L. J. (2001) Development of a Saccharomyces cerevisiae strain with enhanced resistance to phenolic fermentation inhibitors in lignocellulose hydrolysates by heterologous expression of laccase, *Applied and Environmental Microbiology.* **67**, 1163-1170.

136. Bauer, C. G., Kühn, A., Gajovic, N., Skorobogatko, O., Holt, P.-J., Bruce, N. C., Makower, A., Lowe, C. R. & Scheller, F. W. (1999) New enzyme sensors for morphine and codeine based on morphine dehydrogenase and laccase, *Fresenius' Journal of Analytical Chemistry.* **364**, 179-183.

137. Di Fusco, M., Tortolini, C., Deriu, D. & Mazzei, F. (2010) Laccase-based biosensor for the determination of polyphenol index in wine, *Talanta.* **81**, 235-240.

138. Ghindilis, A., Gavrilova, V. & Yaropolov, A. (1992) Laccase-based biosensor for determination of polyphenols: determination of catechols in tea, *Biosensors and Bioelectronics.* **7**, 127-131.

139. Arora, D. S. & Sharma, R. K. (2010) Ligninolytic fungal laccases and their biotechnological applications, *Applied Biochemistry and Biotechnology.* **160**, 1760-1788.

140. Santhanam, N., Vivanco, J. M., Decker, S. R. & Reardon, K. F. (2011) Expression of industrially relevant laccases: prokaryotic style, *Trends in Biotechnology.* **29**, 480-489.

141. Dwivedi, U. N., Singh, P., Pandey, V. P. & Kumar, A. (2011) Structure–function relationship among bacterial, fungal and plant laccases, *Journal of Molecular Catalysis B: Enzymatic.* **68**, 117-128.

142. Margot, J., Bennati-Granier, C., Maillard, J., Blánquez, P., Barry, D. A. & Holliger, C. (2013) Bacterial versus fungal laccase: potential for micropollutant degradation, *AMB Express.* **3**, 63.

143. Ferraroni, M., Myasoedova, N. M., Schmatchenko, V., Leontievsky, A. A., Golovleva, L. A., Scozzafava, A. & Briganti, F. (2007) Crystal structure of a blue laccase from Lentinus tigrinus: evidences for intermediates in the molecular oxygen reductive splitting by multicopper oxidases, *BMC Structural Biology.* **7**, 60.

144. Li, X., Wei, Z., Zhang, M., Peng, X., Yu, G., Teng, M. & Gong, W. (2007) Crystal structures of E. coli laccase CueO at different copper concentrations, *Biochemical and Biophysical Research Communications.* **354**, 21-26.

145. Roberts, S. A., Weichsel, A., Grass, G., Thakali, K., Hazzard, J. T., Tollin, G., Rensing, C. & Montfort, W. R. (2002) Crystal structure and electron transfer kinetics of CueO, a multicopper oxidase required for copper homeostasis in Escherichia coli, *Proceedings of the National Academy of Sciences.* **99**, 2766-2771.

146. Mellano, M. A. & Cooksey, D. A. (1988) Nucleotide sequence and organization of copper resistance genes from Pseudomonas syringae pv. tomato, *Journal of Bacteriology.* **170**, 2879-2883.

147. Brown, N. L., Barrett, S. R., Camakaris, J., Lee, B. T. O. & Rouch, D. A. (1995) Molecular genetics and transport analysis of the copper-resistance determinant (pco) from *Escherichia coli* plasmid pRJ1004, *Molecular Microbiology.* **17**, 1153-1166.

148. Hullo, M.-F., Moszer, I., Danchin, A. & Martin-Verstraete, I. (2001) CotA of Bacillus subtilis Is a Copper-Dependent Laccase, *Journal of Bacteriology.* **183**, 5426-5430.

149. Grass, G. & Rensing, C. (2001) CueO Is a Multi-copper Oxidase That Confers Copper Tolerance in Escherichia coli, *Biochemical and Biophysical Research Communications.* **286**, 902-908.

150. Chandra, R., Raj, A., Purohit, H. J. & Kapley, A. (2007) Characterisation and optimisation of three potential aerobic bacterial strains for kraft lignin degradation from pulp paper waste, *Chemosphere.* **67**, 839-846.

151. Roslan, M. A. M., Amirudin, N. A., Abidin, Z. A. Z. & Omar, S. M. (2015) Isolation of bacteria from the acidic peat swamp forest soil and their lignin degradation potential, *Jurnal Teknologi.* **77**.

152. Sargent, F., Berks, B. C. & Palmer, T. (2006) Pathfinders and trailblazers: a prokaryotic targeting system for transport of folded proteins, *FEMS Microbiology Letters.* **254**, 198-207.

153. Rahmanpour, R., King, L. D. & Bugg, T. D. (2017) Identification of an extracellular bacterial flavoenzyme that can prevent re-polymerisation of lignin fragments, *Biochemical and Biophysical Research Communications.* **482**, 57-61.

154. Magnani, D. & Solioz, M. (2007) How bacteria handle copper in *Molecular Microbiology of Heavy Metals* pp. 259-285, Springer.

155. Outten, F. W., Huffman, D. L., Hale, J. A. & O'Halloran, T. V. (2001) The independent cue and cus Systems confer copper tolerance during aerobic and anaerobic growth in Escherichia coli, *Journal of Biological Chemistry.* **276**, 30670-30677.

156. Cha, J. S. & Cooksey, D. A. (1991) Copper resistance in Pseudomonas syringae mediated by periplasmic and outer membrane proteins, *Proceedings of the National Academy of Sciences.* **88**, 8915-8919.

157. Outten, F. W., Outten, C. E., Hale, J. & O'Halloran, T. V. (2000) Transcriptional Activation of an Escherichia coliCopper Efflux Regulon by the Chromosomal MerR Homologue, CueR, *Journal of Biological Chemistry.* **275**, 31024-31029.

158. Mills, S. D., Jasalavich, C. A. & Cooksey, D. A. (1993) A two-component regulatory system required for copper-inducible expression of the copper resistance operon of Pseudomonas syringae, *Journal of Bacteriology.* **175**, 1656-1664.

159. Puig, S., Rees, E. M. & Thiele, D. J. (2002) The ABCDs of periplasmic copper trafficking, *Structure.* **10**, 1292-1295.

160. Arnesano, F., Banci, L., Bertini, I. & Thompsett, A. R. (2002) Solution Structure of CopC: a cupredoxin-like protein involved in copper homeostasis, *Structure.* **10**, 1337-1347.

161. Arnesano, F., Banci, L., Bertini, I., Mangani, S. & Thompsett, A. R. (2003) A redox switch in CopC: An intriguing copper trafficking protein that binds copper(I) and copper(II) at different sites, *Proceedings of the National Academy of Sciences.* **100**, 3814-3819.

162. Lawton, T. J., Kenney, G. E., Hurley, J. D. & Rosenzweig, A. C. (2016) The CopC Family: structural and bioinformatic insights into a diverse group of periplasmic copper binding proteins, *Biochemistry.* **55**, 2278-2290.

163. Chauhan, P. S., Goradia, B. & Saxena, A. (2017) Bacterial laccase: recent update on production, properties and industrial applications, *3 Biotech.* **7**, 323.

164. Kajita, S., Sugawara, S., Miyazaki, Y., Nakamura, M., Katayama, Y., Shishido, K. & Iimura, Y. (2004) Overproduction of recombinant laccase using a homologous expression system in Coriolus versicolor, *Applied Microbiology and Biotechnology.* **66**, 194-199.

165. Ma, B., Mayfield, M. B. & Gold, M. H. (2003) Homologous expression of Phanerochaete chrysosporium manganese peroxidase, using bialaphos resistance as a dominant selectable marker, *Current Genetics.* **43**, 407-414.

166. Couto, S. R. & Toca-Herrera, J. L. (2007) Laccase production at reactor scale by filamentous fungi, *Biotechnology Advances.* **25**, 558-569.

167. Cassland, P. & Jönsson, L. (1999) Characterization of a gene encoding Trametes versicolor laccase A and improved heterologous expression in Saccharomyces cerevisiae by decreased cultivation temperature, *Applied Microbiology and Biotechnology.* **52**, 393-400.

168. Liu, W., Chao, Y., Liu, S., Bao, H. & Qian, S. (2003) Molecular cloning and characterization of a laccase gene from the basidiomycete Fome lignosus and expression in Pichia pastoris, *Applied Microbiology and Biotechnology.* **63**, 174-181.

169. Conesa, A., Jeenes, D., Archer, D. B., van den Hondel, C. A. & Punt, P. J. (2002) Calnexin overexpression increases manganese peroxidase production in Aspergillus niger, *Applied and Environmental Microbiology.* **68**, 846-851.

170. Robert, V., Mekmouche, Y., R Pailley, P. & Tron, T. (2011) Engineering laccases: in search for novel catalysts, *Current Genomics.* **12**, 123-129.

171. Plotkin, J. B. & Kudla, G. (2011) Synonymous but not the same: the causes and consequences of codon bias, *Nature Reviews Genetics.* **12**, 32.

172. Rosano, G. L. & Ceccarelli, E. A. (2009) Rare codon content affects the solubility of recombinant proteins in a codon bias-adjusted Escherichia coli strain, *Microbial Cell Factories.* **8**, 41.

173. Ducros, V., Brzozowski, A. M., Wilson, K. S., Brown, S. H., Østergaard, P., Schneider, P., Yaver, D. S., Pedersen, A. H. & Davies, G. J. (1998) Crystal structure of the type-2 Cu depleted laccase from Coprinus cinereus at 2.2 Å resolution, *Nature Structural & Molecular Biology.* **5**, 310-316.

174. Galli, I., Musci, G. & di Patti, M. C. B. (2004) Sequential reconstitution of copper sites in the multicopper oxidase CueO, *JBIC Journal of Biological Inorganic Chemistry.* **9**, 90-95.

175. Durao, P., Chen, Z., Fernandes, A. T., Hildebrandt, P., Murgida, D. H., Todorovic, S., Pereira, M. M., Melo, E. P. & Martins, L. O. (2008) Copper incorporation into recombinant CotA laccase from Bacillus subtilis: characterization of fully copper loaded enzymes, *JBIC Journal of Biological Inorganic Chemistry.* **13**, 183-193.

176. Sainsbury, P. D., Hardiman, E. M., Ahmad, M., Otani, H., Seghezzi, N., Eltis, L. D. & Bugg, T. D. (2013) Breaking down lignin to high-value chemicals: the conversion of lignocellulose to vanillin in a gene deletion mutant of Rhodococcus jostii RHA1, *ACS Chemical Biology.* **8**, 2151-2156.

177. Mycroft, Z., Gomis, M., Mines, P., Law, P. & Bugg, T. D. (2015) Biocatalytic conversion of lignin to aromatic dicarboxylic acids in Rhodococcus jostii RHA1 by re-routing aromatic degradation pathways, *Green Chemistry.* **17**, 4974-4979.

178. Rashid, G. M., Duran-Pena, M. J., Rahmanpour, R., Sapsford, D. & Bugg, T. D. (2017) Delignification and enhanced gas release from soil containing lignocellulose by treatment with bacterial lignin degraders, *Journal of Applied Microbiology*.

179. Wang, Z. & Wu, M. (2013) A phylum-level bacterial phylogenetic marker database, *Molecular Biology and Evolution.* **30**, 1258-1262.

180. Besemer, J. & Borodovsky, M. (2005) GeneMark: web software for gene finding in prokaryotes, eukaryotes and viruses, *Nucleic Acids Research.* **33**, W451-W454.

181. Seemann, T. (2014) Prokka: rapid prokaryotic genome annotation, *Bioinformatics.* **30**, 2068-2069.

182. Yoon, S.-H., Ha, S.-M., Kwon, S., Lim, J., Kim, Y., Seo, H. & Chun, J. (2017) Introducing EzBioCloud: a taxonomically united database of 16S rRNA gene sequences and whole-genome assemblies, *International Journal of Systematic and Evolutionary Microbiology.* **67**, 1613-1617.

183. Granja-Travez, R. S., Wilkinson, R. C., Persinoti, G. F., Squina, F. M., Fülöp, V. & Bugg, T. D. (2018) Structural and functional characterisation of multi-copper oxidase CueO from lignin-degrading bacterium Ochrobactrum sp. reveal its activity towards lignin model compounds and lignosulfonate, *The FEBS Journal.* **285**, 1684-1700.

184. Franke, S., Grass, G., Rensing, C. & Nies, D. H. (2003) Molecular analysis of the copper-transporting efflux system CusCFBA of Escherichia coli, *Journal of Bacteriology.* **185**, 3804-3812.

185. Brouwers, G.-J., de Vrind, J. P., Corstjens, P. L., Cornelis, P., Baysse, C. & de Vrind-de Jong, E. W. (1999) cumA, a gene encoding a multicopper oxidase, is involved in Mn2+ oxidation in Pseudomonas putida GB-1, *Applied and Environmental Microbiology.* **65**, 1762-1768.

186. Lee, P. A., Tullman-Ercek, D. & Georgiou, G. (2006) The bacterial twin-arginine translocation pathway, *Annu Rev Microbiol.* **60**, 373-395.

187. Denef, V., Park, J., Tsoi, T., Rouillard, J.-M., Zhang, H., Wibbenmeyer, J., Verstraete, W., Gulari, E., Hashsham, S. & Tiedje, J. (2004) Biphenyl and benzoate metabolism in a genomic context: outlining genome-wide metabolic networks in Burkholderia xenovorans LB400, *Applied and Environmental Microbiology.* **70**, 4961-4970.

188. Childs, R. E. & Bardsley, W. G. (1975) The steady-state kinetics of peroxidase with 2, 2'-azino-di-(3-ethyl-benzthiazoline-6-sulphonic acid) as chromogen, *Biochemical Journal.* **145**, 93.

189. Bauer, R. & Rupe, C. O. (1971) Use of syringaldazine in a photometric method for estimating" free" chlorine in water, *Analytical Chemistry.* **43**, 421-425.

190. Michota-Kaminska, A., Wrzosek, B. & Bukowska, J. (2006) Resonance Raman evidence of immobilization of laccase on self-assembled monolayers of thiols on Ag and Au surfaces, *Applied Spectroscopy.* **60**, 752-757.

191. Adelakun, O. E., Kudanga, T., Green, I. R., le Roes-Hill, M. & Burton, S. G. (2012) Enzymatic modification of 2, 6-dimethoxyphenol for the synthesis of dimers with high antioxidant capacity, *Process Biochemistry.* **47**, 1926-1932.

192. Edens, W. A., Goins, T. Q., Dooley, D. & Henson, J. M. (1999) Purification and characterization of a secreted laccase of Gaeumannomyces graminis var. tritici, *Applied and Environmental Microbiology.* **65**, 3071-3074.

193. Doerge, D. R., Divi, R. L. & Churchwell, M. I. (1997) Identification of the colored guaiacol oxidation product produced by peroxidases, *Analytical Biochemistry.* **250**, 10-17.

194. Devasia, S. & Nair, A. J. (2016) Screening of potent laccase producing organisms based on the oxidation pattern of different phenolic substrates, *International Journal of Current Microbiology and Applied Sciences.* **5**, 127-137.

195. Galai, S., Korri-Youssoufi, H. & Marzouki, M. N. (2014) Characterization of yellow bacterial laccase SmLac/role of redox mediators in azo dye decolorization, *Journal of Chemical Technology and Biotechnology.* **89**, 1741-1750.

196. Koschorreck, K., Richter, S. M., Ene, A. B., Roduner, E., Schmid, R. D. & Urlacher, V. B. (2008) Cloning and characterization of a new laccase from Bacillus licheniformis catalyzing dimerization of phenolic acids, *Applied Microbiology and Biotechnology.* **79**, 217-224.

197. Li, Y., Yin, J., Qu, G., Lv, L., Li, Y., Yang, S. & Wang, X.-G. (2008) Gene cloning, protein purification, and enzymatic properties of multicopper oxidase, from Klebsiella sp. 601, *Canadian Journal of Microbiology.* **54**, 725-733.

198. Kalyani, D., Munk, L., Mikkelsen, J. & Meyer, A. (2016) Molecular and biochemical characterization of a new thermostable bacterial laccase from Meiothermus ruber DSM 1279, *RSC Advances.* **6**, 3910-3918.

199. Miyazaki, K. (2005) A hyperthermophilic laccase from Thermus thermophilus HB27, *Extremophiles.* **9**, 415-425.

200. Harkin, J. M. & Obst, J. R. (1973) Lignification in trees: indication of exclusive peroxidase participation, *Science.* **180**, 296-298.

201. Britton, H. T. S. & Robinson, R. A. (1931) CXCVIII.—Universal buffer solutions and the dissociation constant of veronal, *Journal of the Chemical Society (Resumed)*, 1456-1462.

202. Martins, L. O., Soares, C. M., Pereira, M. M., Teixeira, M., Costa, T., Jones, G. H. & Henriques, A. O. (2002) Molecular and Biochemical Characterization of a Highly Stable

Bacterial Laccase That Occurs as a Structural Component of the Bacillus subtilis Endospore Coat, *Journal of Biological Chemistry.* **277**, 18849-18859.

203. Mohammadian, M., Fathi-Roudsari, M., Mollania, N., Badoei-Dalfard, A. & Khajeh, K. (2010) Enhanced expression of a recombinant bacterial laccase at low temperature and microaerobic conditions: purification and biochemical characterization, *Journal of Industrial Microbiology & Biotechnology.* **37**, 863-869.

204. Eisenthal, R., Danson, M. J. & Hough, D. W. (2007) Catalytic efficiency and kcat/KM: a useful comparator?, *Trends in Biotechnology.* **25**, 247-249.

205. Roth, S. & Spiess, A. C. (2015) Laccases for biorefinery applications: a critical review on challenges and perspectives, *Bioprocess and Biosystems Engineering.* **38**, 2285-2313.

206. Kawai, S., Nakagawa, M. & Ohashi, H. (1999) Aromatic ring cleavage of a non-phenolic β-O-4 lignin model dimer by laccase of Trametes versicolor in the presence of 1-hydroxybenzotriazole, *FEBS Letters.* **446**, 355-358.

207. Crestini, C. & Argyropoulos, D. S. (1998) The early oxidative biodegradation steps of residual kraft lignin models with laccase, *Bioorganic & Medicinal Chemistry.* **6**, 2161-2169.

208. Kawai, S., Asukai, M., Ohya, N., Okita, K., Ito, T. & Ohashi, H. (1999) Degradation of a non-phenolic β-O-4 substructure and of polymeric lignin model compounds by laccase of Coriolus versicolor in the presence of 1-hydroxybenzotriazole, *FEMS Microbiology Letters.* **170**, 51-57.

209. Castro, A. I., Evtuguin, D. V. & Xavier, A. M. (2003) Degradation of biphenyl lignin model compounds by laccase of Trametes versicolor in the presence of 1-hydroxybenzotriazole and heteropolyanion [SiW11VO40] 5−, *Journal of Molecular Catalysis B: Enzymatic.* **22**, 13-20.

210. Fengel, D. & Wegener, G. (1984) Wood: chemistry, ultrastructure, reactions, *Walter de Gruyter.* **613**, 1960-82.

211. Leonowicz, A., Szklarz, G. & Wojtaś-Wasilewska, M. (1985) The effect of fungal laccase on fractionated lignosulphonates (Peritan Na), *Phytochemistry.* **24**, 393-396.

212. Rittstieg, K., Suurnakki, A., Suortti, T., Kruus, K., Guebitz, G. & Buchert, J. (2002) Investigations on the laccase-catalyzed polymerization of lignin model compounds using size-exclusion HPLC, *Enzyme and Microbial Technology.* **31**, 403-410.

213. Heap, L., Green, A., Brown, D., van Dongen, B. & Turner, N. (2014) Role of laccase as an enzymatic pretreatment method to improve lignocellulosic saccharification, *Catalysis Science & Technology.* **4**, 2251-2259.

214. Rittstieg, K., Suurnäkki, A., Suortti, T., Kruus, K., Guebitz, G. M. & Buchert, J. (2003) Polymerization of Guaiacol and a Phenolic β-O-4-Substructure by Trameteshirsuta Laccase in the Presence of ABTS, *Biotechnology Progress.* **19**, 1505-1509.

215. Borgmeyer, J. R. & Crawford, D. L. (1985) Production and characterization of polymeric lignin degradation intermediates from two different Streptomyces spp, *Applied and Environmental Microbiology.* **49**, 273-278.

216. Masai, E., Katayama, Y., Kubota, S., Kawai, S., Yamasaki, M. & Morohoshi, N. (1993) A bacterial enzyme degrading the model lignin compound β-etherase is a member of the glutathione-S-transferase superfamily, *FEBS Letters.* **323**, 135-140.

217. Cázares-García, S. V., Vázquez-Garcidueñas, M. S. & Vázquez-Marrufo, G. (2013) Structural and phylogenetic analysis of laccases from Trichoderma: a bioinformatic approach, *PloS One.* **8**, e55295.

218. Messerschmidt, A. (1997) *Multi-copper oxidases*, World Scientific.

219. Larrondo, L. F., Salas, L., Melo, F., Vicuña, R. & Cullen, D. (2003) A novel extracellular multicopper oxidase from Phanerochaete chrysosporium with ferroxidase activity, *Applied and Environmental Microbiology.* **69**, 6257-6263.

220. Kataoka, K., Komori, H., Ueki, Y., Konno, Y., Kamitaka, Y., Kurose, S., Tsujimura, S., Higuchi, Y., Kano, K. & Seo, D. (2007) Structure and function of the engineered multicopper oxidase CueO from Escherichia coli—deletion of the methionine-rich helical region covering the substrate-binding site, *Journal of Molecular Biology.* **373**, 141-152.

221. Kabsch, W. (2010) Xds, *Acta Crystallographica Section D: Biological Crystallography.* **66**, 125-132.

222. Bailey, S. (1994) Collaborative computational project number 4, *Acta Crystallogr D Biol Crystallogr.* **50**, 760-763.

223. Long, F., Vagin, A. A., Young, P. & Murshudov, G. N. (2008) BALBES: a molecular-replacement pipeline, *Acta Crystallographica Section D: Biological Crystallography.* **64**, 125-132.

224. Solomon, E. I., Sundaram, U. M. & Machonkin, T. E. (1996) Multicopper Oxidases and Oxygenases, *Chemical Reviews.* **96**, 2563-2606.

225. Baker, E. N. (1988) Structure of azurin from Alcaligenes denitrificans refinement at 1· 8 Å resolution and comparison of the two crystallographically independent molecules, *Journal of Molecular Biology.* **203**, 1071-1095.

226. Pieper, U., Eswar, N., Davis, F. P., Braberg, H., Madhusudhan, M. S., Rossi, A., Marti-Renom, M., Karchin, R., Webb, B. M. & Eramian, D. (2006) MODBASE: a database of annotated comparative protein structure models and associated resources, *Nucleic Acids Research.* **34**, D291-D295.

227. Jaiswal, D., Vařeková, R. S., Ionescu, C.-M., Sehnal, D. & Koča, J. (2012) Searching for tunnels of proteins–comparison of approaches and available software tools, *Journal of Cheminformatics.* **4**, P60.

228. Hakulinen, N., Kiiskinen, L.-L., Kruus, K., Saloheimo, M., Paananen, A., Koivula, A. & Rouvinen, J. (2002) Crystal structure of a laccase from Melanocarpus albomyces with an intact trinuclear copper site, *Nature Structural and Molecular Biology.* **9**, 601.

229. Messerschmidt, A., Ladenstein, R., Huber, R., Bolognesi, M., Avigliano, L., Petruzzelli, R., Rossi, A. & Finazzi-Agró, A. (1992) Refined crystal structure of ascorbate oxidase at 1.9 Å resolution, *Journal of Molecular Biology.* **224**, 179-205.

230. Petřek, M., Otyepka, M., Banáš, P., Košinová, P., Koča, J. & Damborský, J. (2006) CAVER: a new tool to explore routes from protein clefts, pockets and cavities, *BMC Bioinformatics.* **7**, 316.

231. Hakulinen, N., Andberg, M., Kallio, J., Koivula, A., Kruus, K. & Rouvinen, J. (2008) A near atomic resolution structure of a Melanocarpus albomyces laccase, *Journal of Structural Biology.* **162**, 29-39.

232. Anzai, Y., Kim, H., Park, J.-Y., Wakabayashi, H. & Oyaizu, H. (2000) Phylogenetic affiliation of the pseudomonads based on 16S rRNA sequence, *International Journal of Systematic and Evolutionary Microbiology.* **50**, 1563-1589.

233. Nelson, K., Weinel, C., Paulsen, I., Dodson, R., Hilbert, H., dos Santos, V. M., Fouts, D., Gill, S., Pop, M. & Holmes, M. (2002) Complete genome sequence and comparative analysis of the metabolically versatile Pseudomonas putida KT2440, *Environmental Microbiology.* **4**, 799-808.

234. Belda, E., Van Heck, R. G., José Lopez-Sanchez, M., Cruveiller, S., Barbe, V., Fraser, C., Klenk, H. P., Petersen, J., Morgat, A. & Nikel, P. I. (2016) The revisited genome of Pseudomonas putida KT2440 enlightens its value as a robust metabolic chassis, *Environmental Microbiology.* **18**, 3403-3424.

235. Huang, W. & Wilks, A. (2017) A rapid seamless method for gene knockout in Pseudomonas aeruginosa, *BMC Microbiology.* **17**, 199.

236. Schäfer, A., Tauch, A., Jäger, W., Kalinowski, J., Thierbach, G. & Pühler, A. (1994) Small mobilizable multi-purpose cloning vectors derived from the Escherichia coli plasmids pK18 and pK19: selection of defined deletions in the chromosome of Corynebacterium glutamicum, *Gene.* **145**, 69-73.

237. Wang, H.-h., Zhou, X.-r., Liu, Q. & Chen, G.-Q. (2011) Biosynthesis of polyhydroxyalkanoate homopolymers by Pseudomonas putida, *Applied Microbiology and Biotechnology.* **89**, 1497-1507.

238. Jiménez, J. I., Miñambres, B., García, J. L. & Díaz, E. (2002) Genomic analysis of the aromatic catabolic pathways from Pseudomonas putida KT2440, *Environmental Microbiology.* **4**, 824-841.

239. Brebu, M. & Vasile, C. (2010) Thermal degradation of lignin—a review, *Cellulose Chemistry & Technology.* **44**, 353.

240. Beckham, G. T., Johnson, C. W., Karp, E. M., Salvachúa, D. & Vardon, D. R. (2016) Opportunities and challenges in biological lignin valorization, *Current Opinion in Biotechnology.* **42**, 40-53.

241. Skálová, T., Dohnálek, J., Østergaard, L. H., Østergaard, P. R., Kolenko, P., Dušková, J., Štěpánková, A. & Hašek, J. (2009) The structure of the small laccase from Streptomyces coelicolor reveals a link between laccases and nitrite reductases, *Journal of Molecular Biology.* **385**, 1165-1178.

242. Van Mellaert, L. & Anné, J. (2001) Gram-positive bacteria as host cells for heterologous production of biopharmaceuticals in *Novel Frontiers in the Production of Compounds for Biomedical use* pp. 277-300, Springer.

243. Outten, F. W., Huffman, D. L., Hale, J. A. & O'Halloran, T. V. (2001) The independent cue and cus Systems confer copper tolerance during aerobic and anaerobic growth inEscherichia coli, *Journal of Biological Chemistry.* **276**, 30670-30677.

10 Appendix

10.1 Appendix 1

Rate of reaction vs substrate concentration for Pp-CopA, Pf-CopA and Oc-CueO.

Graphics: reaction rate vs substrate concentration for Pp-CopA, Pf-CopA and Oc-CueO. The corresponding linearized graphics were used for the determination of steady state kinetic parameters of these enzymes. Pf-CopA is presented in blue markers, Pp-CopA in orange markers, and Oc-CueO in grey markers, with ABT, DMP and SGZ. Left: rate of reaction as a function of substrate concentration. Centre: Eadie-Hofstee plot. Right: Lineweaver Burk plot. The substrate used is shown in the label of the "x" axis, in each graphic in the left side.

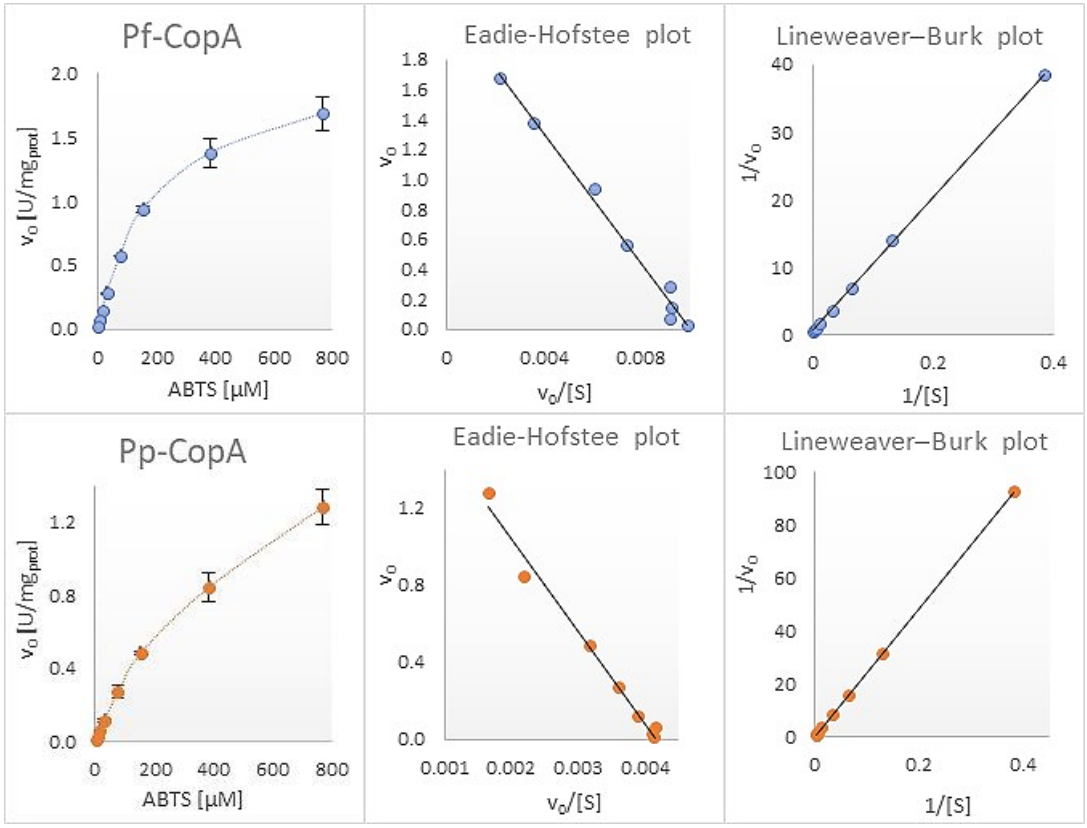

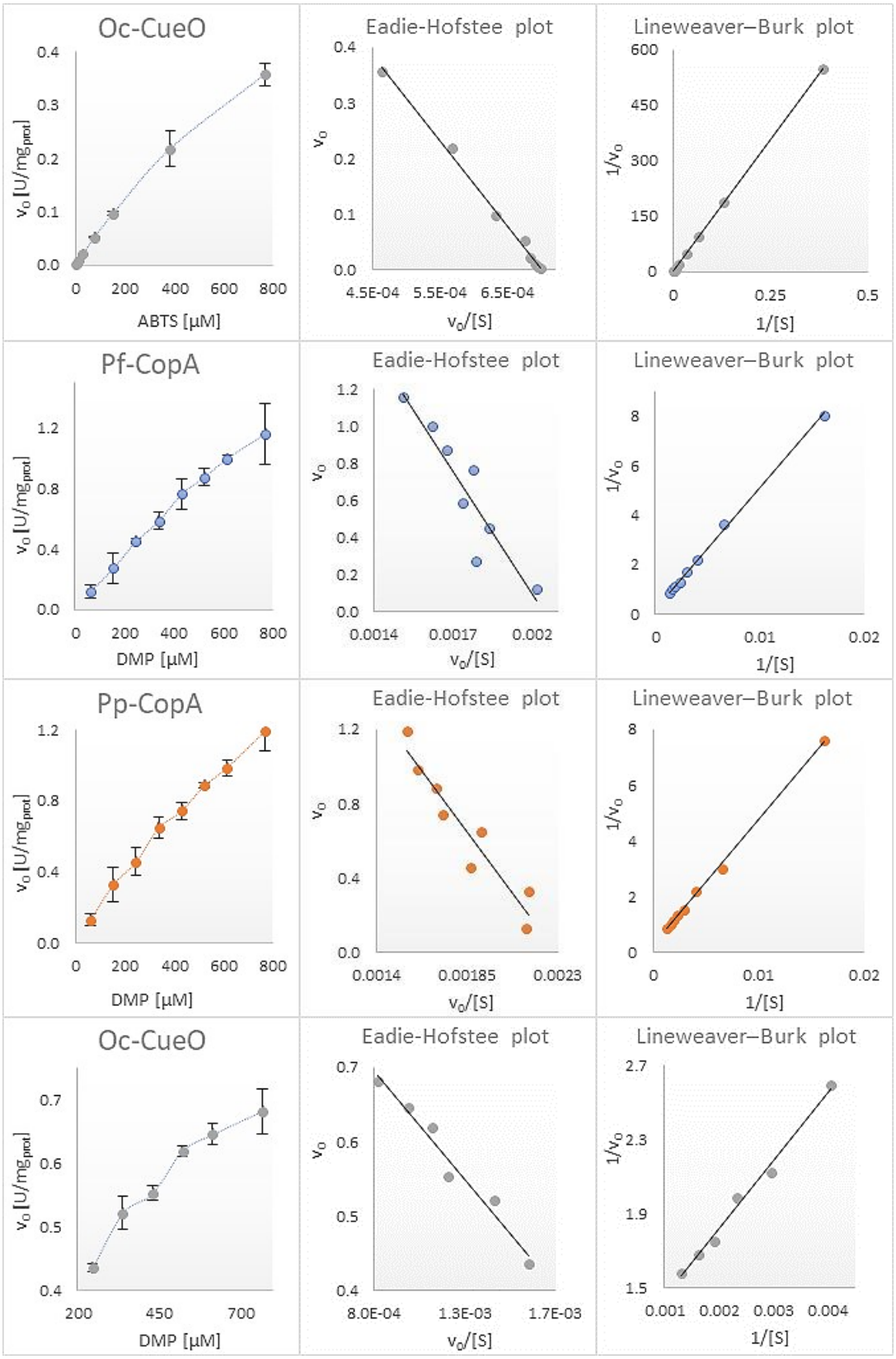
Oc-CueO
Eadie-Hofstee plot
Lineweaver–Burk plot
v0 [U/mgprot]
ABTS [µM]
v0/[S]
1/v0
1/[S]
Pf-CopA
DMP [µM]
Pp-CopA
Oc-CueO

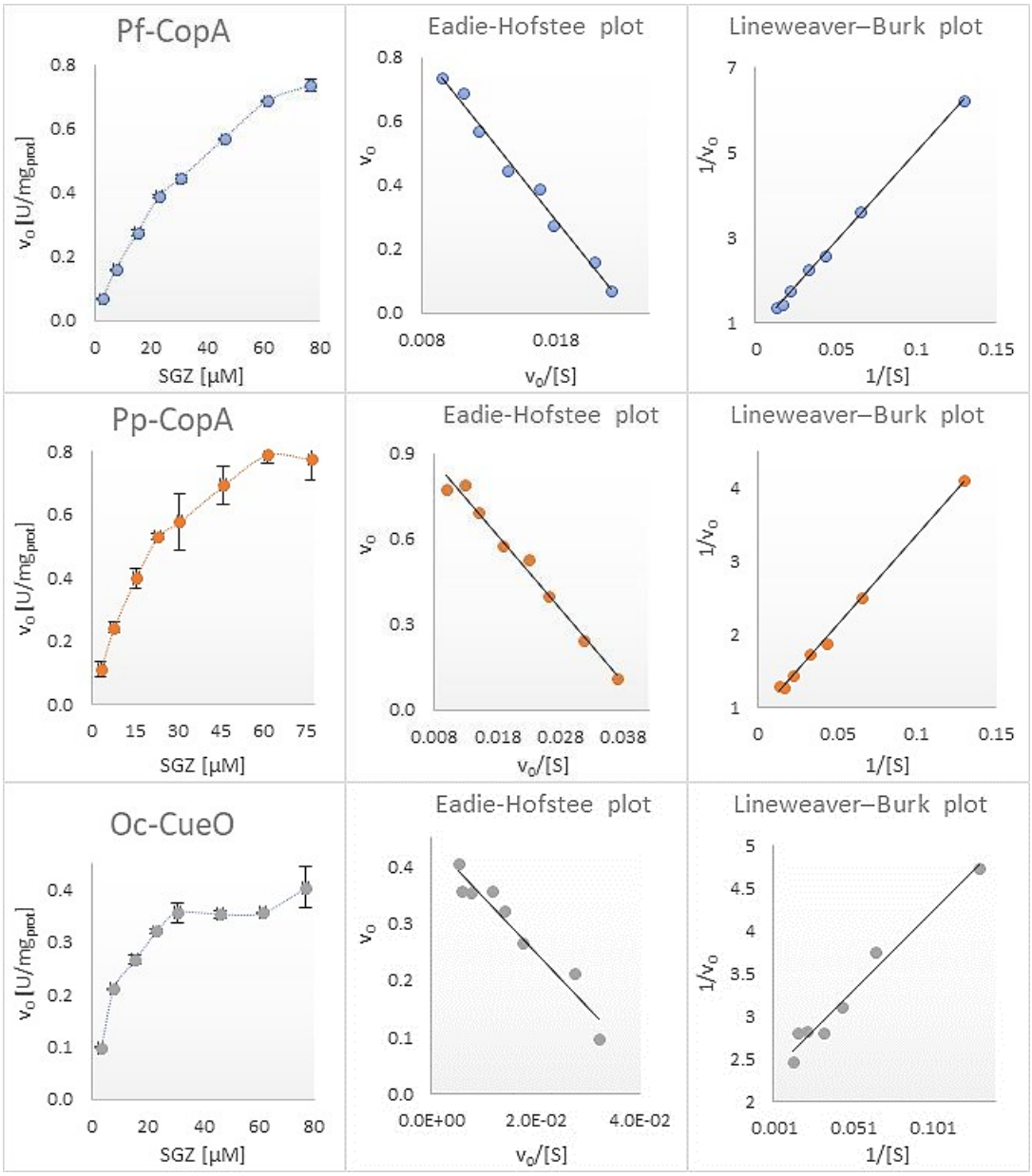
Pf-CopA
Eadie-Hofstee plot
Lineweaver–Burk plot
Pp-CopA
Eadie-Hofstee plot
Lineweaver–Burk plot
Oc-CueO
Eadie-Hofstee plot
Lineweaver–Burk plot
SGZ [µM]
v0 [U/mgprot]
v0/[S]
1/v0
1/[S]

10.2 Appendix 2

HPLC chromatograms for activity of LMCOs with polymeric lignin substrates, and photos of their corresponding reactions.

The list of polymeric lignin used was as follows:

Lignin 1: Poplar ammonia (percolation) organosolv (University of Glasgow)

Lignin 2: Wheat straw organosolv lignin (CIMV)

Lignin 3: Wheat straw protobind lignin (Green value)

Lignin 4: Alkali Kraft lignin (Sigma-Aldrich)

Lignin 5: Na-lignosulfonate softwood ultrafiltrated (Borregaard)

Lignin 6: Ca-lignosulfonate hardwood (Borregaard)

Lignin 7: Wheat straw alkali organosolv lignin (University of Glasgow)

Lignin 8: Wheat straw acid organosolv lignin (University of Glasgow)

Blue line: blank/negative control. Red line: Pp-CopA. Green line: Pf-CopA. Pink line: Oc-CueO. Only reactions carried out in presence of a mediator (1 mM ABTS) are shown, as these reactions presented more variations in the chromatograms than the reactions in absence of a mediator. Lignin 6 (Ca-lignosulfonate hardwood (Borregaard)) gave the formation of a new peak.

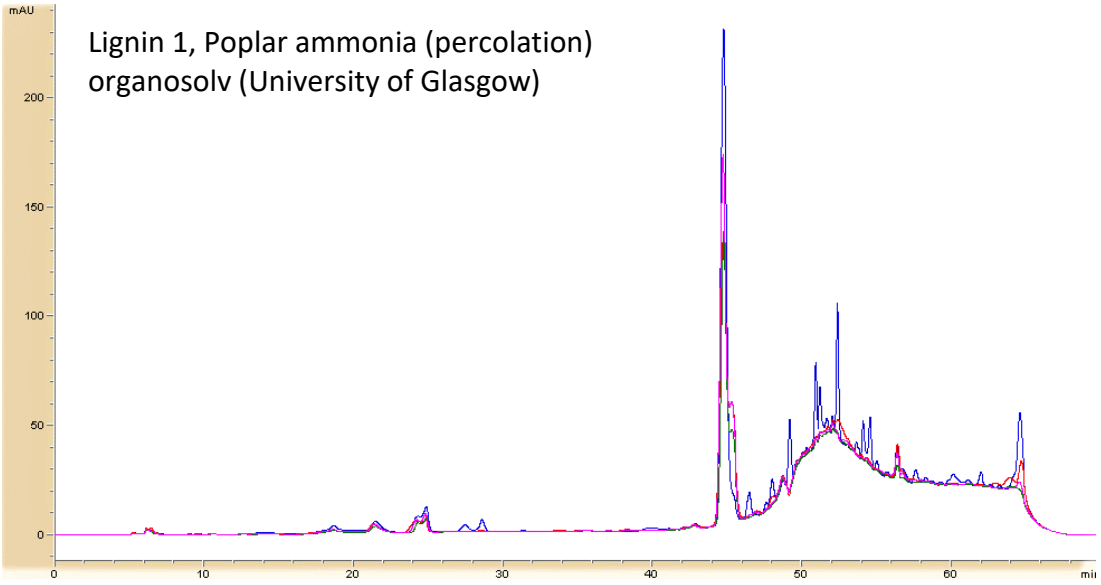

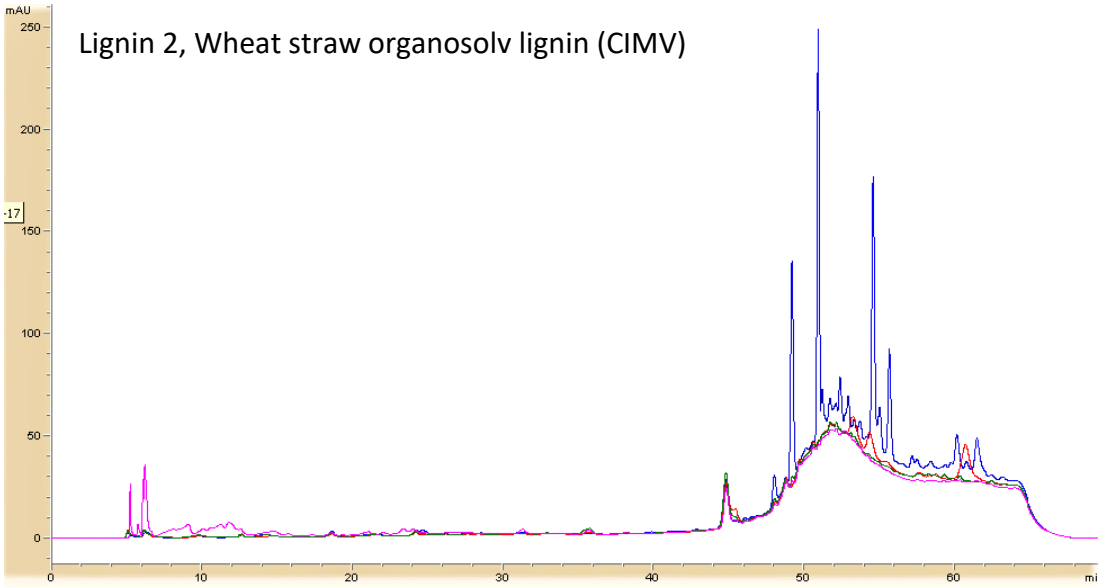
Lignin 2, Wheat straw organosolv lignin (CIMV)
mAU
250
200
150
100
50
0
10
20
30
40
50
60
mi

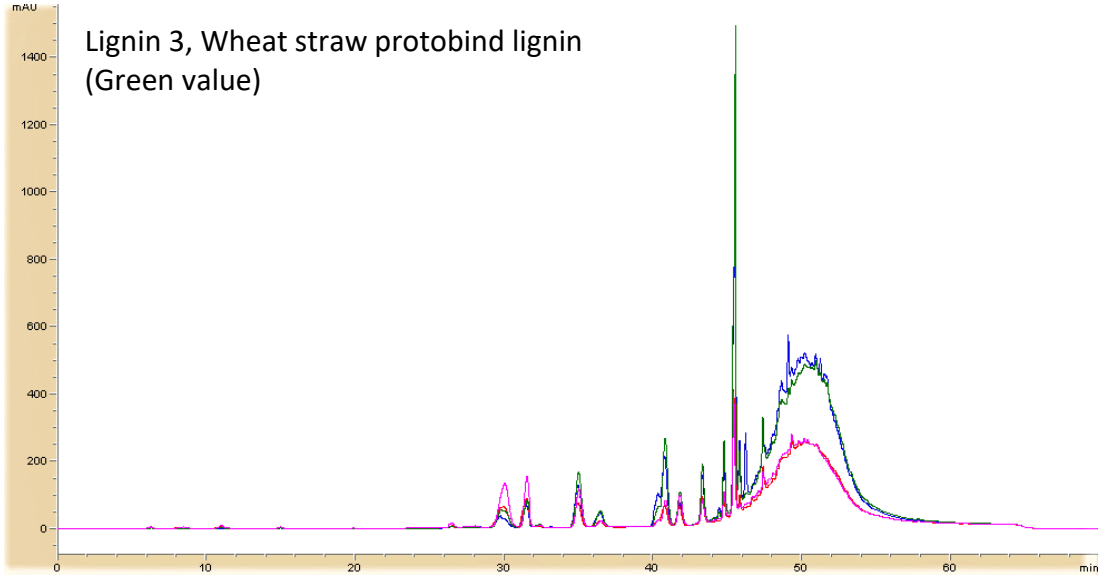
Lignin 3, Wheat straw protobind lignin
(Green value)
mAU
1400
1200
1000
800
600
400
200
0
10
20
30
40
50
60
min

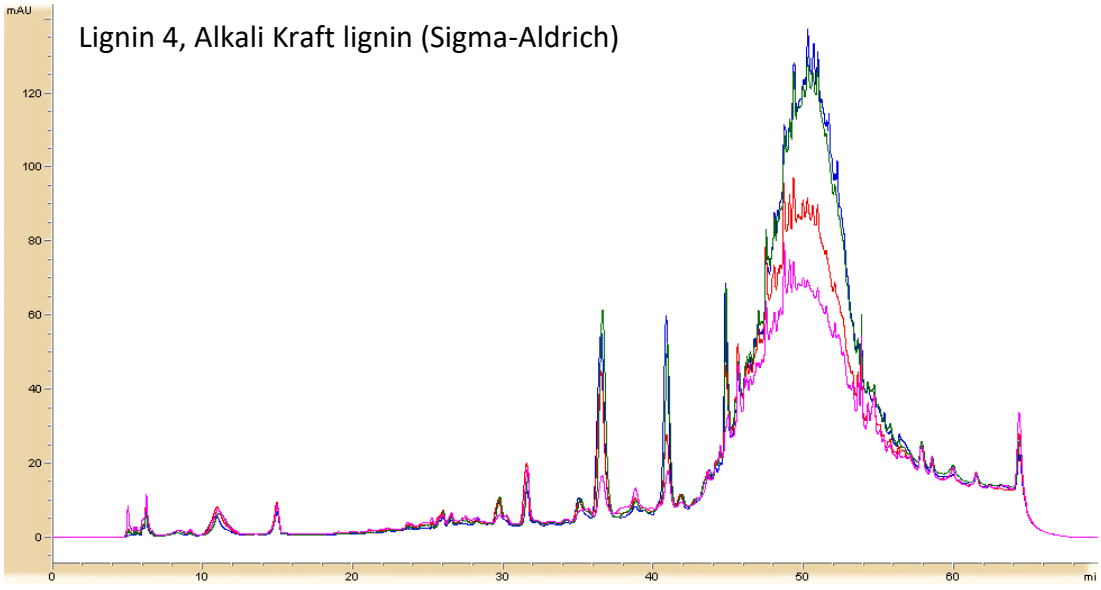
Lignin 4, Alkali Kraft lignin (Sigma-Aldrich)
mAU
120
100
80
60
40
20
0
10
20
30
40
50
60
mi

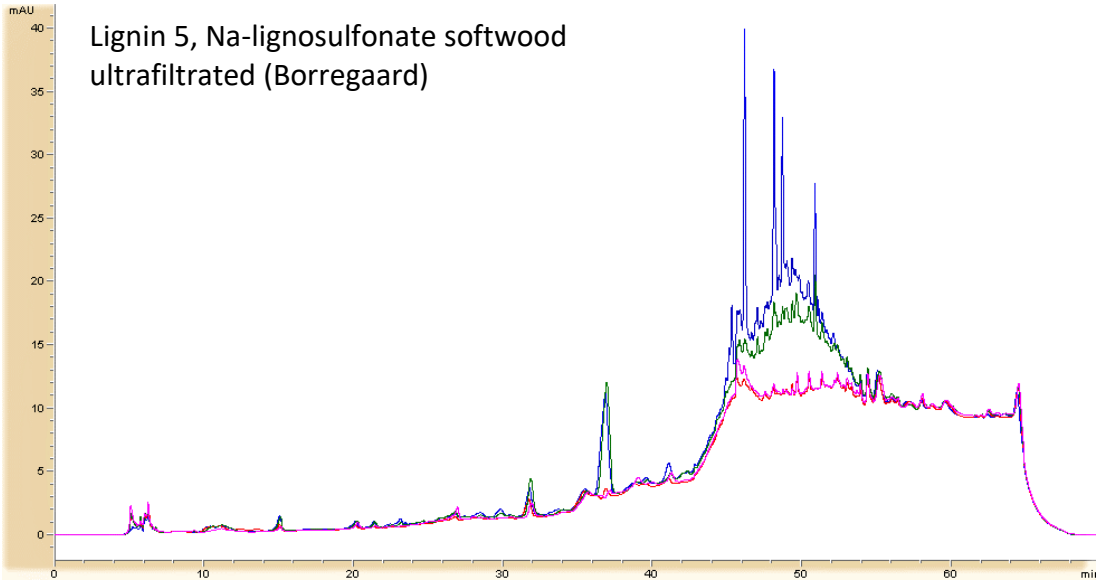
Lignin 5, Na-lignosulfonate softwood ultrafiltrated (Borregaard)
mAU
40
35
30
25
20
15
10
5
0
0
10
20
30
40
50
60

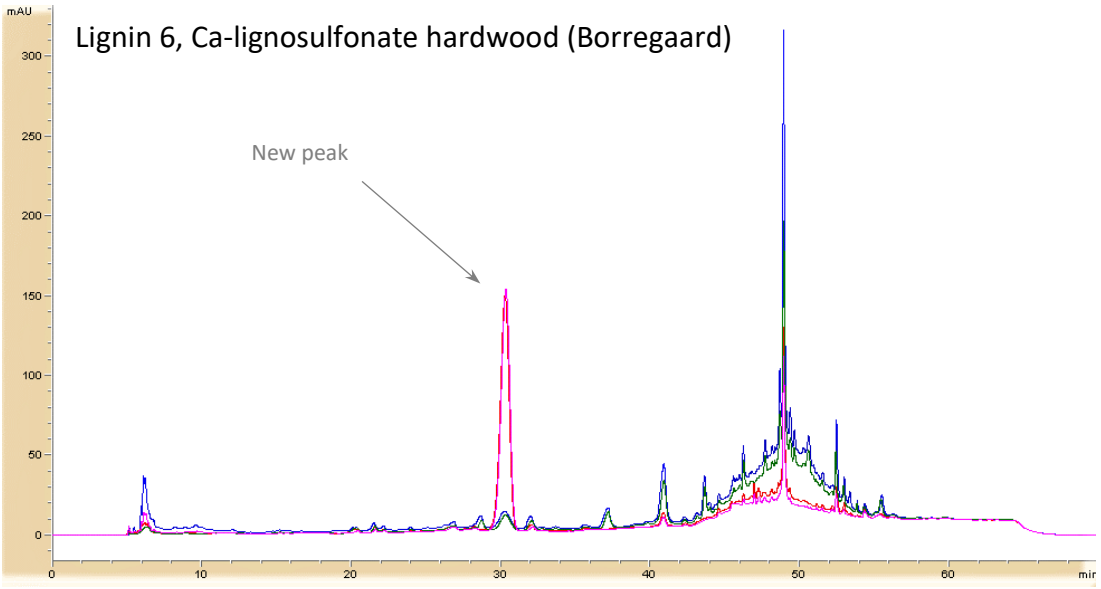
Lignin 6, Ca-lignosulfonate hardwood (Borregaard)
New peak
mAU
300
250
200
150
100
50
0
0
10
20
30
40
50
60

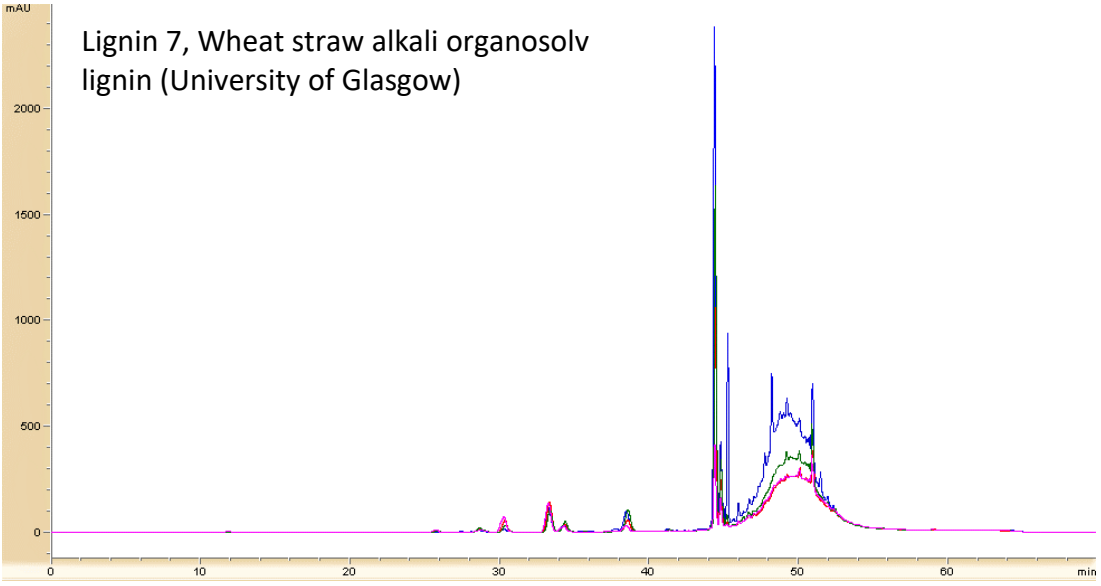
Lignin 7, Wheat straw alkali organosolv lignin (University of Glasgow)
mAU
2000
1500
1000
500
0
0
10
20
30
40
50
60

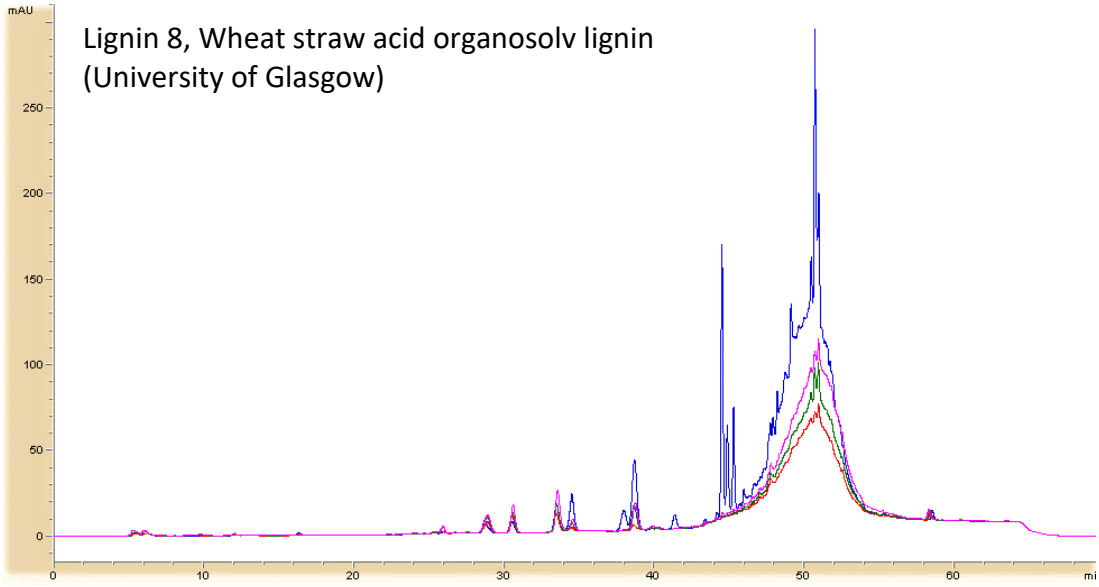
Lignin 8, Wheat straw acid organosolv lignin
(University of Glasgow)
mAU
250
200
150
100
50
0
0
10
20
30
40
50
60
mi

Activity of Recombinant LMCOs against polymeric lignin substrates. For each photo, from left to right, the reactions corresponding to negative control, Pp-CopA, Pf-CopA and Oc-CueO, respectively, are shown. In the same way, the upper part corresponds with the reactions in absence of mediator, whereas the bottom part shows the reactions in presence of 1 mM ABTS as mediator.

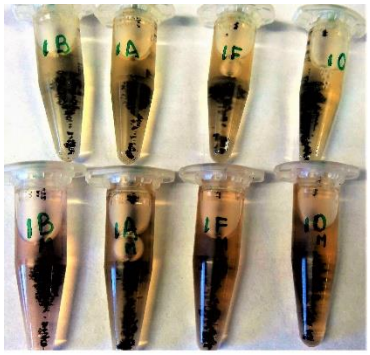

Lignin 1

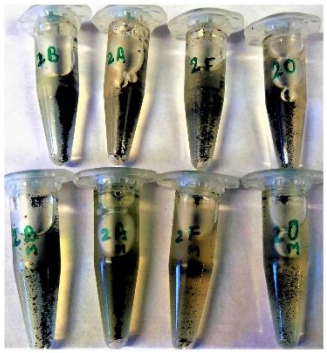

Lignin 2

Lignin 3

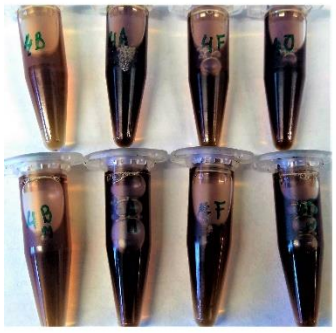

Lignin 4

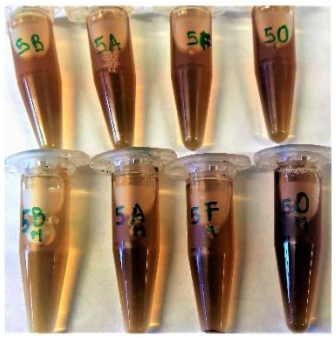

Lignin 5

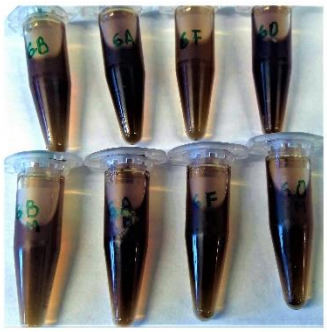

Lignin 6

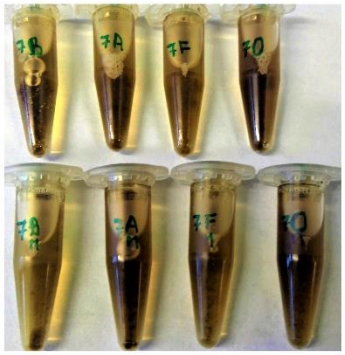

Lignin 7

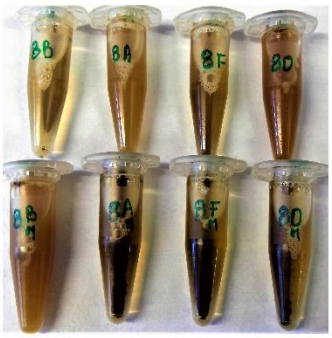

Lignin 8

10.3 Appendix 3

Bacterial and fungal laccases and laccase-like multicopper oxidases sequence alignment

List of putative and annotated fungal and bacterial laccases or multicopper oxidases used for alignment. PDB, means code from Protein Data Bank database; GB, means code from GenBank database; if there is not prefix, code belongs to Uniprot database.

Bacterial laccases or multicopper oxidases					
Sequence number	**Host organism**	**Accession code**	**Sequence number**	**Host organism**	**Accession code**
1	*Pseudomonas putida*	Q88C03	**18**	*Hapalosiphon* sp.	GB WP_053456062.1
2	*Ochrobactrum* sp.	-	**19**	*Gramella forsetii*	GB WP_011709064.1
3	*Pseudomonas fluorescens*	Q4KCN4	**20**	*Marivirga tractuosa*	GB WP_013454223.1
4	*Pseudomonas syringae* pv. tomato	P12374	**21**	*Actinoplanes subtropicus*	GB WP_030438873.1
5	*Bacillus subtilis*	P07788	**22**	*Ralstonia solanacearum*	A0A1L3DK94
6	*Escherichia coli*	A0A0E0XT94	**23**	*Pectobacterium* sp.	GB WP_014701106.1
7	*Aquifex aeolicus*	GB WP_010880708.1	**24**	*Pantoea ananatis*	GB WP_028724718.1
8	*Bacillus* sp.	I6ZLM4	**25**	*Streptomyces (multispecies)*	GB WP_030731323.1
9	*Bacillus* sp.	B9W2C5	**26**	*Bacillus coagulans*	GB WP_014097300.1
10	*Bacillus subtilis*	GB WP_004397739.1	**27**	*Streptomyces silvensis*	GB WP_058850924.1
11	*Streptomyces pristinaespiralis*	ZP_06908025.1	**28**	*Escherichia coli*	P36649
12	*Pseudomonas stutzeri*	A0A182CBL5	**29**	Uncultured bacterium	E9MWD9
13	*Catelliglobosispora koreensis*	GB WP_020519869.1	**30**	uncultured bacterium	F5ANG6
14	*Spirosoma linguale*	GB WP_012931295.1	**31**	Uncultured bacterium	G8IJH7
15	*Thermus* (multispecies)	GB WP_011173754.1	**32**	Uncultured bacterium	F5ANG7
16	*Meiothermus ruber*	GB WP_013012601.1	**33**	Uncultured bacterium	E1ACR6
17	*Nostoc* sp.	GB WP_041555149.1			

Fungal laccases					
Sequence number	**Host organism**	**Accession code**	**Sequence number**	**Host organism**	**Accession code**
34	*Trametes versicolor*	PDB 1GYC	**50**	*Trametes versicolor*	Q12717
35	*(Trametes) Coriolopsis trogii*	PDB 2HRH	**51**	*Phlebia radiata*	Q01679
36	*Botryotinia fuckeliana (Botrytis cinerea)*	Q12570	**52**	*Pleurotus ostreatus*	Q12729
37	*Trametes hirsuta*	Q02497	**53**	*Agaricus bisporus*	Q12541
38	*Trametes villosa*	Q99044	**54**	*Thanatephorus cucumeris*	P56193
39	*Basidiomycete PM1*	Q12571	**55**	*Neosartorya fumigata*	E9RBR0
40	*Cerrena maxima*	D0VWU3	**56**	*Trametes versicolor*	Q12719
41	*Pycnoporus cinnabarinus*	O59896	**57**	*Botryotinia fuckeliana (Botrytis cinerea)*	Q96WM9
42	*Trametes pubescens*	Q8TG93	**58**	*Botryotinia fuckeliana (Botrytis cinerea)*	Q96UM2
43	*Pleurotus ostreatus*	Q12739	**59**	*Neurospora crassa*	P06811
44	*Trametes pubescens*	Q8TG94	**60**	*Botryotinia fuckeliana (Botrytis cinerea)*	Q12570-1
45	*Trametes sp C30*	GB AAF06967.1	**61**	*Podospora anserina*	P78722
46	*Botrytis aclada*	GB AFC76164.1	**62**	*Melanocarpus albomyces*	Q70KY3
47	*Trametes ochracea*	PDB 2HZH	**63**	*Arthroderma benhamiae*	D4APX3
48	*Thanatephorus cucumeris (Rhizoctonia solani)*	Q02075	**64**	*Cryptococcus neoformans*	Q55P57
49	*Trametes cinnabarina*	GB AAC39469.1	**65**	*Emericella nidulans*	P17489

The multiple sequence alignment, with 33 bacterial laccase-like multicopper oxidases (in gray background) and 32 fungal laccases is shown below. Metal-binding residues are coloured in blue; well-conserved residues are coloured in red (**Table 15**). Accession codes (Uniprot, GenBank or Protein Data Bank, databases) are listed above.